Springer Laboratory

Harald Pasch
Muhammad Imran Malik

Advanced Separation Techniques for Polyolefins

Springer

Springer Laboratory

Manuals in Polymer Science

Harald Pasch • Muhammad Imran Malik

Advanced Separation Techniques for Polyolefins

Springer

Harald Pasch
Department of Chemistry and Polymer Science
University of Stellenbosch
Matieland
South Africa

Muhammad Imran Malik
International Center for Chemical and Biological Sciences (ICCBS)
H.E.J. Research Institute of Chemistry
University of Karachi
Karachi
Pakistan

ISSN 0945-6074 ISSN 2196-1174 (electronic)
ISBN 978-3-319-08631-6 ISBN 978-3-319-08632-3 (eBook)
DOI 10.1007/978-3-319-08632-3
Springer Cham Heidelberg New York Dordrecht London

Library of Congress Control Number: 2014949149

Printed on acid-free paper

Springer is part of Springer Science+Business Media (www.springer.com)

Preface

Polyolefins are the most widely used synthetic polymers and their production capacities are rapidly increasing. Polyolefins are produced from very simple monomers containing only carbon and hydrogen, yet they exhibit very complex molecular structures. As all other synthetic polymers, polyolefins are distributed regarding various molecular properties, including molar mass, chemical composition, microstructure and molecular topology.

One consequence of the complex structure of polyolefins is the need for advanced analytical methods that provide accurate and quantitative information on the different parameters of molecular heterogeneity. In addition to analysis of bulk properties by spectroscopic methods, emphasis is on the analysis of property distributions that require suitable fractionation methods. If the material is distributed in more than one molecular property, multidimensional fractionations or the combination of fractionation and spectroscopic analysis might be required. High temperature fractionation methods must be used because most polyolefins are semi-crystalline and do not dissolve in common solvents at ambient temperatures. Powerful and well established methods include high temperature size exclusion chromatography (HT-SEC) for molar mass analysis, temperature rising elution fractionation (TREF) and crystallization analysis fractionation (CRYSTAF) for the analysis of chemical composition and branching. Recently, a number of more advanced methods including high temperature two-dimensional liquid chromatography (HT-2D-LC), temperature gradient interaction chromatography (TGIC) and crystallization elution fractionation (CEF) have been developed.

The fractionation of polyolefins has been addressed in numerous original publications and review articles. The most recent reviews were published by Monrabal (Adv. Polym. Sci., 2013, 257:203–51) and the authors of this book (Adv. Polym. Sci., 2013, 251:77–140) in 2013. These reviews provide an excellent overview on the current status of polyolefin characterization. They do not, however, give any detailed information on experimental protocols and procedures. To date, no textbook has been published that addresses the experimental background of different polyolefin fractionation techniques in great detail. This challenge is now addressed in the present textbook.

Similar to the previous textbooks in the Springer Laboratory Series, this laboratory manual is written for beginners as well as for experienced scientists. The subject of the book is the description of the experimental approach for the analysis

of complex polyolefins. It summarizes important applications in all major fractionation methods with emphasis on multidimensional analytical approaches. The theoretical background, equipment, experimental procedures and applications are discussed for each fractionation technique. It will enable polymer chemists, physicists and material scientists, as well as students of polymer and analytical sciences, to optimize experimental conditions for specific fractionation problems. The main benefit for the reader is that a great variety in instrumentation, separation procedures and applications is given, making it possible to solve simple as well as sophisticated separation tasks.

The book is structured in a similar fashion to the review article of the authors. It commences with a short introduction to the molecular complexity of polyolefins. This is followed by a discussion of crystallization-based fractionation techniques, including TREF, CRYSTAF and CEF. The major part addresses column chromatographic techniques for molar mass, chemical composition and microstructure, and the combination of different fractionations in multidimensional experimental set-ups. Finally, some first information on the application of field-flow fractionation is presented.

This textbook is dedicated to friends and colleagues that contributed (directly or indirectly) to this book by pioneering high temperature fractionation using HPLC, TREF, CRYSTAF, CEF and multidimensional chromatography, most prominently Tibor Macko (Germany) and, among others, Benjamin Monrabal (Spain), Freddy van Damme (The Netherlands), Yefim Brun, Colin Li Pi Shan and Rongjuan Cong (USA), Wolf Hiller, Robert Bruell, Dieter Lilge, Volker Dolle and Peter Montag (Germany), Joao Soares (Canada), Albert van Reenen (South Africa) and a number of former graduate students including Lars-Christian Heinz, Andreas Albrecht, Nyambeni Luruli, Pritish Sinha, Tino Otte, Anton Ginzburg, Stefan de Goede, Elana de Goede and Sadiqali Cheruthazhekatt.

Stellenbosch, South Africa — Harald Pasch
Karachi, Pakistan — Muhammad Imran Malik
May 2014

Symbols and Abbreviations

AF4, AFFFF	asymmetric flow field-flow fractionation
ATR	attenuated total reflectance
A-TREF	analytical temperature rising elution fractionation
BF	branch frequency
BHT	2,6-bis(1,1-dimethylethyl)-4-methylphenol
c	concentration
CCD	chemical composition distribution
CEF	crystallization elution fractionation
CRYSTAF	crystallization analysis fractionation
CSTR	continuous stirred tank reactor
D	diffusion coefficient
2D-LC	two-dimensional liquid chromatography
DLS	dynamic light scattering
DSC	differential scanning calorimetry
DVB	divinyl benzene
EA	ethylene–acrylate
EB	ethylene–butene
ED	ethylene-1-decene
EGMBE	ethyleneglycol monobutylether
EH	ethylene–hexene
ELSD	evaporative light scattering detector
EMA	ethylene–methyl acrylate
EMMA	ethylene–methyl methacrylate
EO	ethylene–octene
EP	ethylene–propylene
EPC	ethylene–propylene copolymer
EPDM	ethylene–propylene–diene rubber
EPR	ethylene–propylene rubber
EVA	ethylene–vinylacetate copolymer
f	frictional drag
FFF	field-flow fractionation
FID	free induction decay
FTIR	Fourier transform infrared spectroscopy
ΔG	Gibbs free energy

ΔG_m	Gibbs free energy of mixing
GPC	gel permeation chromatography
ΔH	interaction enthalpy
ΔH_m	mixing enthalpy
ΔH_u	heat of fusion
HDPE	high density polyethylene
HPLC	high performance liquid chromatography
HT	high temperature
IC	interaction chromatography
i.d.	internal diameter
IPC	impact polypropylene copolymer
IR	infrared
J	net flux
K^*	optical constant in light scattering
K_d	distribution coefficient
l	mean layer thickness
LALLS	low angle laser light scattering
LALS	low angle light scattering
LAM	longitudinal acoustic mode
LC	liquid chromatography
LCB	long chain branching
LCCC	liquid chromatography at critical conditions
LDPE	low density polyethylene
LLDPE	linear low density polyethylene
LS	light scattering
M	molar mass
M_n	number-average molar mass
M_o	molar mass of repeat unit
M_v	viscosity-average molar mass
M_w	weight-average molar mass
MA	methyl acrylate
MALLS	multi-angle laser light scattering
MALS	multi-angle light scattering
MFI	melt flow index
MMA	methyl methacrylate
MMD	molar mass distribution
MT	medium temperature
m_i	mass of species i
n_i	number of species i
N_A	Avogadro's number
NMR	nuclear magnetic resonance
OBC	olefin block copolymer
ODCB	ortho-dichlorobenzene
P	degree of polymerization
$P(\Theta)$	scattered light angular dependence

PE	polyethylene
PMMA	poly(methyl methacrylate)
PP	polypropylene
aPP	atactic polypropylene
iPP	isotactic polypropylene
sPP	syndiotactic polypropylene
PS	polystyrene
P-TREF	preparative temperature rising elution fractionation
PVAc	poly(vinyl acetate)
R, R_g	radius of gyration
R_h	hydrodynamic radius
$R(\Theta)$	intensity of scattered light
RALLS	right angle laser light scattering
RI	refractive index
RT	retention time
ΔS	conformational entropy
SCB	short chain branching
SCBD	short chain branching distribution
SDV	styrene-divinylbenzene copolymer
SEC	size exclusion chromatography
SEM	scanning electron microscopy
SGIC	solvent gradient interaction chromatography
SNR	signal-to-noise ratio
SSA	successive self-nucleation annealing
SSF	successive solution fractionation
T	temperature
T_c	crystallization temperature
T_m	melting temperature
TCB	1,2,4-trichlorobenzene
ThF3	thermal field-flow fractionation
TGA	thermo-gravimetric analysis
TGIC	temperature gradient interaction chromatography
TREF	temperature rising elution fractionation
TriSEC	triple-detector SEC
U	applied force (in FFF)
UHM	ultrahigh molar mass
UV	ultraviolet
V_e	elution volume
V_i	interparticle volume
V_p	pore volume
V_R	retention volume
VA	vinyl acetate
Visco	viscometer
w_i	weight fraction
w%	weight percentage

WAXD	wide-angle X-ray diffraction
ZN	Ziegler-Natta
η	viscosity
$[\eta]$	intrinsic viscosity, Staudinger index
η_o	viscosity of a solvent
η_{rel}	relative viscosity
η_{sp}	specific viscosity
λ	wavelength
λ	retention parameter (in FFF)

Contents

Introduction 1

Polyolefins are the most important and most widely used synthetic polymers; their annual production exceeds 130 million metric tons. Polyolefin production continues to grow rapidly and new polyolefin grades are constantly being introduced in the market [1]. One of the most widely investigated areas of industrial and academic polymer research continues to be the polymerization of olefins to polymers with different microstructures and properties. The interest in polyolefins continues to grow due to the fact that polyolefins are made from simple, cheap and easily accessible monomers. Polyolefins contain only carbon and hydrogen, and can be reused after recycling or degraded by thermal processes to oil and monomers [2]. Incorporation of new monomers in a copolymer system or use of modern catalysts results in new and improved properties. Polyolefins have superior properties, including excellent chemical inertness, high crystallinity resulting in excellent mechanical strength, high thermal stability and high stability against thermo-oxidative degradation.

The metallorganic-catalysed polymerization of olefins by Ziegler and the stereospecific polymerization of propene and α-olefins by Natta [3], as well as the use of metallocene catalysts [4], illustrate the potential of olefin polymerization and the properties of resulting polymers. The development of new and improved analytical techniques and approaches are vital for the analysis of new 'tailor-made' polyolefins. Information on the molecular heterogeneity of new products as well as the monitoring of the polymerization process are necessary for the development of structure–property relationships. Suitable methods to obtain information on molar mass distribution (MMD), chemical composition, tacticity, and molecular topology (branching) are imperative for proper evaluation of a polyolefin material, irrespective of the mechanism of the polymerization.

In the early days of polyolefin development, the main focus was on the characterization and evaluation of the polymerization catalyst and on the polymerization process itself. Materials were characterized by their bulk properties and much effort was directed at elucidating physical properties and crystal structures. With the development of new materials and new polymerization processes, polyolefin

H. Pasch, M.I. Malik, *Advanced Separation Techniques for Polyolefins*, Springer Laboratory, DOI 10.1007/978-3-319-08632-3_1

microstructure became more complex and parameters like chemical composition distribution (CCD) and tacticity became the focus of polyolefin research. Initially, bulk analysis techniques like Fourier transform infrared spectroscopy (FTIR), nuclear magnetic resonance (NMR), microscopy and crystal analysis were used. Later, further advancements led to fractionation techniques such as temperature rising elution fractionation (TREF) and size exclusion chromatography (SEC).

One of the major technical advantages of polyolefins is that they are stable against solvent attack and are insoluble in most of the typical organic solvents. This is, however, a disadvantage for solution based analytical methods. The prerequisite of most polymer fractionation methods is proper solubility of all the components of the sample to obtain representative dilute solutions. The majority of technically important polyolefins are semi-crystalline materials with melting points above 100 °C. Typically, polyolefin materials must be heated above their melting temperatures to achieve complete solubility; hence, high boiling solvents are required in polyolefin analysis. Polyolefin fractionation is usually carried out in 1,2,4-trichlorobenzene (TCB), 1,2-dichlorobenzene, decaline and in some cases cyclohexane at temperatures between 130 and 160 °C [5, 6]. Typically, stabilizers and antioxidants are added to the solvent to prevent degradation.

Polyolefins generally exhibit multiple distributions of molecular parameters, e.g. low density polyethylene (LDPE) and linear low density polyethylene (LLDPE) have long chain branching and CCD, respectively, along with the MMD. Polyolefin materials can be either copolymers or blends of homopolymers. From this point of view, polyolefins are not different from other synthetic polymers, and similar analytical approaches can be used. These approaches, together with specific separation and analysis methods, will be presented in the chapters that follow and typical applications will be discussed.

1.1 Molecular Heterogeneity of Polyolefins

Classical polyolefins contain only carbon and hydrogen, making them the simplest of all synthetic polymers. However, similar to all other synthetic polymers, polyolefins exhibit distributions in molar mass, chemical composition, molecular topology and (sometimes) functional groups. The constitution, configuration and conformation of macromolecules are characterized by their chemical structures. The sequences of repeat units (alternating, random or block in the case of copolymers) must be described in addition to their type and quantity. Several constitutions of macromolecules (head-to-tail vs. head-to-head arrangements, linear vs. branched molecules) can exist in macromolecules with similar chemical compositions. In addition, repeat units can exist in different steric patterns (isotactic, syndiotactic and atactic sequences in the polymer chain) despite having similar constitutions, which is referred to as configurational isomerism. Variations in the polymerization procedure and the composition of the monomer feed can lead to different types of heterogeneities in the products. High density polyethylene (HDPE) is a mostly linear homopolymer that is distributed only regarding molar

mass. In contrast, LDPE is a branched homopolymer and is, therefore, distributed regarding molar mass and molecular topology (branching). The branching in LDPE is called 'long chain branching' (LCB) while in LLDPE the branching is called 'short chain branching' (SCB). SCB stems from the fact that ethylene is copolymerized with other α-olefins, resulting in the formation of branches with typically one (propene) to six (octene) carbon atoms. Accordingly, LLDPE exhibits molar mass and chemical composition distributions. The incorporation of short chain branches reduces the crystallinity of the polyolefin and, therefore, the density of the material.

When a Ziegler (multiple-site) catalyst is used, the incorporation of monomer is not uniform and an average chemical composition will not reflect the molar mass-chemical composition interdependence. To address this interdependence, the chemical composition as a function of molar mass and/or the molar mass as a function of chemical composition must be investigated. A schematic representation of the molecular population in LLDPE is presented in Fig. 1.1 [7].

The MMD curve in Fig. 1.1a shows that the comonomer content, given as the number of CH_3 endgroups per 1,000 carbons (CH_3/1,000C), decreases with increasing molar mass. This indicates that the shorter polymer chains are more branched than the longer polymer chains. The CCD curve in Fig. 1.1b shows bimodality in chemical composition. Similar to Fig. 1.1a, less branching at higher molar masses is found.

The development of single-site (metallocene) catalysts resulted in better defined microstructures with uniform comonomer incorporation and narrow MMDs [8, 9].

Different from ethylene polymerization, the homopolymerization of propylene produces polymers that may exhibit different microstructures in addition to the MMD. Propylene is a chiral monomer and can, thus, form meso and racemo diads along the polymer chain; see Fig. 1.2a. If the polymer chain consists only of meso diads then it is called isotactic polypropylene (iPP); if it consists only of racemo diads then it is called syndiotactic polypropylene (sPP); see Fig. 1.2b.

In addition to the above described types of microstructures, there may be undesired stereo errors in the growing polymer chain that result from missinsertions such as head-to-head or tail-to-tail instead of head-to-tail. Such missinsertions can be identified by NMR spectroscopy.

When propylene is copolymerized with other α-olefins, copolymers are formed that, in addition to MMD and microstructure variations, will exhibit a CCD. It has been shown that the insertion of ethylene units into a growing PP chain will disrupt the chain order and crystallinity will decrease. This is graphically presented in Fig. 1.3, where the decrease in crystallinity as a function of ethylene incorporation is shown [7].

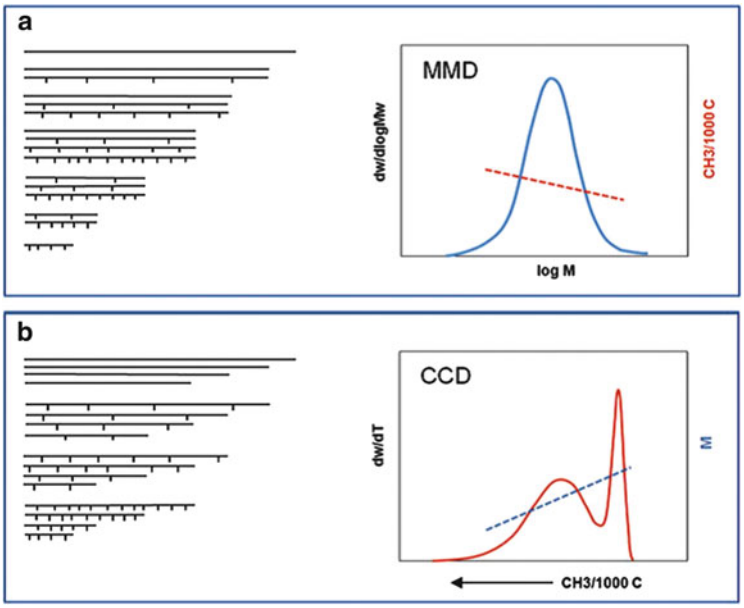

Fig. 1.1 LLDPE molecular population organized by size and the corresponding MMD curve (**a**) and organized by composition (branching) and the corresponding CCD curve (**b**) (reprinted from [7] with permission of Springer Science + Business Media)

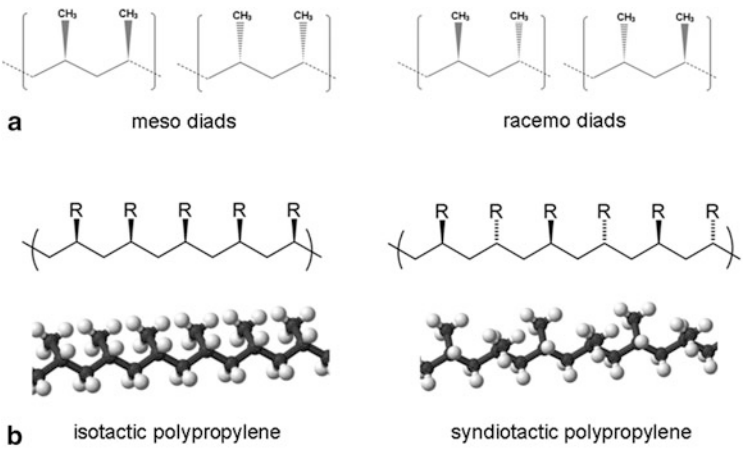

Fig. 1.2 Microstructure of polypropylene: meso and racemo diads (**a**), isotactic and syndiotactic polypropylene (**b**)

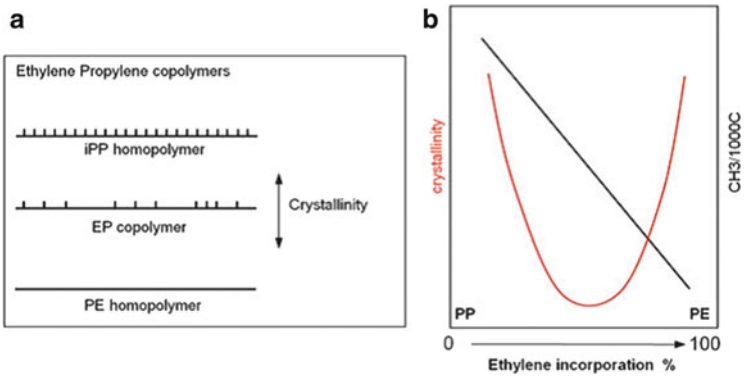

Fig. 1.3 Disruption of chain order by incorporation of ethylene units (**a**) and crystallinity as a function of copolymer composition for random EP copolymers (**b**) (reprinted from [7] with permission of Springer Science + Business Media)

1.2 Analytical Methods for Polyolefins

For the analysis of polyolefins, two types of molecular parameters are most important: MMD and CCD. High temperature SEC is a relatively rapid method for the determination of MMD. The detectors most commonly used for concentration detection are refractive index (RI) and infrared (IR) detectors. More advanced detectors like an online viscometer (Visco) or a light scattering (LS) detector help to determine chain dimensions and branching in terms of the hydrodynamic radius (R_h) or the radius of gyration (R_g). With specific IR detectors, chain branching as a function of MMD can be measured. As is known, SEC separates polymers according to the hydrodynamic size of the molecules in solution [10–12]. The size of polymer molecules in solution is influenced not only by the number of repeat units in the polymer chain but also by the molecular architecture and the chemical composition. Polymer molecules with identical hydrodynamic volumes will co-elute in SEC, although they may have different chemical compositions and different numbers of monomer units. Therefore, the knowledge of MMD obtained by SEC analysis will not be sufficient to define the molecular heterogeneity of complex polyolefins [13, 14].

Two methods are typically used to analyse the compositional heterogeneity of polyolefins: TREF, developed in the late 1970s by Wild, and crystallization analysis fractionation (CRYSTAF), developed by Monrabal in the early 1990s. Both methods fractionate the sample on the basis of crystallizability, which is a function of both chemical composition and molecular architecture. They can be used to fractionate semi-crystalline polyolefin copolymers and blends based on the crystallization of the macromolecules from a hot solution [15–19]. TREF and CRYSTAF are based on slow crystallization and, therefore, require significant periods of time.

Another feature of TREF and CRYSTAF is that only the crystallizing parts are fractionated while the non-crystallizing amorphous parts are not.

More recently, crystallization elution fractionation (CEF), as a refinement of the basic TREF technique, has been pioneered by Monrabal. CEF allows rapid analysis and good separation of a variety of polyolefins [20]. Another new technique based on turbidity fractionation analysis, solution crystallization analysis by laser light scattering (SCALLS), has been used for CCD analysis of polyolefins [21]. This technique yields similar results to CRYSTAF but in shorter periods of time, uses a comparatively low amount of solvent, and has a greater sensitivity in some cases. However, all these techniques are limited to crystallizable samples.

Differential scanning calorimetry (DSC) is a thermal analysis method suitable for studying the melting and crystallization behaviour; it is related to the chemical structure of the polymer chain (chemical composition). DSC has been used as an alternative tool for the qualitative analysis of CCD. ^{13}C-NMR spectroscopy is the method of choice for the analysis of polyolefin microstructure, based on the analysis of comonomer sequences and tactic units. Like all other bulk spectroscopic methods, it provides only the average chemical composition. It is difficult to determine the exact CCD due to the relatively low concentration of individual components in complex polyolefins; thus, a preparative fractionation is required as the first step.

Another well established spectroscopic method, FTIR spectroscopy, provides information regarding comonomer composition, polymer chain configuration, branching and crystallinity. A combined method of chromatography and IR spectroscopy may be employed to map the distribution of monomers in copolymer samples [20]. The coupling of high temperature SEC (HT-SEC) to multiple detectors allows detailed and fast molecular characterization. Several method combinations have been applied to determine the copolymer composition and comonomer distribution along the MMD. TREF combined with SEC and FTIR, SEC with TREF and CRYSTAF and SEC with triple detectors (TriSEC) have been reported to perform such type of analysis [22–26].

It is well established that fractionation and subsequent analysis of the separated fractions is an essential approach to study the heterogeneity in multicomponent systems. Preparative fractionation followed by subsequent analysis of the fractions by SEC and NMR or SEC-FTIR can provide a detailed picture of the chemical composition as a function of molar mass [27]. The selection of the analytical method does not depend only on factors such as accuracy, labour and time demands but also on the versatility and practicability of the approach. Preparative TREF fractionation followed by SEC-FTIR is capable of analysing even very heterogeneous samples with low branching in a rapid and satisfactory manner [28–30]. However, only the average chemical composition per molar mass fraction can be obtained by this approach; due to the heterogeneity of the chemical composition within each molar mass fraction, the CCD cannot be obtained. The main drawback of this approach is that preparative TREF involves time consuming operations such as separation, filtration and drying of the fractions.

CCD (the chain structure, polymer type and chain branching) and MMD determine the thermal properties (melting and crystallization) of semi-crystalline polymers. For a complex copolymer consisting of different chain structures, it is very important to study the relationship between the thermal behaviour and the chemical structure of individual components to optimize the processing conditions and to reduce the production cycle time. For such polymers, crystallization is an important factor, as it determines the final mechanical properties of the material. Various analytical approaches have been reported to correlate the molecular characteristics of polyolefins with their thermal and mechanical properties. The combination of preparative TREF (P-TREF) with standard DSC relates the chemical composition to the thermal properties of olefin copolymers [31]. However, even by this method combination, it is difficult to gain a full understanding of the relationship between the complex chain structure and the crystallization behaviour. An advancement in this field is the use of HyperDSC (high performance DSC) instead of standard DSC [32, 33]. HyperDSC has the ability to measure very small sample masses, while scanning at very high heating rates (up to 500 °C/min). The separation or reduction of reorganizational thermal processes (such as cold crystallization, recrystallization and decomposition that may occur during heating) is promoted by fast scanning rates in HyperDSC. The weak transitions (including weak glass transitions) that are difficult to determine by standard DSC can now be detected successfully by fast scanning DSC technology. This approach (SEC-HyperDSC) will be very useful for the investigation of the relationships between the molecular structure of the polymer chains and their thermal properties (the influence of the molar mass on the thermal properties of the materials).

Liquid chromatography (LC) is an efficient analytical technique for the fast separation of complex polyolefins according to chemical composition [34]. High temperature LC methods were developed recently. They are mainly based on selective precipitation or adsorption mechanisms on different stationary phases. The separated fractions are eluted by using a suitable solvent gradient, which results in the dissolution or desorption of the polymer chains from the stationary phase [35–37]. Recently, the use of a graphitic stationary phase (Hypercarb) for the separation of PP according to tacticity was reported [38]. Using a solvent gradient from 1-decanol to TCB, PP as well as PE and ethylene–propylene copolymers were separated. The fast and efficient separation of polyolefins and olefin copolymers with respect to chemical composition in a short time can only be achieved by the above method [39–44]. A new technique, high temperature thermal gradient interaction chromatography (HT-TGIC), has been reported for the separation of ethylene-1-octene copolymers with a wide range of comonomer contents, based on decreasing the interaction of the polymer chains with the Hypercarb stationary phase by increasing temperature in an isocratic solvent [45]. Among the several analytical techniques reported for the characterization of polyolefins, most recently, high temperature two-dimensional liquid chromatography (HT-2D-LC) has been presented for the 2D mapping of the molecular heterogeneity of polyolefins. In 2D-LC, the chromatographic separation by HT-HPLC is coupled to HT-SEC in

order to obtain a complete separation in terms of both CCD and MMD. This technique enables the generation of 2D characterization data for virtually any polyolefin over a wide compositional range regardless of crystallinity [46–49].

References

1. Kaminsky W (2008) Macromol Chem Phys 209:459
2. Kaminsky W, Arndt M (1997) Polymer synthesis/polymer catalysis. Springer, Berlin, p 143
3. Seymour RB, Cheng T (eds) (1986) History of polyolefins. D. Reidel, Dordrecht, Holland
4. Scheirs J, Kaminsky W (2000) Metallocene-based polyolefins: preparation, properties and technology. Wiley, Hoboken, NJ
5. Mori S, Barth HG (1999) Size exclusion chromatography. Springer, Berlin
6. Striegel AM, Yau WW, Kirkland JJ, Bly DD (2009) Modern size-exclusion liquid chromatography. Wiley, Hoboken, NJ
7. Monrabal B (2013) Adv Polym Sci 257:203
8. Sinn H, Kaminsky W (1980) Adv Organomet Chem 18:99
9. Kaminsky W (2004) J Polym Sci A Polym Chem 42:3911
10. Janca J (1984) Size exclusion liquid chromatography. Marcel Dekker, New York, NY
11. Yau WW, Kirkland JJ, Bly DD (1979) Modern size exclusion chromatography. Wiley, New York, NY
12. Tribe K, Saunders G, Meißner R (2006) Macromol Symp 236:228
13. Piel C, Jannesson E, Qvist A (2009) Macromol Symp 282:41
14. Liu MX, Dwyer JL (1996) Appl Spectrosc 50:349
15. Harding GH, van Reenen AJ (2006) Macromol Chem Phys 207:1680
16. Soares JBP, Hamielec AE (1995) Polymer 36:1639
17. Soares JBP, Anatawarskul S, Adams PMW (2005) Adv Polym Sci 182:1
18. Kissin YV, Fruitwala HA (2007) J Appl Polym Sci 106:3872
19. Pasch H, Brüll R, Wahner U, Monrabal B (2000) Macromol Mater Eng 279:46
20. Monrabal B, Sancho-Tello J, Mayo N, Romero L (2007) Macromol Symp 257:71
21. van Reenen AJ, Brand M, Rohwer E, Walters P (2009) Macromol Symp 282:25
22. Alghyamah AA, Soares JBP (2009) Macromol Symp 285:8
23. Wang W, Kharchenko S, Migler K, Zhu S (2004) Polymer 45:6495
24. Yau WW, Gillespie D (2001) Polymer 42:8947
25. Gabriel C, Lilge D (2001) Polymer 42:297
26. Starck P, Lehmus P, Seppälä JV (1990) Polym Eng Sci 39:1444
27. Hiller W, Pasch H, Macko T, Hofmann M, Ganz J, Spraul M, Braumann U, Streck R, Mason J, van Damme F (2006) J Magn Reson 183:290
28. de Goede E, Mallon P, Pasch H (2010) Macromol Mater Eng 295:366
29. Albrecht A, Heinz LC, Lilge D, Pasch H (2007) Macromol Symp 257:46
30. Macko T, Brüll R, Zhu Y, Wang Y (2010) J Sep Sci 33:3446
31. Mathot VBF (1994) The crystallization and melting region. In: Mathot VBF (ed) Calorimetry and thermal analysis of polymers. Hanser Publishers, Munich, Chapter 9
32. Krumme A, Basiura M, Pijpers T, Poel GV, Heinz LC, Brüll R, Mathot VBF (2011) Mater Sci Eng 17:260
33. Poel GV, Mathot VBF (2007) Thermochim Acta 461:107
34. Pasch H, Trathnigg B (2013) Multidimensional HPLC of polymers. Springer, Berlin
35. Heinz LC, Pasch H (2005) Polymer 46:12040
36. Macko T, Pasch H, Brüll R (2006) J Chromatogr A 1115:81
37. Macko T, Denayer JF, Pasch H, Baron GV (2003) J Sep Sci 26:1569
38. Macko T, Pasch H (2009) Macromolecules 42:6063
39. Pereira LJ (2008) J Liq Chromatogr Rel Tech 31:1687

40. Macko T, Brüll R, Alamo G, Thomann Y, Grumel V (2009) Polymer 50:5443
41. Macko T, Cutillo F, Busico V, Brüll R (2010) Macromol Symp 298:182
42. Dolle V, Albrecht A, Brüll R, Macko T (2011) Macromol Chem Phys 212:959
43. Chitta R, Macko T, Brüll R, Doremaele GV, Heinz LC (2011) J Polym Sci A Polym Chem 49:1840
44. Macko T, Brüll R, Alamo RG, Stadler FJ, Losio S (2011) Anal Bioanal Chem 399:1547
45. Cong R, deGroot W, Parrott A, Yau W, Hazlitt L, Brown R, Miller M, Zhou Z (2011) Macromolecules 44:3062
46. Ginzburg A, Macko T, Dolle V, Brüll R (2010) J Chromatogr A 1217:6867
47. Roy A, Miller MD, Meunier DM, de Groot AW, Winniford WL, van Damme FA, Pell RJ, Lyons JW (2010) Macromolecules 43:3710
48. Ginzburg A, Macko T, Dolle V, Brüll R (2011) Eur Polym J 47:319
49. Chitta R, Ginzburg A, Doremaele G, Macko T, Brüll R (2011) Polymer 52:5953

Crystallization-Based Fractionation Techniques

2

The vast majority of commercial polyolefins are semi-crystalline materials. Depending on the chemical composition and tacticity, their melting temperatures range from ambient to temperatures exceeding 160 °C. Polyolefins form various crystalline structures that can be investigated with microscopic, spectroscopic and scattering techniques.

When a semi-crystalline polyolefin is dissolved in a solvent at high temperature (usually above the melting temperature), followed by a continuous or stepwise decrease of the solution temperature, the polyolefin starts to form crystals that will precipitate out of the solution. The crystallization temperature, the shape and the amount of crystals depend on the molecular structure of the polyolefin, mainly its chemical composition, its tacticity and the degree of branching. Highly crystalline materials will crystallize out of the solution at higher temperatures than materials with lower crystallinity.

Flory–Huggins statistical thermodynamic treatment accounts for melting point depression due to the presence of a diluent in a crystallizing system. The diluent can be a solvent or a comonomer. In either case, the crystallization temperature decreases with increasing diluent concentration. Therefore, for copolymers that do not have long chain branches, the separation by crystallizability can be regarded as a separation according to chemical composition. A precondition is that the concentration of the diluent is low and it does not enter into the crystal lattice of the crystallizing polymer. For copolymers where the non-crystallizing comonomer is the diluent, a linear dependence of the melting or crystallization temperature on the amount of comonomer incorporated is observed. Such linear dependencies have been seen in temperature rising elution fractionation (TREF), differential scanning calorimetry (DSC) and crystallization analysis fractionation (CRYSTAF) experiments [1–4].

The potential of crystallization behaviour of semi-crystalline polymers as an analytical tool was recognized by Desreux and Spiegels [5] in the early history of polyolefin fractionation. TREF, CRYSTAF and crystallization elution fractionation (CEF) are the main techniques that are used today in this category. The differences

H. Pasch, M.I. Malik, *Advanced Separation Techniques for Polyolefins*, Springer Laboratory, DOI 10.1007/978-3-319-08632-3_2

in crystallization behaviours of different polymers are the basis of fractionation in these techniques expressed by differences in crystallizability as a function of temperature. A discussion of the various experimental approaches to obtain final results will be given in the following chapters. Long analysis times and the limitation of the techniques to only the crystallizable part of the sample are the major disadvantages of the techniques in this category. The amorphous part cannot be fractionated and is obtained as a bulk fraction. Historically, TREF analysis required around 100 h to be completed. New developments in the field have reduced TREF analysis time to 3–4 h. CRYSTAF analysis can be accomplished in 100 min while the latest development in crystallization-based techniques—CEF—allows analysis to be completed in less than 30 min.

2.1 Temperature Rising Elution Fractionation

There are numerous excellent reviews on TREF that have been published over the years. These reviews demonstrate very clearly that, to date, TREF is the most important fractionation technique for semi-crystalline polyolefins and is a standard method in the polyolefin industry. Most recent and comprehensive reviews have been presented by Soares and Hamielec [6, 7], Monrabal [8, 9] and Pasch, Malik and Macko [10].

The principles of polymer fractionation by solubility or crystallization such as TREF are based on the Flory–Huggins statistical thermodynamic theory that accounts for melting point depression due to the presence of a diluent and it is expressed by Eq. (2.1) [11–14]:

$$1/T_{\mathrm{m}} - 1/T_{\mathrm{m}}^{0} = -(R/\Delta H_{\mathrm{u}}) \ln N_{\mathrm{A}} \tag{2.1}$$

where $T_{\mathrm{m}}{}^{0}$ is the melting temperature of the pure polymer, T_{m} is the equilibrium melting temperature of the 'diluted' polymer, ΔH_{u} is the heat of fusion per polymer repeat unit, and N_{A} is the mole fraction of the diluent.

Fractionation in TREF resembles a liquid chromatographic separation, comprised of a column, a mobile phase, a set of detectors and a fraction collector. TREF can be performed on analytical and preparative scale, termed A-TREF and P-TREF, respectively. In all cases, a TREF experiment involves the following steps: (1) dissolution of the sample in a suitable solvent at high temperature, (2) crystallization of the polymer on a solid support by decreasing the temperature, (3) dissolution and elution of polymer fractions with different crystallizabilities by increasing the temperature. A schematic presentation of the TREF process is given in Fig. 2.1.

Typical solvents to be used in TREF are high boiling point solvents such as xylene, 1,2,4-trichlorobenzene (TCB), o-dichlorobenzene (ODCB), chloronaphthalene and others. Typical dissolution temperatures are between 120 °C and 160 °C and solution concentrations are around 0.5 wt%. Once the polymer is dissolved, the solution is loaded onto the TREF column which is filled with an inert support, e.g. sea sand, glass beads or stainless steel shots.

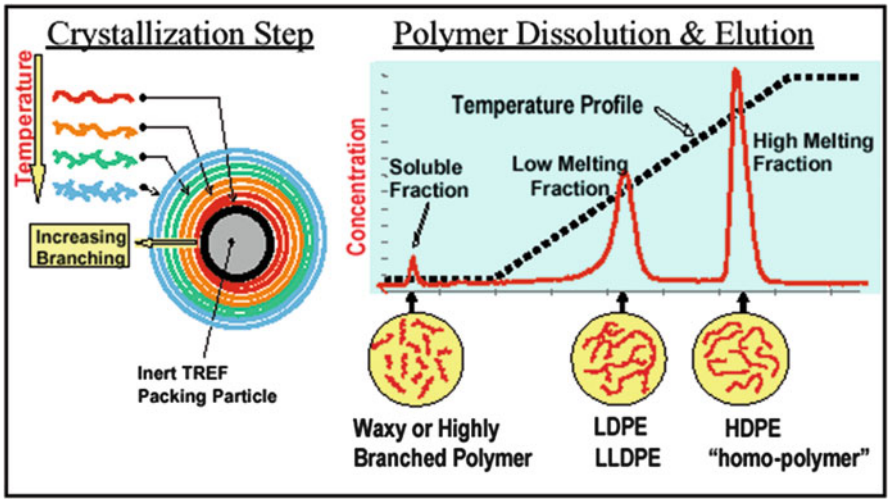

Fig. 2.1 Schematic presentation of the TREF process including the crystallization and the dissolution/elution steps

Alternatively, the polymer solution can be mixed with the support in a beaker or flask. In the next step, the temperature of the column (beaker, flask) is slowly decreased from high to ambient in order to crystallize polymer fractions out of the solution. At the highest temperature, the highly crystalline fractions will precipitate on the solid support followed by fractions of lower crystallinity. Accordingly, onion-type layers of polymer will be formed that have decreasing crystallinities from core to surface, as shown in Fig. 2.1. Non-crystallizing polymer fractions will remain in the solution. The type of crystalline layers will be influenced by the crystallization rate; in order to produce uniform layers crystallization rates as low as 0.1 °C/min are used [10–14].

As has been pointed out earlier, crystallizability is (mainly) a function of chemical composition and molecular topology (branching). Accordingly, linear low density polyethylene (LLDPE) which exhibits a chemical composition distribution crystallizes with regard to the copolymer composition. Low density polyethylene (LDPE) which is a homopolymer but exhibits a branching distribution crystallizes with regard to the number and length of the branches [15].

After the crystallization step is completed, the TREF column contains a slurry of the solid support decorated with polymer sample layers. If crystallization was conducted in a beaker/flask, the slurry is now filled into the TREF column. The next step is the dissolution/elution step. A constant flow of solvent (mobile phase) produced by a standard HPLC pump is applied to the column and all soluble material is eluted. Typical flow rates are 0.5–2 mL/min. At ambient temperature, the 'soluble fraction' consisting of (amorphous) material that did not crystallize elutes; see Fig. 2.1. By slowly increasing the temperature of the column and the mobile phase (0.5–5 °C/min), the crystallized outer layers start to dissolve and elute

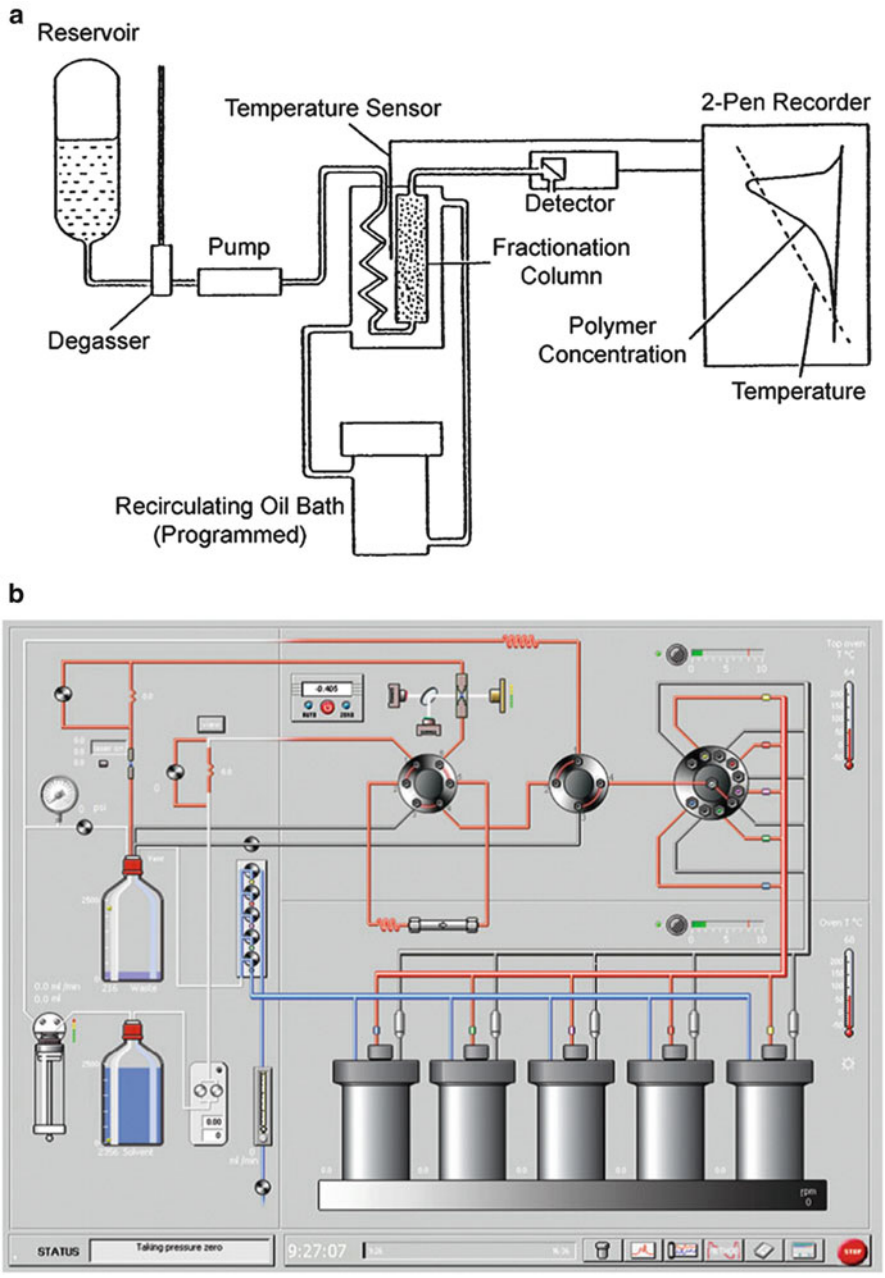

Fig. 2.2 Schematic diagram of analytical TREF (**a**) and fully automated Polymer Char instrument (**b**) (reprinted from [16] and [9] with permission of Springer Science + Business Media)

from the column. Accordingly, elution takes place with increasing temperature in the direction of increasing crystallizability. The latest eluting fractions have the highest crystallizability (lowest comonomer content, lowest degree of branching). The elution process is monitored by standard concentration detectors such as infrared (IR) and evaporative light scattering detectors (ELSD); however, more detailed information can be obtained when additional molar mass sensitive detectors, such as a viscometer (Visco) or light scattering (LS) detector, are used [10–14].

Over the years, different (mainly home-built) instruments have been used; for example see the schematic diagram in Fig. 2.2a [16] or instrument in [17]. Today, the most common instrument is the fully automated TREF instrument produced by Polymer Char, Valencia, Spain; see the schematic diagram in Fig. 2.2b.

Typical TREF curves for olefin block copolymers showing the influence of the α-olefin content in the hard block on the crystallizability are presented in Fig. 2.3. Kuhlman and Klosin investigated the block composition of PE multiblock copolymers as a function of different catalyst systems [18]. The block composition was tuned by a combination of hard and soft catalysts and diethylzinc (DEZ) as chain shuttling agent. With different catalyst compositions, the α-olefin content increased and the crystallization curves moved to lower temperatures from run A to run G. The amorphous part of the samples could not be resolved and eluted at the lowest temperature as a narrow peak.

As can be seen in Fig. 2.3, the TREF experiment produces a plot of elution temperature vs. concentration (wt%) of eluting fraction. For linear copolymers such as LLDPE, the elution temperature is directly proportional to copolymer composition. This has been shown by Boisson and co-workers for LLDPEs containing different comonomers [19]. As is shown in Fig. 2.4, for ethylene copolymers with propene, 1-hexene, 1-octene and 1-octadecene as comonomers, linear calibration curves were obtained. At the same molar composition the TREF dissolution temperature decreased with increasing branch length. Octene and hexene copolymers produced identical calibration curves.

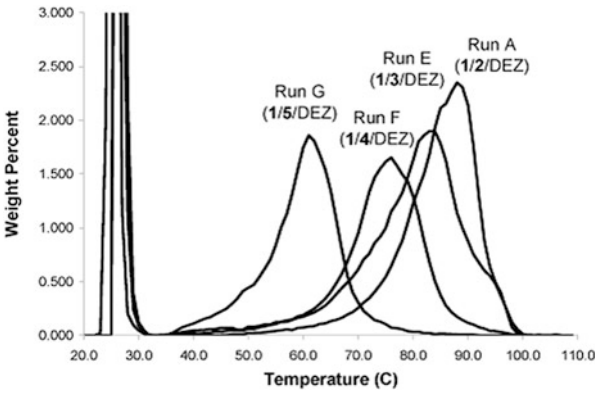

Fig. 2.3 The influence of α-olefin content in the hard block on polymer solubility as shown by TREF separation; sample code indicates catalyst composition (reprinted from [18] with permission of the American Chemical Society)

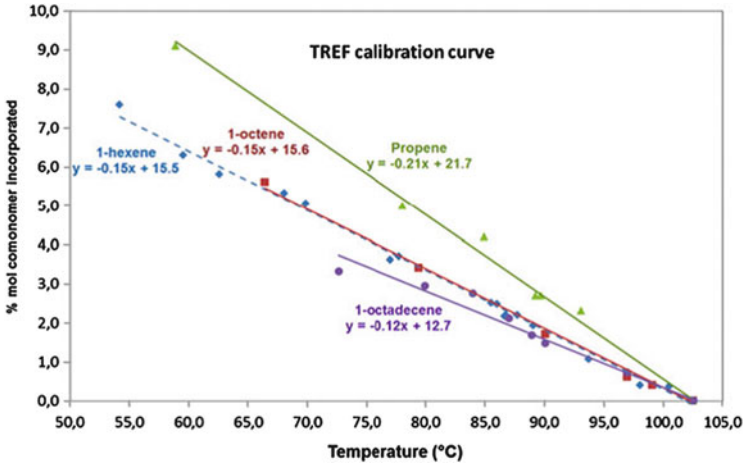

Fig. 2.4 TREF calibration curves for different ethylene copolymers (reprinted from [19] with permission of Wiley-VCH)

The elution in TREF has been shown to be independent of molar mass above 10 kg/mol [1, 2]. As an alternative to the calibration of TREF with well characterized polymer standards, a composition sensitive detector can be used, as has been demonstrated by Monrabal [20, 21]. Using a state-of-the-art IR detector with two simultaneous signals, one signal is used for total concentration while the other signal measures the methyl absorption, which is indicative for comonomer content. The ratio of the two signals gives the CH_3/1,000C value for a typical LLDPE; see Fig. 2.5a. Assuming that the sample has no long chain branches, the value corresponds directly to the copolymer composition. It is remarkable that the CH_3/1,000C calibration curve shows a linear dependence on elution temperature. The composition detector is particularly important in cases where the crystallization behaviour is influenced by copolymer composition and other parameters such as tacticity and branching. A good example for such a situation is the fractionation of high impact polypropylene copolymers (IPCs) where the IR detector reading provides copolymer composition irrespective of polypropylene (PP) tacticity; see Fig. 2.5b [9]. Other detector options are the online viscometer and the multiangle laser light scattering (MALLS) detectors that provide direct molar mass information.

As has been pointed out earlier, TREF is one of the workhorses of the polyolefin industry for characterization of polyolefins with respect to crystallizability. A typical procedure is to fractionate a complex polyolefin by TREF, isolate the fractions and subject them to a range of analyses including size exclusion chromatography (SEC) for molar mass and FTIR/NMR for chemical composition. Other approaches include the analysis of the crystalline structure by X-ray diffraction (XRD) and the thermal properties by differential scanning calorimetry (DSC).

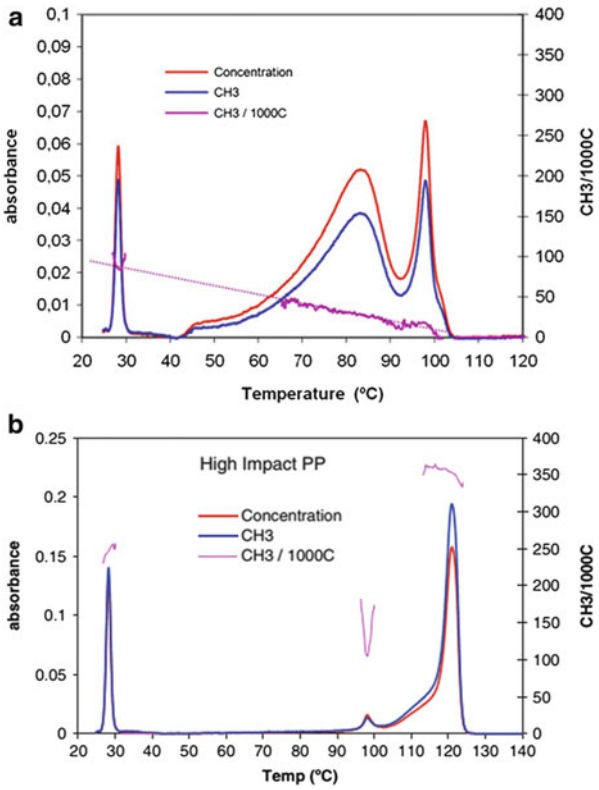

Fig. 2.5 TREF analysis of a LLDPE with an IR detector for composition (**a**) and TREF analysis of an IPC using the same detector (**b**) (reprinted from [9] with permission of Springer Science + Business Media)

A few representative applications of TREF are reviewed as follows. The slow crystallization of PE in extended mode occurs only below molar masses of 2,000 g/mol, as shown by the analysis of TREF fractions using Raman spectroscopy in longitudinal acoustic mode (LAM) and DSC by Tomba et al. [22]. Chain folding takes place at higher molar masses. For a narrow molar mass range, independent crystallization was observed, in contrast to broad molar mass ranges where co-crystallization occurs in the case of polyolefin blends. These results indicated that crystallizable sequences really existed, and could be attributed to chain folding and co-crystallization phenomena. A perfect tool for the direct examination of the distribution of crystallizable sequences length was the Raman technique in LAM mode. DSC was limited only to samples where narrow distributions of crystallizable sequences were expected.

Hassan et al. [23, 24] correlated the preparation procedure of the Ziegler–Natta catalyst, the co-catalyst type, catalyst pretreatment and polymerization conditions with the tacticity of resulting PP by using SEC, NMR and TREF. Zhang and co-workers [25] studied the fractionation of random copolymers of propylene and ethylene by P-TREF, and carried out subsequent analysis of P-TREF fractions by SEC, ^{13}C NMR, DSC and wide-angle X-ray diffraction (WAXD) analysis. Copolymer molecules with varying compositions and molar masses were found in TREF

fractions. Random copolymers of propylene and 1-butene were synthesized by Zhang with Ziegler–Natta catalysts and the molecular microstructure and crystallization behaviour were correlated [26]. Relatively uniform microstructures with long isotactic polypropylene (iPP) sequences and isolated 1-butene comonomer units were found by analysis of TREF fractions using CRYSTAF, SEC and ^{13}C NMR. The increase in 1-butene content decreased the melting temperatures of the copolymers; therefore, higher temperature fractions contained less 1-butene content. Two LLDPE samples (comonomers 1-butene and 1-hexene) with similar densities were fractionated by van Reenen and co-workers. The melt flow index (MFI) values and comonomer contents were measured and the TREF fractions were analysed by high resolution solution and solid state NMR [27]. The type of crystallinity differed significantly in spite of similar degrees of crystallinity for both polymers. Insight into the detailed microstructure as provided by the hyphenation of TREF with NMR was not accessible otherwise. The same group reported on the fractionation of propylene–ethylene random copolymers by P-TREF. The fractions were subsequently analysed by CRYSTAF, DSC, ^{13}C NMR, HT-SEC and WAXD [28]. Their conclusion was that the incorporation of comonomers inhibited crystallization and the increase in ethylene content decreased the crystallization and melting points of the copolymers.

Suzuki et al. investigated the effect of the tacticity distribution on the thermo-oxidative degradation behaviour of PP by using TREF, NMR and thermographic analysis (TGA) [29]. It has been shown that atactic PP is more stable due to the hindered abstraction reaction of tertiary hydrogen. The abstraction of tertiary hydrogen was the rate-determining step in PP degradation and its dependence on tacticity distribution was correlated to the rate of degradation of PP. Therefore, the presence of more meso sequences in the chain will enhance the rate of thermo-oxidative degradation. Gupta et al. developed structure–property relationships for LLDPE by varying the length of short chains and keeping similar overall branching contents [30]. Despite similar TREF profiles, the mechanical properties of the LLDPE films varied significantly which was attributed to the type of the comonomer. Shan and Hazlitt developed a 'block index methodology' by analysing P-TREF fractions by A-TREF [31]. The comonomer content of olefin block copolymer fractions was higher than that of fractions of random copolymers eluting at the same temperature. The block index methodology of Shan and Hazlitt revealed the degree of intrachain comonomer distribution of olefin copolymers.

A comparison of HT-HPLC, CRYSTAF and TREF results for the chemical composition distribution (CCD) of ethylene–acrylate (EA) copolymers was presented by Pasch and co-workers [32]. A combinatory investigation of NMR, TREF, DSC and scanning electron microscopy (SEM) techniques was employed by Wang and co-workers for studying the compositional heterogeneity, phase structure and melting behaviour of PP prepared by two spherical $TiCl_4/MgCl_2$ catalysts [33]. PP homopolymers, PE homopolymers and ethylene-co-propylene copolymers with different ethylene segment lengths were the main components of the reactor alloys prepared by complex ethylene–propylene (EP) copolymerization. A sample prepared by a different procedure was slightly different; it contained PP

homopolymer, EP segmented polymer and EP random copolymer. The mechanical properties of the different materials were correlated with the molecular architectures and phase structures of the products. Amer and van Reenen reported on the TREF fractionation of iPP to obtain fractions with different molar masses but similar tacticities [34]. The DSC results of the fractions indicated that the configuration (tacticity) and the molar mass of the PP strongly affected the crystallization behaviour.

Cross-fractionation techniques such as SEC-TREF or TREF-SEC were used for the deconvolution of bivariate MMD/CCD distributions of polyolefin copolymers. The results were used to identify the number of active catalyst sites and the relation of the type of active sites with the microstructure of polyolefins produced with multiple-site catalysts [35]. Model ethylene-1-butene and ethylene-1-octene copolymers were used to validate the approach. The correlation of molecular structure and mechanical properties of ethylene-1-hexene copolymer film grade resins produced by a metallocene catalyst by varying the molar mass and branching distribution was studied by Alamo and co-workers [36]. Molar mass fractionation was achieved by solvent/non-solvent techniques, while fractionation with respect to 1-hexene content was obtained by P-TREF. The hyphenation of TREF with SEC-FTIR offered a simple alternative to conventional and time-consuming methods for characterizing the compositional heterogeneity of IPCs [37].

The idea to combine different polyolefin fractionation methods to address the multiple molecular distributions was developed by Nakano and Goto; they combined TREF and SEC to address the bivariate distribution in chemical composition and molar mass [38]. The resulting instrument was the first fully automated instrument that combined the chemical composition fractionation by TREF and the subsequent molar mass analysis of the TREF fractions by SEC.

When combining SEC and TREF there are, in principle, two options: SEC-TREF or TREF-SEC. The SEC-TREF approach was followed by Aust et al. [39] to analyse a medium density PE, while Faldi and Soares used TREF-SEC for the fractionation of a LLDPE [40]. Shan et al. developed a custom-built TREF-SEC instrument [41] which was used later by Gillespie et al. for SEC-TREF experiments [42]. Yau demonstrated the potential of a 3D-SEC-TREF apparatus which was used for the investigation of polyolefin microstructures [43]. A refractive index (RI) detector, a LS detector and a dual wavelength IR detector were used as online detectors, as shown in Fig. 2.6.

Monrabal and co-workers [44] pioneered the development of a user-friendly automated cross-fractionation apparatus (TREF-SEC) to fully characterize polyolefins with bivariate distributions; see Fig. 2.7. Short chain branching distributions have been analysed as a function of molar mass. The instrument was based on the design of a TREF 300 unit. The concentration detector employed is a dual band IR4 infrared detector. Further online detectors, such as methyl-sensitive IR sensors, Visco and LS detectors, can be added to enhance the amount of information.

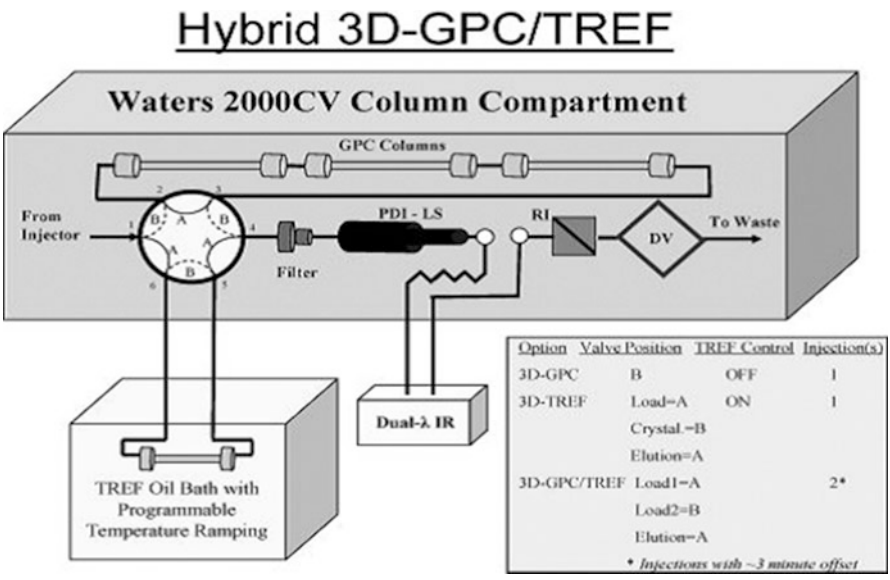

Fig. 2.6 Configuration of a hybrid 3D-SEC-TREF system (reprinted from [43] with permission of Wiley-VCH)

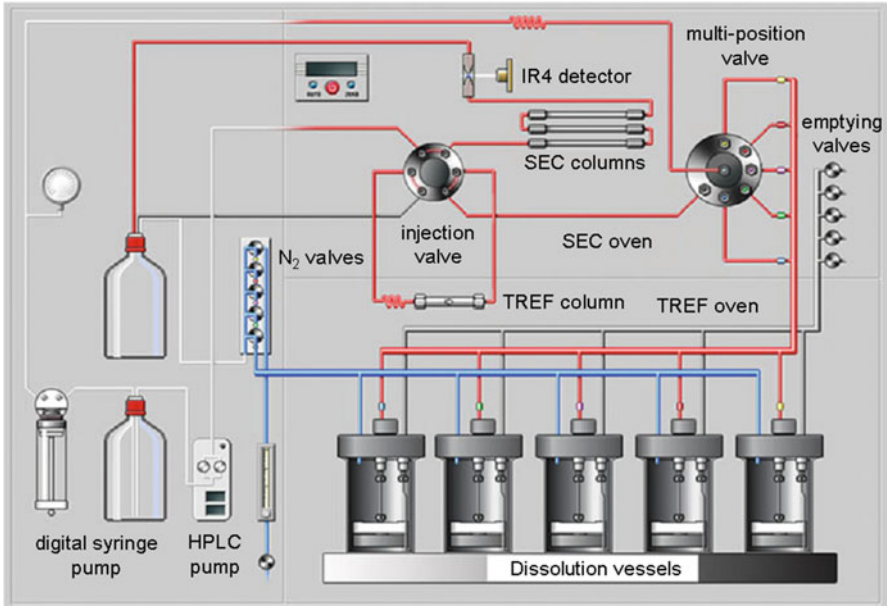

Fig. 2.7 Schematic diagram of an automated cross-fractionation instrument. Injection valve shown in 'load' position A; 'inject' position marked as B (reprinted from [44] with permission of Wiley-VCH)

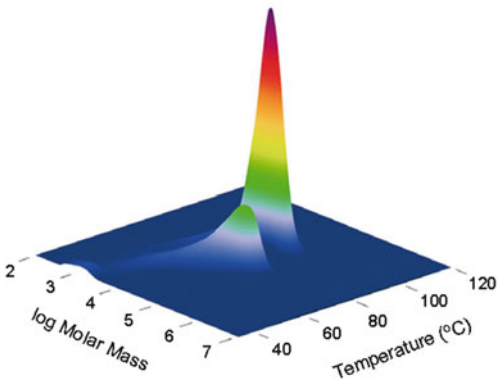

Fig. 2.8 MMD × CCD surface plot of a two-component PE blend (reprinted from [45] with permission of Polymer Char, Valencia, Spain)

In the TREF fractionation part, there are five stainless steel vessels equipped with internal filters and magnetic stir bars for dissolution and the subsequent sequential analysis. Dissolution of the sample is achieved by heating the TREF oven to 150 °C. The injection valve is moved to the 'load' position in order to load typically 1–3 mg of the sample into the TREF column through an internal filter. The injection valve is kept at the load position in the next step when crystallization of the sample is carried out. After complete crystallization and segregation of the polymer in the TREF column, a discontinuous elution at increasing temperature steps is carried out. A predefined dissolution time at each temperature is given for different fractions. The injection valve is then switched to the 'inject' position to elute the dissolved polymer fractions from the TREF column into the SEC column set. The flow through the TREF column is stopped again after elution of the given fraction by switching the injection valve to the 'load' position. The oven temperature is increased for dissolution of the next fraction. This process allows molar mass analysis of the TREF fractions that are collected with respect to increasing crystallinity. The final chromatogram is recorded by an IR4 infrared detector and the oven temperature signals are plotted against the raw IR signals. As a result of the cross-fractionation process, a 3D plot can be obtained, where the TREF elution temperature is plotted against the molar mass (from SEC) and the IR detector intensity (as a measure of concentration); see Fig. 2.8.

2.1.1 Fractionation of Ethylene–Octene Copolymers [46]

Ethylene–octene (EO) copolymers are one of the most important commercial polyolefin materials. EO copolymers constitute a significant share of the total market of LLDPE. With a total polyolefin market of more than 120 million tons, LLDPE has a market share of more than 17 %, with an increasing tendency to replace LDPE [47].

The higher tensile strength, superior impact and puncture resistance of LLDPE makes it more popular than LDPE. Thinner films of LLDPE can be produced

without compromising on strength, thus saving material and reducing costs. The toughness of LLDPE opens new horizons of application areas. The major share in global applications of LLDPE is film applications that include food and non-food packaging, shrink/stretch film and non-packaging applications. Metallocene or single-site catalysts revolutionized LLDPE research. New resins were synthesized that allow faster and more stable operations along with improved downgauging of films. Processing of LLDPE grades is also facilitated by improved and more effective methods. Today, major application areas of LLDPE are agricultural greenhouse films, multi-layer cast stretch films, lamination packaging films and medium to heavy duty bags.

2.1.1.1 Aim

An important step in the development of new or improved materials is the correlation of molecular structure and material properties. For molecular structure elucidation of complex polyolefins, TREF has been shown to be an invaluable tool. For LLDPE, TREF fractionation produces copolymer fractions that differ in comonomer content. These fractions are then analysed by spectroscopic methods (chemical composition, microstructure), SEC (molar mass) and calorimetric methods (melting and crystallization behaviour) for the development of structure–property correlations. A very useful approach is the online combination of TREF and FTIR spectroscopy, which will be discussed in the present application.

2.1.1.2 Materials

- *Polymers*. Ethylene-1-octene copolymers: sample 1 is a commercial random copolymer, sample 2 is a laboratory product. PE homopolymer (SRM1484a from the National Institute of Standards and Technology, Gaithersburg, USA; M_w 119.6 kg/mol). Eicosane

2.1.1.3 Equipment

- *TREF system*. CRYSTAF-TREF 200+ (Polymer Char, Valencia, Spain).
- *Detector*. FTIR flow cell (Polymer Laboratories, Church Stretton, UK), 1 mm optical path length, 70 μL volume, CaF_2 windows. The cell was placed in a TENSOR 27 FTIR spectrometer (Bruker, Rheinstetten, Germany).
- *Solvent*. TCB stabilized with 2,6-di-*tert*-butyl-4-methylphenol (BHT).
- *TREF column temperature*. Temperature gradient between 140 °C and 25 °C.
- *TREF sample concentration*. 40–150 mg in 20 mL TCB per reactor vessel.

2.1.1.4 Preparatory Investigations

One of the challenges that TREF presents is to extract quantitative compositional information on the copolymers from the TREF elution profile. The raw data are presented as a plot of TREF elution temperature vs. eluate concentration. The correlation between the TREF elution temperature and the copolymer composition (wt% comonomer) can be obtained in different ways. Typically, a set of well defined copolymers with narrow CCDs and known compositions (from NMR) is measured by TREF and the peak maximum elution temperature for each sample is determined. This peak maximum elution temperature is then plotted against the wt

% comonomer to give a suitable calibration curve. Quite frequently, copolymer composition is expressed as the number of methyl groups per 1,000 carbons (CH_3/1,000C).

A much more feasible approach is the 'real time' measurement of the copolymer composition using an online FTIR detector. In this case, the analysis relies on the measurement of the absorption bands of the backbone methylene groups (at 2,855 cm^{-1} and 2,926 cm^{-1}) corresponding to the total concentration and the methyl groups (at 2,874 cm^{-1} and 2,957 cm^{-1}) corresponding to the concentration of the comonomer [48, 49]. As the intensities of the IR absorption bands do not directly correspond to concentration, a calibration of the FTIR data must be conducted. In the present case, blends of a linear PE and a low molar mass hydrocarbon (e.g. eicosane) as well as well defined single-site catalyst resins were used. It is known that for high molar mass linear PE the methyl chain ends contribute little to the visible complexity of the spectrum. Thus, the linear PE provided the total polymer concentration (CH_2) while the endgroups of the hydrocarbon provided the methyl group concentration (CH_3). Figure 2.9 shows expanded IR spectra of the linear PE and the hydrocarbon with corresponding peak deconvolutions to determine the polymer concentration and the methyl content.

Based on the analysis of the corresponding absorption bands, the polymer concentration ([C]) and the methyl content ([CH_3]) can be monitored as a function of the elution temperature. From these concentrations, the branch frequency (BF) can be calculated using Eq. (2.2).

$$\mathrm{BF} = (14,000 \times [\mathrm{CH_3}])/(15\,[\mathrm{C}] - 14n\,[\mathrm{CH_3}]) \tag{2.2}$$

n: depends on monomer, for octene $n = 5$

The BF is a direct measure for the LLDPE copolymer composition.

2.1.1.5 Measurement and Evaluation

It is known that both cooling and heating rates influence the TREF results. These parameters must, therefore, be selected very carefully. For the present LLDPE

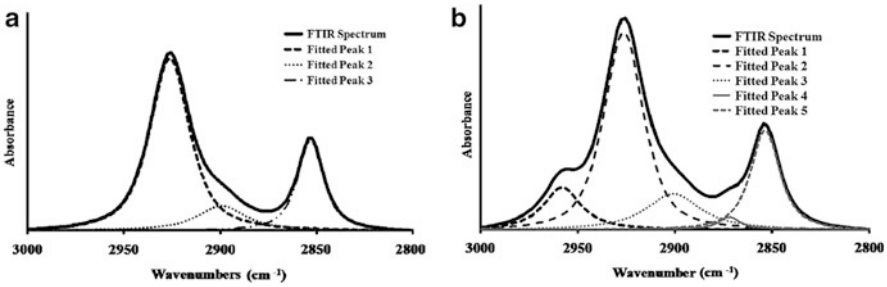

Fig. 2.9 Expanded IR spectra of linear PE (**a**) and eicosane (**b**) with peak deconvolutions for the methylene and methyl absorption bands, the shoulder at 2,900 cm^{-1} is a CH_2 combination absorption (reprinted from [46] with permission of Wiley-VCH)

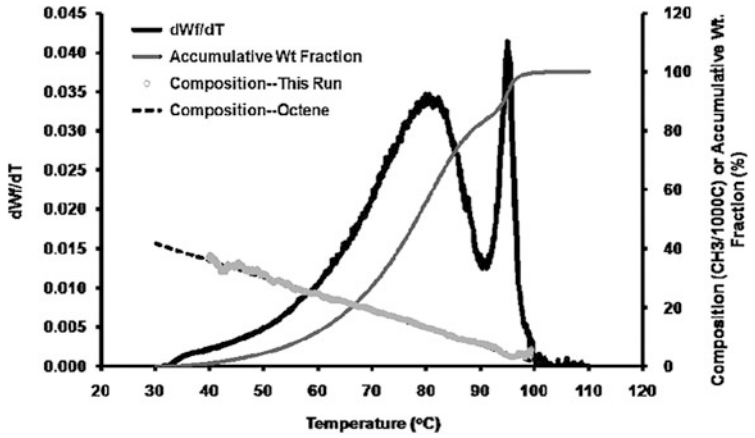

Fig. 2.10 TREF–FTIR profile of a random EO copolymer (reprinted from [46] with permission of Wiley-VCH)

samples, a cooling rate of 0.20 °C/min was used; the heating rate was 0.25 °C/min. For the elution step, a flow rate of 0.75 mL/min was used.

The TREF-FTIR curve of a random EO copolymer is presented in Fig. 2.10. 'dWf/dT' is the differential mass per temperature increment; the accumulative weight fraction is calculated based on the mass profile. The comonomer content is expressed as CH_3/1,000C.

Figure 2.10 shows a typical TREF profile with a component that elutes at high temperature, producing a sharp elution peak and a range of components that elute in a broad peak between 30 °C and 90 °C. A different TREF profile is obtained for a blocky EO copolymer produced by chain shuttling technology, see Fig. 2.11 [50]. This sample shows no elution peak at high temperature but a broad elution peak between 30 °C and 90 °C. Different from the random sample, the olefin block copolymer exhibits a narrow elution peak at 25 °C.

The TREF curve of the random EO copolymer is quite representative for a LLDPE. The online FTIR detection shows that the octene content of the copolymer decreases with increasing TREF elution temperature. The highest eluting fraction does not contain octene and is, therefore, PE. The elution temperature of 96 °C is in agreement with linear (high density) PE. The copolymer components eluting between 30 °C and 90 °C are due to EO copolymer molecules with different EO contents. The lowest eluting fractions have an octene content of about 40 CH_3/1,000C. It is interesting to note that the TREF elution temperature is linearly dependent on the octene content of the copolymer. This makes it very easy to produce a calibration curve that stretches towards higher octene contents. The online FTIR detection also provides the total concentration of the sample components. Figure 2.10 indicates that the present sample contains about 10 % of PE.

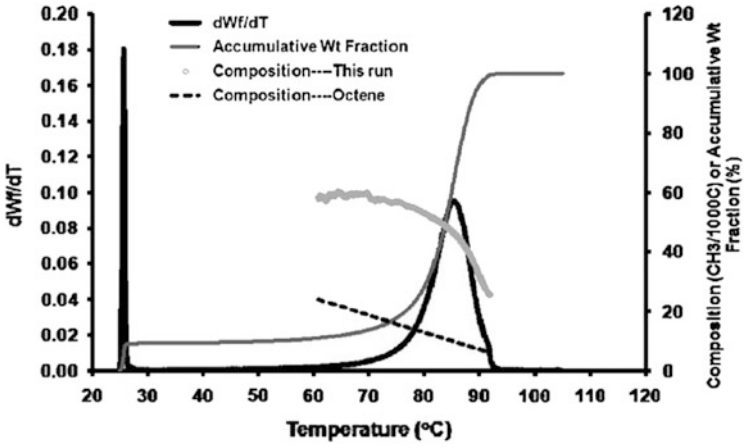

Fig. 2.11 TREF–FTIR profile of a blocky EO copolymer (reprinted from [46] with permission of Wiley-VCH)

A different type of TREF behaviour is seen for the blocky EO copolymer in Fig. 2.11. There is no component (PE) eluting beyond 90 °C. As in the previous case, the copolymer fractions elute in agreement with their octene content. A narrow TREF elution peak at 25 °C indicates that the sample contains material that did not crystallize in the crystallization step. The elution step starts at 25 °C and the 'soluble fraction' elutes first from the TREF column. This soluble material contains copolymer molecules with high octene contents and may even contain (amorphous) polyoctene (this comprises about 10 % of the total sample). It is an important limitation of TREF that only the crystallizable material can be fractionated. The fractionation of all components irrespective of the crystallizability can be achieved by means of column-based interaction chromatography as will be shown in Part 3.

Another remarkable feature of Fig. 2.11 is the difference between the actually measured octene content and the calibration curve that was obtained from the random EO copolymer sample. The figure clearly shows that the real octene content at a given elution temperature of the block copolymer is significantly higher than it is for the random copolymer. This is clear proof of the fact that the crystallization/elution temperature is not only influenced by the 'bulk' octene content but also by the microstructure (blockiness, type of branches) [31].

2.1.2 Fractionation of Impact Polypropylene Copolymers [37]

Another unique class of complex polyolefins is heterophase ethylene–propylene copolymers (EPCs). The major advantage of this class is improved low temperature impact strength of PP, therefore, they are frequently referred to as 'Impact PP copolymers (IPCs)'. The common procedure for IPC production is via a two-reactor

sequential gas-phase polymerization in the presence of a Ziegler–Natta catalyst [51]. A complex mixture of reaction products is formed that ranges from amorphous random EPCs to crystalline iPP. This wide range of reaction products is attributed to the sequential polymerization procedure and the heterogeneous nature of the catalyst. Different monomer sequence distributions and sequence lengths lead to varying degrees of crystallinity. Accordingly, EPCs are semi-crystalline to varying extents [52–54] and are also referred to as EP block copolymers [55–57], although this terminology is misleading, regarding the nature of the mixture of end products obtained.

The distribution of ethylene and propylene sequences, the sequence lengths and the tacticities determine the final properties of IPC. Therefore, the detailed characterization of IPCs is an important subject, focusing on fractionation as well as spectroscopic analysis. Structural parameters of bulk EPCs have been investigated using ^{13}C-NMR as a method of choice [58]. The information on comonomer contents, distribution of monomers and tacticity could also be obtained by FTIR [59]. DSC is the method of choice to study the melting and crystallization behaviour of IPC. DSC is able to distinguish random copolymers from blends and block structures found in EPCs [60]. The complexity of IPC products makes fractionation techniques an integral part of the characterization protocol. Separation of the different components have been achieved by analytical and preparative TREF [52, 55, 57, 61, 62]. The hyphenation of TREF fractionation with ^{13}C-NMR, DSC and FTIR allows a comprehensive characterization of impact PP but it is a time-consuming procedure.

2.1.2.1 Aim

The present application describes the preparative TREF fractionation of a commercial IPC that is followed by a detailed investigation of the molecular structure of the fractions. In addition to NMR, DSC and SEC as the standard analytical methods, coupled SEC-FTIR shall be used to analyse the chemical composition as a function of molar mass.

2.1.2.2 Materials

- *Polymers*. Non-stabilized commercial IPC from SASOL Polymers (Secunda, South Africa) with the following bulk properties: ethylene content 10.5 mol%, isotacticity 88.8 % (mmmm), M_w 354 kg/mol, molar mass dispersity 3.18.

2.1.2.3 Equipment

- *TREF system*. In-house built preparative TREF apparatus. For crystallization, 3 g of polymer, ca. 2 wt% Irganox 1010 (Ciba Speciality Chemicals, Switzerland) and 300 mL of solvent were placed in a glass reactor and dissolved at 130 °C. The reactor was transferred to an oil bath maintained at 130 °C. As the crystallization support, pre-heated sea sand (white quartz; Aldrich, South Africa) was added to the reactor. The reactor was cooled at a rate of 1 °C/h. A stainless steel column was packed with the crystallized mixture and transferred to a modified GC oven. The temperature of the oven was increased at a steady rate

while pre-heated solvent was pumped through the column. Fractions were collected at pre-determined intervals, solvent was evaporated, fractions were recovered by precipitation in acetone and then finally dried to a constant weight.

- *Solvent*. Xylene
- *TREF column temperature*. Temperature gradient between 130 °C and 30 °C.
- *TREF sample concentration*. 3 g of polymer in 300 mL of solvent.
- *SEC*. PL 220 high temperature chromatograph (Polymer Laboratories, Varian Inc., Church Stretton, UK) at 150 °C equipped with three 300 × 7.5 mm i.d. PLgel Olexis columns and a differential RI detector. BHT stabilized TCB was the eluent at a flow rate of 1 mL/min. Sample concentration was 0.5 mg/mL in TCB and injection volume in all cases was 200 μL. Narrowly distributed polystyrene (PS) standards (Polymer Standards Service GmbH, Mainz, Germany) were used for calibration.
- *FTIR spectroscopy*. Attenuated total reflectance (ATR) measurements were recorded on a Nicolet Nexus 670 FTIR spectrometer (Thermo Electron, Waltham, USA) with a SensIR ATR attachment, equipped with a diamond reflective crystal, incidence angle of 45°. Spectra recorded from 4,000 to 650 cm^{-1} were obtained from a collection of 64 scans at a resolution of 2 cm^{-1}.
- *DSC*. Mettler 822 DSC instrument (Mettler Toledo, Greifensee, Switzerland), calibrated with indium metal according to standard procedures, heating rate of 10 °C/min from 25 °C to 200 °C. Second heating cycle data were used for thermal analysis calculations. Measurements were carried out in a nitrogen atmosphere.
- *NMR*. 600 MHz Varian^{unity} INOVA NMR spectrometer (Varian Inc., Palo Alto, USA) operating at 125 MHz for carbon at 120 °C, 5 mm PFG switchable broadband probe, samples were prepared to a concentration of 6 wt% in deuterated tetrachloroethane (Aldrich, South Africa), 90° flip angle of approximately 6 μs, continuous proton decoupling, acquisition time 1.8 s, pulse delay time 15 s.
- *SEC-FTIR*. PL XT-220 (Polymer Laboratories, Church Stretton, UK) operating at 140 °C was coupled to a solvent evaporation FTIR interface LC-Transform (Series 300, Lab Connections, Carrboro, USA), stage and nozzle temperatures 160 °C and 150 °C, respectively, transfer line temperature 150 °C, solutes deposited on heated germanium disc and subsequently analysed by FTIR, analysis of SEC-FTIR results using Omnic software package (Thermo Electron, Waltham, USA).

2.1.2.4 TREF Fractionation

The preparative TREF fractions of the sample were collected at 30 °C, 60 °C, 80 °C, 90 °C, 100 °C, 110 °C, 120 °C and 130 °C. Figure 2.12 depicts the weight distribution (W_i%) and weight fraction per temperature increment (W_i%/ΔT) of the eight P-TREF fractions. The 30 °C fraction and fractions eluting in the range 110–130 °C constitute the largest weight percentage of sample 3V, as is shown by the fractionation diagram. The principle of TREF fractionation is based on crystallizability; therefore, fractions collected at 30 °C are expected to be

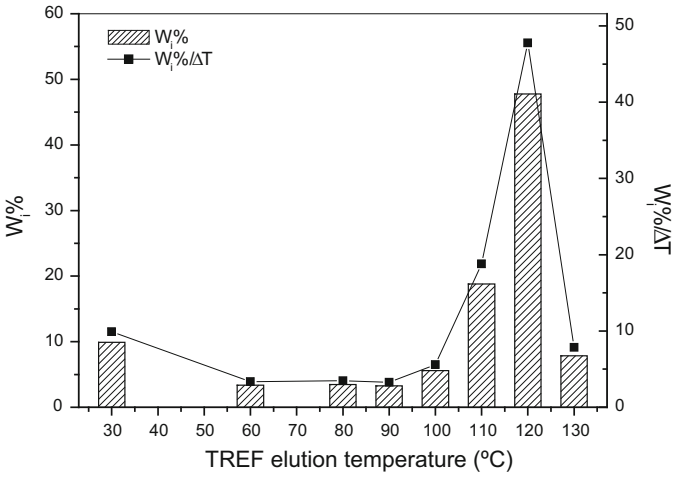

Fig. 2.12 Weight distribution and weight fraction per temperature increment for the TREF fractions of IPC (reprinted from [37] with permission of Wiley-VCH)

amorphous, while highly crystalline fractions are expected at higher temperatures (around 120 °C). The fractions obtained between these two extreme temperatures are assumed to be semi-crystalline with compositional differences. All fractions were analysed by DSC, ^{13}C-NMR and SEC-FTIR for determination of their chemical composition and thermal properties.

The relationships established by Ray et al. [63] and Randall [64] were used to calculate the comonomer contents and monomer sequence distributions from NMR; see Table 2.1. The method described by Kanezaki et al. [65] was used to obtain the isotacticity (% mmmm) data for the PP part; see Table 2.2.

The results indicate that the TREF fractionation was governed by decreasing comonomer content and increasing isotacticity. The fractionation also depended upon the increasing sequence length; the average length (n_x) of both ethylene and propylene sequences increased with increasing elution temperature. The first four fractions have high concentrations of PE and EP diads which indicate the linking of ethylene and propylene segments to some extent. On the other hand, the concentration of PE and EP diads becomes virtually zero in the highest eluting fractions. Therefore, higher eluting fractions consist of long iPP homopolymer sequences along with a small amount of PE homopolymer.

The fraction obtained at 30 °C contains equal amounts of ethylene and propylene with a high number of EP junctions, indicating the strong presence of EP random copolymers. However, some atactic PP and ethylene homopolymer may also be present. The higher temperature fractions that elute at 60 °C, 80 °C and 90 °C contain long sequences of both ethylene and propylene along with a fair number of EP junctions. This indicates that longer segments of propylene and ethylene are linked. The sequential gas-phase polymerization cannot produce true block structures; hence these are called ‘blocky’ copolymers.

Table 2.1 ^{13}C-NMR monomer sequence analysis and tacticity data of the bulk 3V sample and its TREF fractions (reprinted from [37] with permission of Wiley-VCH)

Sample	P	E	PP	PE/EP	EE	PPP	PPE/EPP	EPE	EEE	EEP/PEE	PEP	%mmmm
3V	89.52	10.48	86.36	6.34	7.32	84.19	3.63	1.70	5.75	3.18	1.58	88.82
30 °C	49.55	50.45	34.43	30.23	34.39	49.39	0.14	0.02	25.78	13.42	1.80	24.70
60 °C	45.11	54.89	34.15	21.92	43.87	28.74	11.64	4.73	37.56	12.43	1.65	36.13
80 °C	44.46	55.54	38.29	12.32	48.99	37.74	3.96	3.11	44.47	7.47	1.00	64.91
90 °C	54.31	45.69	52.66	3.31	43.83	54.26	0.04	0.01	42.25	2.37	0.06	71.21
100 °C	90.27	9.73	89.96	0.63	9.11	89.37	0.90	0.00	8.50	0.02	0.11	85.74
110 °C	94.85	5.15	94.85	0.00	4.37	91.86	2.99	0.00	2.81	0.00	0.00	86.54
120 °C	99.39	0.61	99.39	0.00	0.61	99.39	0.00	0.00	0.61	0.00	0.00	91.52

Table 2.2 The Average ethylene (n_E) and propylene (n_P) sequence lengths of sample 3 V and its TREF fractions (reprinted from [37] with permission of Wiley-VCH)

Sample	n_E	n_P
3V	3.31	28.86
30 °C	5.41	3.32
60 °C	5.00	4.12
80 °C	8.95	7.21
90 °C	27.51	32.84
100 °C	29.99	287.23
110 °C	n.d.	n.d.
120 °C	n.d.	n.d.

n.d. not determined

2.1.2.5 Fraction Analysis and Evaluation

The molar masses of the bulk polymer and the TREF fractions were analysed by SEC. As can be seen in Fig. 2.13, a number of fractions exhibit monomodal MMDs while others are bimodal. Such molar mass bimodality might indicate compositional heterogeneity. This has frequently been observed for the mid-elution temperature fractions of IPC fractionated by TREF [62, 66, 67] where semi-crystalline EPC and PP homopolymer co-elute due to the isotacticity distribution found in PP [62, 68]. PP homopolymer will not elute entirely at high TREF temperatures, because PP fractions of lower isotacticity will become soluble within the same lower temperature range of the semi-crystalline EPC phase of corresponding crystallizability.

Additional evidence for the complexity of the TREF fractions is obtained from the thermal behaviour, as shown in Fig. 2.14 for the DSC heating curves.

As expected, no melting or crystallization is observed for the 30 °C fraction. This fraction is amorphous and contains random EP rubber and (perhaps) some low molar mass PP with a low isotacticity. The higher temperature fractions (110 °C and 120 °C) have a single, distinct melting peak around 160 °C, which confirms the monomodality of fractions containing predominantly iPP. The fractions eluting at lower temperatures (60–100 °C) show bimodalities with two melt endotherms, indicating the presence of two distinct crystallizable components. Furthermore, the fractions show an increase in melting temperatures for both endotherms from the 60 °C fraction to the 100 °C fraction, which is a clear indication of an increase in crystallinity of both components with increasing elution temperature. The appearance of two melt endotherms for the mid-elution fractions confirms the assumption derived from the SEC curves that these fractions exhibit a significant compositional heterogeneity. SEC, however, separates according to molecular size and not chemical composition. Therefore, bimodality in the SEC profiles does not conclusively prove a chemical heterogeneity. One way to overcome this problem is to couple SEC with a selective detector such as FTIR, as has been shown in Sect. 2.1.1. In the present case, however, the LC-Transform interface is used instead of a flow cell. The operation of this device has been described elsewhere and a number of important applications have been presented [14, 69]. The advantage of this

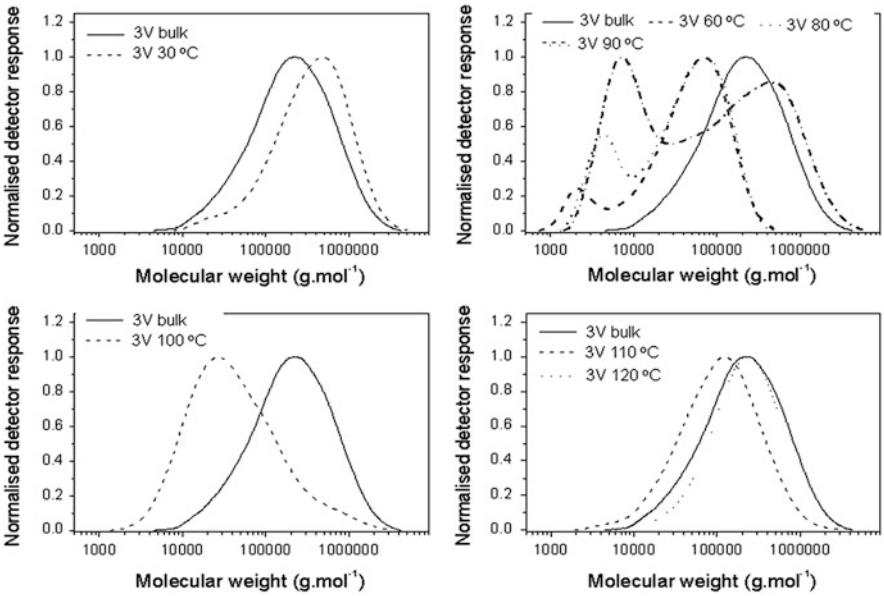

Fig. 2.13 Molar mass distributions of the bulk IPC and the TREF fractions (reprinted from [37] with permission of Wiley-VCH)

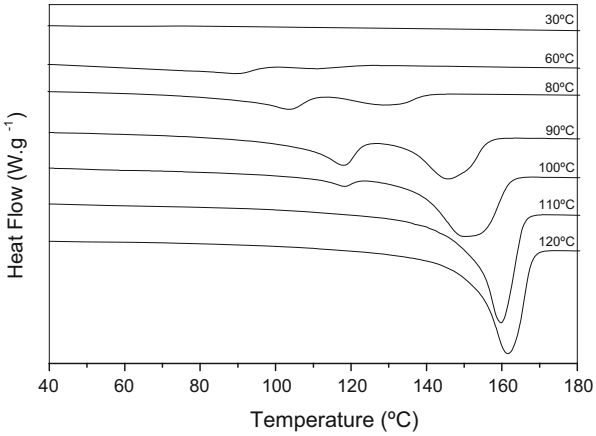

Fig. 2.14 Melt endotherms of the TREF fractions of IPC as obtained by DSC (reprinted from [37] with permission of Wiley-VCH)

approach is that not only can two wavelengths (e.g. for total concentration and methyl group content) be monitored, but for each SEC slice a complete FTIR spectrum is generated. The results of the SEC-FTIR analysis of the TREF fractions are summarized in Figs. 2.15 and 2.16.

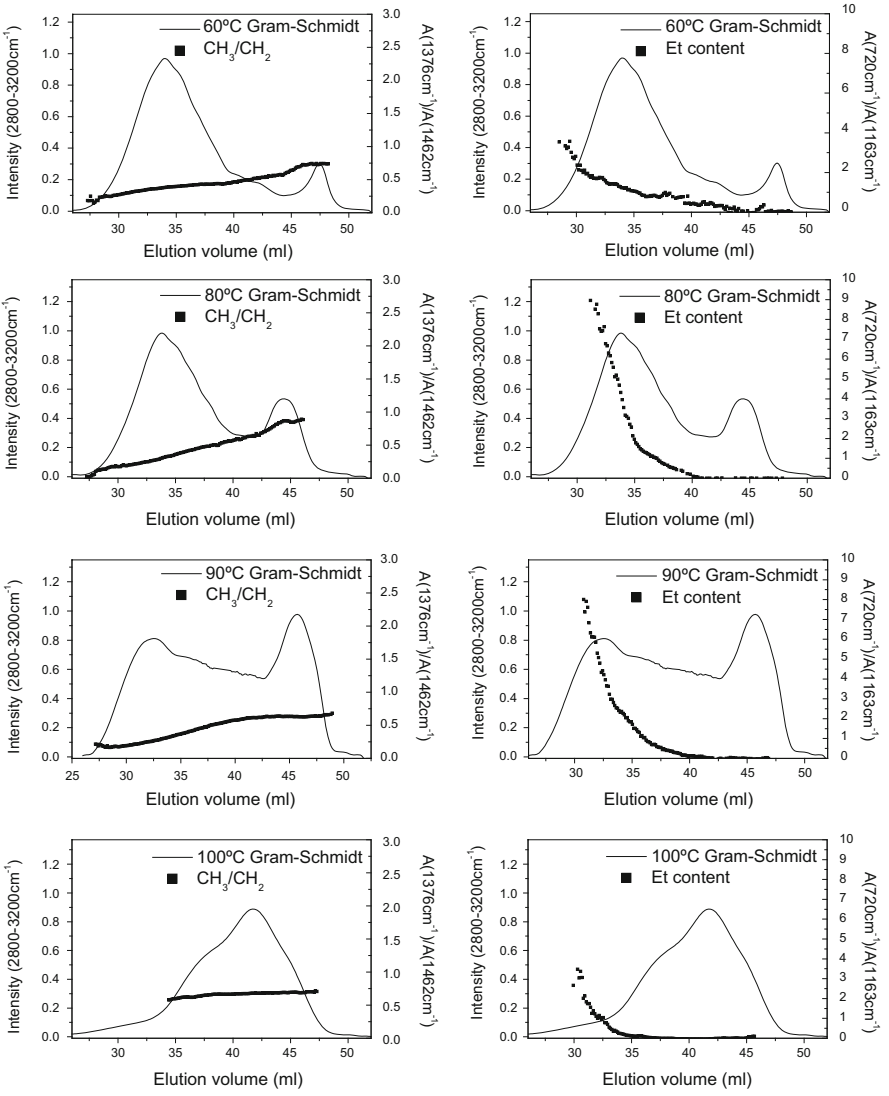

Fig. 2.15 SEC-FTIR analysis of the ethylene and propylene distribution within the 60 °C, 80 °C, 90 °C and 100 °C TREF fractions of IPC (reprinted from [37] with permission of Wiley-VCH)

The Gram–Schmidt plots represent the total FTIR absorption over the 2,800–3,200 cm^{-1} range of the spectrum. The shape of the plot resembles SEC curves, which show distributions of molar masses from higher to lower as the elution volume increases. In the Gram–Schmidt plot, CH_3/CH_2 corresponds to the distribution of propylene and 'Et content' corresponds to the ethylene content profile. The areas of the absorption bands at 1,376 cm^{-1} and 1,462 cm^{-1} correspond to CH_3 and CH_2, respectively, and are used for quantification of the propylene content

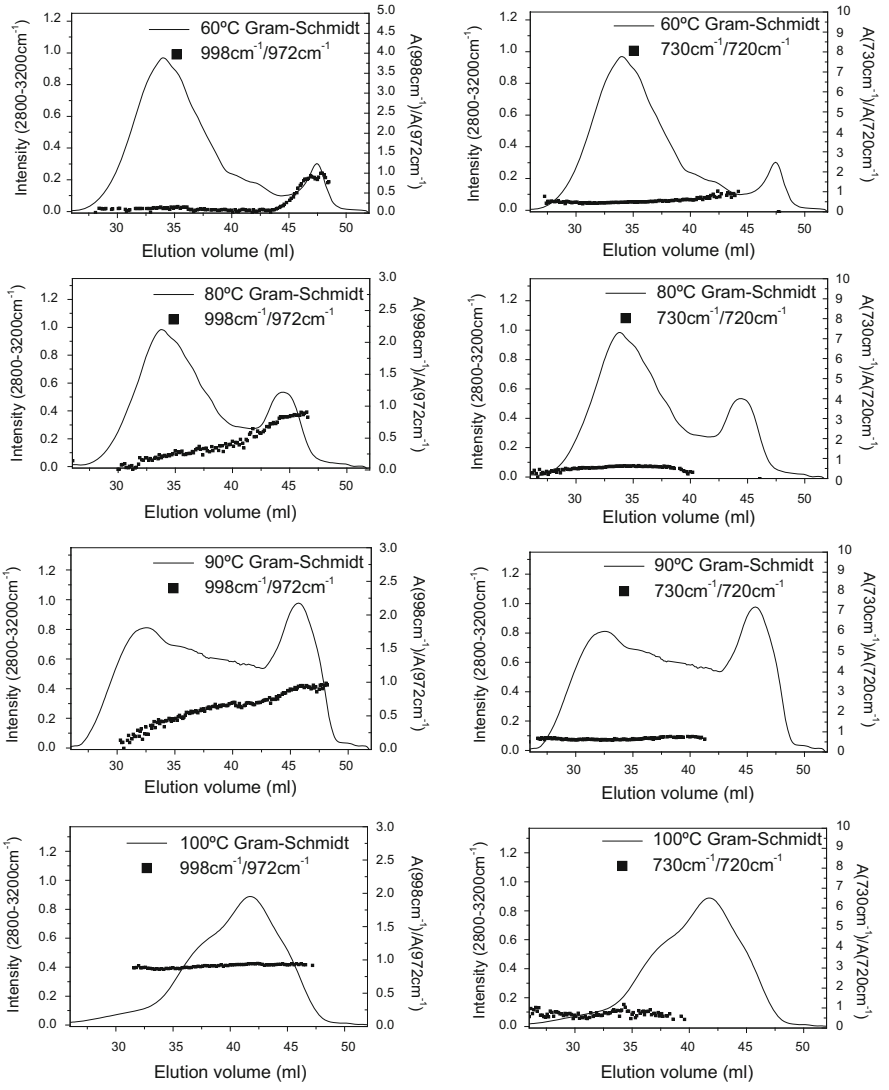

Fig. 2.16 SEC-FTIR analysis of the ethylene and propylene crystallinity distributions within the 60 °C, 80 °C, 90 °C and 100 °C TREF fractions of IPC (reprinted from [37] with permission of Wiley-VCH)

[70–72]. The total polymer concentration is measured by the intensity of the CH_2 band, whereas the presence of CH_3 groups indicates branching and is characteristic of PP units. The chain branching in PE may also result in the band at 1,378 cm^{-1}; therefore, the validity of using the ratio of 1,378 cm^{-1}/1,462 cm^{-1} was investigated. This was achieved by constructing the ethylene profile across the molar mass curve. The ratio of the areas of the bands at 720 cm^{-1} and 1,163 cm^{-1}

was used for the ethylene content quantification within an EP block copolymer [73]. The gradual increase in the CH_3/CH_2 ratio across the bimodal MMDs is observed for the first three fractions eluting at 60 °C, 80 °C and 90 °C, respectively. This indicates the higher propylene content in the lower molar mass component; see Fig. 2.15. The ethylene content decreases gradually from the higher molar mass side of the distribution until it reaches zero within the lower molar mass region, as indicated by the ratios of the 720 cm^{-1}/1,162 cm^{-1} bands. This is a clear indication that ethylene is only present in the higher molar mass components and the band at 1,378 cm^{-1} represents the methyl groups in PP only.

There is a visible difference in the compositions of the lower and high molar mass components of the bimodal distribution. PP homopolymers are the sole component of the lower molar mass region, in contrast to the high molar mass part which is composed of EPCs with varying monomer distributions. The ethylene-rich copolymers appear on the higher molar mass side. The propylene content increases towards the lower molar mass side of the distribution. The 100 °C fraction forms the transition between blocky copolymers and iPP fractions eluting at higher temperature, as predicted by ^{13}C-NMR. The Gram–Schmidt curve constructed from the CH_3/CH_2 ratio shows lower values for regions of higher molar mass (low elution volume) compared to the low molar mass region, indicating the differences in the propylene content in both regions of the MMD. This is a clear sign that the propylene content is lower in the region of higher molar masses. The results are in good agreement with the ratio of 720 cm^{-1}/1,163 cm^{-1}, which decreases to zero in the direction of higher elution volumes. The presence of EPC in the higher molar mass shoulder in the 100 °C fraction is therefore confirmed by SEC-FTIR analysis. The two melt endotherms in each of these fractions determined by DSC analysis suggest the presence of both crystalline ethylene and propylene segments. The specific crystalline entities for both monomers are associated with specific IR bands; therefore, the construction of ethylene and propylene crystallinity profiles should be possible from SEC-FTIR. The 998 cm^{-1} and 841 cm^{-1} bands are associated with long repeating monomer units in the crystalline 3_1 helix of PP [74–77]. The short helix segments are associated with the 972 cm^{-1} band of the FTIR spectrum. There is a linear correlation between the intensities of the 998 cm^{-1} and 841 cm^{-1} bands and the density of PP as a measure of its crystallinity [78]. PP tacticity can, therefore, be determined by the ratio of the 998 cm^{-1} and 972 cm^{-1} absorption bands, providing the degree of spectral crystallinity in PP.

FTIR spectroscopy also provides information on the relative crystallinity of ethylene segments in EPCs along with propylene segments. The 720 cm^{-1} band originates from long methylene sequences. With the increase in crystallinity of PE, the intensity of the 730 cm^{-1} component increases at the cost of splitting of the 720 cm^{-1} band [79, 80]. The band at 730 cm^{-1} is recognized as a true crystallinity band [75]. Therefore, the relative crystallinity in PE is related to the ratio of the band intensities at 720 cm^{-1} and 730 cm^{-1} [80–82]. The ratios of 998 cm^{-1}/972 cm^{-1} and 730 cm^{-1}/720 cm^{-1} are constructed across the Gram–Schmidt

curves to examine the distribution of ethylene and propylene crystallinity across the molar mass profiles; see Fig. 2.16.

The low elution volume component of the 60 °C fraction shows a very low level of propylene isotacticity or crystallinity. The higher elution volume component (corresponding to lower molar mass) shows higher ratios of 998 cm^{-1}/972 cm^{-1}, indicating the presence of PP homopolymer. Crystalline ethylene sequences are present only in the lower elution volume component, which can be identified as the semi-crystalline EPC component of this fraction. The absence of the 730 cm^{-1} and 720 cm^{-1} absorption bands resulted in the discontinuation of this profile within the higher elution volume component of the distribution.

In the case of the 80 °C and 90 °C fractions, the ratio of the 998 cm^{-1}/972 cm^{-1} absorption bands increases across the bimodal distribution towards higher elution volumes where PP homopolymer is located. Ethylene crystallinity is only seen in the lower elution volume component. This is the region where EPC elutes. Therefore, crystalline ethylene and propylene segments are found in the EPC phase and highly crystalline isotactic PP is found in the lower molar mass PP phase. The crystalline ethylene segments of the EPC are represented by lower temperature melt endotherms in the DSC heating curve. The higher temperature melt endotherm in the DSC heating curve is due to melting of propylene segments of EPC and PP homopolymer. A uniform propylene concentration is detected in the 100 °C fraction across the Gram–Schmidt curve. The higher elution volume end of the PP homopolymer component of preceding fractions and this fraction show similar values for the 998 cm^{-1}/972 cm^{-1} ratio. There is only a slight variation at the lower elution volume shoulder, where EPC elutes, as indicated by the CH_3/CH_2 ratio. Crystalline ethylene segments are also detected only in the low elution volume shoulder of the Gram–Schmidt plot. The SEC-FTIR results for ethylene and propylene crystallinity agree well with DSC results on the thermal behaviour of the fractions.

2.1.3 Analysis of Thermo-oxidatively Degraded Polypropylene [83]

Polyolefins are susceptible to degradation which takes place throughout the life cycle of the material. Degradation occurs during polymerization, processing, application and recycling. It influences the polymer properties, thereby limiting the lifetime of the materials and leading to economic losses [84, 85]. To reduce the degradation of a particular material, the sources of degradation and the degradation pathways must be understood. This is a strong motivation to search for new analytical methods to analyse and monitor the degradation of polyolefins [86]. A particular aspect is the increasing importance of polymer recycling with the aim not to downgrade the material.

One can distinguish between photo-oxidative and thermo-oxidative degradation. Polyolefins can also be attacked by strong acids [87]. The generally accepted free radical oxidation model of polyolefins involves radical initiation, propagation and termination reactions [88, 89]. Following an initiation reaction, which usually

results from the thermal or photo-initiated dissociation of chemical bonds, alkyl radicals react with molecular oxygen to form peroxy radicals [90]. The oxygen-containing functionalities like ketones, alcohols, carboxylic acids, esters and γ-lactones are due to the propagation reactions [91–96]. Fractionation is an important approach to obtain information about degradation and the distribution of degradation products. CRYSTAF and TREF separate semi-crystalline polyolefins based on crystallizability. These methods in combination with spectroscopic methods shall now be used for the analysis of degraded polyolefins.

2.1.3.1 Aim

In Sect. 2.1.2, the compositional heterogeneity of a commercial IPC was measured by hyphenation of TREF fractionation with SEC-FTIR analysis. The chemical composition as function of MMD of all fractions was determined. The morphological nature of the components was further confirmed by determination of ethylene and propylene crystallinity distributions across the MMDs.

In the present application, the thermo-oxidative degradation of IPC shall be addressed. IPC is degraded at different times and temperatures like in previous reports on PP and PP-1-pentene copolymers [97, 98]. The bulk sample analysis by SEC, FTIR, SEC-FTIR, CRYSTAF and DSC is used to monitor the process of degradation. A degraded sample is fractionated by P-TREF and the fractions are analysed for molar mass and chemical composition in order to obtain information on degradation of individual components of IPC. A comparison of two different IPC samples with regard to chemical composition will be presented. The degree of degradation as a function molar mass, chemical composition and crystallinity will be determined for the fractions of degraded materials. Finally, samples shall be evaluated and compared with respect to thermo-oxidative stability.

2.1.3.2 Materials

- *Polymers*. The bulk properties of two non-stabilized commercial IPCs from SASOL Polymers (Secunda, South Africa) are presented in Table 2.3 (samples were labelled 3V and 4V, O h indicates original samples before degradation). To prevent degradation during film extrusion and sample preparation, 0.05 % of phosphite processing stabilizer, Irgafos 168, was added for compounding of the materials. Dry-blending of the IPC powder and Irgafos 168 was followed by melt-blending at 200 °C on a Brabender PL 2000-6 single-screw extruder equipped with a 19 mm diameter screw, length-to-diameter ratio of 25 and screw speeds of 40–100 rpm. The extrudates were cooled and pelletized. Thin films (1 g of material, ca. 160 μm) were prepared by compression moulding at 190 °C. A typical compression cycle consisted of melting of the pellets for 1.5 min and compression at 10–12 bar for another 1.5 min, with subsequent quench cooling in an ice/water mixture.
- *Accelerated oven ageing*. The thermo-oxidative degradation of thin films at 90 °C and 110 °C was accomplished in a heat-circulating oven with digital temperature control (SMC manufacturing, Cape Town, South Africa). The visual (for physical changes) and FTIR (for chemical changes) monitoring of the degradation followed the degradation process and samples were removed at

Table 2.3 Summary of the molecular properties of IPC samples 3V and 4V

Sample	[Ethylene] (mol%)	Isotacticity (%mmmm)	M_w (g/mol)	M_n (g/mol)	M_w/M_n	T_m (°C)	T_c (°C)	ΔH_m (J/g)
3V-0h	10.48	88.82	354,400	114,600	3.18	118.15	162.56	93.84
4V-0h	16.42	83.17	351,900	86,600	4.06	116.28	160.69	72.45

Ethylene content and isotacticity (%mmmm): determined by ^{13}C-NMR; M_w, M_n and M_w/M_n measured by HT-SEC; T_m, T_m and ΔH_m measured by DSC

regular intervals for further analysis. The degradation process was discontinued when samples snapped or flaked on bending. The degraded films were homogenized by shredding the film into small pieces and re-melting into a single film for a very brief time. Films removed from the oven at advanced stages of degradation were brittle and shattered easily. Plasticity was, however, restored after the re-moulding process.

2.1.3.3 Equipment

- *SEC*. Polymer Laboratories PL 220 high temperature chromatograph (Polymer Laboratories, Church Stretton, UK) at 150 °C, equipped with three 300 × 7.5 mm i.d. PLgel Olexis columns and a differential RI detector. The eluent was TCB stabilized with BHT, at a flow rate 1 mL/min. Sample concentration was 0.5 mg/mL in TCB and the injection volume was 200 μL. Calibration was done with PS.
- *FTIR Spectroscopy*. Nicolet Nexus 670 FTIR spectrometer (Thermo Electron, Waltham, USA). Spectra were recorded from 4,000 to 650 cm^{-1}. Spectra were obtained from a collection of 64 scans at a resolution of 2 cm^{-1}.
- *DSC*. Mettler 822 DSC instrument (Mettler Toledo, Greifensee, Switzerland), calibrated with indium metal according to standard procedures, heating rate of 10 °C/min from 25 °C to 200 °C. Data obtained during the second heating cycle were used for thermal analysis calculations. Measurements were conducted in a nitrogen atmosphere.
- *NMR*. 600 MHz Varian^{unity} INOVA NMR spectrometer (Varian, Palo Alto, USA) operating at 125 MHz for carbon at 120 °C, 5 mm PFG switchable broadband probe, samples were prepared to a concentration of 6 wt% in deuterated tetrachloroethane (Aldrich, South Africa), 90° flip angle of approximately 6 μs, continuous proton decoupling, acquisition time 1.8 s, pulse delay time 15 s.
- *TREF*. In-house built preparative TREF apparatus. For crystallization, 3 g of polymer, ca. 2 wt% Irganox 1010 (Ciba Speciality Chemicals, Switzerland) and 300 mL of solvent were placed in a glass reactor and dissolved at 130 °C. The reactor was transferred to an oil bath maintained at 130 °C. As the crystallization support, pre-heated sea sand (white quartz; Aldrich, South Africa) was added to the reactor. The reactor was cooled at the rate of 1 °C/h. A stainless steel column was packed with the crystallized mixture and transferred to a modified GC oven. The temperature of the oven was increased at a steady rate while pre-heated solvent was pumped through the column. Fractions were collected at pre-determined intervals, solvent was evaporated, fractions were recovered by precipitation in acetone and then finally dried to a constant weight.
- *Solvent*. Xylene.
- *TREF column temperature*. Temperature gradient between 130 °C and 30 °C.
- *TREF sample concentration*. 3 g of polymer in 300 mL of solvent.
- *CRYSTAF*. CRYSTAF apparatus Model 200 (Polymer Char, Valencia, Spain). 20 mg of the sample was dissolved in 40 mL ODCB. Stainless steel reactors for crystallization were equipped with an automatic stirring and filtration device and crystallization was carried out under agitation. The dissolution at 160 °C was

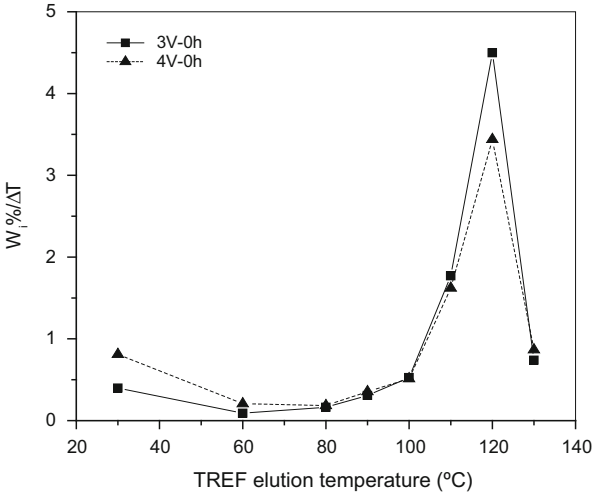

Fig. 2.17 Crystallization curves of IPC samples 3V and 4V obtained by TREF ($W_i\%/\Delta T$) (reprinted from [83] with permission of Wiley-VCH)

followed by cooling to 100 °C for stabilization and then to 30 °C at a cooling rate of 0.1 °C/min. Fractions were collected automatically and an IR detector was used to determine the concentration of the solution at the chosen wavelength of 3.5 μm.

2.1.3.4 TREF Fractionation and Analysis of Non-degraded Samples

Samples were fractionated by preparative TREF and fractions were collected at 30 °C, 60 °C, 80 °C, 90 °C, 100 °C, 110 °C, 120 °C and 130 °C; see Fig. 2.17.

Although the maxima of the TREF curves at 120 °C are similar for the two samples, the intensity of the 4V crystallization peak is lower than that of sample 3V and a larger TREF soluble fraction at 30 °C is detected for sample 4V. The higher percentage of ethylene comonomer in sample 4V will result in larger amounts of non-crystallizable material.

To study the heterogeneity of the copolymers, TREF fractions were analysed by ^{13}C-NMR, SEC and DSC. The comonomer content and isotacticity data of the TREF fractions of the samples as obtained by ^{13}C-NMR are presented in Fig. 2.18a, b. In both samples, the isotacticity increases with increasing TREF elution temperature indicating that the fractionation of the PP phase is governed by tacticity. The ethylene content decreases in the same direction. Significant differences are found between the two samples. In parallel to the increasing isotacticity and decreasing comonomer content, the melting temperatures increase with increasing TREF elution temperature; see Fig. 2.18d. For the molar masses of the different fractions, as obtained by SEC, no clear trend can be observed. However, the soluble fraction appears to have the highest molar mass, see Fig. 2.18c.

Figure 2.18a shows that for both copolymers the ethylene content decreases towards higher elution temperatures. The first three fractions of copolymer 4V contain considerably higher concentrations of ethylene. The next four fractions of copolymer 4V are similar to copolymer 3V as far as ethylene content is concerned.

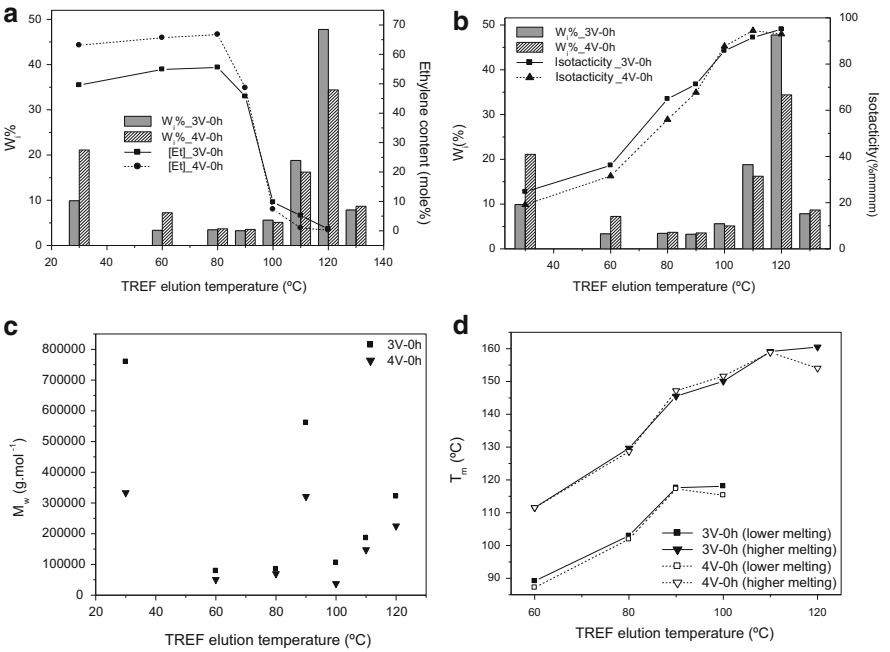

Fig. 2.18 Analytical results for the TREF fractions of IPC samples 3V and 4V, ethylene content (**a**), isotacticity (**b**), average molar masses M_w (**c**) and DSC melting temperatures (**d**) (reprinted from [83] with permission of Wiley-VCH)

It seems that random copolymer fractions incorporated the excessive ethylene comonomer introduced during polymerization. This introduces shorter segments of ethylene and propylene in the EP rubber (EPR) and 'transition' copolymers. Therefore, the nature of random and semi-crystalline EPCs should be more affected by higher comonomer contents compared to the PP matrix. This is in agreement with the polymerization process, where iPP is produced in the first reactor while the formation of EPCs takes place only in the second reactor. In DSC, two melt endotherms were observed in the 60–100 °C fractions of both samples, see Fig. 2.18d, indicating that the 60 °C, 80 °C, 90 °C and 100 °C fractions consist of co-eluting PP with lower isotacticity and semi-crystalline EP copolymers. The crystallizable ethylene sequences in the EPC phase correspond to the lower of the two melt endotherms, whereas the higher melt endotherm is due to the propylene sequences from both the EPC and PP homopolymer phases.

Table 2.4 summarizes the compositional differences between the two samples. The 30 °C fraction was identified as EPR. The co-eluting components of EPC and low isotacticity PP with short sequences of ethylene and propylene form the 60 °C and 80 °C fractions. The same constituents are present in the 90 °C and 100 °C fractions but with higher isotacticity of PP and longer ethylene and propylene

Table 2.4 Compositional heterogeneity of IPC samples 3V and 4V

	T_e			
	30 °C	60–80 °C	90–100 °C	110–130 °C
Sample	EPR + aPP	'Transition' EPC + low isotacticity PP	'Blocky' EPC + high isotacticity PP	Isotactic PP + PE
3V-0h	9.90	6.83	8.86	74.72
4V-0h	21.11	10.94	8.67	59.28

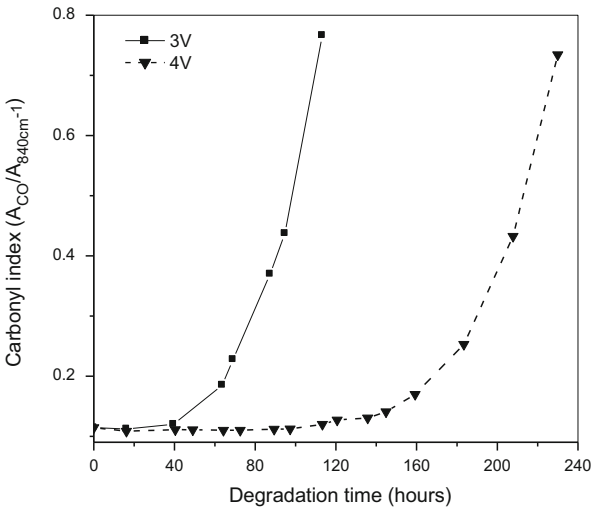

Fig. 2.19 Carbonyl index changes in IPC samples 3V and 4V (reprinted from [83] with permission of Wiley-VCH)

sequences. iPP is the major constituent of the 110–130 °C fractions, with traces of PE homopolymer.

2.1.3.5 Analysis of Degraded Bulk Samples

The accelerated thermo-oxidative degradation of thin films of samples 3V and 4V was executed under similar conditions. After predetermined times, samples of both grades were taken from the oven and analysed further. FTIR data and the progress of embrittlement of complete film areas were used for monitoring the progress of degradation. The differences in the embrittlement rate of both samples were compared. The 3V films showed faster embrittlement compared to sample 4V. The rate and extent of degradation of both samples was compared quantitatively by means of the carbonyl index. The carbonyl index was calculated as the peak height ratio of the maximum of the carbonyl band at 1,804–1,580 cm^{-1} and the reference band at 840 cm^{-1}; see Fig. 2.19.

Copolymer 3V degraded at a faster rate and with a shorter induction time of about 40 h compared to sample 4V. Sample 4V showed signs of degradation in the form of gradual enhancement of the carbonyl index only after 100 h of ageing. A steady rate of degradation was observed for both samples after the induction period. However, the steeper slope of the carbonyl index curve of sample 3V indicates the

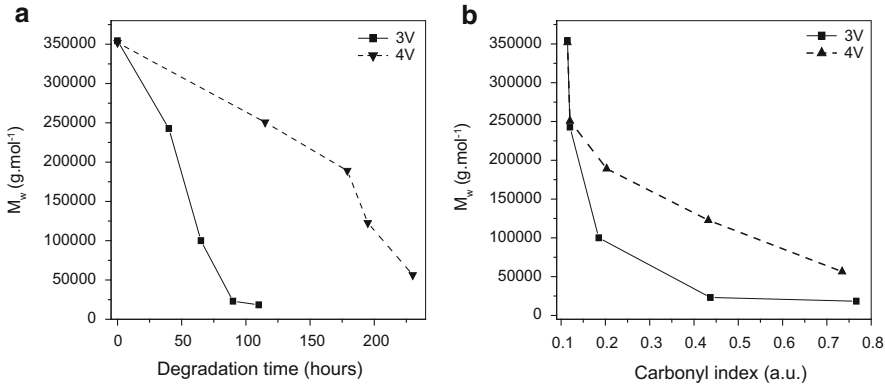

Fig. 2.20 Comparison of M_w decrease of samples 3V and 4V as a function of degradation time (**a**) and carbonyl index (**b**) (reprinted from [83] with permission of Wiley-VCH)

faster degradation rate compared to sample 4V. The decrease in M_w with increasing degradation time is presented in Fig. 2.20a. The M_w changes as a function of the carbonyl index (obtained with ongoing degradation) for both the samples are presented in Fig. 2.20b. The different rates of degradation can be seen clearly by changes in molar mass upon ongoing degradation, despite of the fact that the nondegraded samples have identical molar masses. The molar mass decrease to approximately 250,000 g/mol was noted during the first stages of degradation (up to 40 h and 115 h for samples 3V and 4V, respectively). However, the M_w decrease for sample 3V was considerably faster compared to sample 4V after longer degradation times. This confirms the higher degradation rates in the copolymer with lower contents of comonomer and isotacticity.

The thermal behaviour of the two samples is presented in Fig. 2.21, showing the changes in CRYSTAF T_c, as well as DSC T_c, T_m and ΔH_m.

The three molecular parameters, namely carbonyl index, molar mass and either CRYSTAF T_c or DSC T_c or T_m, can be combined to study the effect of molar mass and carbonyl concentration on the crystallization and melting temperature of the degraded copolymers; see Fig. 2.22a, b. The influence of degradation on the interrelationship between three seemingly independent parameters is clearly indicated by these presentations, irrespective of the different time scales of the degradation of IPC samples 3V and 4V.

2.1.3.6 TREF Fractionation and Analysis of the Degraded Samples

The degraded samples were recrystallized in TREF. The same fraction collection TREF profile as for the nondegraded samples was used. The nondegraded and degraded samples were compared at different degradation times with regard to the weight fractions per temperature increment ($W_i\%/\Delta T$); see Fig. 2.23. The crystallization peaks shifted to lower temperatures from 120 °C for nondegraded and

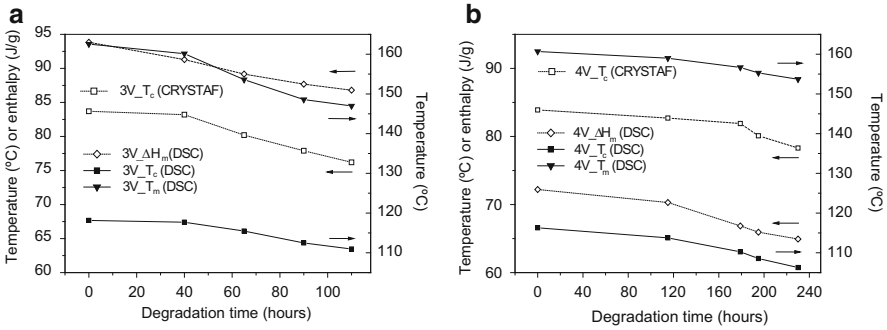

Fig. 2.21 Comparison of the changes in crystallization and melting behaviour as a function of degradation time for samples 3V (**a**) and 4V (**b**) (reprinted from [83] with permission of Wiley-VCH)

slightly degraded samples to 110 °C for samples degraded for longer times. CRYSTAF measurements show the selective degradation of the higher isotacticity fractions. The results are confirmed by the decrease in intensity and shift towards lower values for crystallization peak temperature along with an increase in the amount of material eluting at the lowest elution temperature.

The SEC results of selected fractions of the degraded samples are shown in Fig. 2.24. For the highest eluting fractions, the shifts in molar mass of the two samples are very similar. This is expected, because these fractions consist mainly of iPP. The 60–90 °C fractions exhibit bimodal distributions due to low isotacticity PP and EPC. As can be expected, little differences are observed between the samples in terms of molar mass changes of the low isotacticity PP component. The EPC component, however, shows slightly different molar mass shifts in the two samples. The most significant differences in the molar mass changes are, however, seen within the 30 °C fractions. These fractions consist mainly of EPR. The higher comonomer content and lower isotacticity of EPR of sample 4V seemingly make it more stable than sample 3V. The stability of the 60–90 °C fractions of sample 4V seems to be improved by the higher ethylene content.

The results indicate a longer induction period and slower increase in carbonyl functionalities, as well as a slower decrease in M_w for sample 4V. The delayed onset and slower oxidation rate in IPCs with higher ethylene content are attributed to the introduction of more stable ethylene units in the polymer chain. The number of tertiary PP carbons that can undergo dissociation reactions is believed to be eliminated by the presence of ethylene units. The presence of the 3_1 helix in crystalline PP promotes the bimolecular decomposition reaction that is of lower activation energy than the unimolecular decomposition occurring in more random conformations; hence, higher isotacticity of the PP unit also increases the rate of oxidation. The samples currently being studied have only small differences in ethylene content and isotacticity, and relatively large differences in the amount of amorphous material. Nonetheless, they show a considerable difference in their degradation behaviour. The analysis of the fractions of both copolymers by SEC

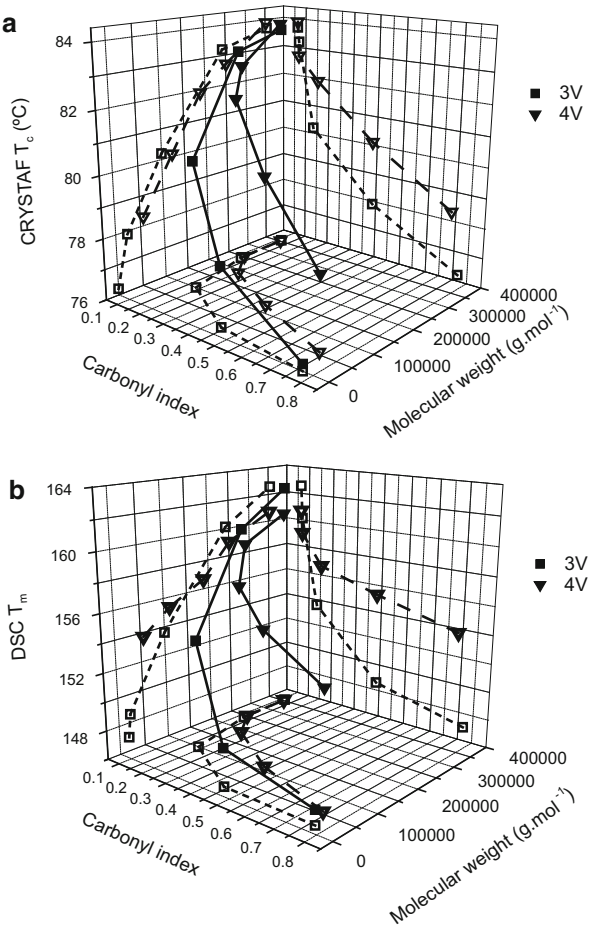

Fig. 2.22 Comparison of differences in the relationships between carbonyl index, molar mass and CRYSTAF T_c (**a**) and DSC T_m (**b**) for samples 3V (*squares*) and 4V (*triangles*) (reprinted from [83] with permission of Wiley-VCH)

and DSC agreed quite well. The 30 °C and 90 °C fractions of samples 3V and 4V show slight differences in their molar masses. The fractions collected at similar TREF elution temperatures for both products have almost identical T_m and T_c values. The similarity in distribution of isotacticity of the PP phase and the sequence length of ethylene and propylene of the EPC component of corresponding fractions of the two copolymers is illustrated by the results. However, weight percentages of the fractions eluting at corresponding elution temperatures are different for the two samples. For copolymer 4V, larger amounts of amorphous fractions (30–90 °C) and smaller amounts of more crystalline fractions (110 °C and 120 °C) are collected during P-TREF compared to product 3V. Similar amounts

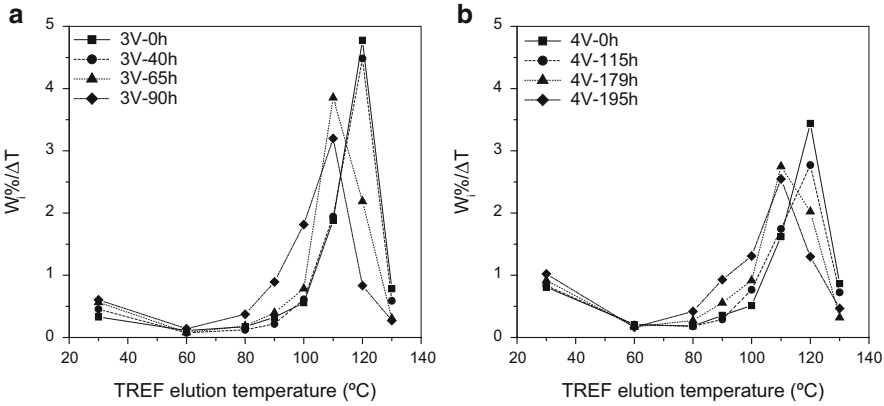

Fig. 2.23 TREF weight fraction per temperature increment curves ($W_i\%/\Delta T$) for the degraded samples 3V (**a**) and 4V (**b**) at different degradation times (reprinted from [83] with permission of Wiley-VCH)

were obtained for the middle fraction collected at 100 °C. The subsequent analysis of the fractions by ^{13}C-NMR, DSC, SEC and CRYSTAF demonstrated that the major constituents of the corresponding fractions of both products are the same; only the amounts differed.

Sample 4V showed a delayed induction and a slower oxidation rate. The reason for this behaviour is the higher ethylene content and lower isotacticity of the bulk sample. Further explanations of this behaviour include the relative amounts of the four major components within the two samples. Larger concentrations of amorphous EPR and transition EPC accompanied by a lower concentration of iPP were found in copolymer 4V by TREF analysis of the nondegraded sample. iPP degrades preferentially, for reasons explained earlier, despite of the presence of large amounts of amorphous material. Data from hyphenation of TREF fractionation with ^{13}C-NMR suggested that in the polymerization of sample 4V, the excess ethylene that is added during the second stage is located in the EPR and the transition EPC fractions.

The degradation behaviour of the two samples shows interesting trends. The most important factors that determine the degradation behaviour are the amount and distribution of ethylene in the four components of IPC. An increase in ethylene content induces higher chemical stability and a barrier effect of the comonomer in intrachain hydroperoxide formation. These effects account for the increase in oxidation induction time and stability. The morphology of IPCs is also affected by the amount of ethylene. The morphological variations include the shapes and sizes of the dispersed EPR phase and the nature of the segmented EPCs that act as compatibilizer at the interface between the EPR inclusions and the iPP matrix. The role of this interface is vital in the migration and combination of free radicals during the degradation of heterophase EPCs. It is therefore concluded that the stability differences between the two grades are attributed to their morphological disparity.

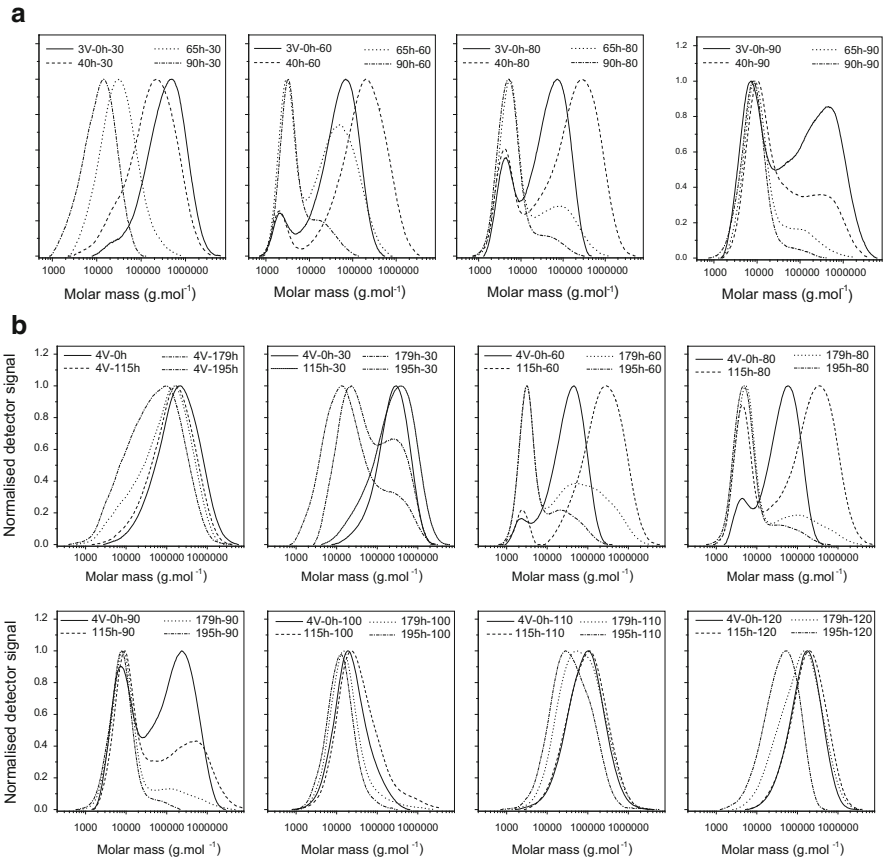

Fig. 2.24 Changes in molar mass distributions of TREF fractions from degraded samples 3V (**a**) and 4V (**b**). Sample codes are as follows: first number—degradation time in h, second number—TREF elution temperature (reprinted from [83] with permission of Wiley-VCH)

The unique morphology of these copolymers plays a very important role in governing the degradation, along with the effect of chemical composition. The study was extended to thicker specimens where oxygen diffusion is expected to play a greater role. FTIR microscopy and a conventional technique involving layer-by-layer milling followed by SEC, FTIR and CRYSTAF analyses were used to study the spatial heterogeneity within the copolymers 3V and 4V [99]. Details of hyphenation of TREF-SEC-FTIR are discussed in [100].

2.2 Crystallization Analysis Fractionation

Besides all the merits of TREF, one of the important shortcomings is the very long time that is required for the slow crystallization and elution steps. This makes a TREF experiment a very time-consuming procedure that requires from a few hours to a few days, depending on the experimental protocol. CRYSTAF was developed by Monrabal in 1999 to overcome this problem and to speed up the CCD analysis of olefin copolymers [8, 101]. CRYSTAF is based on the same principles of separation by crystallizability from dilute solutions but, instead of two steps—crystallization and elution, it makes use of only one step—crystallization. This crystallization takes place in a stirred vessel with no support. The polyolefin sample is dissolved at high temperature, followed by a slow decrease of the temperature of the solution. Depending on the composition of the sample, fractions of different crystallizability (chemical composition) precipitate out of solution at different temperatures.

The crystallization process is continuously monitored as a function of temperature using a suitable detector, typically a dual wavelength IR detector. Aliquots of the polymer solution are analysed by the detector after filtration through the internal filter in the vessel. The detector reading is assumed to provide relative concentration information. Consequently, a profile of polymer concentration in the solution as a function of temperature is obtained; it is termed as a cumulative CRYSTAF profile. As the temperature of the solution is decreased, an increasing fraction of polymer in solution crystallizes out and, accordingly, polymer concentration in solution decreases. Similar to TREF, a correlation between polymer concentration in solution at a given temperature and chemical composition is developed through a calibration curve. Copolymer standards with narrow CCDs are used to create the calibration curve for particular experimental conditions (cooling rate, comonomer type, solvent, etc.). The typical means of obtaining polyolefins with narrow CCDs are P-TREF fractionation or direct synthesis using single-site catalysts.

Polymer Char (Valencia, Spain) is the only supplier of CRYSTAF instrumentation; the schematic diagram of their commercial version is illustrated in Fig. 2.25. The instrument is equipped with five stainless steel crystallization vessels with stirrers and a temperature programmable oven for parallel analysis. A nitrogen line, a waste line and a sampling line with an inline filter are provided to all five vessels. A dual wavelength online IR detector is connected to the sampling line. The detector is also heated to 150 °C and polymer concentration in solution as a function of temperature is measured. A good solvent for the polymers such as TCB is used for dissolution of the sample, while keeping the concentration of the polymer in solution between 0.1 mg/mL and 1.0 mg/mL. Interchain interactions and co-crystallization could occur if higher concentrations are used. On the other hand, low concentrations can lead to poor signal-to-noise ratio (SNR). Experience and literature suggest that the most suitable stirring rate during dissolution and stabilization is 200 rpm. The stirring rate should be reduced to 100 rpm during crystallization. The Co-crystallization should be avoided by cooling at a very slow rate. A typical cooling rate is kept at 0.1–0.2 °C/min during the crystallization step.

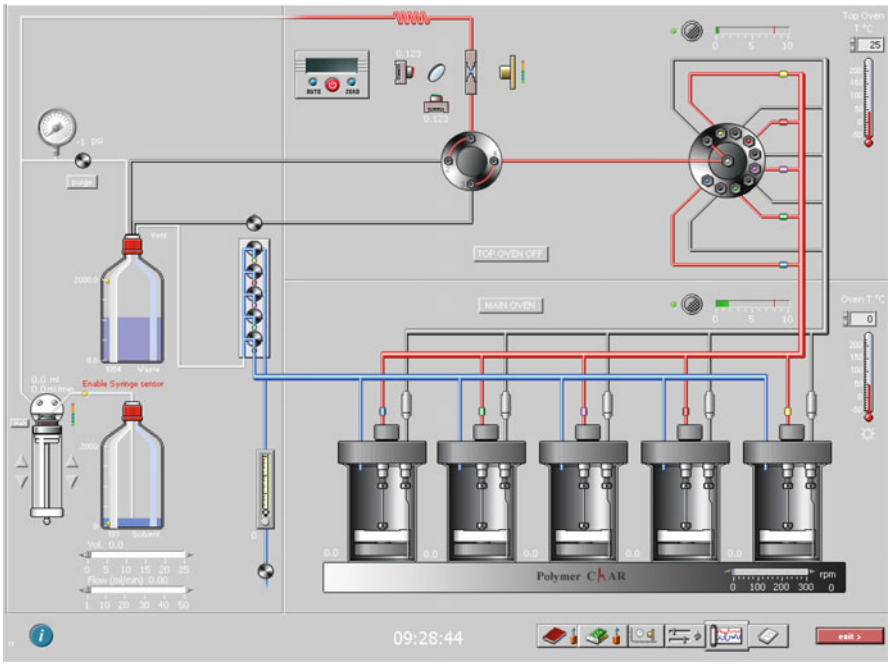

Fig. 2.25 Systematic diagram of a CRYSTAF instrument (Polymer Char, Spain) (screenshot from instrument)

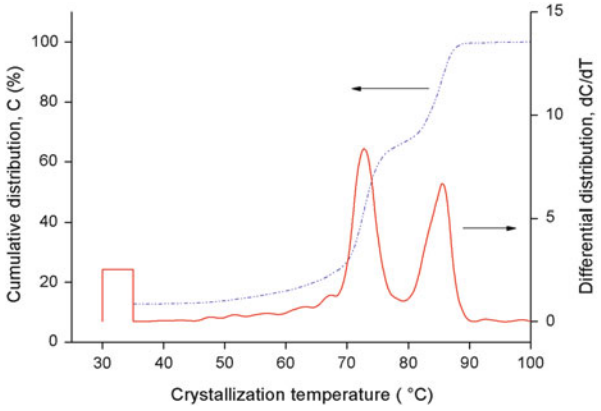

Fig. 2.26 Cumulative and differential CRYSTAF profiles of a blend of HDPE and PP

The differentiation of the integral CRYSTAF profile at each temperature provides the amount of polymer crystallizing at each temperature. The CRYSTAF plot presents the polymer crystallized as a function of temperature. It is the most widely used and lucid representation of CRYSTAF results. Figure 2.26 depicts the integral and differential profile for a blend of HDPE and PP. The molar mass of the polymer,

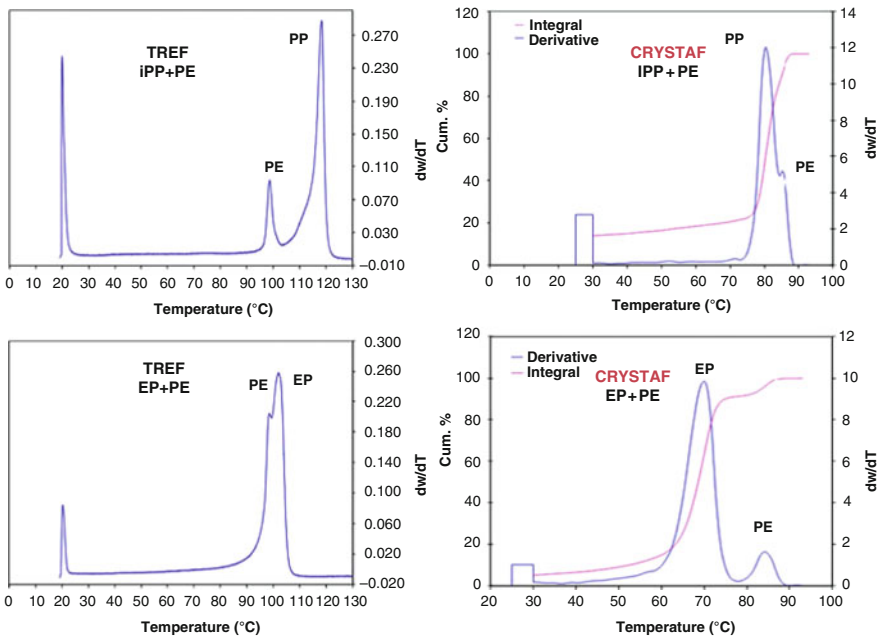

Fig. 2.27 TREF and CRYSTAF analysis of PE–PP combinations showing the different fractionation capabilities (reprinted from [9] with permission of Springer Science + Business Media)

the comonomer type and content, the cooling rate and co-crystallization effects must be taken into account for reliable CRYSTAF profiles, as is the case with TREF. Comprehensive reviews on crystallization-based techniques summarize the state of the art up to 2005 [12, 102]. More recent information is given in [9, 10].

As pointed out earlier, CRYSTAF was developed originally as a faster version of crystallization fractionation and it was assumed that TREF and CRYSTAF would produce similar results. This is not entirely correct, as can be seen from a comparison that was presented by by Monrabal [9]. TREF data are generated in the dissolution step while CRYSTAF data refer to the crystallization step. Each step works differently, e.g. for iPP, PE and EP copolymers; see Fig. 2.27. In TREF, iPP and PE are adequately fractionated, with iPP eluting at a higher temperature. This is not the case in CRYSTAF due to the undercooling effect for iPP resulting in crystallization of iPP and PE at nearly the same temperature. On the other hand, CRYSTAF fractionates EP and PE adequately, while in TREF the resolution of this fractionation is rather poor.

2.2.1 Characterization of Homogeneous Ethylene–Octene Copolymers [103]

For the last 30 years LLDPE has been produced mainly using multiple-site (Ziegler–Natta, ZN) catalysts. These copolymers have broad (multimodal) CCDs, which has a strong impact on product performance. The CCD of olefin copolymers is also referred to as short chain branching distribution (SCBD).

The fractionation of EO copolymers by TREF has been discussed in Sect. 2.1.1. It has been shown that ZN LLDPEs contain a highly crystalline fraction of HDPE and fractions of very low crystallinity that have high comonomer contents.

2.2.1.1 Aim

In the present application, the CCD of homogeneous EO copolymers shall be analysed by CRYSTAF. Such LLDPEs are typically produced by using a single-site (constrained geometry) catalyst. The correlation between crystallization temperature and comonomer content shall be investigated and the data shall be used for calibrating CRYSTAF/TREF. Finally, the behaviour of these homogeneous LLDPEs shall be compared to a commercial ZN LLDPE.

2.2.1.2 Materials

- *Polymers*. A series of 17 samples of EO copolymers produced by Dow Chemical in a solution process with a constrained geometry catalyst, sample densities 0.868–0.935 g/cm^3, melt indexes (at 190 °C, with 2.16 kg, according to ASTM D1238) are 0.5–30 dg/min.

2.2.1.3 Equipment

- *CRYSTAF system*. Commercial CRYSTAF instrument model 100 (Polymer Char, Valencia, Spain).
- *Detector*. Built-in dual wavelength IR detector with heated flow-through micro cell at 150 °C.
- *Solvent*. TCB.
- *Crystallization protocol*. Crystallization between 90 °C and 30 °C (in selected cases between 90 °C and 5 °C) at a rate of 0.2 °C/min.
- *Sample concentration*. 30 mg in 30 mL TCB.

2.2.1.4 Preparatory Investigations

As a first step of the investigation, the homogeneous EO copolymers were measured. Figure 2.28 shows the CRYSTAF curves of three representative samples. As expected, the samples exhibit monomodal and narrow crystallization profiles, which are a clear indication of their narrow CCDs.

The CRYSTAF results of all samples are summarized in Table 2.5 and compared to other analytical data.

The calculation of the weight and number average crystallization temperatures T_w and T_n, respectively, and the parameters measuring the broadness of the CCD, are as follows:

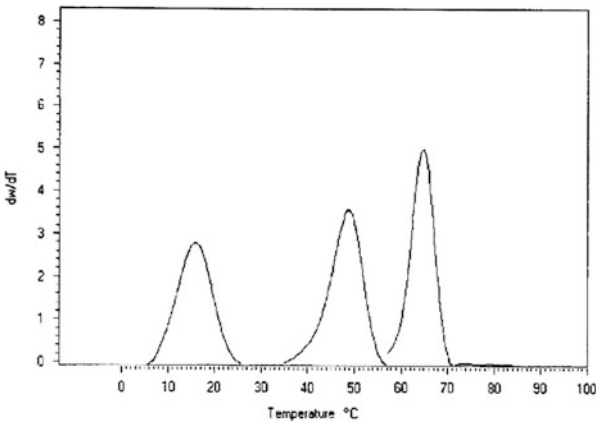

Fig. 2.28 CRYSTAF analysis of three homogeneous LLDPEs (reprinted from [103] with permission of J. Wiley & Sons)

Table 2.5 CRYSTAF and analytical results for EO copolymer samples (reprinted from [103] with permission of J. Wiley & Sons)

T_c (°C)	T_w (°C)	Sigma	R	Weight % Octene	Density	M.I.
8.9	6.8	5.2	–	41	0.868	0.5
16.2	13.7	7.3	–	38	0.875	3
23.1	12.4	12.8	–	36	0.88	18
32	27.2	9.9	–	30.6	0.885	1
40.7	38.1	7.7	–	23.1	0.895	1.6
50.9	47.4	8	6	19.1	0.902	1
49.5	47.4	6.3	2.3	19.5	0.902	3
48.8	45.9	7.9	10.5	19.3	0.902	3
45.5	41.2	9.8	14.2	19.7	0.902	30
59.1	57.4	4.9	1	13.8	0.91	0.5
58.7	57.3	4.3	0.6	14.3	0.91	1
56	54.7	5.5	1.2	15.1	0.91	3.5
59.4	56.7	6.5	1.8	14.8	0.911	6
56.6	52.1	8.7	3.7	15.1	0.913	30
57	50.3	9.3	4.6	15.2	0.913	30
64.8	63.6	4.2	0.5	10.8	0.915	1
						2
78.7	78.1	4.1	0.5	2.5	0.935	

T_c is the peak crystallization temperature, T_w is the weight-average crystallization temperature, Sigma and R are parameters defining the broadness of the CCD as per equations 2.3 and 2.4

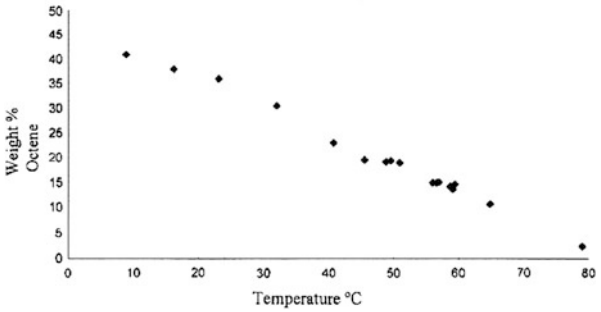

Fig. 2.29 CRYSTAF calibration curve based on homogeneous EO copolymers (reprinted from [103] with permission of J. Wiley & Sons)

$$T_w = \frac{\Sigma c_i \cdot T_i}{\Sigma c_i} \quad T_n = \frac{\Sigma c_i}{\Sigma c_i / T_i} \tag{2.3}$$

$$\sigma = \sqrt{\frac{\Sigma c_i \left(T_i^2 - T_w^2\right)}{\Sigma c_i}} \quad R = \left(\frac{T_w}{T_n} - 1\right) \cdot 100 \tag{2.4}$$

2.2.1.5 Discussion and Evaluation

As is seen in Table 2.5, most of the copolymer samples exhibit narrow CCDs. This makes them good candidates as calibration standards for CRYSTAF and TREF. Such calibrations are required to relate the crystallization (or elution) temperature to the comonomer content. For such copolymers, it is assumed that they are strictly linear and do not have long chain branches. Based on comonomer contents, analysed by ^{13}C-NMR spectroscopy, a calibration plot of crystallization temperature vs. wt% octene can be constructed. As is seen in Fig. 2.29, a straight line is obtained that indicates (1) a good correlation with the equilibrium theory of Flory, and (2) the crystallization temperature is practically independent of molar mass (see melt index in Table 2.5).

The present calibration curve can be used to quantify the CCD of EO copolymers irrespective of their origin and production process. As an example, the CRYSTAF analysis of a heterogeneous ZN LLDPE material is shown in Fig. 2.30.

In contrast to the CCDs in Fig. 2.28, this polymer shows a broad CCD, with a component that crystallizes at high temperature (HDPE), a range of components that crystallize between 70 °C and 30 °C (crystallizable EO copolymers with increasing EO contents) and non-crystallizable components (EO copolymers with a high octene content). In CRYSTAF, the non-crystallizable (soluble) components are presented as a rectangular concentration profile. The temperature axis as shown in Fig. 2.30 can be converted into a 'wt% octene' axis using the calibration curve in Fig. 2.29.

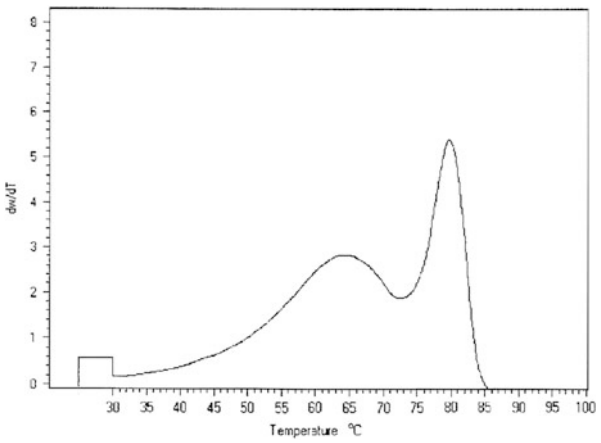

Fig. 2.30 CRYSTAF analysis of a heterogeneous ZN LLDPE (reprinted from [103] with permission of J. Wiley & Sons)

2.2.2 Analysis of Blends of Polyethylene and Polypropylene [104]

Polymer blends are very important commercial materials that combine useful properties of different polymers in a single product without involving any chemical reaction. The approach provides a good alternative to developing new tailor-made polymeric structures. The blending is a particularly feasible and commercially viable approach for polyolefins. Polyolefin blends ranging from blends of homopolymers to blends of homo- and copolymers are commercially available to achieve some selected application properties.

There are no universal methods available for the identification and quantitative determination of blend components and this is a demanding analytical challenge. The most widely used techniques for this purpose are spectroscopic techniques such as FTIR and NMR. These are averaging techniques; they are unable to differentiate between mixtures of two homopolymers and a copolymer with similar chemical compositions. Therefore, a separation step is often required prior to spectroscopic analysis for proper characterization of these complex polymers. This is particularly challenging for polyolefin blends because they dissolve only at high temperatures.

The most widely used method to separate polymer blends is the separation according to molar mass by SEC. This is only a viable method if the blend components have sufficiently different molar masses. DSC or TREF provide other approaches for compositional analysis by determining the melting and crystallization behaviour, respectively. DSC is advantageous in the analysis of blends due to the required equipment being simple and widely available. Another advantage of using DSC for blend analysis is that very small amounts of components can be detected. However, quantitative analysis by DSC is problematic. Thermal history problems that must be considered in DSC are eliminated in TREF as crystallization takes place from dilute solutions. TREF has been successfully used for the separation of copolymers and polymer blends [16, 105–109]. The separation and quantification of different components of the blends of HDPE, LDPE, LLDPE

and PP are possible. The long analysis times and the inefficiency in separating PE and EP copolymers are the only limitations of TREF.

2.2.2.1 Aim

In the present application, the capabilities of CRYSTAF for the fractionation of polyolefin blends shall be explored. CRYSTAF is faster than TREF and is based on a single crystallization step of the blend components out of the solution. The detection limit of each component shall be determined and compared to DSC for investigation of blends of metallocene-catalysed PE and PP. The successful separation and quantification of blends of commercial HDPE, LDPE and PP shall be demonstrated. Finally, the analysis of recycled polyolefins by CRYSTAF shall be discussed. It shall be demonstrated that CRYSTAF can be the workhorse of the polyolefin industry for routine analysis of complex polyolefin blends to obtain direct quantitative results.

2.2.2.2 Materials

- *Polymers*. Laboratory products of metallocene-catalysed PE and PP, and commercial HDPE, LDPE and PP.

2.2.2.3 Equipment

- *CRYSTAF system*. CRYSTAF instrument model 200 (Polymer Char, Valencia, Spain).
- *Detector*. Built-in dual wavelength IR detector with heated flow-through micro cell at 150 °C.
- *Solvent*. TCB.
- *Crystallization protocol*. Crystallization between 100 °C and 30 °C, at a rate of 0.1 °C/min.
- *Sample concentration*. 30 mg in 30 mL TCB.
- *DSC*. Perkin-Elmer DSC 7 (Perkin-Elmer, Waltham, USA), heating and cooling rates of 10 °C/min were applied. DSC curves of the second heating cycle were used for analysis.
- *SEC*. Waters 150 HT-SEC apparatus (Waters Inc., Milford, USA) equipped with a differential refractometer, oven temperature 145 °C, mobile phase TCB, column set: Styragel 500 Å + HT3 + HT4 + HT5 + HT6, flow rate 1 mL/min.

2.2.2.4 Preparatory Investigations

Blends of metallocene-catalysed PE and PP were analysed by SEC and DSC as a first step. The molar masses of the blend components (PE 342 kg/mol and PP 143 kg/mol) are not very different. Therefore, SEC was not the technique of choice for this separation. The MMDs for PE/PP blends of varying compositions are shown in Fig. 2.31.

DSC separates with regard to melting or crystallization temperatures. PE melts at 132 °C while PP melts at 147 °C. The difference is sufficiently large to obtain well resolved melting peaks. As long as the concentration of PP exceeds 20 %, both components can be easily identified; see Fig. 2.32. For blends containing low

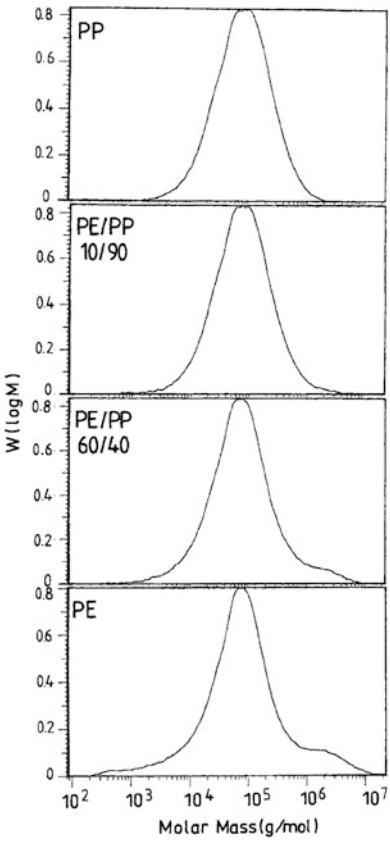

Fig. 2.31 SEC separation of metallocene-catalysed PE and PP and a PE/PP blend (reprinted from [104] with permission of Wiley-VCH)

amounts of PP, it is difficult to detect the PP peak in a routine experiment. The melt enthalpy is a function of crystallinity and thermal history of the sample; therefore, quantitative information on blend composition is rather difficult to obtain, unless further information on the samples is obtained by additional measurements.

2.2.2.5 CRYSTAF Fractionations

The CRYSTAF results of a variety of PE/PP blends are presented in Fig. 2.33. The crystallization temperatures of the blend components are clearly different. PE crystallizes at higher temperature (86.3 °C) compared to PP (70.5 °C). Narrow and well resolved crystallization peaks are obtained for both PE and PP. A true concentration profile is obtained directly, unlike with DSC. Therefore, the relative concentrations of the components can be calculated directly from the experimental results without further assumptions.

In contrast to DSC, very low concentrations of the blend components can be detected, as seen in Fig. 2.33. The detection limits for both components are very low (5 wt% for PP and 2–3 wt% for PE). As can be seen in Fig. 2.34, the experimental

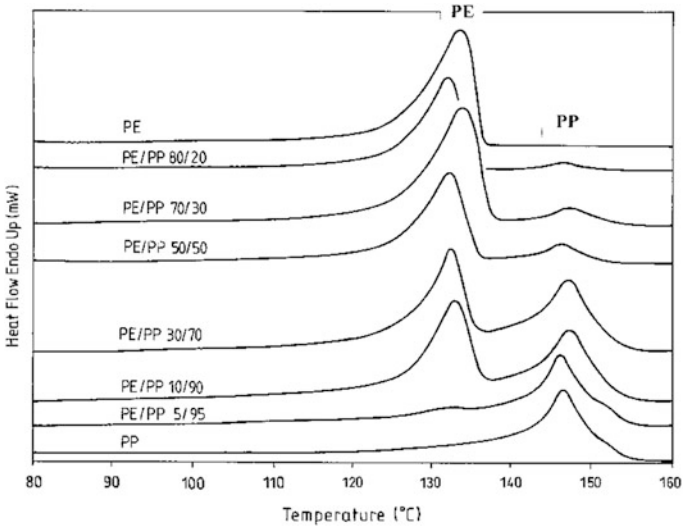

Fig. 2.32 DSC analysis of metallocene-catalysed PE and PP and PE/PP blends (reprinted from [104] with permission of Wiley-VCH)

blend composition as calculated by CRYSTAF agrees quite well with the nominal composition of the samples over the entire range of compositions.

2.2.2.6 Discussion and Evaluation

ZN-catalysed polyolefins and their blends still dominate industrial applications. DSC is not capable of analysing different blends of HDPE and LDPE because the melting temperatures of both components are quite similar and the DSC peaks are rather broad. The CRYSTAF analysis revealed excellent separation of blends with varying compositions of HDPE (Lupolen 5261Z) and LDPE (Lupolen 1800H), as can be seen in Fig. 2.35. The sharp crystalline peak for HDPE appeared at 88.0 °C and a small fraction of less than 5 % crystallized at lower temperature suggesting small amounts of less crystalline PE. At an even lower temperature of 59.1 °C, a broad crystallization peak for LLDPE is obtained.

The CRYSTAF analysis revealed well separated crystallization peaks for blends of HDPE and LDPE that can be quantified easily in the composition range of HDPE/LDPE 90/10 to 10/90. The lower detection limit for HDPE is less than 4 wt% in this case. The detection limit for LDPE is higher because HDPE itself contains some less crystalline material. The lower detection limit for LDPE in the present case is 10 wt%. Figure 2.36 demonstrates the comparison of CRYSTAF results with the nominal composition of the sample. Excellent agreement is found over the entire range of compositions.

An increasingly important topic is the characterization of waste plastics or materials resulting from recycling processes. Recycled plastics frequently contain several diverse components and these must be analysed with regard to their PP,

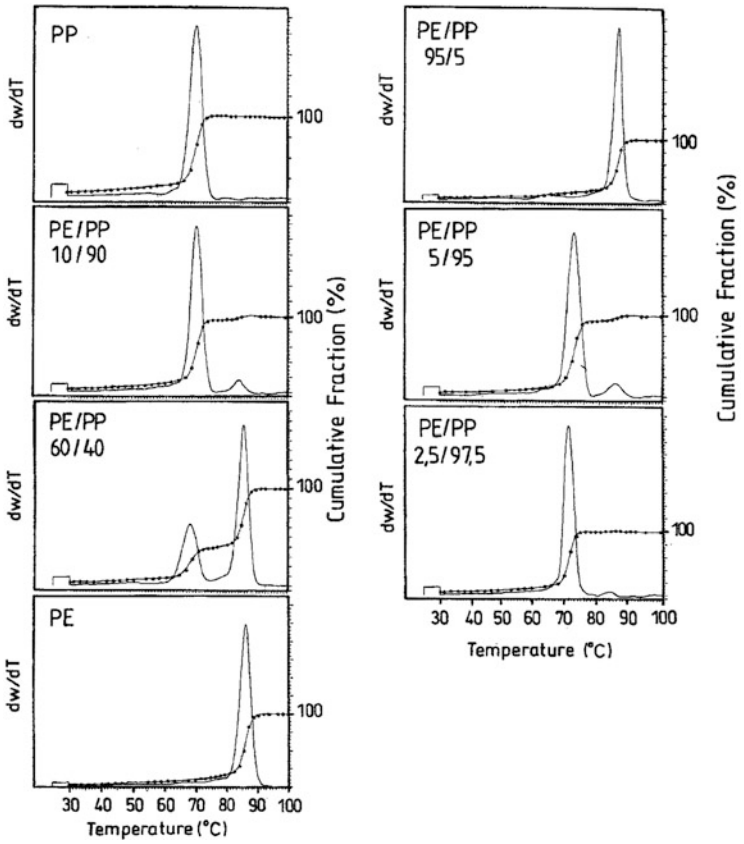

Fig. 2.33 CRYSTAF analysis of metallocene-catalysed PE and PP and PE/PP blends (reprinted from [104] with permission of Wiley-VCH)

HDPE and LDPE contents. DSC can be used to determine PP in such materials but as explained earlier the determination of the ratio of HDPE and LDPE in such materials by DSC is rather difficult. CRYSTAF is the method of choice for the analysis of such materials and three components can be easily identified and quantified. Figure 2.37 displays a comparison of CRYSTAF and DSC results of a waste plastic material. The three components, namely HDPE, PP and LDPE, can be recognized by their crystallization peaks and the peak areas directly reveal the concentration of the components. The crystallization peaks of the three components show slight overlapping. Nonetheless, the relative amounts of the three components can be determined to be about 40/27/33 wt%.

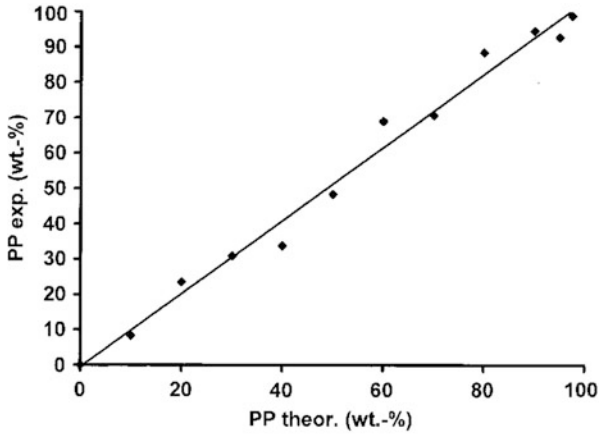

Fig. 2.34 Comparison of experimental and nominal PP content in PE/PP blends (reprinted from [104] with permission of Wiley-VCH)

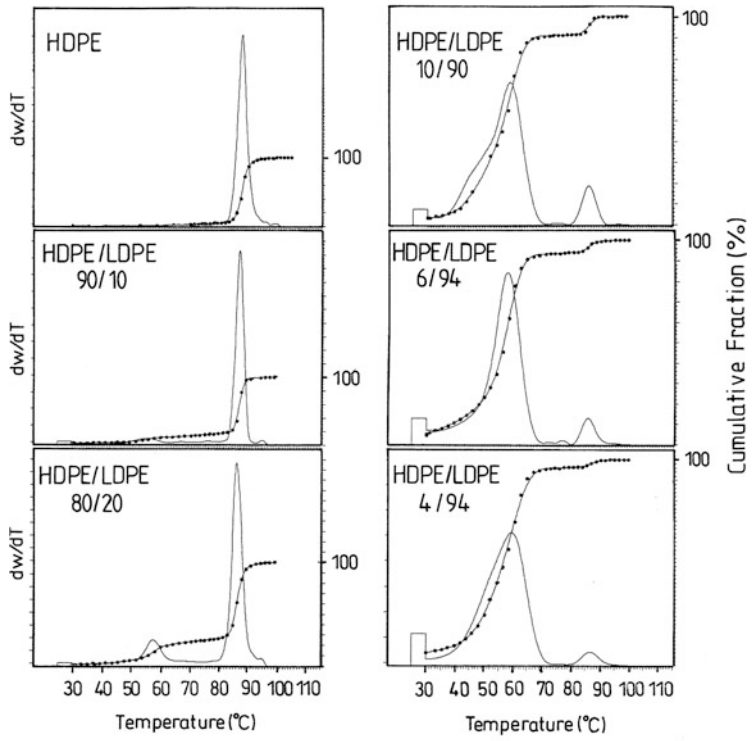

Fig. 2.35 CRYSTAF analysis of HDPE/LDPE blends (reprinted from [104] with permission of Wiley-VCH)

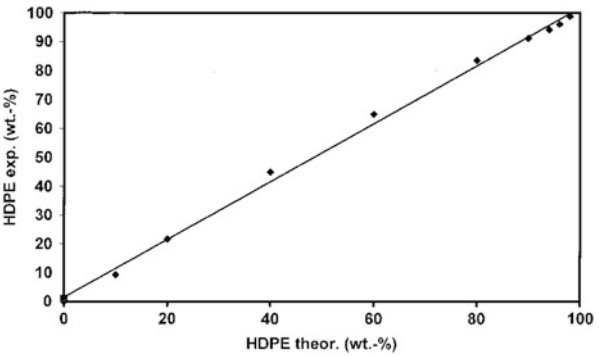

Fig. 2.36 Comparison of experimental and nominal HDPE content in HDPE/LDPE blends (reprinted from [104] with permission of Wiley-VCH)

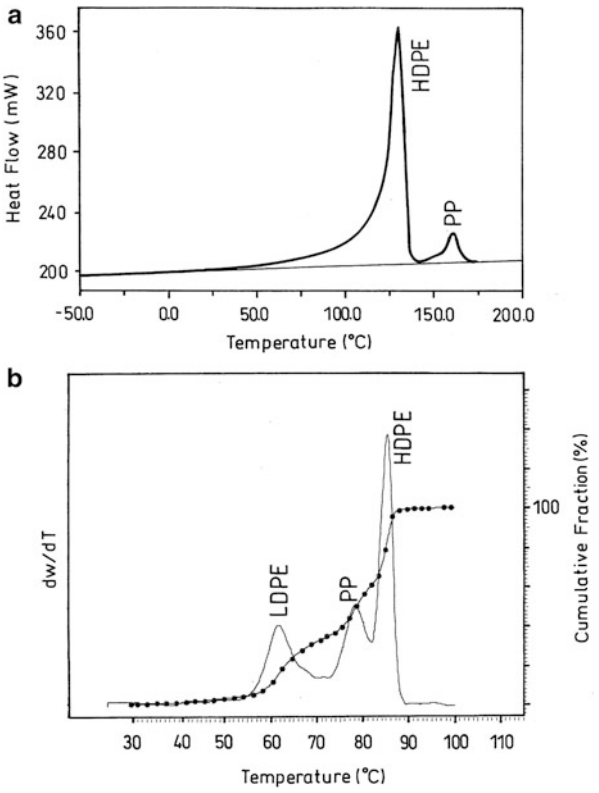

Fig. 2.37 Comparison of DSC (**a**) and CRYSTAF (**b**) of a waste plastic sample containing HDPE, LDPE and PP (reprinted from [104] with permission of Wiley-VCH)

2.2.3 Analysis of Copolymers of Propylene and Higher α-Olefins [110]

Random copolymers of ethylene and higher α-olefins are important commercial materials that are typically classified as LLDPE. In contrast to the technical

applications of LLDPE, random copolymers of propylene and higher α-olefins are less frequently investigated and used. Most of the work that has been done over the years has dealt with copolymers of propylene and ethylene, one example being IPCs; see, e.g. Sect. 2.1.2.

As has been discussed earlier (Sect. 2.2.1) there is a direct correlation between the crystallization temperature and the copolymer composition. This has been documented for LLDPEs with butene, hexene or octene as comonomers. The crystallization behaviour of random copolymers of ethylene was reviewed by Alamo and Mandelkern [111]. According to them, a linear relationship describes the melting temperature of ethylene/higher α-olefin copolymers versus the comonomer content up to 4 mol%. The type of comonomer has no effect on the melting temperature. In agreement with these findings, the CRYSTAF and TREF analysis of narrow LLDPE fractions revealed a linear correlation between crystallization temperature and comonomer content [8, 16]. The CRYSTAF and TREF apparatus were calibrated by the crystallization temperature of single-site ethylene-1-octene (EO) copolymers and the calibration was subsequently used for the analysis of broadly distributed industrial LLDPE samples [103].

2.2.3.1 Aim

There are numerous studies on the melting and crystallization behaviour of ethylene-α-olefin copolymers. However, copolymers based on propylene have not received much attention. In the present study, these copolymers shall be investigated by DSC and CRYSTAF. The influence of the comonomer shall be investigated for propylene copolymers with 1-octene, 1-decene, 1-tetradecene and 1-octadecene.

2.2.3.2 Materials

- *Polymers*. The copolymerizations were conducted according to the procedure described in [110]. The catalyst was $(CH_3)_2Si$(2-methylbenz[e]indenyl)$ZrCl_2$. The copolymer compositions are summarized in Table 2.6. The molar masses were determined by SEC.

2.2.3.3 Equipment

- *CRYSTAF system*. CRYSTAF instrument model 200 (Polymer Char, Valencia, Spain).
- *Detector*. Built-in dual wavelength IR detector with heated flow-through micro cell at 150 °C.
- *Solvent*. TCB.
- *Crystallization protocol*. Crystallization between 100 °C and 30 °C at a rate of 0.1 °C/min.
- *Sample concentration*. 20 mg in 30 mL TCB.
- *DSC*. Pyris 1 (Perkin-Elmer, Waltham, USA). Samples were cooled to −50 °C and then heated to 180 °C. From 180 °C, samples were again cooled to −50 °C. The cooling rate was kept at 10 °C/min. T_c was determined from the maximum

Table 2.6 Comonomer content, melting temperature T_m, crystallization temperature from melt T_c (melt) (DSC), crystallization temperature from solution T_c (sol) (CRYSTAF), molar masses and molar mass dispersities (adopted from [110] with permission of Wiley-VCH)

Sample	Comonomer	Comonomer (mol-%)	T_m (°C)	T_c (melt) (°C)	T_c (sol) (°C)	$\overline{M}_w$(g/mol)	$\overline{M}_w/\overline{M}_n$
3.1	None	0	149.0	112.4	75.4	460,700	2.80
8.8	1-Octene	0.47	141.1	101.6	66.4	600,200	2.34
8.5		0.55	140.1	99.0	62.9	539,700	2.47
8.7		0.57	142.1	99.1	63.7	421,500	2.19
8.4		0.86	137.1	90.0	58.9	456,900	2.25
8.6		1.27	125.7	77.4	50.8	156,200	3.11
8.2		2.89	108.2	66.7	34.9	303,800	1.94
8.9		3.43	106.4	64.8	30	304,500	2.15
10.6	1-Decene	0.42	145.9	96.4	63.4	466,200	2.30
10.8		0.47	144.4	98.6	65.9	448,800	2.64
10.7		0.72	140.6	95.2	58.3	428,300	2.24
10.5		0.78	145.9	100.9	63.7	272,100	2.28
10.4		1.07	138.2	89.7	57.1	427,700	2.21
10.3		1.39	128.1	84.7	49	372,700	2.39
10.2		2.31	115.4	67.0	38.7	297,400	2.10
10.9		2.39	111.9	70.1	30	346,800	2.05
14.8	1-Tetradecene	0.26	144.1	98.2	65.8	282,700	2.29
14.7		0.5	143.2	96.2	59.4	240,700	2.14
14.4		0.63	142.3	93.2	57.7	572,300	2.23
14.5		0.68	136.3	91.9	55.2	553,500	2.54
14.6		0.77	144.3	94.4	60.1	369,700	2.35
14.3		0.89	130.8	89.7	51.5	639,200	2.51
14.1		1.05	126.5	81.7	47	413,200	2.15
14.10		2.33	114.5	66.9	34.5	415,500	2.15
14.2		2.76	108.4	64.3	30	395,100	2.31
18.6	1-Octadecene	0.47	143.3	101.5	61.4	279,700	2.21
18.8		0.51	142.1	106.3	62.9	223,700	2.44
18.4		0.66	139.1	94.3	59	764,300	2.20
18.5		0.81	137.8	88.9	55.5	486,200	2.27
18.10		1.09	131.4	86.9	50.6	494,600	2.05
18.9		1.49	127.4	86.4	45	307,700	2.02
18.11		1.89	122.8	81.5	38.7	442,000	1.99
18.2		2.04	124.5	–	41.2	380,500	1.95

of the exotherm in the cooling cycle. While the sample was heated from −50 °C to 180 °C at a heating rate of 10 °C/min, the melting endotherm was recorded. T_m was determined from the peak maximum of the second heating cycle.

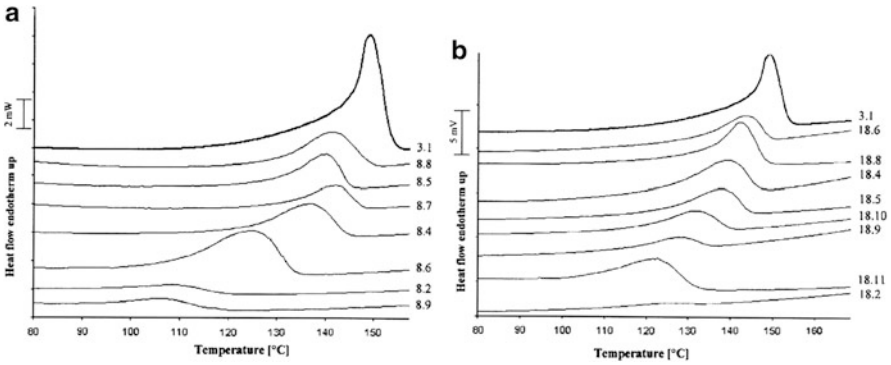

Fig. 2.38 DSC analysis of metallocene-catalysed propylene-α-olefin copolymers, second heating cycle, comonomer 1-octene (**a**), comonomer 1-octadecene (**b**) (reprinted from [110] with permission of Wiley-VCH)

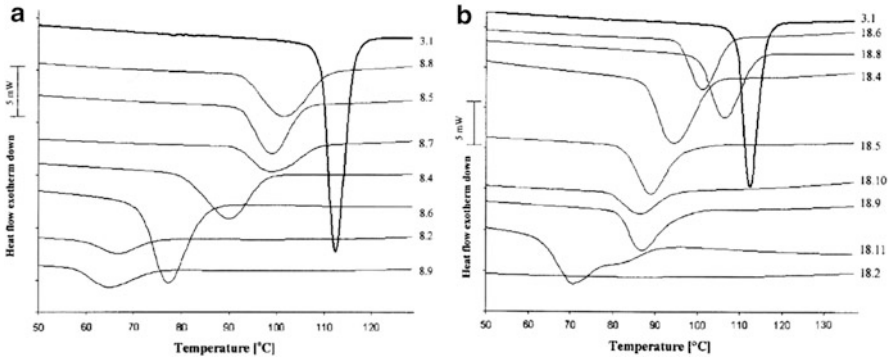

Fig. 2.39 DSC analysis of metallocene-catalysed propylene-α-olefin copolymers, first cooling cycle, comonomer 1-octene (**a**), comonomer 1-octadecene (**b**) (reprinted from [110] with permission of Wiley-VCH)

2.2.3.4 CRYSTAF and DSC Measurements

The copolymers were prepared by solution polymerization using a single-site catalyst. Conversions were kept to below 50 %. Comonomer contents were restricted to an upper limit of 3.5 mol%. ^{13}C-NMR spectroscopy was used to determine the amount of comonomer incorporated into the copolymer. All copolymers had high molar masses and low molar mass dispersities. The analytical data for the copolymers are summarized in Table 2.6.

The discussion of the thermal behaviour of the copolymers focuses on the 1-octene and the 1-octadecene copolymers as the two extremes. Their DSC heating and cooling curves are summarized in Figs. 2.38 and 2.39. The DSC curves are positioned according to the amount of comonomer incorporated. The peak melting temperature, T_m, was recorded from the maximum of the endotherm and the crystallization temperature from melt, T_c (melt), was recorded from the maximum

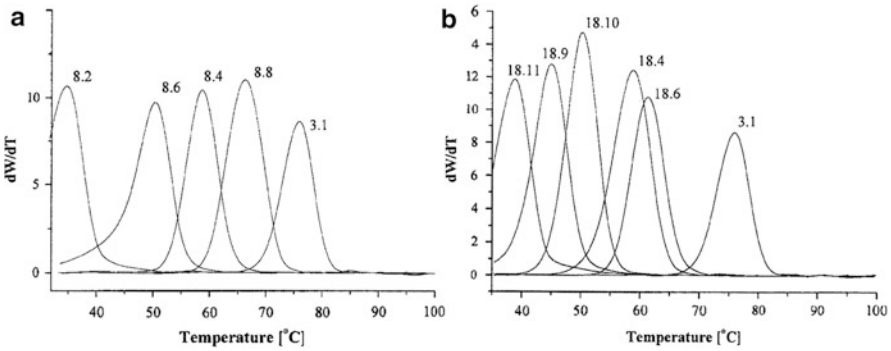

Fig. 2.40 CRYSTAF analysis of metallocene-catalysed propylene-α-olefin copolymers, comonomer 1-octene (**a**), comonomer 1-octadecene (**b**) (reprinted from [110] with permission of Wiley-VCH)

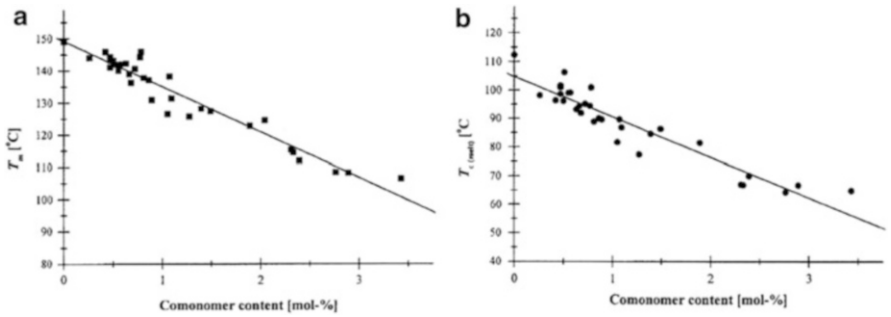

Fig. 2.41 Melting temperature T_m (**a**) and crystallization temperature T_c (melt) (**b**) as a function of copolymer composition, determined by DSC (reprinted from [110] with permission of Wiley-VCH)

of the exotherm. The melting temperatures obtained during the second heating cycle were considered in order to ensure identical thermal histories of the investigated copolymers.

The CRYSTAF analysis of the 1-octene and the 1-octadecene copolymers is shown in Fig. 2.40. Copolymers with higher comonomer contents (e.g. entries 8.2 and 18.11) partially crystallize at temperatures lower than 30 °C. This is not relevant in the current study because only the peak maximum temperatures are used in the discussion.

2.2.3.5 Discussion and Evaluation

The dependence of the melting temperature determined by DSC follows the expected linear relationship according to the Flory–Huggins theory. As expected, the nature of the comonomer does not influence the melting point depression. Figure 2.41a demonstrates the melting points of all synthesized propylene/α-olefin

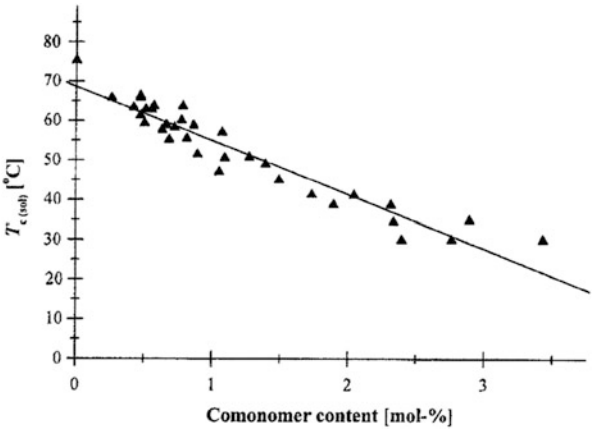

Fig. 2.42 Crystallization temperature T_c (sol) as a function of copolymer composition, determined by CRYSTAF (reprinted from [110] with permission of Wiley-VCH)

copolymers as a function of the comonomer content. It can be clearly seen that melting point depression is independent of the type of comonomer. The molar mass of the copolymers was not treated as an independent variable as the molar masses were sufficiently high not to be an influencing factor.

For the investigation of the crystallization behaviour, a constant cooling rate was applied to the crystallization from the melt (DSC) and from dilute solution (CRYSTAF). It is well accepted from TREF studies of polyolefins that above a molar mass of 15 kg/mol the crystallization behaviour is independent of the chain length [5]. The molar masses of propylene/higher α-olefin copolymers in the current study are well above this threshold; therefore crystallization behaviour is presumed to be independent of molar mass. DSC measurements provided T_c (melt), and are plotted against comonomer content of all copolymers; see Fig. 2.41b. The decrease of T_c (melt) with increasing comonomer content seems to be independent of the nature of the respective comonomers. The explanation given earlier for depression in the melting point being independent of the comonomer type is valid in this case too. After plotting the peak crystallization temperature from solution, T_c (sol) obtained by CRYSTAF versus the amount of comonomer incorporated, a straight line relationship is found. Similar to T_m and T_c (melt), T_c (sol) is independent of the nature of the comonomer; see Fig. 2.42.

All the illustrated regression curves summarized in Fig. 2.43 follow the linear relationship $y = -Ax + B$. The degree of the temperature depression for the melting process or the crystallization from melt as well as from dilute solution is described by coefficient A that is constant within experimental error, as can be seen in Table 2.7. The parallel lines for the regression curves in Fig. 2.43 manifest this fact. However, the crystallization from dilute solution occurs at significantly lower temperature than the crystallization process from melt.

It is important to mention here that the comonomers used in the current study had sufficiently bulky side chains to be excluded from all crystalline structures. The effect of lower α-olefins might not be the same. The copolymers composed of

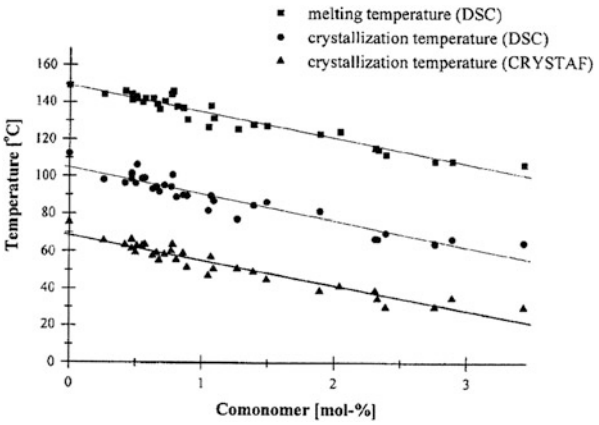

Fig. 2.43 T_m, T_c (melt) and T_c (sol) as a function of copolymer composition (reprinted from [110] with permission of Wiley-VCH)

Table 2.7 Regression curves calculated using least square regression analysis assuming the function $y = -Ax + B$ (y = melting/crystallization temperature in °C, x = comonomer content in mol%)

	A (°C/mol%)	B (°C)	R^2
Melting (DSC)	14.1 ± 0.7	149.1 ± 1.0	0.93
Crystallization (DSC)	14.2 ± 0.9	104.7 ± 1.3	0.88
Crystallization (CRYSTAF)	13.7 ± 0.8	68.6 ± 1.1	0.91

The best fit was obtained with the constants A and B. The coefficient of fit was R^2 (adopted from [110] with permission of Wiley-VCH)

propylene-1-butene showed crystalline behaviour over the entire range of compositions, indicating the co-crystallization of 1-butene with propylene [112].

2.3 Crystallization Elution Fractionation

A further refinement of crystallization-based fractionation techniques was recently introduced by Monrabal et al. with the development of crystallization elution fractionation (CEF) [113]. Combining the advantages of TREF and CRYSTAF, the aim of CEF is to improve the separation and to decrease the fractionation time. This is achieved by using dynamic crystallization as the first step of the process. In TREF, crystallization takes place in the column statically and all polymer fractions crystallize on the solid support at the same location, forming onion-like crystalline layers; see Fig. 2.1. In CEF, crystallization of the different polymer fractions takes place at different locations in the column. This is achieved by applying a small flow of the solvent in the column.

Figure 2.44 demonstrates the differences between normal TREF, dynamic crystallization and CEF. Figure 2.44a depicts the typical TREF process, where the first step is sample loading at high temperature, followed by stepwise crystallization of the polymer components by crystallizability. The same sample loading is the first

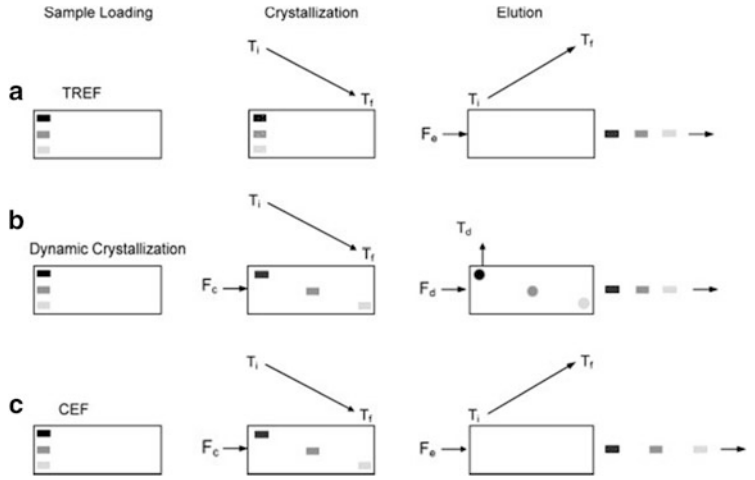

Fig. 2.44 Separation diagram by crystallizability. TREF (**a**), dynamic crystallization (**b**), CEF (**c**) (reprinted from [114] with permission of Wiley-VCH).

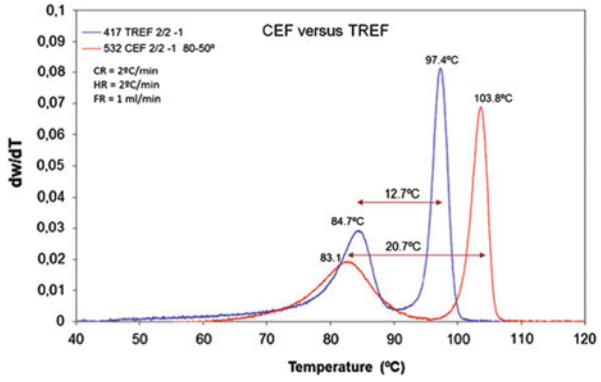

Fig. 2.45 Separation of two metallocene-type resins of very similar densities by TREF and CEF, cooling rate 2 °C/min, CEF crystallization flow 0.4 mL/min, elution flow 1 mL/min (reprinted from [9] with permission of Springer Science + Business Media)

step in dynamic crystallization where a continuous solvent flow is maintained through the column during the cooling process; see Fig. 2.44b. The polymer components that reach their crystallization temperatures will segregate and anchor on the support while other components in solution move along until they reach their crystallization temperatures. The physical separation of the polymer components is achieved with regard to crystallizability within the column in the crystallization cycle. The key to improving separation during the crystallization step is the flow rate. After the completion of crystallization, the solvent flow is stopped and dissolution of the polymer components is achieved by heating the column to higher

temperatures. To elute all different fractions, the solvent flow is started again at an appropriate rate.

The advantages of the two processes explained in Fig. 2.44a, b are combined in CEF. The sample loading step is the first step. It is the same for all three methods. The crystallization with a continuous flow through the column enhances the physical separation according to crystallinity during this step and this dynamic crystallization is combined with the typical TREF elution cycle as a next step; see Fig. 2.44c. The set-up resulted in enhanced resolution in a shorter time frame.

CEF has been shown to provide reproducible and very fast analyses of the compositional distribution of complex polyolefins, one application being in high-throughput experimentation [114]. Analysis times of less than 30 min could be achieved. The gain in separation from TREF to CEF is presented in Fig. 2.45 for a blend of two metallocene-type resins [9]. The crystallization peaks of the two components are separated by 20.7 °C for CEF compared to only 12.7 °C for TREF.

2.3.1 Analysis of Complex Polyolefins by CEF [113]

As mentioned earlier, CEF is faster than TREF and CRYSTAF, and significantly improved fractionations are obtained. This makes CEF an interesting alternative to the more conventional polyolefin fractionation techniques. CEF experiments can be conducted in a standard TREF instrument as they only require a typical tunable column oven and a HPLC pump to deliver the solvent flow. Similar to TREF, a range of different detectors can be used to monitor concentration, chemical composition and molar mass.

2.3.1.1 Aim

In the present application, a range of different complex polyolefins shall be fractionated. The experimental approach of CEF shall be described and the quality of fractionations obtained shall be discussed.

2.3.1.2 Materials

- *Polymers*. Metallocene-type resins with densities of 0.902 g/mL and 0.937 g/mL, Elite™ resin of Dow Chemical, LLDPE

2.3.1.3 Equipment

- *CEF*. CEF Instrument (Polymer Char, Valencia, Spain); see Fig. 2.46.
- *Detectors*. Dual wavelength IR detector, dual capillary viscometer.
- *Solvent*. ODCB.
- *Crystallization and elution protocol*. As described in the text.

2.3.1.4 CEF Measurements and Discussion

The fractionation of a typical complex polyolefin, Elite™ from Dow Chemical, is shown in Fig. 2.47. This fractionation was accomplished in only 23 min using very fast crystallization and heating rates (10 °C/min for both). Nevertheless, excellent

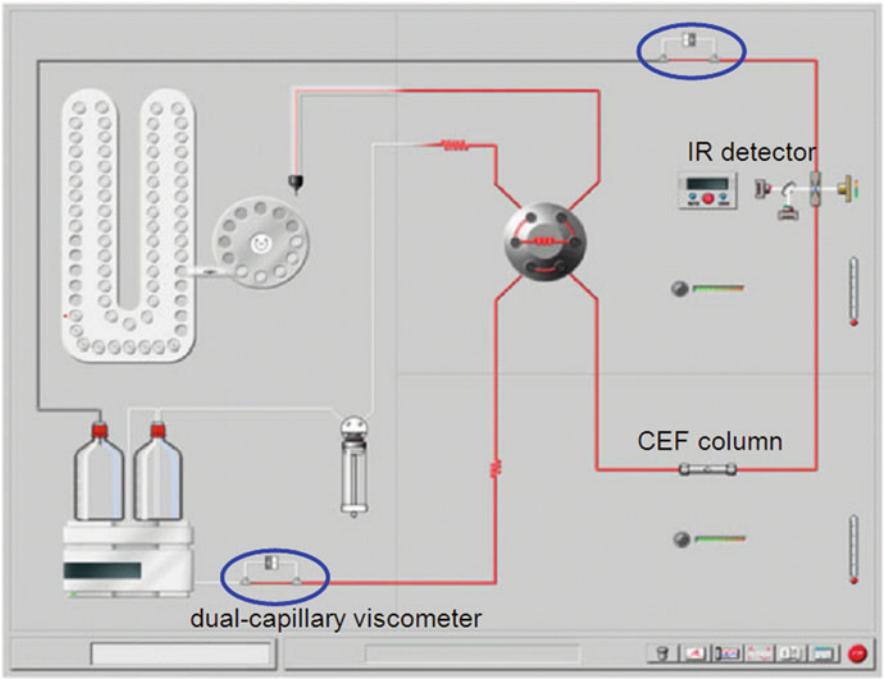

Fig. 2.46 Schematic diagram of instrument combining TREF, dynamic crystallization and CEF (reprinted from [113] with permission of Wiley-VCH)

separation into the different components is achieved. The reproducibility of multiple fractionations is very good, as can be seen in Fig. 2.48 for the same resin. This makes CEF a preferred choice for conducting fast and repeated fractionations, for example, of an unknown material. Sufficiently large fractions can be accumulated that allow further analyses, e.g. by NMR spectroscopy.

The separation of a LLDPE by multidetector CEF is presented in Fig. 2.49. The dual wavelength IR detector provides the concentration reading while the ratio of the CH_2 and CH_3 signals from the IR detector provides the copolymer composition (CH_3/1,000C). The molar mass is obtained from the online capillary viscometer reading that provides the intrinsic viscosity distribution.

To summarize, CEF is an interesting alternative method to TREF and CRYSTAF and can be performed in a simplified TREF instrument. Better information can be obtained in a fraction of the time that is required for TREF or CRYSTAF.

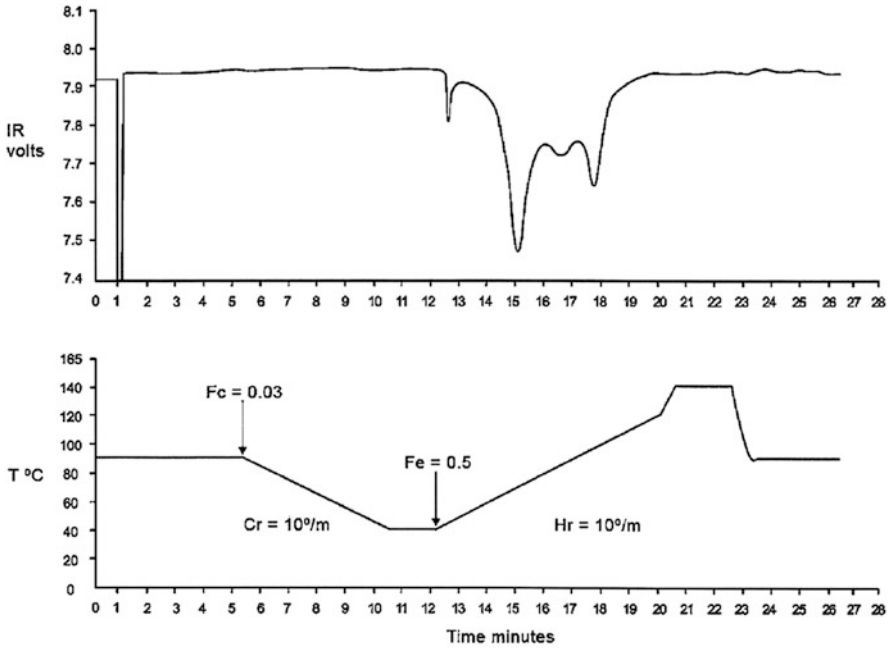

Fig. 2.47 CEF analysis of Elite™ resin: *top diagram* shows the IR concentration reading, *bottom diagram* shows the crystallization and elution temperature profiles (reprinted from [113] with permission of Wiley-VCH)

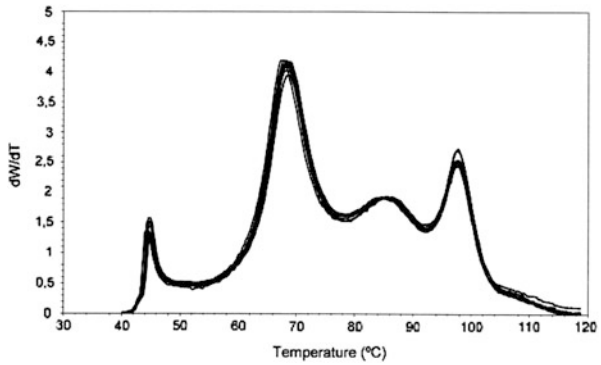

Fig. 2.48 Multiple CEF analyses (10 times) of Elite™ resin: crystallization rate 5 °C/min, heating rate 10 °C/min, elution flow rate 0.5 mL/min (reprinted from [113] with permission of Wiley-VCH)

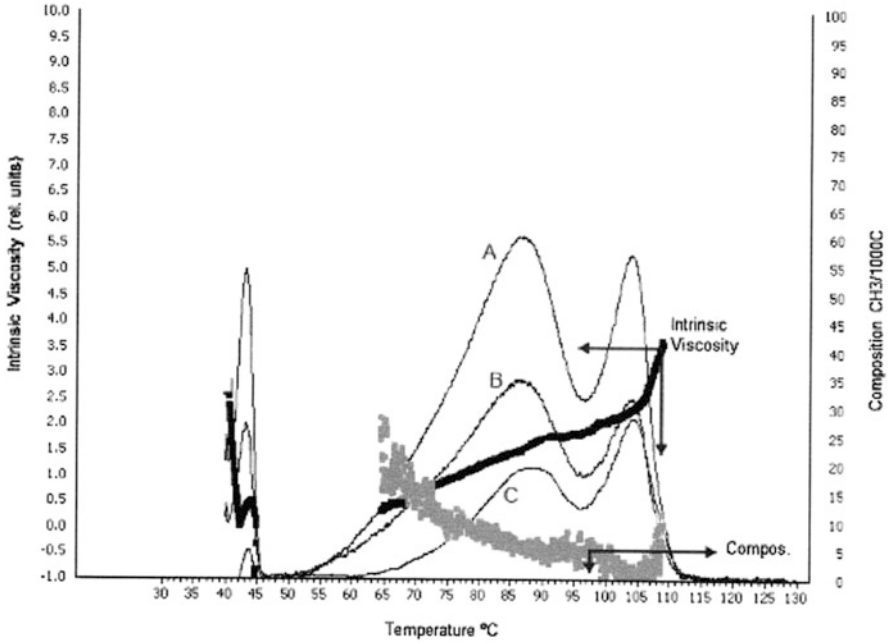

Fig. 2.49 CEF analysis of LLDPE: A—concentration, B—composition, C—intrinsic viscosity (reprinted from [113] with permission of Wiley-VCH)

References

1. Wild L, Ryle T, Knobeloch D, Peat IR (1982) J Polym Sci Polym Phys Ed 20:441
2. Wild L, Blatz C (1993) In: Chung T (ed) New advances in polyolefins. Plenum, New York, NY
3. Alamo R, Mandelkern L (1989) Macromolecules 22:1273
4. Monrabal B (1994) J Appl Polym Sci 52:491
5. Desreux V, Spiegels ML (1950) Bull Soc Chim Belg 59:476
6. Soares JBP, Hamielec AE (1999) In: Petrick RA (ed) Modern techniques for polymer characterization. Wiley, New York, NY, p 1
7. Anatawaraskul S, Soares JBP, Wood-Adams PM (2005) Adv Polym Sci 182:1
8. Monrabal B (2000) Temperature rising elution fractionation and crystallization analysis fractionation. In: Meyers RA (ed) Encyclopedia of analytical chemistry. Wiley, Chichester, p 9074
9. Monrabal B (2013) Adv Polym Sci 257:203
10. Pasch H, Malik MI, Macko T (2013) Adv Polym Sci 251:77
11. Flory PJ (1948) Trans Farad Soc 51:848
12. Flory PJ (1953) Principles of polymer chemistry. Cornell University Press, Ithaca, NY
13. Wunderlich B (1980) Macromolecular physics, vol 3. Academic, New York, NY
14. Huggins ML, Okamoto H (1967) Chapter A: Theoretical considerations. In: Cantow MJ (ed) Polymer fractionation. Academic, New York, NY
15. Mueller A, Arnal L (2005) Progr Polym Sci 30:559

16. Wild L (1991) Adv Polym Sci 98:1
17. Hazlitt LG (1990) J Appl Polym Sci Appl Polym Symp 45:25
18. Kuhlman RL, Klosin J (2010) Macromolecules 43:7903
19. Cossoul E, Baverel L, Martigny E, Macko T, Boisson C, Boyron O (2013) Macromol Symp 330:42
20. Monrabal B (2007) Microstructure characterization of polyolefins. In: Abstracts: advances in polyolefins, 23–26 September 2007, ACS, Division of Polymer Chemistry, Santa Rosa
21. http://www.polymerchar.com/pdf/Gel_Permeation_Chromatograph_with_integrated_Infrared_Detector_IR5_MCT_for_Polyolefin_Analysis.pdf
22. Tomba JP, Carella JM, Pastor JM (2005) J Polym Sci B Polym Phys 43:3083
23. Hasan ATMK, Liu B, Terano M (2005) Polym Bull 54:22
24. Hasan ATMK, Fang Y, Liu B, Terano M (2010) Polymer 51:362
25. Liu Y, Bo S, Zhu Y, Zhang W (2005) J Appl Polym Sci 97:232
26. Zhang Y (2006) J Appl Polym Sci 99:845
27. Assumption HJ, Vermeulen JP, Jarrett WL, Mathias LJ, van Reenen AJ (2006) Polymer 47:67
28. Harding GW, van Reenen AJ (2006) Macromol Chem Phys 207:1680
29. Suzuki S, Nakamura Y, Hasan ATMK, Liu B, Terano M, Nakatani H (2005) Polym Bull 54:311
30. Gupta P, Wilkes GL, Sukhadia AM, Krishnaswamy RK, Lamborn MJ, Wharry SM, Tso CC, DesLauriers PJ, Mansfield T, Beyer FL (2005) Polymer 46:8819
31. Shan CLP, Hazlitt LG (2007) Macromol Symp 257:80
32. Albrecht A, Brüll R, Macko T, Sinha P, Pasch H (2008) Macromol Chem Phys 209:1909
33. Zhu H, Monrabal B, Han CC, Wang D (2008) Macromolecules 41:826
34. Amer I, van Reenen A (2009) Macromol Symp 282:33
35. Anantawaraskul S, Bongsontia W, Soares JBP (2009) Macromol Symp 282:167
36. Vadlamudi M, Subramanian G, Shanbhag S, Alamo RG, Varma-Nai M, Fiscus DM, Brown GM, Lu C, Ruff CJ (2009) Macromol Symp 282:1
37. de Goede E, Mallon P, Pasch H (2010) Macromol Mater Eng 295:366
38. Nakano M, Goto Y (1981) J Appl Polym Sci 26:4217
39. Aust N, Beytollahi-Amtmann I, Lederer K (1995) Int J Polym Anal Char 1:245
40. Faldi A, Soares JBP (2001) Polymer 42:3057
41. Li Pi Shan C, Gillespie D, Hazlitt L (2005) The Dow Company, Ecorep, Lyon
42. Gillespie D, Hazlitt L, Li Pi Shan C (2006) Proceedings of the 1st International Conference on Polyolefin Characterization (ICPC), Houston, October 2006
43. Yau WW (2007) Macromol Symp 257:29
44. Ortin A, Monrabal B, Sancho-Tello J (2007) Macromol Symp 257:13
45. http://www.polymerchar.com/pdf/Automated_Crossfractionation_Chromatography_CFC.pdf
46. Zhang Z (2009) Macromol Symp 282:111
47. http://www.chemsystems.com/about/cs/news/items/POPS09_Executive%20Report.cfm
48. DesLauriers PJ, Rohlfing DC, Hsieh ET (2002) Polymer 43:159
49. Fox JJ, Martin AE (1937) Proc Royal Soc Lond 162:419
50. Arriola DJ, Carnahan EM, Hustad PD, Kuhlman RL (2006) Science 321:714
51. Galli P, Haylock JC, Simonazzi T (1995) Manufacturing and properties of polypropylene copolymers. In: Karger-Kocsis J (ed) Polypropylene: structure, blends and composites, vol 3. Chapman & Hall, London
52. Mirabella F (1993) Polymer 34:1729
53. Usami T, Gotoh Y, Umemoto H, Takayama S (1993) J Appl Polym Sci Appl Polym Symp 52:145
54. Fan Z, Zhang Y, Xu J, Wang H, Feng L (2001) Polymer 42:5559
55. Xu J, Feng L, Yang S, Wu Y (1997) Polymer 38:4381
56. Sun Z, Yu F, Qi Y (1991) Polymer 32:1059

57. Feng Y, Hay JN (1998) Polymer 39:6723
58. Randall JC (1989) JMS-Rev Macromol Chem Phys C29:201
59. Tosi C, Ciampelli F (1973) Adv Polym Sci 12:87
60. Baker BB, Bonesteel JK, Keating MY (1990) Thermochim Acta 166:53
61. Xu J, Fu Z, Fan Z, Feng L (2002) Eur Polym J 38:1739
62. Zacur R, Goizueta G, Capiati N (1999) Polym Eng Sci 39:921
63. Ray GJ, Johnson PE, Knox JR (1977) Macromolecules 10:773
64. Randall JC (1978) Macromolecules 11:33
65. Kanezaki T, Kume K, Sato K, Asakura T (1993) Polymer 34:3129
66. Zacur R, Goizueta G, Capiati N (2000) Polym Eng Sci 40:1921
67. Nakatani H, Manabe N, Yokota Y, Minami H, Suzuki S, Yamaguchi F, Terano M (2007) Polym Int 56:1152
68. Kakugo M, Miyatake T, Mizunuma K, Kawai Y (1988) Macromolecules 21:2309
69. Pasch H, Trathnigg B (2013) Multidimensional HPLC of polymers. Springer, Berlin
70. Verstrate G, Cozewith C, West RK, Davis WM, Capone GA (1999) Macromolecules 32:3837
71. Ozzetti RA, De Oliveira Filho AP, Schuchardt U, Mandelli DJ (2000) Appl Polym Sci 85:734
72. Albrecht A, Heinz LC, Lilge D, Pasch H (2007) Macromol Symp 257:46
73. Bly RM, Kiener PE, Fries BA (1966) Anal Chem 38:217
74. Luongo JPJ (1960) Appl Polym Sci 3:302
75. Andreassen E (1999) Infrared and Raman spectroscopy of polypropylene. In: Karger-Kocsis J (ed) Polypropylene: an A-Z reference. Kluwer, Dordrecht, p 320
76. Painter PC, Watzek M, Koenig JL (1977) Polymer 18:1169
77. Monasse B, Haudin JM (1995) Molecular structure of polypropylene homo- and copolymers. In: Karger-Kocsis J (ed) Polypropylene: structure, blends and composites. Chapman & Hall, London
78. Quynn RG, Riley JL, Young DA, Noether HDJ (1959) Appl Polym Sci 2:166
79. Stein RS, Sutherland GBBM (1953) J Chem Phys 21:370
80. Tobin MC, Carrano MJJ (1957) Polym Sci 24:93
81. Drushel HV, Iddings FA (1963) Anal Chem 35:28
82. Snyder RG, Maroncelli M, Strauss HL, Hallmark VM (1986) J Phys Chem 90:5623
83. de Goede E, Mallon P, Pasch H (2012) Macromol Mater Eng 297:26
84. Struik LCE (1987) Polymer 28:1521
85. Halim Hamid S (2000) Handbook of polymer degradation. Marcel Dekker, New York, NY
86. Michaeli W, Bittner M (1992) In: Menges G, Michaeli W, Bittner M (eds) Recycling von Kunststoffen. Carl Hanser, München
87. Kroschwitz J (1986) Encycl Polym Sci. Wiley, New York, NY
88. Bolland JL, Gee G (1946) Trans Faraday Soc 42:236
89. Bolland JL, Gee G (1946) Trans Faraday Soc 44:669
90. Gugumus G (1995) Polym Degrad Stab 49:28
91. Niki E, Dekker C, Mayo FR (1973) J Polym Sci Part A Polym Chem 11:2813
92. Adams JH (1970) J Polym Sci Part A-1 8:1077
93. Adams JH, Goodrich JE (1970) J Polym Sci Part A-1 8:1269
94. Lacoste J, Vaillant D, Carlsson DJ (1993) J Polym Sci Part A Polym Chem 31:715
95. Gijsman P, Kroon M, van Oorschot M (1996) Polym Degrad Stab 51:8
96. Lacoste J, Carlsson DJ (1992) J Polym Sci Part A Polym Chem 30:493
97. de Goede S, Brüll R, Pasch H, Marshall N (2003) Macromol Symp 193:35
98. de Goede S, Brüll R, Pasch H, Marshall N (2004) e-polymers no. 012
99. de Goede E, Mallon P, Pasch H (2011) Macromol Mater Eng 296:1018
100. Pasch H, de Goede E, Mallon P (2012) Macromol Symp 312:174
101. Monrabal B (1991) Crystallization analysis fractionation. US Patent 5,222,390
102. Soares JBP, Anantawaraskul S (2005) J Polym Sci Part B Polym Phys 43:1557
103. Monrabal B, Blanco J, Nieto J, Soares JBP (1999) J Polym Sci Part A Polym Chem 37:89
104. Pasch H, Brüll R, Wahner U, Monrabal B (2000) Macromol Mater Eng 279:46

105. Wild L (1993) Trends Polym Sci 1:50
106. Karoglanian SA, Harrison IR (1996) Polym Eng Sci 36:731
107. Soares JBP, Hamiliec AE (1995) Polymer 36:1639
108. Mara JJ, Menard KP (1994) Acta Polym 45:378
109. Joskowicz PL, Munoz A, Barrera J, Mueller AJ (1995) Macromol Chem Phys 196:385
110. Brüll R, Pasch H, Raubenheimer HG, Sanderson RD, van Reenen AJ, Wahner UM (2001) Macromol Chem Phys 202:1281
111. Alamo RG, Mandelkern L (1994) Thermochim Acta 238:155
112. Arnold M, Henschke O, Knorr J (1996) Macromol Chem Phys 197:563
113. Monrabal B, del Hierro P (2011) Anal Bioanal Chem 399:1557
114. Monrabal B, Sancho-Tello J, Mayo N, Romero L (2007) Macromol Symp 257:71

Column-Based Chromatographic Techniques

3

Crystallization-based fractionation techniques are powerful methods for the chemical composition fractionation of semi-crystalline polyolefins. The crystallizing components are fractionated according to their crystallizability, which for copolymers is a function of copolymer composition. The non-crystallizing part cannot be fractionated and is obtained as a bulk fraction ('soluble fraction'). Crystallization-based fractionation techniques are far less sensitive to molar mass than they are to chemical composition. In the past, different methods of temperature and solvent–nonsolvent based fractionations have been used, as summarized by Francuskiewicz [1].

In contrast to crystallization-based fractionation techniques, liquid chromatography (LC) exploits specific interactions of the analyte with the separation medium to achieve a separation according to molar mass, chemical composition or molecular topology. In the case of LC, the separation medium is a stationary phase. An alternative is field-flow fractionation (FFF), where the separation medium is a channel that is exposed to an external field.

In column- and channel-based fractionation techniques, the sample is completely dissolved in a suitable solvent (the mobile phase) and then injected into the separation medium. There, the sample may precipitate or remain in solution. In any case, the separation is based on the interaction of all analyte molecules with the separation medium irrespective of crystallinity. Different from crystallization-based fractionation, in column- or channel-based fractionations all components of the analyte are separated regarding specific molecular parameters.

Column-based fractionation techniques have been used in polymer analysis for more than 60 years. First, size exclusion chromatography (SEC) was introduced, followed by different methods of interaction chromatography. The former separates according to hydrodynamic volume of polymer species in solution, therefore providing information on molecular size and molar mass. In contrast, the latter is used mainly for separations according to chemical composition, functionality and molecular topology. Extensive information on the theory and the experimental

H. Pasch, M.I. Malik, *Advanced Separation Techniques for Polyolefins*, Springer Laboratory, DOI 10.1007/978-3-319-08632-3_3

aspects of column-based fractionations for the analysis of complex polymers is given in a number of monographs [2–5].

For the molar mass analysis of polyolefins, high-temperature (HT) SEC has been used routinely for more than 40 years [6–8]. The commercial versions of corresponding HT chromatography instruments have been available since 1964. Several detectors such as refractive index (RI), viscometer (Visco), light scattering (LS) or infrared (IR) may be equipped with the instruments. Due to the niche market of HT-SEC instruments, only a few types of instruments are available, including the Agilent PL-GPC 220 [9], the Malvern/Viscotek HT-GPC [10] and the GPCIR of Polymer Char [11].

SEC at elevated temperatures (HT-SEC) is a fast, reliable and precise method for the measurement of molar mass averages, molar mass dispersity and the complete molar mass distribution (MMD) of polyolefins. Different detectors and calibration options can be added to modify the technique according to the complexity of the samples [12, 13]. Different options include (1) conventional HT-SEC with a concentration detector, (2) HT-SEC-LS and (3) HT-SEC-Visco. Three online detectors are frequently used in a single SEC system, termed a triple-detector SEC (TriSEC). In TriSEC, an online viscometer and a multiangle laser light scattering (MALLS) instrument are coupled to SEC in addition to a concentration detector such as RI. With TriSEC, absolute molar mass determination is possible for polymers that are very different in chemical composition and molecular conformation. The usefulness of the TriSEC approach has been demonstrated in a number of applications [14–20].

In this part, different modes of column-based chromatographic techniques for the analysis of complex polyolefins will be discussed. Multidetector HT-SEC will be used for molar mass analysis while chemical composition analysis will be conducted using different modes of HT interaction chromatography. The multidimensional analysis of complex polyolefins by two-dimensional liquid chromatography (2D-LC) or the coupling with powerful spectroscopic detectors will be presented.

3.1 Multidetector Size Exclusion Chromatography

As mentioned earlier, most polyolefins are soluble only at high temperatures. This is a challenge for column-based chromatography because the complete system from sample injection to the detector must be kept at high temperature to prevent the polyolefin fractions from precipitating out of solution. Most polyolefins dissolve only at temperatures above their melting points, usually between 110 °C and 160 °C. Accordingly, high boiling point solvents must be used, the most popular being 1,2,4-trichlorobenzene (TCB), ortho-dichlorobenzene (ODCB), decalin, methylcyclohexane, α-chloronaphthalene and tetrachloroethylene [21–24].

The severe operating conditions in HT-SEC affect not only the sample and the mobile phase but also the stationary phase. It must withstand high temperatures for extended periods of times (several years) without deteriorating or changing its

Table 3.1 SEC analysis using molar mass-sensitive detectors (adapted from [20] with permission of J. Wiley & Sons)

Method	Information content	
	Primary	Secondary
Regular SEC		MMD
SEC-LALLS	MMD	
SEC-MALLS	MMD	RGD
SEC-VIS	IVD	MMD, RGD, copolymer M_n
SEC-VIS-LS	IVD, MMD, RGD	Copolymer M_n

LALLS low-angle laser light scattering, *IVD* intrinsic viscosity distribution, *RGD* radius of gyration distribution

separation capabilities. Typical stationary phases for HT-SEC are polymeric materials based on cross-linked polystyrene (PS-DVB gels). Various dissolution procedures are used. Generally, a dissolution time between 1 h and 6 h at a temperature of 140–180 °C is recommended. During the dissolution process, the sample may be shaken or stirred. For protection against thermo-oxidative degradation, phenolic antioxidants (e.g. butylated hydroxytoluene, BHT) are usually added in concentrations of 0.2 mg/mL up to 1.5 mg/mL [25, 26] to the mobile phase. Care must be taken to avoid the presence of oxygen, vigorous stirring and sample filtering because these factors may lead to sample degradation. Polyolefin chains may degrade during sample preparation or during the SEC separation itself [27–29]. The thermo-oxidative degradation or the chain scission due to shear stress in the SEC column is the main cause of the potential reduction of the polyolefin molar masses [25, 27].

Depending on the complexity of the sample to be analysed, there are several possible techniques; these mainly differ in terms of the added detectors and calibration options [16]. As mentioned earlier, Tri-SEC makes use of three types of detectors, namely concentration detectors, online viscometers and MALLS detectors. The combination of SEC separation with molar mass-sensitive detectors is an effective tool for the analysis of complex polyolefins. The value of coupling SEC to LS and Visco is summarized in Tables 3.1 and 3.2 (adopted from a critical review of these techniques [20]).

The information obtained is divided into two classes: the highly precise and accurate information that does not require any external calibration and is independent of SEC operation variables is placed in the category ‘primary information’, whereas ‘secondary information’ is less precise and requires external calibration. These are general considerations for polymers but they are equally valid for polyolefins. Further options of powerful and selective detectors for HT-SEC are Fourier transform infrared (FTIR) and proton nuclear magnetic resonance (^{1}H-NMR) spectroscopy. The experimental details of these couplings will be discussed in separate sections.

Table 3.2 Generalization of molar mass-sensitive detectors (adapted from [20] with permission of J. Wiley & Sons)

Intended measurements	LALLS/MALLS	Viscometer
MMD	Requires precise n and dn/dc, not affected by non-exclusion effects	Requires universal calibration and K, a-parameters
IVD	–	Directly from experiment, not affected by non-exclusion effects
RGD	MALLS only	Calculated from $[\eta]$M
Conformation and branching	R_g vs. M plot, MALLS only	$[\eta]$ vs. M plot, R_g vs. M plot
Chemically heterogeneous polymer analysis	Limited	Better
Noise, particulates, bubbles	Strongly affected	Less affected

3.1.1 Molar Mass Analysis by SEC-RI-MALLS

SEC is a relative method and requires calibration to relate the experimentally determined elution volume to molar mass. This is classically done with a set of calibration standards of known molar masses. This approach is not suitable for complex polymers because at a given elution volume, molecules with different molar masses can co-elute depending on their chemical composition and topology [2–5]. Multidetector systems have been developed to overcome the problems associated with the SEC of complex polymers. Employing multiple concentration detectors is a pragmatic approach and reveals the chemical composition of each slice of the SEC curve provided the response factors of the components are sufficiently different for both concentration detectors. Typically, a combination of RI and ultraviolet (UV) is used in ambient temperature SEC. A diode-array detector can also be used. If the components of the polymer sample do not contain any UV absorbing group, the combination of RI and density detection is a viable approach. In HT-SEC, the only detection option is RI combined with an evaporative light scattering detector (ELSD). UV detectors cannot be used due to the high absorption of the mobile phase (TCB or ODCB). Coupling of SEC to spectroscopic detectors like FTIR, NMR or mass spectrometry may yield additional structural information [30].

The coupling of SEC to molar mass-sensitive detectors is the most useful approach for molar mass analysis of complex polymers, and the analysis of polyolefins is no exception. The detector response of the molar mass-sensitive detectors depends upon both molar mass and concentration; therefore, the combination with a concentration-sensitive detector is imperative; see Fig. 3.1. The available molar mass-sensitive detectors include the differential viscometer, the LALLS and MALLS detectors.

Fig. 3.1 HT-SEC system with built-in dual wavelength IR detector for concentration and chemical composition detection; system can be coupled to external MALLS detector (taken from [11] with permission of Polymer Char)

In an LS detector, the scattered light of a laser beam passing through the detector cell is measured at angles other than zero. The (excess) intensity $R(\theta)$ of the scattered light at the angle θ is related to the weight average of molar mass, M_w:

$$K^* c \,/\, R(\Theta) \;=\; [1/M_w P(\Theta)] \;+\; 2A_2 c \tag{3.1}$$

wherein c is the concentration of the polymer, A_2 is the second virial coefficient and $P(\theta)$ describes the scattered light angular dependence. K^* is an optical constant containing Avogadro's number N_A, the wavelength λ_0, the refractive index n_0 of the solvent and the RI increment dn/dc of the sample:

$$K^* \;=\; 4\pi^2 {n_0}^2 (dn/dc)^2 / \left(\lambda_0^4 N_A\right) \tag{3.2}$$

M_w is obtained from the intercept at $\theta = 0$ and the radius of gyration (R_g) from the slope in a plot of $K^*c/R(\theta)$ versus $\sin^2(\theta/2)$. Since the concentration of the injected sample is kept rather low, A_2 can be neglected. Thus, the molar mass at each elution volume increment can be determined if the optical properties (n_0 and dn/dc) of the polymer solution are known.

$$M_{w,i} \;=\; R(\Theta)_i / K^* P(\Theta)_i c_i \tag{3.3}$$

$P(\Theta)$ is close to unity and $M_{w,i}$ can be calculated directly if a low-angle LS instrument is used. The mean square radius of gyration $<{R_g}^2>$ at each elution volume can also be obtained from $P(\Theta)$ in the case of a multi-angle LS instrument:

$$1/P(\Theta)_i = 1 + q^2 < R_g^2 >_i /3$$
$$q = (4\pi/\lambda_0)\sin(\Theta/2) \tag{3.4}$$

In practice, however, the measurement of R_g is only possible for molecules larger than 20 nm in diameter. Furthermore, information on molecular conformation can be obtained by measuring the R_g as a function of M_w [31–33].

Molar mass determination requires knowledge of the specific RI increment dn/dc which in the case of complex polyolefins depends on chemical composition. Copolymer RI increments $(dn/dc)_{copo}$ can accurately be calculated for chemically monodisperse fractions if the comonomer weight fractions w_i and the homopolymer values are known, which is rarely the case. LS investigations of copolymers are even further complicated by the fact that SEC does not separate into chemically monodisperse fractions. Accordingly, due to compositional heterogeneity the RI increment of a particular scattering centre may be different from the total dn/dc of the corresponding SEC slice. Therefore, in general, only apparent molar masses for copolymers can be measured. Another influencing factor is the RI of the solvent.

3.1.1.1 Aim

In the following application a low-density PE that has a molar mass distribution and a branching distribution shall be analysed. The analysis shall be conducted on a triple-detector system with the IR detector providing eluate concentration and chemical composition, the MALLS detector providing the weight average molar mass and the viscosity detector providing the intrinsic viscosity.

3.1.1.2 Materials

- *Polymers*. Low-density PE NBS 1476 (NIST, Gaithersburg, USA), narrow dispersity polystyrene calibration standards (Polymer Standards Service GmbH, Mainz, Germany).

3.1.1.3 Equipment

- *SEC*. GPC-IR-3D (Polymer Char, Valencia, Spain).
- *Detectors*. IR4 for concentration and composition and four-capillary viscometer (both Polymer Char, Valencia, Spain), Heleos 8 MALLS (Wyatt Technology, Santa Barbara, USA). MALLS laser wavelength was 659.2 nm.
- *Columns*. Three linear Olexis columns (13 µm average particle size), column temperature 140 °C.
- *Solvent*. TCB stabilized with 300 ppm BHT.
- *Sample concentration*. 16 mg in 8 mL TCB.
- *Injection volume*. 200 µL.
- *Flow rate*. 1.0 mL/min.

3.1.1.4 Preparatory Investigations

Before investigating the sample, the SEC system was calibrated using narrow dispersity PS calibration standards. Using a PE as standard, a factor Q was applied to transform PS values to PE values.

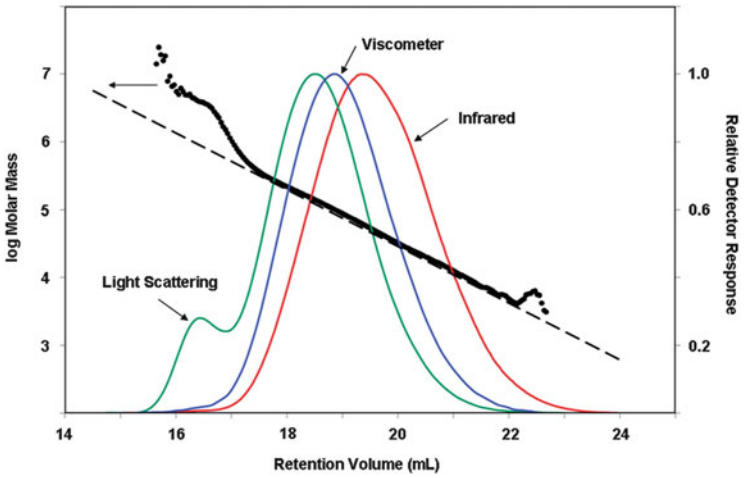

Fig. 3.2 HT-SEC analysis of a low-density polyethylene NBS 1476 using a triple-detector system (taken from [11] with permission of Polymer Char)

When the viscometer was used for molar mass calculation then a universal calibration curve based on the PS standards was used. For the analysis of the LS measurements, the RI increment was determined using a differential refractometer. For the sample under investigation, dn/dc was 0.104. A scattering angle of 90° was used for the molar mass analysis.

3.1.1.5 Measurement and Evaluation

The LDPE sample was dissolved in the mobile phase and injected into the SEC system. Elution of the sample components was monitored with the IR, Visco and MALLS detectors. The results of the analysis are presented in Fig. 3.2.

The plot presents the elution profiles derived from the concentration detector with PS calibration (IR4), the viscometer detector using universal calibration (Visco) and the MALLS detector (LS) measuring the scattered light intensity at 90°. As can be seen, the elution profiles shift towards higher retention volumes from LS to Visco and IR. This effect is known and is related to the higher sensitivity of the molar mass detectors Visco and LS for the high molar mass portion of the distribution. The molar mass calibration curve is derived from the MALLS signal.

Based on the $[\eta]$ values from the viscometer and the M_w values from the MALLS detector as a function of retention volume, a Mark–Houwink plot can be constructed that provides information on long chain branching (LCB); see Fig. 3.3. The intrinsic viscosity distribution (log IV) of the linear PE reference is shown and indicates that the sample was properly separated according to hydrodynamic volume.

The corresponding intrinsic viscosity distribution of the branched sample is presented, corrected for short chain branching (SCB). The SCB correction was based on the IR4 detector signals. The value of LCB can be calculated from the

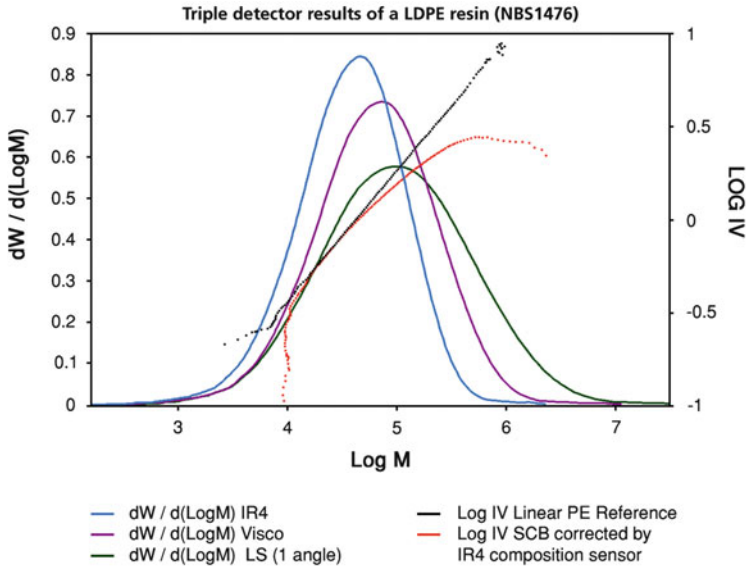

Fig. 3.3 Mark–Houwink plot of an LDPE NBS 1476 using a triple-detector system (personal communication from Polymer Char)

Mark–Houwink plot, and the value used to convert g into g' has been of $\varepsilon = 0.9$ units. The mean square radius of gyration of the branched polymer to that of the linear species of the same molar mass is given by g, whereas g' is the ratio of the intrinsic viscosities. Although the sample is a homopolymer and there is no comonomer incorporation, some short chain branches are generated in the high pressure polymerization process. This SCB is responsible for the log IV curve shifting from the linear reference.

3.1.2 Branching Analysis by Coupled SEC-FTIR

Determination of the chemical composition distribution (CCD) together with the MMD of polyolefin copolymers or polyolefin blends is vital for the detailed analysis and the development of structure–property correlations. Information about average chemical compositions can be obtained by FTIR or NMR. The chemical composition as a function of molar mass can be obtained by direct coupling of HT-SEC to these spectroscopic methods.

The robustness, simplicity and cost-effectiveness of coupling of HT-LC with FTIR make it an important technique. Due to the cost-effectiveness of LC-FTIR, it is usually a preferred method over costly LC-NMR (unless specifically required). There are two methods of hyphenation of LC with FTIR: (1) online mode via a flow cell and (2) off-line mode via a solvent elimination interface. The limited pool of solvents/mobile phases that exhibit sufficiently large spectral windows is the major

limitation of flow cells. Generally, this is a major challenge in polymer analysis; but fortunately, in the case of polyolefins, TCB is the most frequently used solvent/mobile phase and it is sufficiently transparent in the wavenumber range of 2,700–3,000 cm^{-1} that is used for polyolefin detection. ODCB or tetrachloroethylene are good alternatives for TCB in HT-SEC. Compositional heterogeneity or SCB can be analysed successfully by on-flow SEC-FTIR [7, 8, 12, 13, 34–36]. This will be discussed in more detail in the following application. The ratio-recorded transmittance spectra generate the chromatogram, where the spectrum of the pure mobile phase is used as background. Sample concentrations are kept rather low in the range of 1–3 mg/mL, whereas larger injection volumes (400–1,000 μL) are used for better signal-to-noise ratio. The bands of FTIR spectra used for levels of methyl and methylene end groups are 2,958 cm^{-1} and 2,928 cm^{-1}, respectively [7, 8, 34]. These bands can be effectively used for low-density materials. Multivariable statistical techniques are preferred for high-density materials with low degree of branching [36].

As a typical example, two ethylene-1-hexene resins are compared in Fig. 3.4. Both resins were synthesized using Ziegler-Natta (ZN) catalysts but with varying comonomer contents [13]. Typically, the degree of branching is expressed as 'branches per 1,000 total carbons'. Similar approaches are applicable to other polymers with provision of the availability of a spectral window for detection of the polymer species.

Recently, by using a bandpass filter instead of a steel mesh attenuator and changing data processing, a significantly increased SNR in SEC-FTIR was obtained by Piel et al. [37]. They were able to achieve four times higher signals by using the bandpass filter. The proposed method was used by them for the determination of

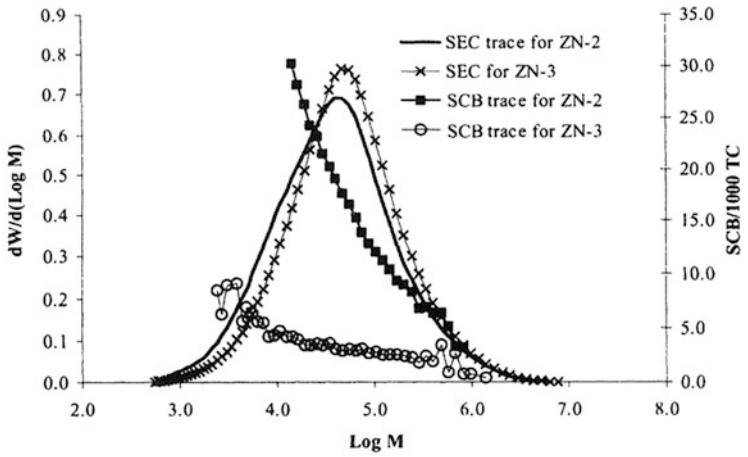

Fig. 3.4 SEC-FTIR analysis of LLDPE, comparison of comonomer incorporation in Ziegler-Natta catalysed ethylene-1-hexene resins using high (ZN-2) and low (ZN-3) comonomer levels (reprinted with permission from [13], copyright (2004) of the American Chemical Society)

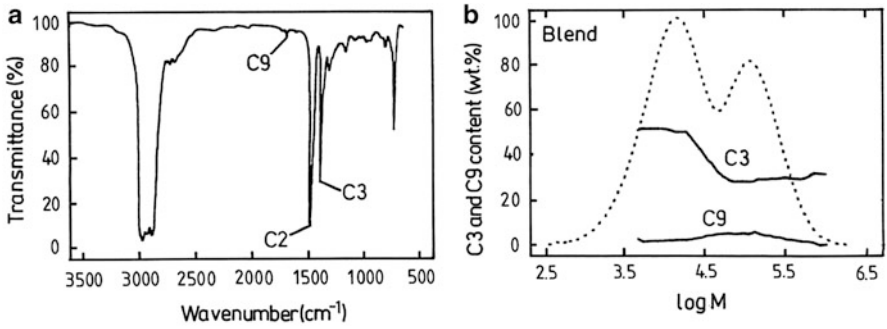

Fig. 3.5 FTIR spectrum of an EPDM copolymer (**a**) and HT-SEC/FTIR analysis of the blend of two EPDM copolymers (**b**) (reprinted from [6] with permission of Springer Science + Business Media)

SCB. Analytical temperature rising elution fractionation (A-TREF) coupled to FTIR can also be applied for SCB analysis.

The range of applicability of FTIR as a detector in LC can be broadened if the mobile phase can be removed prior to detection. The fractions are then measured without any interference from solvents. This concept was realized with the development of the LC-Transform interface. Details of LC Transform can be found in [4–6].

The analysis of a blend of two ethylene-propylene-diene rubbers (EPDMs) with different molar masses and chemical compositions is presented in Fig. 3.5 [38]. Figure 3.5a shows the FTIR spectrum of an EPDM copolymer. The absorption peak at 1,380 cm^{-1} is used for the determination of propylene while the peak at 1,690 cm^{-1} is used for determination of ethylidene norbornene. Figure 3.5b presents the percentage of the two monomers as a function of molar mass. The propylene content of the higher molar mass copolymer was found to be lower compared to the lower molar mass polymer.

Using this experimental set-up, a multitude of different materials can be analysed, including α-olefin copolymers and polyolefin blends. In addition to the analysis of macromolecular components, the technique can be used for the detection and quantification of additives.

There are a number of publications addressing the application of the LC-Transform system for polymer analysis. These include the SEC-FTIR analysis of ethylene-vinyl acetate (EVA) copolymers [39], ethylene-methyl methacrylate (EMMA) copolymers [40, 41], ethylene-styrene copolymers [42], HDPE and PP [43]. The thermo-oxidative degradation of polyolefins has also been studied in

several publications [43–47]. The complex structure of polyolefins has been investigated by a combination of TREF and SEC-FTIR [48, 49]. The application of the LC-Transform system for the analysis of complex polyolefins regarding chemical composition by solvent gradient interaction chromatography will be addressed in Sect. 3.2.1.

The challenges associated with the further improvement in sensitivity are related to the loss of IR sensitivity in the reflectance mirrors of the optics module and the deposition of the effluents in rather narrow tracks on the substrate. The configuration of the recently commercialized DiscovIR-LCTM interface by Spectra Analysis Inc. (Marlborough, MA, USA) accounts for the energy loss in the optics module by using IR microscopy [50]. This single unit instrument eliminates the solvent from LC eluate and deposits the chromatogram as a track as a function of retention time. The scanning of the track takes place by a built-in FTIR microscope in real time. The oxidation of compounds is prevented by deposition under high vacuum and low temperatures (−140 to 100 °C). ZnSe is the deposition matrix, which allows measurements in the transmission mode. Several applications of this interface have been reported; however, so far none for the analysis of polyolefins.

3.1.3 Analysis of a Polymer Blend by Coupled SEC-^{1}H NMR [51]

The direct coupling of high-temperature liquid chromatography to ^{1}H NMR is a further advancement in the analysis of complex polyolefins. With the introduction of a high-temperature flow-through NMR probe by Bruker, the equipment for such a coupling became available. Hiller et al. elaborated details of the experimental set-up and the construction of the LC-NMR interface [51]. Briefly, the workable operating temperature of the probe was now enhanced to 150 °C. The active flow cell in the probe has a volume of 120 μL. It is a dual inverse ^{1}H/^{13}C probe with pulsed field gradients. At the interface of SEC and NMR, a two-position stop-flow valve is mounted. The valve directs the flow from the SEC to the NMR or to waste, as can be seen in Fig. 3.6. On-flow experiments, automatic stop-flow experiments and time slicing are possible with this set-up.

3.1.3.1 Aim

The HT-SEC-NMR method shall be used for the separation and analysis of a ternary polymer blend comprising two homopolymers and the corresponding copolymer. SEC shall separate the components by molar mass while ^{1}H-NMR shall provide identification and structural details of the components.

3.1.3.2 Materials

- *Polymers*. Two samples of PE with number average molar masses of 1,100 g/mol ($M_w/M_n = 1.1$) and 60,000 g/mol ($M_w/M_n = 1.5$), respectively, one sample of PMMA with a number average molar mass of 263,000 g/mol ($M_w/M_n = 1.06$), and one sample of poly[(ethylene)-co-(methyl methacrylate)] (PE-PMMA) with a number average molar mass of 10,600 g/mol ($M_w/M_n = 2.3$).

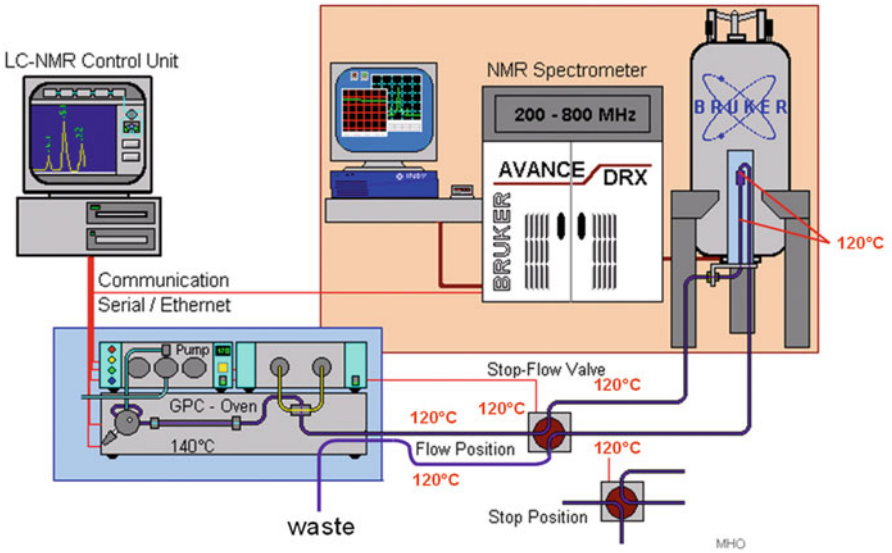

Fig. 3.6 Experimental set-up of the high-temperature SEC-NMR (SEC: 130 °C; LC probe, stop-flow valve and transfer lines: 120 °C) (reprinted from [51] with permission of Elsevier)

PE and PMMA were products of Polymer Standards GmbH (Mainz, Germany). The PE-PMMA copolymer was prepared by the group of H. Höcker [52] at RWTH (Aachen, Germany). The monomer composition measured by ^{1}H-NMR was 87.6:12.4 mol% (E/MMA).

- *Polymer blends*. Blend A: PE (1,100 g/mol) + PMMA + PE-PMMA, Blend B: PE (60,000 g/mol) + PMMA + PE-PMMA. The blend components were mixed in ratios of 1:1:1 (2 mg/mL for each component) in both cases.

3.1.3.3 Equipment

- *SEC*. Waters 150C (Waters Inc., Milford, USA).
- *NMR*. 400 MHz spectrometer AVANCE (Bruker BioSpin GmbH, Rheinstetten, Germany). The measurements were performed with a high-temperature flow probe containing a 120 µL flow cell. The probe was an inverse detection probe equipped with a shielded pulsed field-gradient coil. The gradient strength was 53 G/cm. The 90° ^{1}H pulse was 6.7 µs. WET solvent suppression [53] was applied to TCB. Three frequencies were suppressed. The SEC-NMR system was controlled by Hystar software (Bruker Bio-Spin GmbH, Rheinstetten, Germany).
- *Columns*. Styragel HT-2, HT-3, HT-4, HT-5 and HT-6, all of 10 µm average particle size, and column sizes of 300 mm × 8 mm i.d. (Waters Inc., Eschborn, Germany).
- *Solvent*. TCB.
- *Sample concentration*. 2 mg/mL in TCB.

- *Injection volume*. 300 µL.
- *Flow rate*. 0.5 mL/min.

3.1.3.4 Analysis of the Blends

The blend components were dissolved in TCB at 130 °C. The SEC operating temperature was also 130 °C. The NMR accessory was kept at a temperature of 120 or 130 °C. Similar to ambient temperature LC-NMR, specific solvent signals must be suppressed [54]. The suppression of the three aromatic proton signals of the solvent was achieved by WET (water suppression through T_1 effects) suppression without adding a lock solvent. A wide molar mass range (100–1,000,000 g/mol) was covered by the SEC column set.

Figure 3.7 shows the on-flow run of blend A. Two data sets were generated comprising the raw data, including the impurities of the solvent in Fig. 3.7a and the corrected plot by subtracting signals, which correspond to impurities of the solvent in Fig. 3.7b.

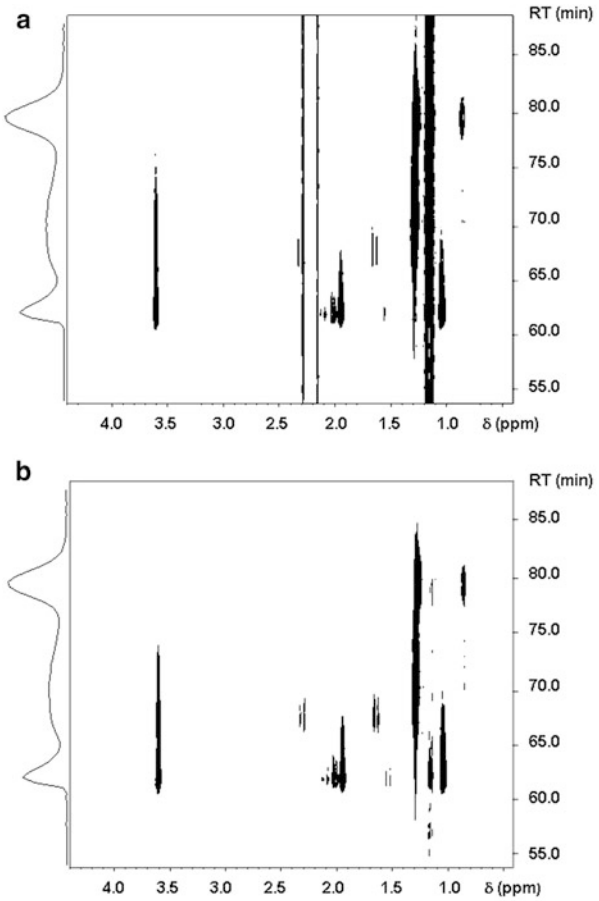

Fig. 3.7 SEC-NMR on-flow run of blend A at 130 °C in TCB (**a**) and corrected on-flow run (**b**), column set 1 (reprinted from [51] with permission of Elsevier)

These impurities were found in all three grades of TCB used: 'TCB for synthesis', redistilled TCB and the most expensive 'TCB for HPLC'. The impurities in TCB appear as residual solvent signals at about 1.18 ppm, 1.28 ppm, 2.15 ppm and 2.3 ppm. The signals of the solvent impurities partially overlap the signals of polymer components. As depicted, much better information on the composition of the sample components is obtained when corrected plots are used.

The blend components elute in the order of decreasing molar masses. The molar mass of PMMA is the highest and it elutes first, followed by the intermediate molar mass PE-PMMA copolymer and the lowest molar mass PE. The spectra of the early eluting fractions show signals for PMMA but not for ethylene. In contrast, the late eluting fractions exhibit signals for ethylene but not for MMA, and can be assigned to PE. Between the two homopolymers, the elution of the copolymer can be measured by detecting signals for both MMA and ethylene. Figure 3.7b also shows the vertical projections taken from the sum of the ^{1}H-NMR signals. They can be used as the chromatogram which also indicates three separated peaks.

Several different traces as obtained by the on-flow experiment are shown in Fig. 3.8. The different components are clearly indicated. Syndiotactic PMMA corresponds to the first trace (a), the second trace (b) belongs to the copolymer with mainly isotactic MMA units and the third trace (*c*) is due to PE homopolymer. The CH_3 end group is also evident at 0.86 ppm; however, precise molar mass calculation is not possible due to low SNR for the CH_3 group. Besides the SNR problem, it should also be noticed that the T_1 relaxation time of the CH_3 group is larger than that of the CH_2 group resulting in a lower intensity of the CH_3 signal. However, quantitative analysis of the monomer compositions of the blend components is possible using the corresponding signals.

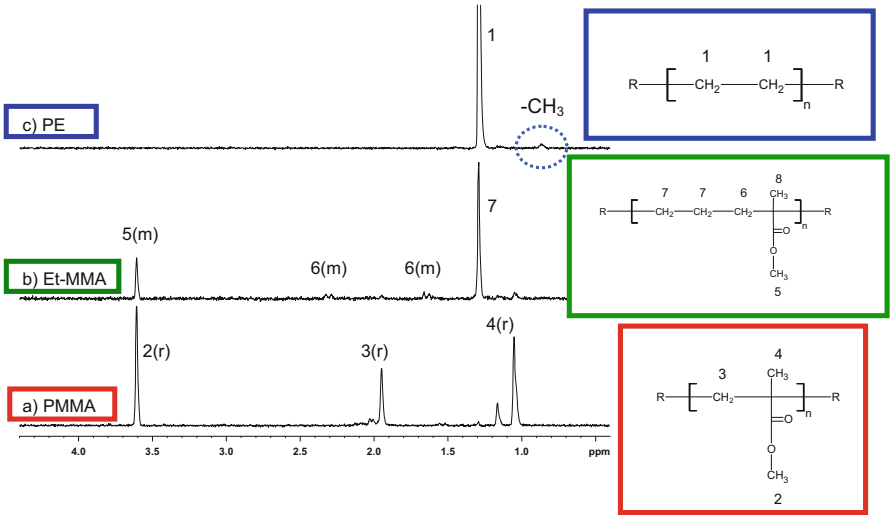

Fig. 3.8 ^{1}H traces of the on-flow run of Fig. 3.7b, (**a**) PMMA (RT = 60.5 min), (**b**) PE-PMMA copolymer (RT = 66.0 min), (**c**) PE 1100 g/mol (RT = 79.4 min) (reprinted from [51] with permission of Elsevier)

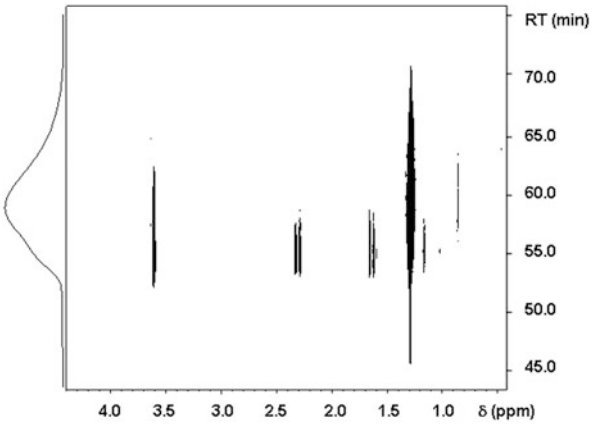

Fig. 3.9 SEC-NMR on-flow run of PE-PMMA copolymer at 120 °C in TCB, corrected by subtraction of the impurities of TCB (reprinted from [51] with permission of Elsevier)

3.1.3.5 Analysis of the PE-PMMA Block Copolymer

Investigation of the CCD of the PE-PMMA copolymer was carried out by an on-flow experiment, the results of which are shown in Fig. 3.9. Twenty-four scans per free induction decay (FID) were recorded in the present case.

For the quantitative analysis of the chemical composition as a function of molar mass, the copolymer was analysed more in detail by conducting an off-line HSQC (heteronuclear single quantum coherence) experiment [54]; see the plot in Fig. 3.10. The signals of the CH_2 groups of the ethylene units totally overlap with the signal of the α-CH_3 group of the MMA. Therefore, ethylene content determination was calculated from using the difference of the sum of signals $7 + 8m + 8r$ and the methoxy group 5(*m*,*r*) of MMA. The syndiotactic part of MMA is indicated by the signals (*r*) while the signals (*m*) are assigned to the isotactic MMA.

The distributions of the different structural moieties corresponding to MMA and ethylene were determined from the on-flow NMR spectra and correlated to the corresponding retention times; see Fig. 3.11. It shows that the MMA monomer units appear mainly at lower retention times, corresponding to higher molar masses. At a retention time of 63.5 min, the maximum amount of MMA (46.2 mol%) was observed. On the other hand, the very high molar mass part of the chromatogram has a higher ethylene content, which decreases to a minimum content until a retention time of 63.5 min, and finally almost pure PE with a low molar mass is detected (higher elution volume). Therefore, it can be concluded that the sample is very heterogeneous and also contains PE as a homopolymer.

The introduction of a new cryoprobe for HT NMR provides a dramatic increase in SNR. Even ^{13}C-NMR analyses are possible with very small quantities of material. The analysis of sample concentrations as low as 0.9–3.2 mg/mL is possible in reasonable acquisition time. Conventional probes used for ^{13}C-NMR require significantly higher concentrations [55, 56]. Cong et al. [57] reported on the collection of fractions from 20 chromatographic runs and their subsequent analysis by NMR after evaporation of the mobile phase. The content of octene in the

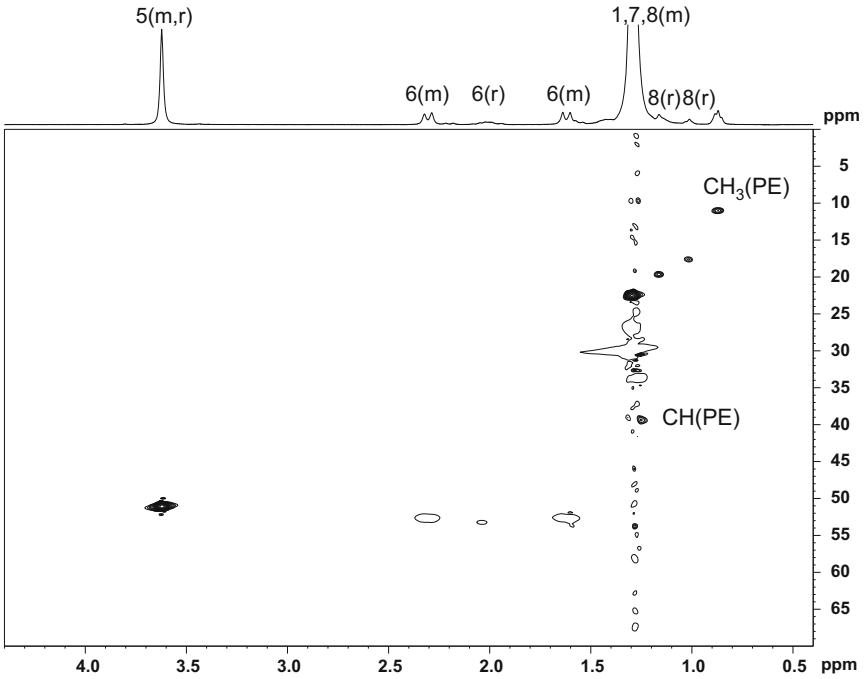

Fig. 3.10 Off-line ^{1}H-^{13}C gradient HSQC of PE-PMMA at 100 °C in TCB (no lock solvent added), 256 increments, 8 scans per increment, empty cross-peaks correspond to CH_2, filled cross-peaks are CH or CH_3 (reprinted from [51] with permission of Elsevier)

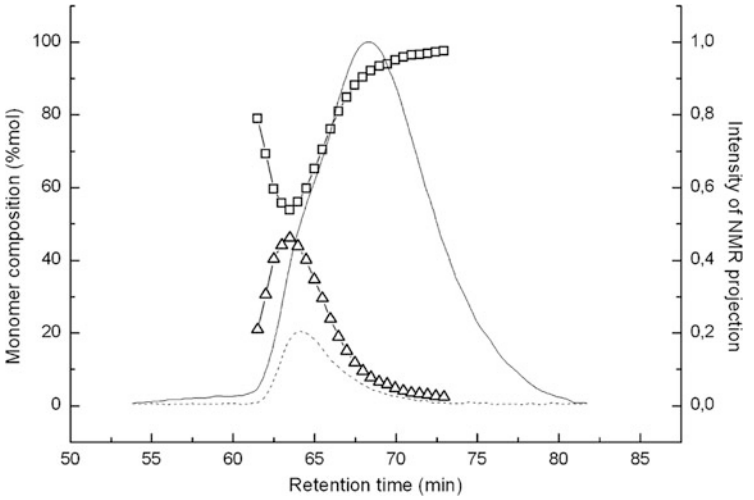

Fig. 3.11 Monomer composition of PE-PMMA copolymer vs. retention time calculated from Fig. 3.9, *open square* = mol% ethylene, *open triangle* = mol% MMA, *solid line*: NMR projection of the signal at 1.29 ppm, *dashed line*: NMR projection of the methoxy group (reprinted from [51] with permission of Elsevier)

collected copolymer fractions was determined using the new cryoprobe. Therefore, the practical applicability and excellent improvement in detectability of polyolefins in NMR were demonstrated.

3.2 Solvent Gradient Interaction Chromatography

TREF, CRYSTAF and crystallization elution fractionation (CEF) are excellent methods for the fractionation of polyolefins according to chemical composition. As has been pointed out earlier, these techniques relate only to the crystallizable part of the sample while the non-crystallizable (amorphous) part is obtained as a bulk fraction. Another problem associated with the crystallization-based fractionation techniques is that they are quite time-consuming. CEF overcomes the long analysis times but is still based on crystallization.

An excellent and fast separation of complex polymers can be achieved by high performance liquid chromatography (HPLC). HPLC separation is based on chemical composition rather than crystallizability, contrary to crystallization-based techniques discussed in Part 2. Different mechanisms that are operative in HPLC separations include adsorption-desorption and precipitation-redissolution. Precipitation and adsorption processes are usually combined in gradient HPLC. Previously, standard methods for the separation of polymers with respect to chemical composition, including solvent gradient chromatography or liquid chromatography at critical conditions (LCCC), were limited to ambient or slightly elevated temperatures [58, 59]. The maximum operating temperature for such separations was 80 °C. Polyolefins dissolve above their melting points; hence, this temperature is not sufficient for their dissolution. Frequently, the minimum required temperature for dissolution of polyolefins is 120 °C. Therefore, it was a real challenge to develop high-temperature (>120 °C) HPLC methods for polyolefin fractionation with regard to chemical composition.

In 2003, first attempts to establish interactive chromatographic methods for polyolefins were reported by Macko et al. [60, 61]. They used an isocratic system for the separation of PE-PP blends. The elution behaviours of PE and PP differed significantly. PP eluted first in SEC mode, while PE eluted later irrespective of its molar mass under limiting conditions. The method, however, had several limitations, including limited resolution and poor solubility of the samples. The studies showed that a major challenge in the development of HPLC methods is the solubility of polyolefins. Therefore, the solubility of polyolefins in different solvents was studied by using cloud point titrations [62]. In the process of method development of interaction chromatography, zeolites were tested as selective stationary phases [63–66]. On specific zeolites, PE can be adsorbed from some polar nonsolvents as well as from good solvents, such as decalin or TCB (typical solvents for SEC of polyolefins). Depending on the nature of the column packing, full or partial adsorption of PE and PP was found [67, 68]. By using tetrachloroethane or trichloropropane as mobile phases on silica gel and other macroporous sorbents,

significant retention of PP and PE was also observed [69]. A summary of the elution behaviours of PP and PE on different column packings is given in [70].

Early investigations were conducted on instruments for HT-SEC where a mixed mobile phase was delivered isocratically or a solvent gradient was formed by adding a second HPLC pump to the system. The reproducibility of this experimental set-up was rather low and a technically more advanced instrument was required that possesses the flexibility to conduct both isocratic and solvent gradient separations under reproducible conditions.

The recovery of high molar mass polymers is often a problem; it requires gradient elution to ensure complete elution and full recovery. The first instrument that allowed solvent gradients while working at higher temperatures was introduced in 2004 after joint efforts of Polymer Laboratories, Ltd. (Church Stretton, England) and the group of Pasch and Macko [71]. This instrument contained a high pressure gradient pump that permitted pumping of a single solvent (for SEC) or premixed mixtures of solvents in isocratic mode (for LCCC) as well as the running of binary solvent gradients (for HPLC); see Fig. 3.12.

Sample preparation and injection at higher temperatures (up to 220 °C) were possible by a robotic sample handling system in the chromatograph. The introduction of a 6-port column switching valve inside the column compartment enabled fast column and mobile phase screening. The instrument was equipped with two detectors: a high-temperature differential RI detector for isocratic elution (e.g. SEC and LCCC) and an ELSD for gradient and isocratic elution modes. A heated transfer line was used to avoid any temperature drops while transferring the eluate to the ELSD.

For a number of years, the Polymer Laboratories instrument was the only commercially available instrument for HT-HPLC. It was subsequently used to develop a number of important methods for the separation of complex polyolefins.

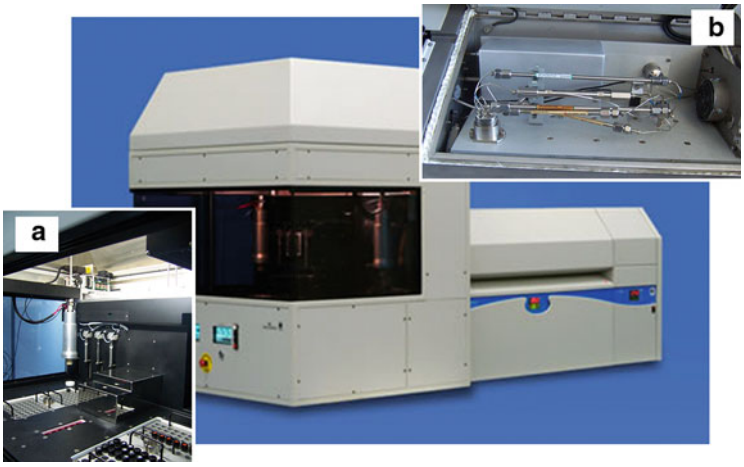

Fig. 3.12 Polymer Labs HT-HPLC instrument with sample robot (**a**) and column switching valve (**b**) (reprinted from [6] with permission of Springer Science + Business Media)

Fig. 3.13 Polymer Char SGIC 2D instrument (reprinted from [72] with permission of Polymer Char)

In 2010/2011, a new instrument for solvent gradient HT-HPLC was introduced by Polymer Char that is suitable for one-dimensional HPLC as well as for 2D HPLC × SEC fractionations; see Fig. 3.13 [72]. In isocratic mode, this instrument can use an IR detector instead of the ELSD, and it is compatible with standard molar mass-sensitive detectors.

A detailed discussion of a number of major developments in the field has recently been presented by Pasch et al. [6] and Monrabal [73]. Different experimental protocols have been developed that make use of the different modes of interaction chromatography of polymers. LCCC has been used for the separation of PE-PS blends [74]; see Fig. 3.14. At critical conditions, polymers of identical chemical composition show no separation and elute at one elution volume, without any effect of the MMD. Examples of such chromatographic behaviour at ambient temperature have been published for more than 150 sorbent-eluent systems [75]. The concept of critical conditions at higher temperatures was introduced by Pasch et al. by developing critical conditions of PMMA at 140 °C. The established critical conditions of PMMA were subsequently used for the identification and separation of EMMA block copolymers [41].

Using a solvent gradient of ethyleneglycol monobutylether (EGMBE)-TCB on silica gel, a baseline separation of PE and PP was achieved [76]. In the initial mobile phase composition, PE was insoluble and was precipitated on the column, whereas PP showed size exclusion behaviour. During the gradient, the content of TCB was increased continuously allowing dissolution and subsequent elution of precipitated PE. The quantitative separation of blends of different polyolefins by LC at 140 °C at a wide range of concentrations was demonstrated for the first time. The separation of EP copolymers into ethylene-rich and propylene-rich parts was also shown [77]. The application of the described chromatographic approach for the separation of EPCs [78] and for the separation of various polyolefins with respect to chemical composition was later published [79].

The separation of random EVA copolymers according to chemical composition based on adsorption-desorption by HT-HPLC was shown by the same group. The complete separation of copolymers with different compositions was achieved on a silica gel column with decaline-cyclohexanone as the mobile phase; see Fig. 3.15.

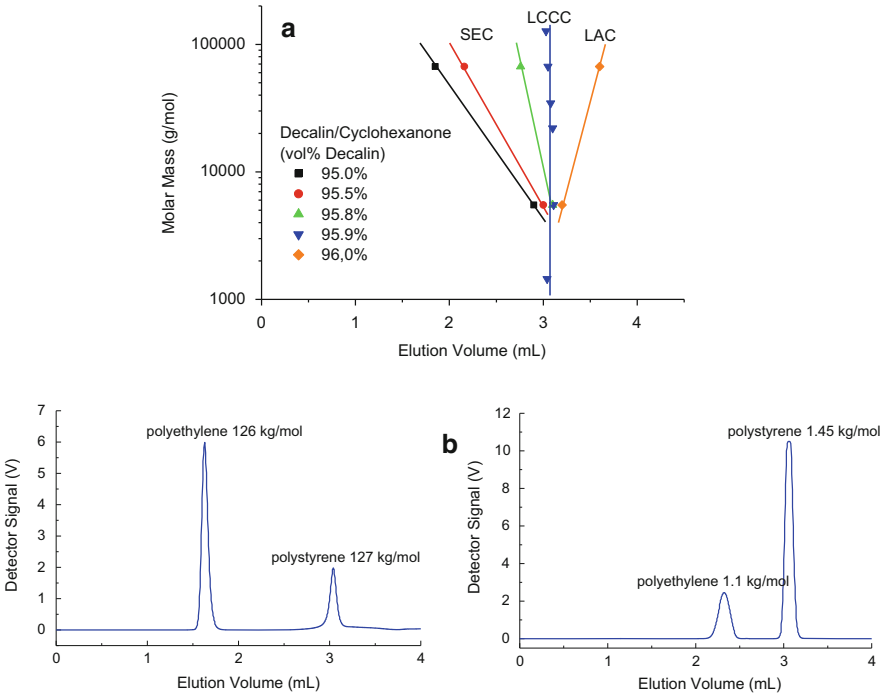

Fig. 3.14 Effect of mobile phase composition on the elution behaviour of polystyrene standards (**a**) and chromatograms of PS-PE blends (**b**). Mobile phase: decalin-cyclohexanone (in vol%). Column: Lichrosorb 100, 250 mm × 4.6 mm i.d. Temperature: 140 °C. Detector: PL-ELS 1000. Flow rate: 1 mL/min (reprinted from [74] with permission of Taylor&Francis)

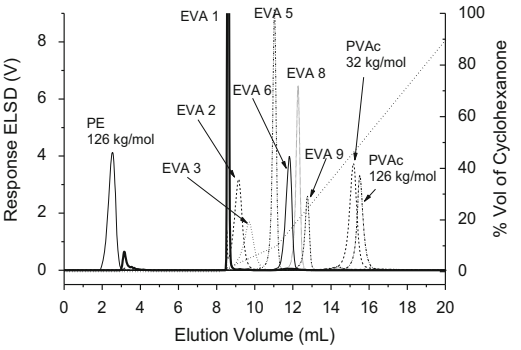

Sample	M_w [kg/mol]	VA [wt.%]
EVA 1	330	5
EVA 2	270	12
EVA 3	330	14
EVA 5	144	28
EVA 6	430	45
EVA 8	370	60
EVA 9	267	70

Fig. 3.15 Overlay of the chromatograms of EVA copolymers; stationary phase: Polygosil 1000; mobile phase: gradient decalin/cyclohexanone (*dotted line*); temperature: 140 °C; detector: ELSD; sample solvent: decalin (TCB for the PVAc standards) (reprinted with permission from [80], copyright (2007) of the American Chemical Society)

The method allowed the separation of copolymers from the respective PE and PVA homopolymers. This was a breakthrough in the analysis of polyolefins as it allowed separation of olefin copolymers with regard to chemical composition irrespective of their crystalline or amorphous nature. The entire range of chemical compositions was covered, contrary to traditional crystallization-based techniques that work only for the crystalline part. Both PE and PVAc were soluble in the components of the binary mobile phase. The nonpolar component of the mobile phase, decalin, promoted adsorption of PVAc on silica gel. Cyclohexanone, on the other hand, is a polar solvent that promoted desorption and elution of the adsorbed polymer species [80]. The coupling of this highly selective copolymer separation with FTIR spectroscopy revealed the CCD of the samples. The LC-Transform interface was employed for the hyphenation of LC to FTIR [81].

The most important achievement, however, was the discovery by Macko and Pasch that a specific carbon-based stationary phase—Hypercarb [82]—enables highly selective separations of polyolefins. Hypercarb was originally developed by Knox and co-workers [83] and had been used in HPLC analysis of small molecules; it was, however, never applied to the separation of synthetic polymers. Macko et al. found that porous carbon adsorbs linear PE from 1-decanol as the mobile phase at 160 °C [84–86]. The retained polymer was desorbed from the column using a linear gradient from 1-decanol to TCB. Moreover, this HPLC system separated isotactic, atactic and syndiotactic PP from each other; see Fig. 3.16. It was shown further that the same chromatographic system separates ethylene-hexene and propene-1-alkene copolymers according to their chemical compositions [87, 88]. Macko et al. demonstrated the usefulness of the approach for EPCs [89] and copolymers of propylene with different tacticities [90]. Moreover, terpolymers of ethylene, propylene and a diene monomer (EPDM) were separated [91]. It was found that both comonomers, ethylene and diene, are adsorbed. On the other hand, adsorption of EP, ethylene-butene (EB), ethylene-hexene (EH), ethylene-octene (EO) or ethylene-1-decene (ED) copolymers depends linearly on the average content of ethylene [92].

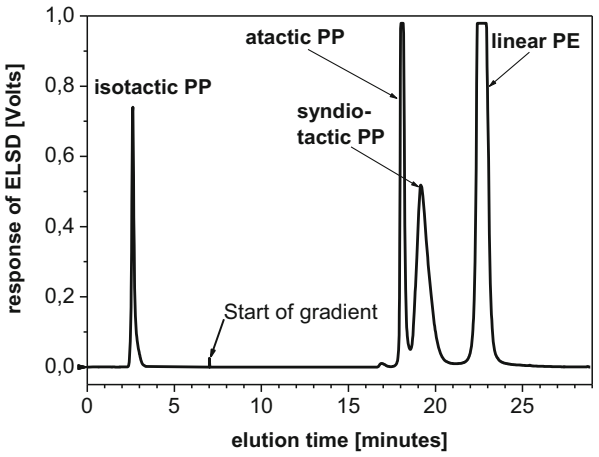

Fig. 3.16 Separation of a blend of isotactic, syndiotactic and atactic PP and linear PE; stationary phase: Hypercarb; mobile phase: gradient 1-decanol/TCB; temperature: 160 °C; detector: ELSD (reprinted with permission from [85], copyright (2009) of the American Chemical Society)

3.2.1 Analysis of Ethylene-Methyl Acrylate Copolymers [40]

3.2.1.1 Aim

Commercial interest in copolymers of ethylene and methyl acrylate (MA) is increasing due to its various applications, e.g. the production of films, foams or hot melt adhesives (depending upon their comonomer contents). As is true for all copolymers, ethylene-methyl acrylate (EMA) copolymers exhibit MMD and CCD. For the optimization of synthetic procedures and the development of structure–property correlations, a comprehensive characterization of these copolymers is required. EMA copolymers with low MA contents may be semi-crystalline materials that can be separated according to composition by TREF or CRYSTAF. With higher MA contents, the materials are fully amorphous and thus cannot be separated by crystallization-based techniques. It is, therefore, the aim of the present application to separate EMA copolymers irrespective of crystallinity by HT-HPLC. Quantitative chemical compositions shall be determined by FTIR spectroscopy.

3.2.1.2 Materials

- *Calibration standards*. Linear PE standards (PSS GmbH, Mainz, Germany)
- *Polymers*. EMA copolymers were obtained from Exxon Mobil Chemical (Meerhout, Belgium), Du Pont (Geneva, Switzerland) and Arkema (Paris, France). Their characteristics are summarized in Table 3.3.

3.2.1.3 Equipment

- *Chromatographic system*. PL XT-220 (Polymer Laboratories, Varian Inc, Church Stretton, England) was used as the high-temperature gradient HPLC system. A robotic sample handling system PL-XTR (Polymer Laboratories) was used for dissolution and injection at higher temperature. The temperature of the whole system, comprising the sample block, injection needle, injection port and the transfer line between the auto sampler and the column compartment, was set to 140 °C. The flow rate was set to 1 mL/min. The dissolution time was 2 h to ensure complete dissolution of the samples.
- *Columns*. Perfectsil 300 Å (particle diameter 5 μm, pore volume 1.05 mL/g, void volume $V_0 = 3.21$ mL) and Polygosil 1,000 Å (particle diameter 10 μm, $V_0 = 3.15$ mL) (MZ Analysentechnik, Mainz, Germany). Column size 250 mm × 4.6 mm i.d.
- *Mobile phase*. Decalin-cyclohexanone.
- *Detectors*. ELSD PL-ELS 1000 (Polymer Laboratories, Church Stretton, England). An air flow rate of 1.5 L/min, a nebulizer temperature of 160 °C and an evaporator temperature of 270 °C were set on the ELSD. The LC-Transform FTIR interface (Series 300, Lab Connections, Carrboro, USA) was used. The settings of the LC-Transform were stage temperature of 150 °C, nozzle temperature of 139 °C and rotation speed of germanium disc of 10° per minute. A Nicolet Protegè 460 (Thermo Electron, Waltham, USA) was used for FTIR spectroscopy of the deposited sample fractions. WinGPC-Software (Polymer

Table 3.3 Weight average molar mass (M_w), molar mass dispersity (M_w/M_n) and methyl acrylate (MA) content given by the producers (adapted from [40] with permission of Wiley-VCH)

Sample code	Producer	M_w (kg/mol)	M_w/M_n	MA (wt%)
EMA 1	Exxon Mobil	282	4.9	23.5
EMA 2		183	3.7	27
EMA 3	Arkema	279	6.8	9
EMA 4		264	6.5	14
EMA 5		289	7.2	18
EMA 6		250	7.2	28
EMA 7	DuPont	240	5.8	9
EMA 8		197	4.7	18
EMA 9		189	4.0	24
EMA 10		235	4.6	24
EMA 11		245	5.3	25

Standards Service GmbH, Mainz, Germany) was used for data collection and processing.

- *Column temperature*. 140 °C.
- *Sample concentration*. 1–1.2 mg/mL. All samples were dissolved in TCB or decalin.
- *Injection volume*. 50 µL.

3.2.1.4 Preparatory Investigations

Suitable stationary and mobile phases have to be found to identify chromatographic conditions for the separation of EMA copolymers. The EMA copolymers are composed of polar acrylate units and nonpolar ethylene units. When using a polar (normal phase) stationary phase, acrylate units will interact with the stationary phase whereas ethylene units will not contribute to retention. Therefore, as the acrylate content increases, the elution volume of copolymer will increase. Based on these assumptions, a bare silica column was selected as the stationary phase. TCB, decalin, cyclohexanone and dibenzylether were identified as solvents for both homo- and copolymers.

A chromatographic method that has been originally developed to fractionate EVA copolymers in a decalin-cyclohexanone gradient [80] was first tested. Some separation of the EMA copolymers was obtained using this system. As can be seen in Fig. 3.17, EMA 1 (23.5 wt% MA) and EMA 2 (27 wt%) elute in the order of increasing MA content. It is interesting to note that EMA 10 (24 wt%) and EMA 11 (25 wt%) show quite broad elution peaks. The sharp peak, which is observed for these samples at 11.8 mL, can be explained by weakly adsorbing copolymer fractions with a low acrylate content, which can be desorbed by a small amount of the desorption promoting solvent, e.g. cyclohexanone.

To improve the separation of EMA copolymers, a step gradient of decalin-cyclohexanone was applied. A number of stationary phases were tested; Perfectsil 300 gave the best performance.

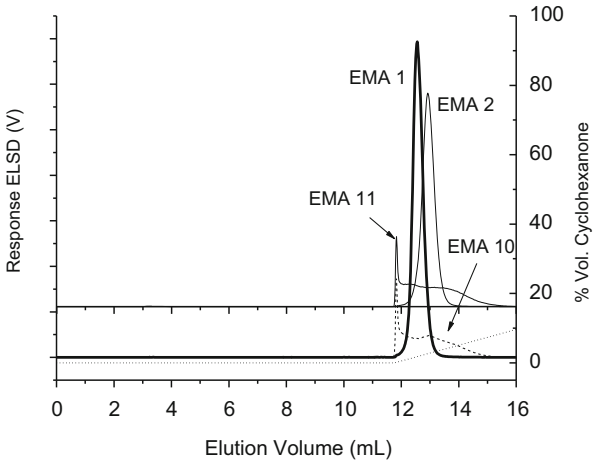

Fig. 3.17 Overlay of the chromatograms of EMA copolymers; stationary phase: Polygosil 1000, mobile phase: decalin-cyclohexanone (*dotted line*) 0–12 mL 100 % decalin, then linear gradient to 90 % decalin at 16 mL; temperature: 140 °C; detector: ELSD; sample solvent: decalin (reprinted from [40] with permission of Wiley-VCH)

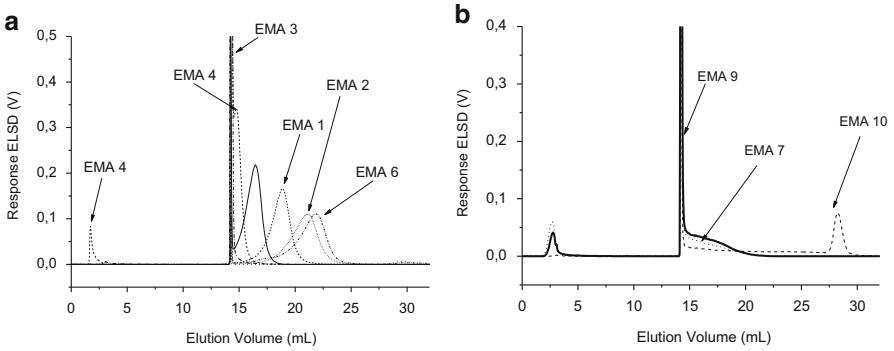

Fig. 3.18 Overlay of the chromatograms of EMA copolymers (**a** and **b**); stationary phase: Perfectsil 300; mobile phase: gradient decalin-cyclohexanone, 0–13 mL 100 % decalin, then linear gradient to 90 % decalin at 27 mL, then linear gradient to 80 % decalin at 30 mL; temperature: 140 °C; detector: ELSD; sample solvent: decalin (reprinted from [40] with permission of Wiley-VCH)

3.2.1.5 Measurement and Evaluation

The separation of several EMA copolymers with varying MA contents (9–28 wt%) was achieved with respect to chemical composition as can be seen in Fig. 3.18a, b. The samples under investigation showed clear differences. EMA 1–6 eluted as narrow peaks, whereas EMA 7, 9 and 10 eluted as broader peaks, which are a clear indication of broad CCD.

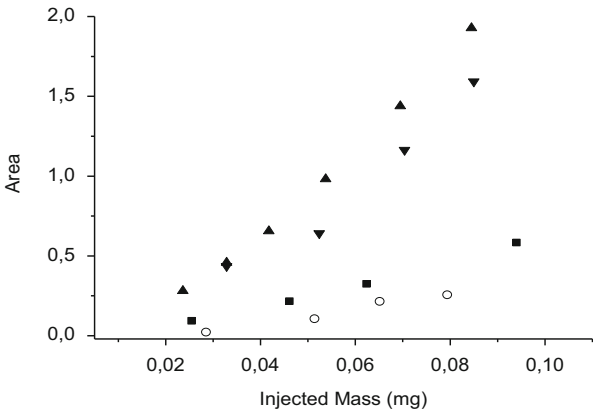

Fig. 3.19 Calibration of the chromatographic system described in Fig. 3.18 with PE 60 kg/mol (*filled triangle*), EMA 3 (*filled inverted triangle*), EMA 5 (*filled square*) and EMA 6 (*open circle*) (reprinted from [40] with permission of Wiley-VCH)

The additional peaks in EMA 4 (between 1.5 mL and 2.5 mL), EMA 7 and EMA 9 (between 2.5 mL and 3 mL) were close to the exclusion volume of the column ($V_0 = 3.21$ mL). These peaks indicate the presence of non-adsorbing species in EMA 4 and weakly adsorbing species in EMA 7 and EMA 9.

As is known, the ELSD response is not strictly independent of the structure of the analyte and depends upon several factors, namely constant instrument parameters (flow rate, temperature, sample loop volume, etc.), the concentration of the analyte and the composition of the mobile phase. The description of the effects of these parameters (concentration, molar mass and chemical composition of the analyte, as well as the composition of the mobile phase) on the detector response is given for the gradient system decalin-cyclohexanone in [80]. The detector response versus amount of sample injected for EMA 3, 5 and 6 and PE homopolymer ($M_w = 60$ kg/mol) is shown in Fig. 3.19. These indicate very clearly that the copolymer composition has a major effect on the ELSD response.

Direct identification of the components of the eluate is not possible by ELSD alone. The coupling of gradient HPLC to FTIR spectroscopy via the LC-Transform was used to obtain the CCD of the eluted fractions. A rotating germanium disc was used to deposit the eluate from the chromatograph, and the mobile phase was evaporated under vacuum. The solvent evaporation rate was adjusted by tuning the spray temperature in order to obtain homogeneous deposition of the polymer. To obtain absolute values for the MA content, a calibration was carried out. ^{1}H-NMR spectroscopy was used to measure the chemical composition of the bulk samples. The correlation of absolute content of MA (by NMR analysis) in the bulk samples to the peak area ratios from FTIR analysis of the bulk samples deposited on the germanium disc is shown in Fig. 3.20c. Figure 3.20a, b show the Gram-Schmidt (GS) plots, which reflect the sample concentration and the MA content along the elution volume.

An increase of the MA content in the main peak with the elution time is found for all samples except EMA 3 and 4. For the other samples, the amount of MA in the copolymers increases with the elution volume, i.e. separation according to chemical

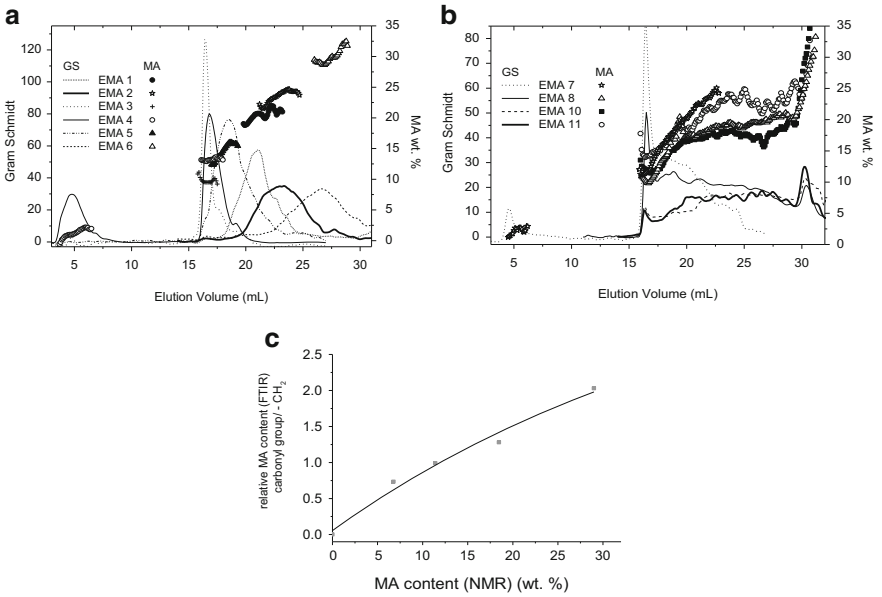

Fig. 3.20 Overlay of the results from HPLC-FTIR analysis of EMA 1–6 (**a**), EMA 7, 8, 10 and 11 (**b**) and the correlation between the MA content measured by ^{1}H-NMR and the peak area ratio of the carbonyl group (1,730 cm^{-1}) to the CH_2 group (1,450 cm^{-1}) measured by FTIR (**c**) (reprinted from [40] with permission of Wiley-VCH)

composition really takes place and the analysed samples are chemically inhomogeneous. From these results, two sets of samples can be distinguished: the first one (EMA 7, 8, 10 and 11) with a broad CCD and the second one (EMA 1–6) with a narrow CCD and a MA gradient of <5 wt%. Among these, EMA 3 and 4 show the most homogeneous chemical composition of about 9 wt% and 13.2 wt% MA, respectively, along the elution volume. In both sets of samples, copolymers with a second elution peak between 4 mL and 5 mL, namely EMA 4 and 7, were identified. The MA content in the second peak ranges between 1 wt% and 2.5 wt % (EMA 7) and between 0 wt% and 2 wt% (EMA 4). The presence of PE homopolymer in sample EMA 4 can be verified by FTIR spectra at selected elution volumes. At an elution volume of 4 mL, no carbonyl absorption band was detected, while in the FTIR spectrum at 5 mL the carbonyl absorption band was clearly identified. Thus the PE fraction in EMA 4 is most likely to be a PE homopolymer.

After plotting the elution volume at the peak maximum as a function of the calculated average MA content for samples EMA 1–6, a linear relationship between elution volumes of 16 mL and 28 mL is obtained; see Fig. 3.21.

The elution behaviours of EMA 1 (23.5 wt%) and EMA 10 (24 wt%) are different despite their similar average chemical compositions (Fig. 3.20a, b). This can be attributed to their different CCDs and architectural differences (degree of

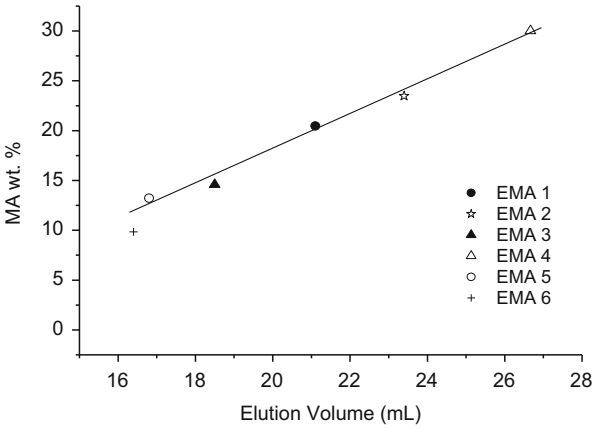

Fig. 3.21 Relationship between the elution volume and the content of methyl acrylate in the copolymer (reprinted from [40] with permission of Wiley-VCH)

Table 3.4 Triads (mol%) and total branch content per 1,000C of EMA copolymers (adapted from [40] with permission of Wiley-VCH)

Sample	Total branch/ 1,000C	Triads				
		EEE (mol%)	MEE (mol%)	MEM (mol%)	EME (mol%)	EMM (mol%)
EMA 1	11.7	74.4	15.6	3.2	7.5	0.4
EMA 10	13.1	68.5	14.7	4	7.4	0.9

blockiness). Hence, quantitative ^{13}C-NMR spectroscopy was used to study these samples. The calculated triads of EMA 1 and EMA 10 are summarized in Table 3.4.

The total branching content per 1,000 carbons of both samples is similar. Therefore, the differences in elution behaviour are assumed to be due to CCD. However, the investigation of the effect of the microstructure on elution behaviour of copolymers is an important future challenge. The copolymerization parameter ($r_1 = 0.045$ and $r_2 = 5.3$ for EMA) explains the presence of microblocks in both samples. These parameters favour the cross-propagation reaction for the ethylene radical compared to the homopropagation reaction for the end acrylate radical [93–95].

3.2.2 Separation of Ethylene-Propylene Copolymers [89]

3.2.2.1 Aim

Ethylene-propylene copolymers are the most important semi-crystalline copolymer materials. Their crystallinity changes as a function of chemical composition and ranges from highly crystalline to mostly amorphous. As has been discussed earlier, it is not only the average chemical composition but also the chemical heterogeneity that determines the crystallization behaviour and eventually the application

Table 3.5 Weight average molar mass (M_w), molar mass dispersity (M_w/M_n) and ethylene content of EP copolymers given by the producers

Sample code	M_w (kg/mol)	M_w/M_n	Ethylene (wt%)
EP-2	112.2	2.45	2.3
EP-4	118.8	2.44	4.0
EP-15	70.0	2.42	14.6
EP-23	61.6	2.08	22.6
EP-49	62.0	2.86	49.0
EP-74	54.7	2.54	73.5
EP-81	163.9	3.01	81.3
EP-91	268.5	2.78	91.0
EP-99	260.8	3.63	98.6

properties of the material. HT-HPLC is the only method that can provide a complete chemical composition separation irrespective of crystallinity. Making use of the different interactions of the polymer segments with the stationary phase, separations in the direction of increasing or decreasing comonomer contents can be obtained. In the present application a novel stationary phase—Hypercarb—shall be used. Hypercarb has been shown to be extremely selective regarding ethylene segments in a variety of homo- and copolymers [6, 73, 85].

3.2.2.2 Materials

- *Calibration standards*. Linear PE standards (PSS GmbH, Mainz, Germany).
- *Polymers*. Samples of EP copolymers as described in [89]. The copolymerization reactions were carried out in a stirred tank reactor operating in semi-continuous mode at 70 °C and 5 bar. The molecular characterization data obtained with HT-SEC and NMR spectroscopy are summarized in Table 3.5.

3.2.2.3 Equipment

- *Chromatographic system*. PL XT-220 (Polymer Laboratories, Varian Inc, Church Stretton, England) was used as the high-temperature gradient HPLC system. A robotic sample handling system PL-XTR (Polymer Laboratories) was used for dissolution and injection at higher temperature. The flow rate was set at 0.5 mL/min. The samples were dissolved in 1-decanol.
- *CRYSTAF*. Model CRYSTAF-TREF 300 (Polymer Char, Valencia, Spain). Polymer solutions with a concentration close to 0.5 mg/mL were prepared in TCB at 160 °C. The crystallization was carried out in the temperature range 95–30 °C with a cooling rate of 0.1 °C/min.
- *Columns*. Hypercarb 100 mm × 4.6 mm i.d., particle diameter 5 μm, pore diameter 200 Å (Thermo Fisher Scientific, Waltham, MA).
- *Mobile phase*. 1-decanol-TCB.
- *Detectors*. ELSD PL-ELS 1000 (Polymer Laboratories, Church Stretton, England). The air flow rate was 1.5 L/min, the nebulizer temperature was 160 °C and the an evaporator temperature was 260 °C.
- *Column temperature*. 160 °C.
- *Sample concentration*. 1–2 mg/mL. All samples were dissolved in 1-decanol.
- *Injection volume*. 13 μL.

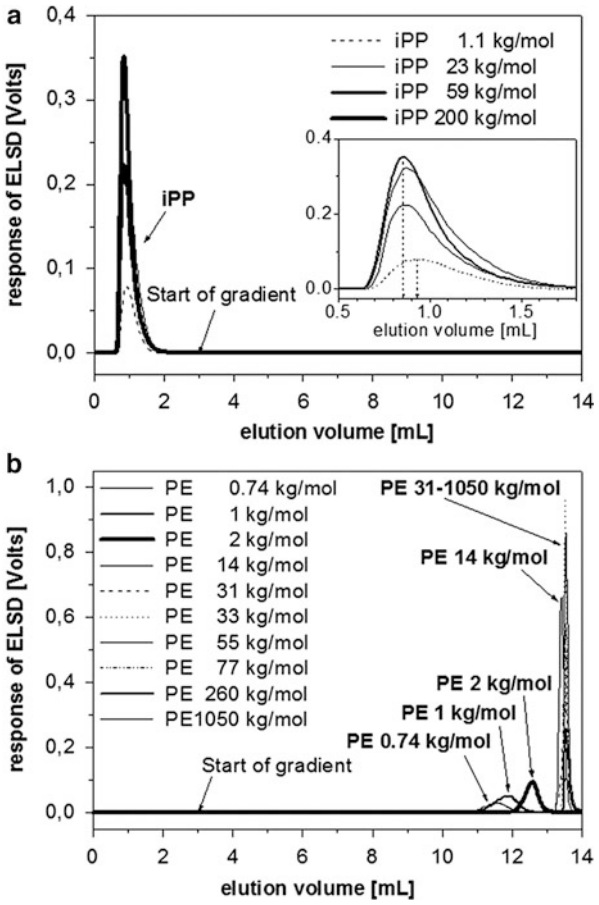

Fig. 3.22 Overlay of chromatograms for iPP (**a**) and PE (**b**). Column: Hypercarb. Mobile phase: 1-decanol and linear gradient from 0 % to 100 % TCB in 10 min. Flow rate: 0.5 mL/min. Temperature: 160 °C (reprinted from [89] with permission of J. Wiley & Sons)

3.2.2.4 Preparatory Investigations

In a first set of experiments, the interactions of PE and PP with the stationary phase Hypercarb were investigated. The samples were dissolved in 1-decanol at 160 °C and then injected into the column that was kept at the same temperature. The sample solvent was used as the starting mobile phase. A linear gradient starting from 100 % 1-decanol and going to 100 % TCB was employed later to achieve separation (the start of the gradient is marked in the chromatograms). The separation of linear PE standards and iPP with varying average molar masses is shown in Fig. 3.22. iPP is not retained and elutes before the start of the gradient in the SEC mode (Fig. 3.22a). PE adsorbs on the column from 1-decanol (starting composition of gradient). The introduction of TCB in the mobile phase promotes desorption of PE and elution takes place with respect to the molar mass of the corresponding PE (Fig. 3.22b).

The given chromatographic conditions work perfectly for the separation of binary blends of iPP and PE, as can be seen in Fig. 3.23 for combinations of

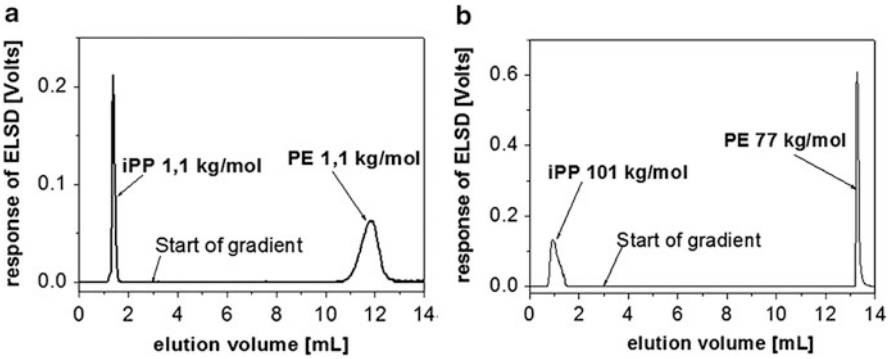

Fig. 3.23 Overlay of chromatograms for iPP-PE blends. (**a**) Blend of iPP 1.1 kg/mol and PE 1.1 kg/mol, (**b**) blend of iPP 101 kg/mol and PE 77 kg/mol. Column: Hypercarb. Mobile phase: 1-decanol and linear gradient from 0 % to 100 % TCB in 10 min. Flow rate: 0.5 mL/min. Temperature: 160 °C (reprinted from [89] with permission of J. Wiley & Sons)

blend components with different molar masses. iPP elutes more or less irrespective of molar mass at elution volumes of 1–2 mL. PE, which strongly interacts with the stationary phase, elutes in the direction of higher molar masses at elution volumes beyond 10 mL.

3.2.2.5 Measurement and Evaluation

The separation of a number of EP copolymers is shown in Fig. 3.24a, b. The elution volume of the samples generally increases with increasing average concentration of ethylene irrespective of the average molar masses of the samples (which differ significantly). Hence, the separation achieved is independent of the molar mass; it is mainly governed by the chemical composition. The samples with higher ethylene contents (EP15–EP99) elute after the start of the gradient whereas the samples with low ethylene contents (EP2 and EP4) elute mainly before the gradient. Similar to iPP, the adsorptive interactions in the present system are not sufficiently strong to adsorb copolymers with such low ethylene contents. However, adsorption of all copolymer samples can be achieved by replacing 1-decanol with 2-ethyl-1-hexanol (Fig. 3.24c, d). Larger retention volumes are obtained by using 2-ethyl-1-hexanol because of stronger interaction between copolymers and sorbent (about 16 mL in Fig. 3.24 vs. 13 mL in Fig. 3.23).

In a next set of experiments, the HPLC behaviour of the copolymers was compared to their crystallization behaviour, as analysed by CRYSTAF. As can be expected, most samples contain crystallizable and amorphous components (see Fig. 3.25). Samples EP2 and EP99 do not contain significant amounts of amorphous material. On the other hand, those samples that contain between 20 wt% and 80 wt % of comonomer have very low crystallization temperatures and contain large amounts of non-crystallizable material.

Figure 3.26 provides a good summary of the experimental results clearly showing the difference between HT-HPLC and CRYSTAF. In HT-HPLC,

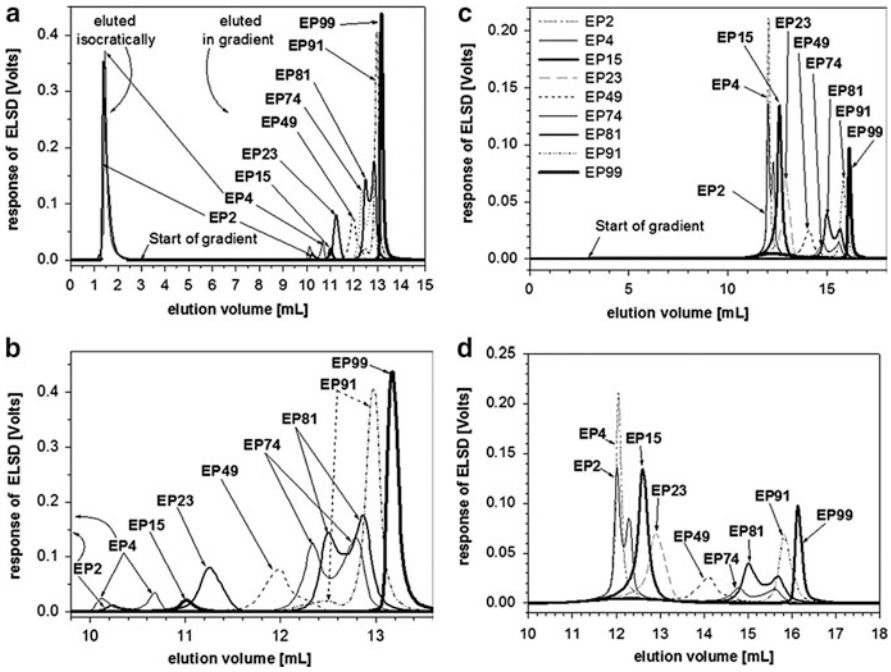

Fig. 3.24 Overlay of chromatograms for EP copolymers. Column: Hypercarb. Mobile phase: 1-decanol (**a**, **b**) or 2-ethyl-1-hexanol (**c**, **d**) and linear gradient from 0 % to 100 % TCB in 10 min. Flow rate: 0.5 mL/min. Temperature: 160 °C. (**b**) and (**d**) are enlarged parts of (**a**) and (**c**), respectively (reprinted from [89] with permission of J. Wiley & Sons)

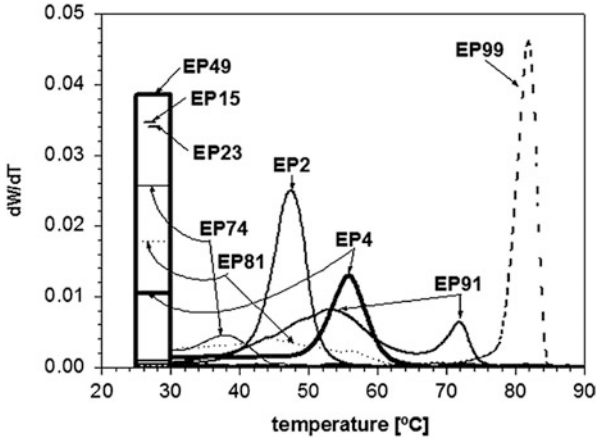

Fig. 3.25 First derivative of the concentration profiles obtained from CRYSTAF analysis of EP copolymers (reprinted from [89] with permission of J. Wiley & Sons)

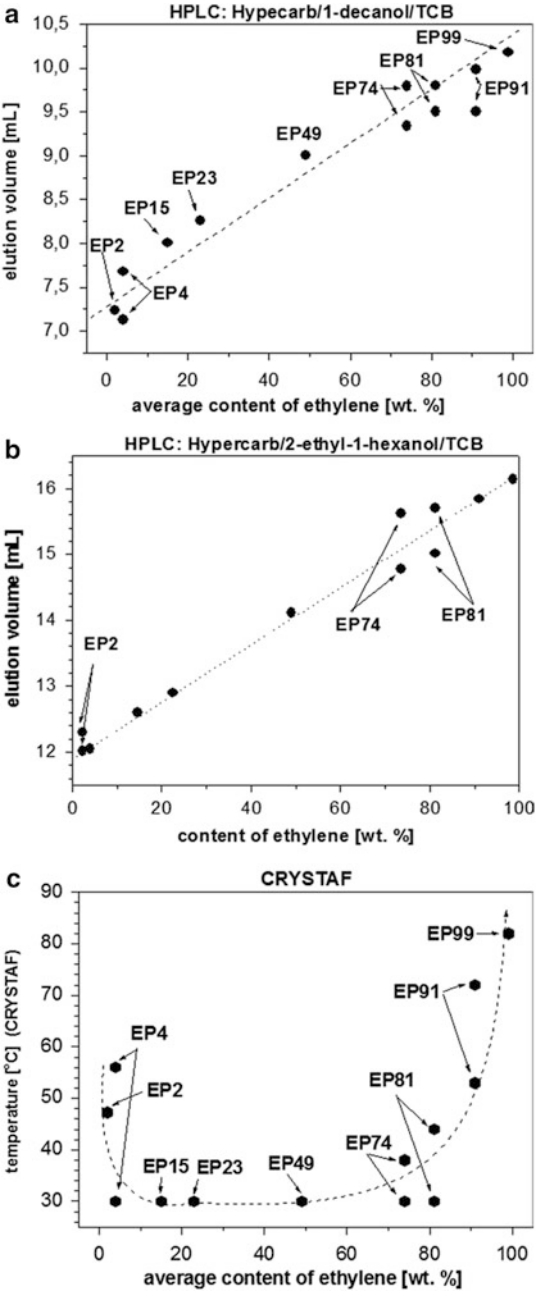

Fig. 3.26 Relationship between elution volume (HT-HPLC, **a** and **b**) or crystallization temperature (CRYSTAF, **c**), respectively, and copolymer composition (reprinted from [89] with permission of J. Wiley & Sons)

fractionation occurs more or less strictly regarding the ethylene content of the samples; see Fig. 3.26a, b. In CRYSTAF, on the other hand, fractionation occurs regarding longer (crystallizable) homopolymer sequences. This is true for longer propylene (low ethylene content) as well as longer ethylene (high ethylene content) sequences; see Fig. 3.26c.

3.2.3 Analysis of 1-Alkene Copolymers [87]

Besides ethylene and propylene homo- and copolymers, the copolymers of these monomers with higher 1-alkenes play an important role in technical applications. The most important materials of this group are copolymers of ethylene and 1-butene, 1-hexene or 1-octene. They are known as linear low-density polyethylenes (LLDPE) and they are mainly used as films in packaging. Other interesting materials, although not frequently used in technical applications yet, are copolymers of propylene with higher 1-alkenes.

3.2.3.1 Aim

Solvent gradient interaction chromatography has been shown to be a powerful tool for the separation of olefin copolymers according to chemical composition. In Sect. 3.2.2 the fractionation of ethylene-propylene copolymers has been presented. In the present section, the fractionation of copolymers with higher 1-alkenes shall be discussed. The focus will be on propylene copolymers with 1-butene, 1-hexene, 1-octene, 1-tetradecene and 1-octadecene. The behaviour of these copolymers will be compared to the behaviour of ethylene-1-hexene copolymers which are typical LLDPEs.

3.2.3.2 Materials

- *Polymers*. Copolymers of various origins were used. Their comonomer contents and molar masses are summarized in Table 3.6.

3.2.3.3 Equipment

- *Chromatographic system*. High-temperature chromatograph PL-GPC 210 (Polymer Labs, Church Stretton, UK) containing a gradient HPLC pump model 1200 (Agilent). The flow rate was 0.5 mL/min; samples were dissolved in 1-decanol.
- *Columns*. Hypercarb (Thermo Scientific, Dreieich, Germany), 100 mm × 4.6 mm i.d., average particle size 5 µm, surface area 120 m^2/g, average pore size 120 Å.
- *Mobile phase*. 1-decanol-TCB.
- *Detectors*. ELSD PL-ELS 1000 (Polymer Laboratories, Church Stretton, England). The air flow rate was 1.5 L/min, the nebulizer temperature was 160 °C and the evaporator temperature was 260 °C.
- *Column temperature*. 160 °C.
- *Sample concentration*. 1–2 mg/mL. All samples were dissolved in 1-decanol.
- *Injection volume*. 13 µL.

Table 3.6 Weight average molar mass (M_w), molar mass dispersity (M_w/M_n) and comonomer content of the copolymers as given by the producers (adapted from [87] with permission of Elsevier)

Sample code[a]	M_w (kg/mol)	M_w/M_n	Comonomer (wt%)
iPP-C2-1	147	2.1	5.8
iPP-C2-2	262	2.0	18.8
iPP-C4-1	125	1.7	1.4
iPP-C4-2	107	2.0	5.9
iPP-C4-3	226	1.8	8.6
iPP-C6-1	130	1.8	1.3
iPP-C6-2	150	2.1	5.6
iPP-C6-3	220	2.1	7.2
iPP-C12-1	283	2.3	0.26
iPP-C12-2	554	2.5	0.68
iPP-C12-3	639	2.5	0.89
iPP-C12-4	416	2.2	2.33
iPP-C12-5	395	2.3	2.76
iPP-C16-1	126	1.8	1.5
iPP-C16-2	104	1.8	4.5
iPP-C16-3	193	1.8	7.6
sPP-C3-1	185	1.8	0.7
sPP-C3-2	139	1.9	1.5
sPP-C3-3	113	1.9	2.4
sPP-C3-4	104	1.9	4.5
PE-C4-1	–	–	3.6
PE-C4-2	–	–	9.2
PE-C4-3	–	–	19.0
PE-C4-4	–	–	43.0
PE-C4-5	–	–	62.1

[a]Comonomers: C2 1-butene, C3 1-pentene, C4 1-hexene, C6 1-octene, C12 1-tetradecene, C16 1-octadecene

3.2.3.4 Preparatory Investigations

As was discussed earlier, the Hypercarb stationary phase is a very good choice for the separation of PP by tacticity and the separation of EP copolymers. It has been shown that iPP elutes before the solvent gradient while sPP and PE adsorb and elute only with the solvent gradient. For the EP copolymers, the mechanism of interaction has been shown to be based on the alignment of linear PE segments on the flat surface of the graphite sheets of the Hypercarb. Chain molecules with side groups (copolymers, branched polymers) cannot form closely packed layers with the graphite surface and are, therefore, less strongly adsorbed [96, 97].

To confirm the separation capabilities of the stationary phase, a set of blends of iPP, sPP and PE having different molar masses were prepared and separated. The elution profiles obtained were very similar to the ones presented in Fig. 3.16.

3.2.3.5 Measurement and Evaluation

Using Hypercarb as the stationary phase and the 1-decanol-TCB solvent gradient, the propylene copolymers were separated. As can be seen in Fig. 3.27, the copolymers with the shorter 1-olefins (1-butene, 1-hexene, 1-octene) did not adsorb on the stationary phase but eluted in the SEC mode before the start of the solvent gradient. For the 1-octene copolymers a small portion of material was detected that eluted later with the solvent gradient. These are probably the copolymer molecules with the highest comonomer content.

A different behaviour is obtained for copolymers with longer branches; see Fig. 3.28 for the propylene copolymers with 1-tetradecene and 1-octadecene. The elution volume increases with increasing 1-alkene content indicating that the longer alkyl branches adsorb on the stationary phase. This is in excellent agreement with the behaviour of ethylene copolymers where the longer ethylene segments interact with the stationary phase. It can be concluded that, although the iPP polymer backbone does not adsorb, substituents (branches) with a minimum number of ethylene units (>6) promote adsorption.

As has been shown earlier, the retention of PP is stereospecific, i.e. iPP is not retained, while sPP adsorbs on the Hypercarb stationary phase. When short alkyl branches are introduced into the sPP structure, the interactions with the graphite surface are disturbed and adsorption decreases. This is shown in Fig. 3.29 for propylene-1-pentene copolymers.

A similar trend is found for ethylene-1-hexene copolymers; see Fig. 3.30. The C4 branches in these copolymers are too short to interact with the stationary phase. Adsorption takes place only based on the long ethylene sequences. Accordingly, retention decreases with increasing comonomer content.

In the present application, ELS detection is used. It is known that peak intensity in ELS detection is influenced by a number of factors, including the composition of the analyte and the mobile phase. As can be seen in Fig. 3.30, the peak intensity decreases with increasing comonomer content although similar sample amounts were injected. At the same time samples of different compositions elute at different elution volumes and, hence, get exposed to different solvent compositions. This situation must be taken into account when the ELSD signal intensity is converted into concentration. Typically, an ELSD calibration must be conducted.

In conclusion, the retention behaviour as a function of copolymer type and composition is summarized in Fig. 3.31. The fact that copolymers containing the same backbone but different comonomers (branches) behave differently may open the way to characterize polyolefins regarding their branching microstructure.

3.3 Temperature Gradient Interaction Chromatography

Solvent gradient interaction chromatography (SGIC) is a very powerful technique for the chemical composition separation of polyolefins, but it does have a few limitations: one is the limited number of detectors that can be used. When using a solvent gradient, typical concentration detectors such as RI and IR cannot be used.

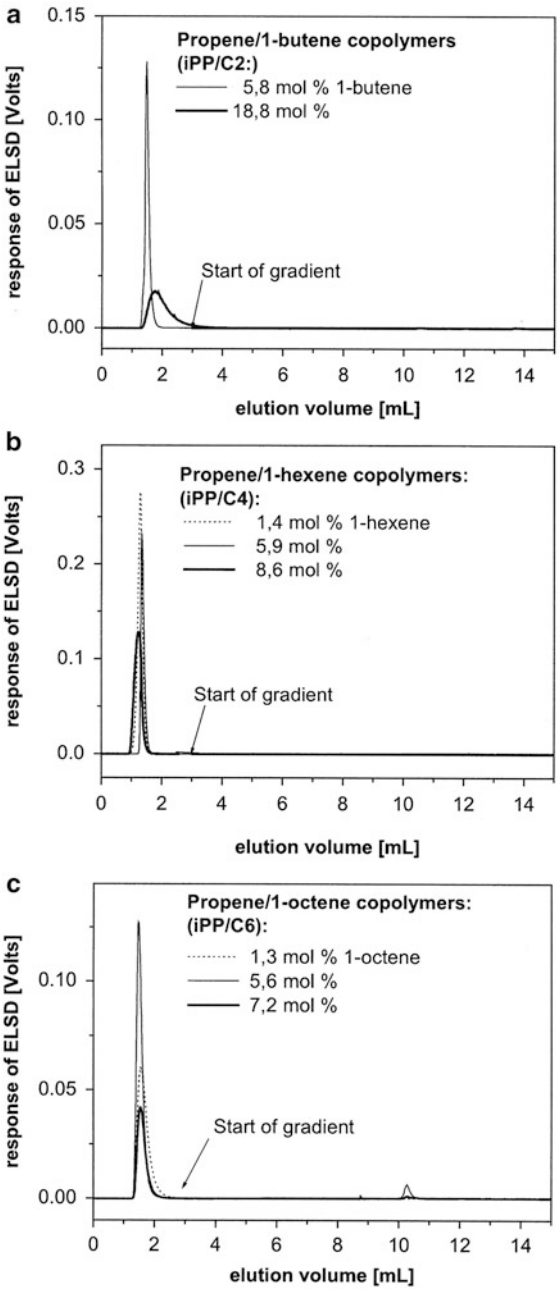

Fig. 3.27 Overlay of chromatograms for 1-alkene copolymers, comonomer content is indicated, (**a**) iPP-C2, (**b**) iPP-C4, (**c**) iPP-C6, solvent gradient: linear from 100 % 1-decanol to 100 % TCB in 10 min (reprinted from [87] with permission of Elsevier)

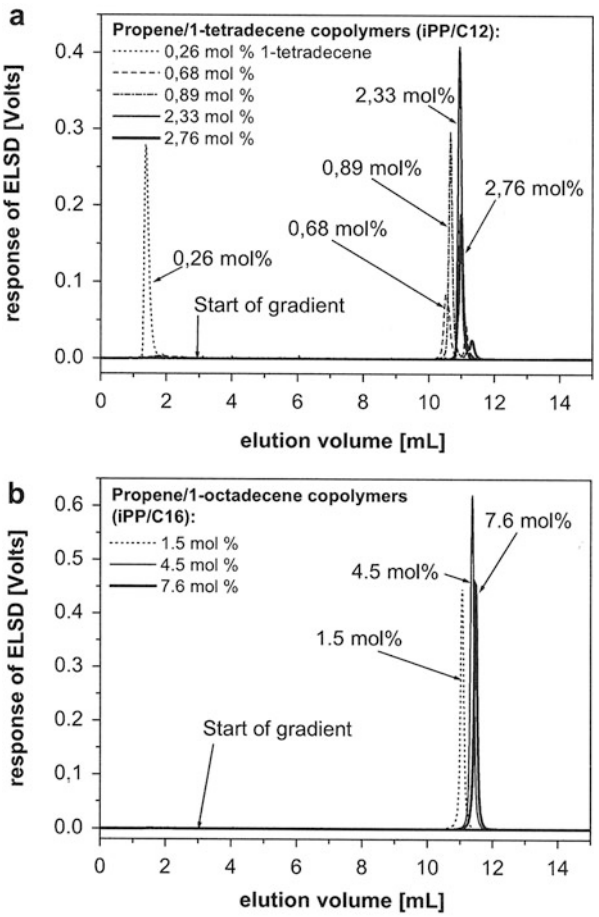

Fig. 3.28 Overlay of chromatograms for 1-alkene copolymers, comonomer content is indicated, (**a**) iPP-C12, (**b**) iPP-C16, solvent gradient: linear from 100 % 1-decanol to 100 % TCB in 10 min (reprinted from [87] with permission of Elsevier)

The solvent gradient also poses major limitations on the use of molar mass-sensitive detectors such as viscometers and LS detectors.

It is known that the adsorption of a polymer on a stationary phase is a function of temperature [98]. This phenomenon has been applied to the separation of synthetic polymers by a number of authors including Lochmüller et al. [99] for poly(ethylene glycol) and (most prominently) Chang and co-workers [59, 100, 101] for a variety of polymers. Very recently, Cong et al. described experimental conditions for the application of temperature changes to the separation of polyolefins [57]. In 'temperature gradient interaction chromatography' (TGIC), the solvent gradient is replaced by a thermal gradient using an isocratic mobile phase composition. The separation of EO copolymers was achieved by the interaction of the polyolefin with a graphite surface (Hypercarb) in a thermodynamically good solvent for PE. The solvent used was ODCB.

The results obtained were quite similar to those obtained with the solvent gradient approach, but, instead of using an ELS detector, detection was conducted

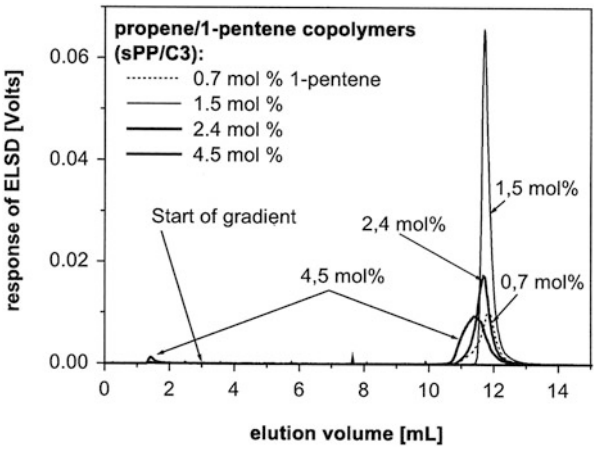

Fig. 3.29 Overlay of chromatograms for propylene-1-pentene copolymers, comonomer content is indicated, solvent gradient: linear from 100 % 1-decanol to 100 % TCB in 10 min (reprinted from [87] with permission of Elsevier)

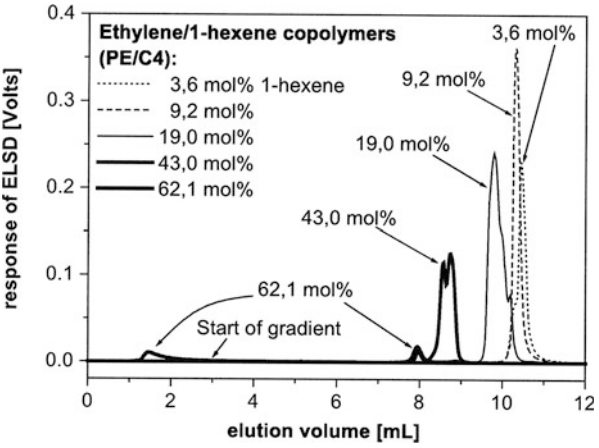

Fig. 3.30 Overlay of chromatograms for ethylene-1-hexene copolymers, comonomer content is indicated, solvent gradient: linear from 100 % 1-decanol to 100 % TCB in 10 min (reprinted from [87] with permission of Elsevier)

by a combination of IR, MALLS and Visco. A linear relationship between the elution time (elution temperature) and the copolymer composition was obtained. It was found that elution is independent of molar mass above 20 kg/mol.

The samples were dissolved in ODCB and injected into the column flushed with the solvent. After injection, a temperature gradient was applied; see Fig. 3.32. As a consequence, the samples eluted from the column in an elution order of decreasing comonomer content. The authors claimed that co-crystallization does not play a role in TGIC.

The work of Cong et al. [57] was followed by a number of detailed studies on the mechanism of TGIC. Monrabal explained the interaction with the graphite surface by weak van der Waals forces. In addition, he postulated that the flat surface of the graphene sheets interacts favourably with linear PE chains while copolymers or iPP show some steric hindrance causing a decrease in adsorption. The fact that flat surfaces enhance interaction was proven by Monrabal who showed that different

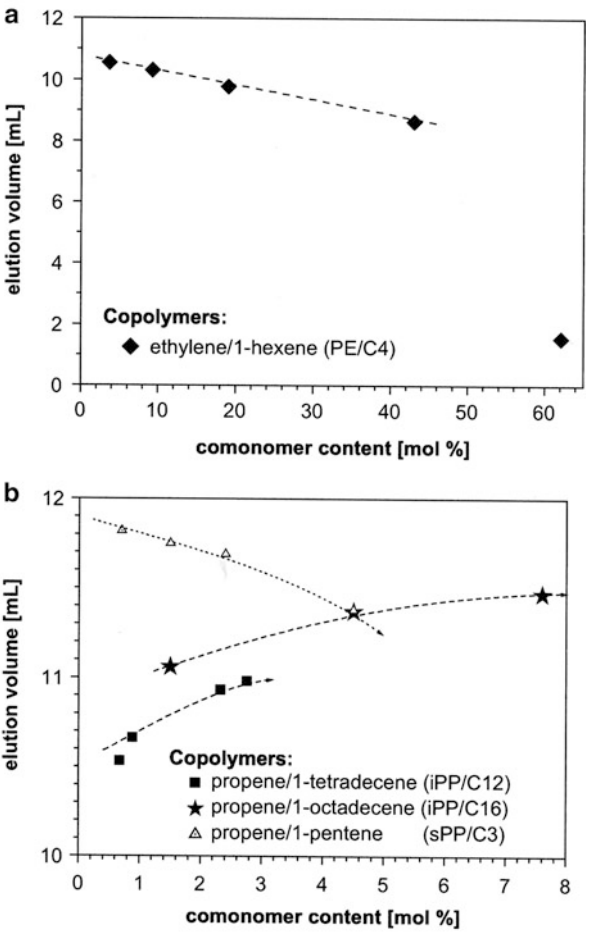

Fig. 3.31 Dependence of the elution volume on copolymer type and composition, (**a**) ethylene-1-hexene copolymers, (**b**) propylene-1-alkene copolymers (reprinted from [87] with permission of Elsevier)

surface chemistries show similar selectivities for ethylene copolymers [73, 102]. This is shown in Fig. 3.33 for a comparison of Hypercarb and a molybdenum sulphide stationary phase.

3.3.1 Separation of Ethylene-Octene Copolymers [57]

3.3.1.1 Aim

The separation of olefin copolymers according to chemical composition has been accomplished by SGIC; see Sect. 3.2.3 for more details. TREF and CRYSTAF have been used to fractionate EO copolymers by composition; these fractionations, however, are limited to the crystallizable part of the samples. The separation of these important copolymers over a broad range of compositions including non-crystalline components shall be conducted using HT-TGIC. The aim is to

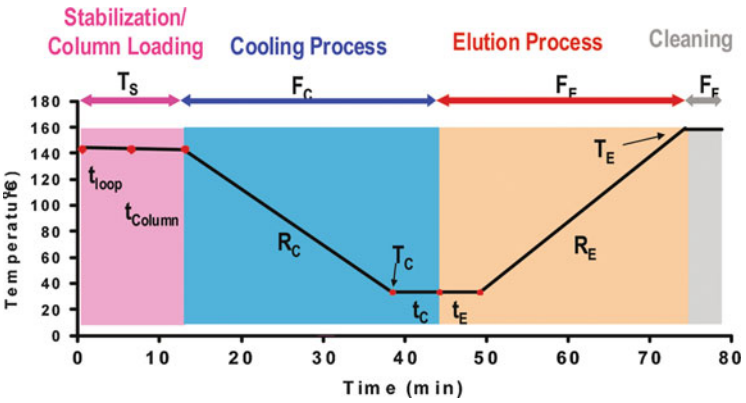

Fig. 3.32 Schematic of HT-TGIC experimental set-up, the definition of each variable is described in Table 3.7 (reprinted from [57], copyright (2011) of the American Chemical Society)

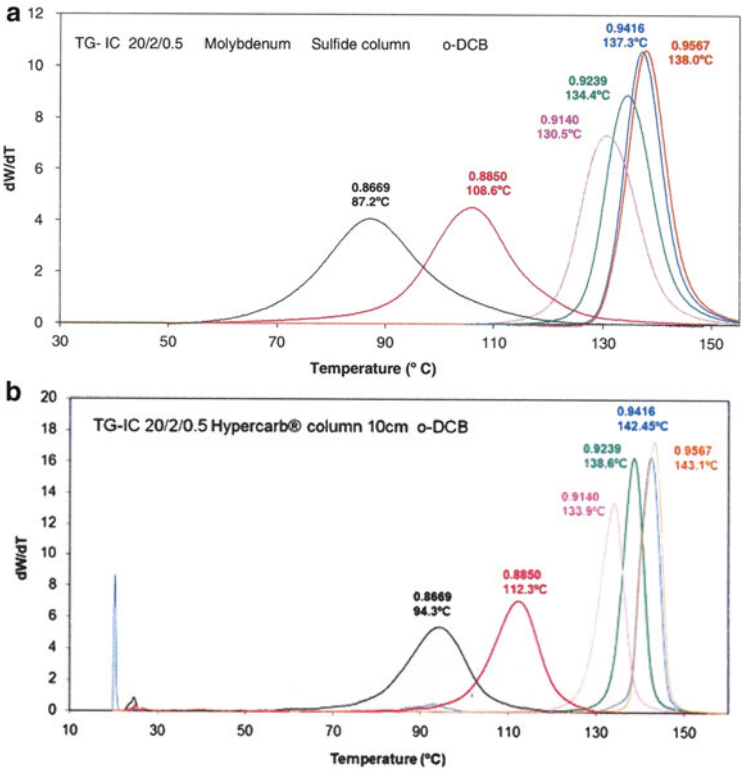

Fig. 3.33 HT-TGIC analysis of a number of ethylene-octene copolymers on Hypercarb (**a**) and molybdenum sulphide (**b**) as stationary phases, numbers indicate sample densities and elution temperatures (reprinted from [102] with permission of Wiley-VCH)

Table 3.7 Definition of the experimental variables for TGIC (adapted from [57], copyright (2011) of the American Chemical Society)

Variable	Symbol	Description
Stabilization and sample loading process		
Stabilization rate (°C/min)	R_S	Thermal rate for the temperature changing from the dissolution temperature to the stabilization temperature
Stabilization temperature (°C)	T_S	Temperature during stabilization and at the start of cooling process
Stabilization time (min)	t_{LOOP}	Amount of time the sample stays in the injection loop in the top oven of CEF before being loaded into the column
Precooling time (min)	t_{COLUMN}	Amount of time the sample stays in the front of the column before cooling process begins
Cooling process		
Cooling rate (°C/min)	R_C	Thermal rate of the main oven (where TGIC column is located) during cooling process
Final temp of cooling process (°C)	T_C	Final temperature at the end of cooling process
Postcooling time	t_C	Time that the sample stays in the column at the final temperature of cooling process
Flow rate of pump during cooling process (mL/min)	F_C	Flow rate during cooling process; it can be zero (static cooling process) or nonzero (dynamic cooling process)
Elution process		
Elution rate (°C/min)	R_E	Thermal rate of the main oven (where TGIC column is located) during elution process
Final temperature of elution process (°C)	T_E	Final temperature at the end of elution
Soluble fraction time	t_E	Amount of time that the main oven stays at the final temperature of cooling process while pump being at flow rate of elution process before increasing temperature; data collection begins here; the purpose is to have a well separate SF peak in chromatogram
Flow rate of pump during elution process (mL/min)	F_E	Flow rate during elution process

separate EO copolymers completely, irrespective of crystallinity, and exclusively regarding adsorptive interactions.

3.3.1.2 Materials

- *Standards*. Linear HDPE standards with peak molar masses of 2.1–1,100 kg/mol (Polymer Labs, Church Stretton, UK).
- *Polymers*. EO copolymers synthesized using a constrained geometry catalyst from Dow Chemical (Freeport, USA). The compositions and molar masses of the copolymers are summarized in Table 3.8.

Table 3.8 Weight average molar mass (M_w), molar mass dispersity (M_w/M_n) and comonomer content of EO copolymers as given by the producers (adapted from [57], copyright (2011) of the American Chemical Society)

Sample code	M_w (kg/mol)	M_w/M_n	Octene (mol%)
EO-1	115	2.6	0
EO-2	104.5	2.1	1.3
EO-3	102.9	2.3	4.0
EO-4	111.2	2.0	8.5
EO-5	123.4	2.0	13.9
EO-6	159.9	2.6	19.0
EO-7	174.5	2.6	21.7
EO-8	235.7	3.3	32.5
EO-9	39.6	2.0	50.7

3.3.1.3 Equipment

- *TGIC instrument*. CEF instrument (Polymer Char, Valencia, Spain) connected to a Spectra Chrom model CF-1 fraction collector (Spectrum Chromatography, Houston, USA). For the prep fractionations, nine fractions were collected at 2 min intervals. Twenty repetitive injections were made.
- *Columns*. Hypercarb (Thermo Scientific, Dreieich, Germany), 100 mm × 4.6 mm i.d., average particle size 7 μm, average pore size 250 Å.
- *Mobile phase*. ODCB.
- *Detectors*. Two-channel IR-4 (PolymerChar, Valencia, Spain), two-angle (15° and 90°) LS detector (Precision Detectors), two-capillary viscometer.
- *Column temperature*. Temperature gradient.
- *Sample concentration*. 2 mg/mL. All samples are dissolved in ODCB at 160 °C.
- *Injection volume*. 200 μL.

3.3.1.4 Preparatory Investigations

The HT-TGIC experiment consists of the following steps: (1) injection of the sample at a constant temperature, (2) adsorption of the polymer on the column by decreasing the column temperature and (3) elution of the polymer components by increasing the column temperature with a moderate solvent flow. The column process (2) can be carried out with (similar to CEF) or without flow. To obtain optimum separation, a number of experimental variables can be changed including the column cooling and heating rates, and the solvent flow. The definition of the experimental variables of TGIC is listed in Table 3.7.

In the present case, the optimum experimental conditions are the following: stabilization temperature (T_s) 140 °C, stabilization rate (R_s) 40 °C/min, stabilization time (t_{loop}) 2 min and precooling time (t_{column}) 2 min. Many other factors can affect the results. To simplify the identification of any specific HT-TGIC run conditions, the following run-ID convention was adopted by Cong et al. [57]: TGIC 140 °C_0 °C_175 °C_6 °C/min_3 °C/min_0.03 mL/min_0.5 mL/min, representing the following experimental conditions: stabilization temperature (°C)_final temperature during cooling process (°C)_final temperature during elution process (°C)_cooling rate during cooling process (°C/min)_heating rate during elution process (°C/min)_flow rate during cooling process (mL/min)_flow rate during elution process (mL/min), respectively.

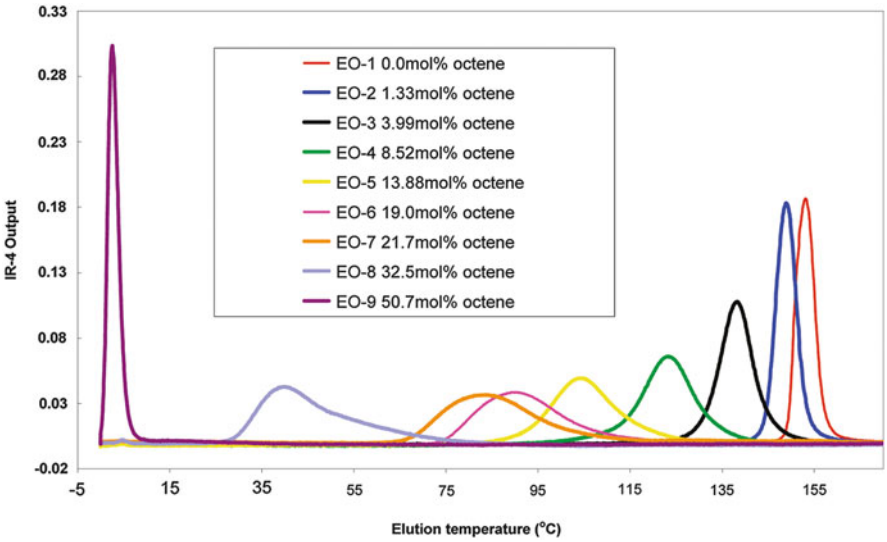

Fig. 3.34 HT-TGIC chromatograms of EO-1 to EO-9, Hypercarb column, TGIC experimental conditions (stabilization temperature 140 °C; final temperature during cooling process 0 °C; final temperature during elution process 175 °C; cooling rate during cooling process 6 °C/min; heating rate during elution process 3 °C/min; flow rate during cooling process 0.03 mL/min; flow rate during elution process 0.5 mL/min (reprinted from [57], copyright (2011) of the American Chemical Society)

3.3.1.5 Measurement and Evaluation

Using the above experimental conditions, the EO copolymers were separated by HT-TGIC. An overlay of the chromatograms of the samples is presented in Fig. 3.34. The overlay shows clearly that the samples were separated according to the comonomer content. The highest elution temperature (150.4 °C) was obtained for the PE homopolymer EO-1. This elution temperature is roughly 49 °C higher than the TREF/CEF elution temperatures and it is 15 °C higher than the melting temperature obtained by DSC. This is a clear indication for the adsorptive interactions taking place with the Hypercarb stationary phase. The peak elution temperature is a linear function of the octene content of the copolymers as can be seen in Fig. 3.35.

Regarding the range of copolymer compositions, samples containing up to 50 mol% of octene can be separated. This is a significantly larger compositional range compared to TREF and CEF. It does not, however, cover the whole range of compositions from 0 % to 100 % comonomer.

The separation mechanism in HT-TGIC was further studied by preparative fractionation of sample EO-4 and subsequent analysis of the fractions by ^{13}C-NMR spectroscopy. The prep TGIC chromatogram is given in Fig. 3.36a and the compositions of the fractions as obtained by ^{13}C-NMR are given in Fig. 3.36b. This experiment shows again that separation takes place based on octene content of the copolymer.

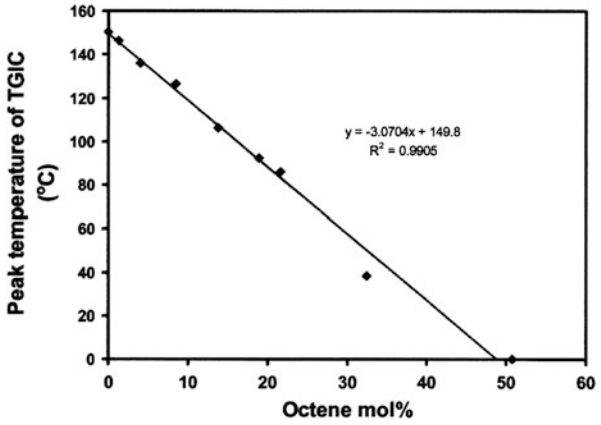

Fig. 3.35 Plot of the peak elution temperature of HT-TGIC vs. octene content of EO copolymer; for experimental conditions see Fig. 3.34 (reprinted from [57], copyright (2011) of the American Chemical Society)

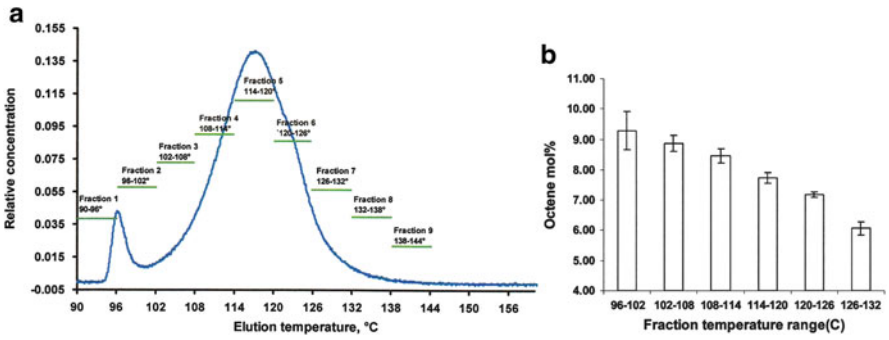

Fig. 3.36 Prep TGIC chromatogram of sample EO-4 (**a**) and octene content of the fractions as determined by ^{13}C-NMR (**b**) (reprinted from [57], copyright (2011) of the American Chemical Society)

The molar mass dependence of the elution temperature was investigated by analysing a set of HDPE calibration standards. It was found that samples with lower molar masses eluted at lower temperatures. When increasing the molar mass, the elution temperature stabilized at about 153 °C and from molar masses of about 20 kg/mol upwards this elution temperature was obtained irrespective of molar mass. The co-crystallization was analysed by separating EO copolymer blends and it was found that co-crystallization does not occur in HT-TGIC.

3.4 Two-Dimensional Liquid Chromatography

The most relevant structural parameters of a complex polyolefin are MMD and CCD. Other structural features such as branching (SCB and LCB distributions) as well as the distribution of functional groups are not less important but are more difficult to analyse.

For the last three decades, the analysis of the bivariate CCD-MMD distribution was limited to the combination of TREF and SEC. As early as 1981, the first automatic TREF-SEC instrument was introduced by Nakano and Goto [103]. They were able to present the molecular heterogeneity of complex polyolefins in 3D diagrams where the TREF elution temperature (as a measure of CCD), the molar mass and the detector output (as a measure of concentration) were plotted against each other; see e.g., Fig. 2.8. A fully automated cross-fractionation instrument was introduced by Polymer Char in 2005, see schematic diagram in Fig. 2.7 [104].

In one of the latest developments, HT-TGIC was coupled to SEC for the analysis of the molecular heterogeneity of EPDM [105]. In this case, the EPDM was not fractionated by crystallizability but by adsorptive interaction with a graphitic stationary phase. The contour diagram of a typical EPDM sample, together with the reconstructed CCD and MMD plots, is shown in Fig. 3.37. The quantitative copolymer composition was determined using a dual wavelength IR detector revealing the numberr of CH_3 groups per 1,000 carbons.

Over the last 20 years, comprehensive 2D-LC has developed into a powerful analytical technique for the analysis of the molecular heterogeneity of complex polymers [4, 5]. Coupling of different liquid chromatographic separation methods enables the high resolution of multiple distinctive molecular distributions. Until recently, however, the application of 2D-LC was limited to ambient temperature; it was only in 2009 that the introduction of a commercial instrument based on HT-2D-LC was announced. In this instrument, isocratic and solvent gradient separations can be conducted in the first dimension to provide information on the chemical composition (functionality, branching) of olefin copolymers and polyolefin blends. A photograph of the instrument is shown in Fig. 3.38. It comprises a separate sample dissolution and injection module, a solvent delivery module and a chromatographic unit containing two separate column ovens for the HPLC and the SEC columns. The instrument is equipped with RI, IR and ELSD detectors, with options to add a MALLS or viscometer detector.

Ginzburg et al. [106, 107] and Roy et al. [108] published the first results on 2D-LC for polyolefins. The system used by Roy et al. [108] was the same as described by Macko et al. [84, 85, 87]. The separation of EO copolymers with regard to chemical composition and molar mass was achieved on this system. Online coupling of gradient HPLC and SEC for the separation of blends of PP stereoisomers, ethylene-propylene rubbers (EPRs), ethylene-norbornene copolymers and ethylene-1-hexene copolymers was employed by Ginzburg et al. [106]. Hypercarb as the stationary phase and 1-decanol-TCB as the mobile phase were used for all separations at an operating temperature of 160 °C. As an example, the 2D contour diagram (composition vs. molar mass) of one of the

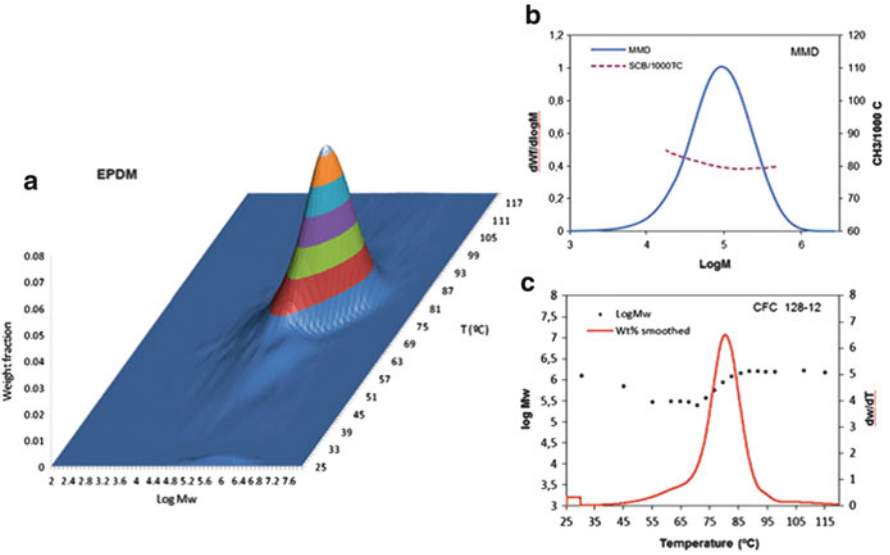

Fig. 3.37 TGIC-SEC analysis of an EPDM sample (**a**), reconstructed MMD with SCB reading (**b**) and reconstructed TGIC temperature plot with M_w reading (**c**) (reprinted from [73] with permission of Springer Science + Business Media)

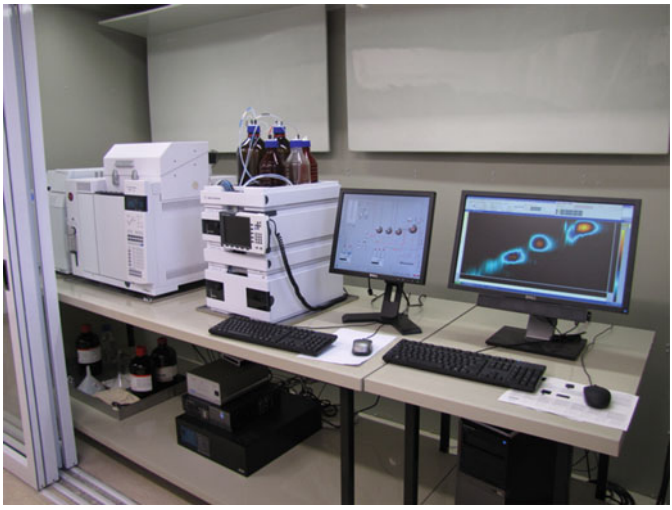

Fig. 3.38 High-temperature 2D-LC system of PolymerChar (Valencia, Spain)

systems is shown in Fig. 3.39a. The capabilities of HT-2D-LC are convincingly presented in this application. A complex mixture of PE and PPs with different tacticities has also been separated as illustrated in Fig. 3.39b.

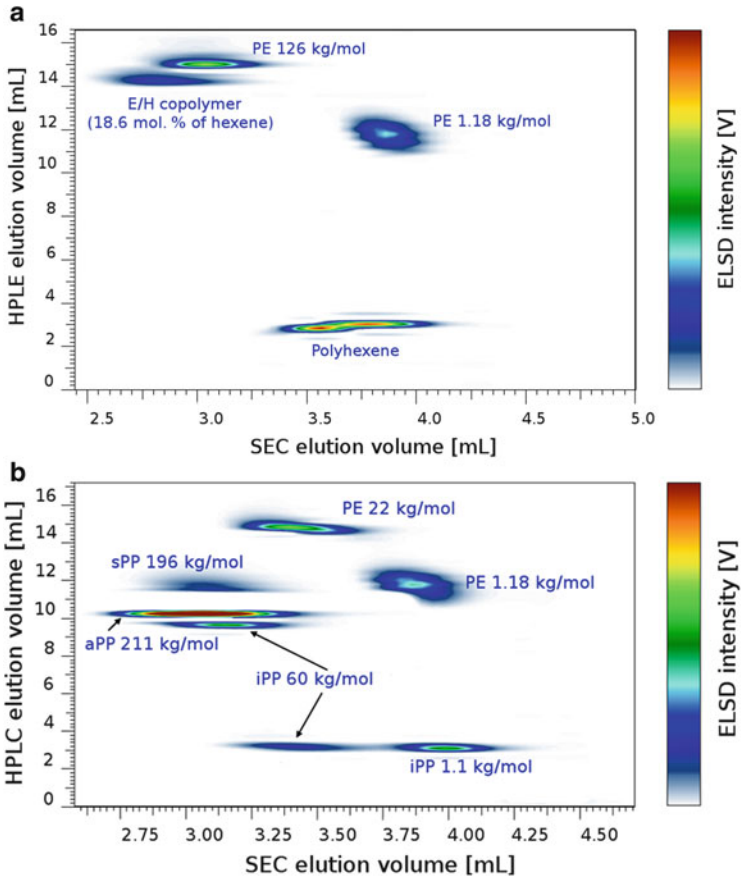

Fig. 3.39 Contour diagram of the HT-2D-LC separation of (**a**) a blend of PE, poly-1-hexene and an ethylene-1-hexene copolymer and (**b**) a blend of PE and PPs with different tacticities; stationary phase: Hypercarb (first dimension) and PL Rapide H (second dimension); mobile phase: gradient 1-decanol/TCB (first dimension) and TCB (second dimension); temperature: 160 °C; detector: ELSD (reprinted from [107] with permission of Elsevier Limited)

Ginzburg et al. [106] demonstrated that both axes of the contour plot may be calibrated for the HT-2D-LC separation of EVA copolymers. PE standards were used to calibrate the SEC separation, while EVA copolymers with known VA content were utilized for calibration of HPLC. Moreover, the utilization of TCB as mobile phase in coupling of HPLC to SEC enables the application of RI, IR, Visco or LS detectors as was demonstrated by Lee et al. for the 2D-LC separation of EP and EO copolymers [109]. The calculation of molar masses of polymers eluting from the 2D-LC system was carried out on the basis of signals from the IR and LS detectors.

The different separation principles of 2D-LC and TREF-SEC resulted in dissimilar contour plots as obtained from both types of hyphenations. The separation in

TREF is governed by the crystallization-dissolution behaviour of the samples in contrast to interactive HPLC, which is based on selective adsorption and desorption of the macromolecules. It is one of the major advantages of 2D-LC over TREF-SEC that it enables one to address all sample components irrespective of their crystallinity.

The following two applications of HT-2D-LC have been published previously in [5]. They are reproduced here because they serve as excellent examples for the power of this technique.

3.4.1 Analysis of Polypropylenes by Tacticity and Molar Mass [107]

3.4.1.1 Aim

Polyolefins are similar to other synthetic polymers in that they are complex with regard to different parameters of molecular heterogeneity. PPs exhibit a MMD and a distribution regarding tacticity. Due to the chiral centre of propylene, different catalysts and polymerization conditions may result in the formation of iPP and sPP polymer chains or subunits. When different tactic units are distributed along the polymer chain, the material is atactic (aPP). The average tacticity of PP can be analysed by FTIR or NMR spectroscopy. In FTIR spectroscopy, the information relates to a global % tacticity while NMR provides the types and concentrations of tactic triads or pentads depending on the technical parameters of the spectrometer. Quantitative information on the composition of a single polymer chain cannot be provided nor can a blend (of, e.g., iPP, sPP and aPP) be differentiated from a PP containing different tactic units. It has been shown in a number of applications that the Hypercarb stationary phase exhibits a remarkable selectivity towards different polyolefin structures; see Sects. 3.2.2 and 3.2.3. This stationary phase shall now be used for the separation of PP according to tactivity. The molar mass of the different tactic polymers shall be analysed by online coupled SEC.

3.4.1.2 Materials

- *Calibration standards*. Linear PE and PP standards (PSS GmbH, Mainz, Germany).
- *Polymers*. sPP with M_w 196 kg/mol (Sigma-Aldrich, Munich, Germany), aPP with M_w 211 kg/mol (LyondellBasell, Ferrara, Italy), iPP with M_w 45 kg/mol (University of Stellenbosch, South Africa).

3.4.1.3 Equipment

- *Chromatographic system*. A prototype chromatographic system for HT-2D-LC analysis constructed by Polymer Char (Valencia, Spain) was used for all experiments. The system has an autosampler, two separate ovens, valves and two pumps equipped with vacuum degassers (Agilent, Waldbronn, Germany). The first oven is for thermostating the SEC column while the other one is used to thermostat the HPLC column. The injector and a switching valve are housed in the latter. An electronically controlled 8-port valve EC8W (VICI Valco

instruments, Houston, Texas, USA) equipped with two 200 µL loops was employed for hyphenation of HT-HPLC and HT-SEC. The 8-port valve was switched every 2 min in order to inject 200 µL of effluent from the HPLC into the SEC column from the moment of injection in the HPLC column (50 µL injection loop). The 2D-LC system was handled with software provided by Polymer Char (Valencia, Spain). The data acquisition and evaluation was performed by WinGPC-Software v. 7.0 (Polymer Standards Service, Mainz, Germany).

- *Columns*. Chromatograph 1: Hypercarb column (Thermo Scientific, Dreieich, Germany) packed with porous graphite particles with the following parameters: column size 250 mm × 4.6 mm i.d., average particle size 5 µm, surface area 120 m^2/g, average pore size 250 Å. Chromatograph 2: PL Rapide H, 150 mm × 7.5 mm (Polymer Laboratories, Church Stretton, England).
- *Mobile phase*. Chromatograph 1: linear gradient 1-decanol to TCB starting with 100 % of 1-decanol for 40 min, the volume fraction of TCB was linearly increased to 100 % within 80 min and then held constant for 80 min. The flow rate was 0.1 mL/min. Chromatograph 2: TCB with a flow rate of 2.5 mL/min.
- *Detectors*. ELSD PL-ELS 1000 (Polymer Laboratories, Church Stretton, England). The following parameters were set on the ELSD: air flow rate 1.5 L/min, nebulizer temperature 160 °C, evaporator temperature 260 °C.
- *Column temperature*. 160 °C.
- *Sample concentration*. 2–3 mg/mL. All samples were dissolved in 1-decanol.
- *Injection volume*. 50 µL (first dimension).

3.4.1.4 Preparatory Investigations

The separation in the first dimension was conducted according to the method that was published by Macko and Pasch [85] using Hypercarb as the stationary phase and a solvent gradient of 1-decanol-TCB. The separation is according to tacticity of PP and chemical composition, separating PP and PE. In preliminary investigations, it has been found that iPP elutes in two peaks. The first peak elutes in decanol before the start of the gradient while the second peak elutes with the solvent gradient. To investigate this phenomenon in more detail, iPP samples with different molar masses were analysed by HT-2D-LC; see Fig. 3.40.

The contour plots prove that in all cases the portion of iPP, which elutes in the gradient, has a larger molar mass than the fraction that elutes in 1-decanol. Moreover, the higher the molar mass of the injected iPP standard, the larger is the fraction that elutes in the gradient. The standard with M_w 350 kg/mol is almost completely retained and elutes mostly with the gradient. At present it is not quite clear what the reason for the elution behaviour is. This should be considered in future investigations.

3.4.1.5 Measurement and Evaluation

The separation of a blend of iPP, sPP, aPP and PE is presented in Fig. 3.41. As expected, all components are fully separated from each other. Their molar masses are different, as is proven by the different elution volumes in the second dimension.

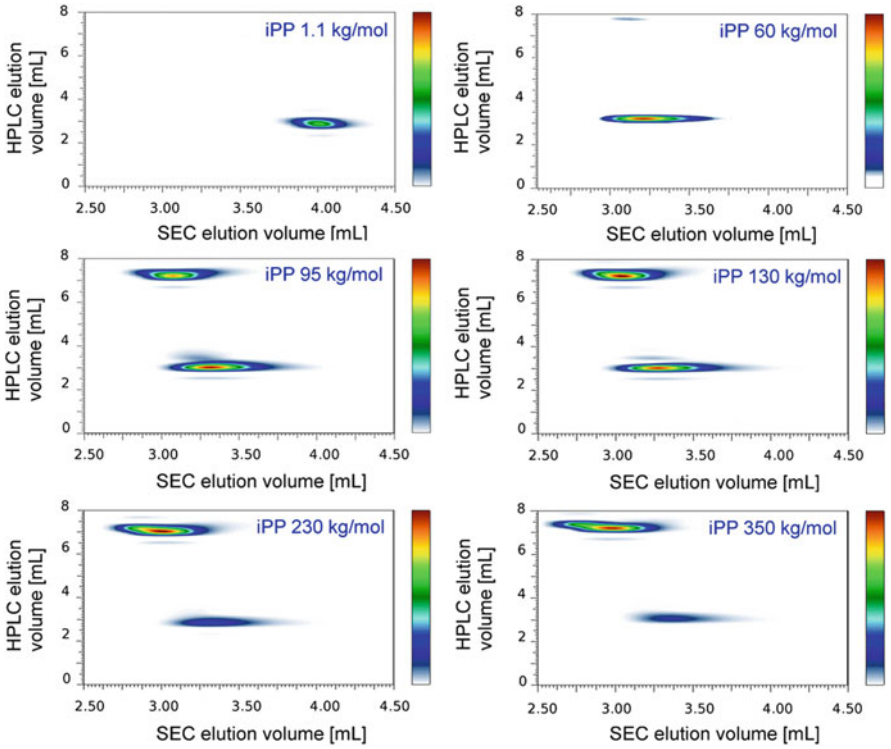

Fig. 3.40 2D-LC plots of iPP samples with different molar masses. First dimension: Hypercarb, mobile phase: gradient decanol-TCB; second dimension: PL Rapide, TCB; detector: ELSD, column temperature 160 °C (reprinted from [107] with permission of Elsevier)

It can be clearly seen that aPP and sPP have significantly higher molar masses than iPP and PE.

A most important yet difficult topic in 2D-LC is calibration of the second dimension to determine the molar masses of the separated species. In a comprehensive 2D-LC set-up, two chromatographic modes (HPLC and SEC) are coupled online. This means that the polymer sample is introduced into the SEC column in a mixed solvent via an automated switching valve. In the present case the composition of the mixed solvent changes from pure 1-decanol to 1-decanol/TCB. The hydrodynamic volume of the macromolecules may vary in different solvents, which may result in slight variations from the SEC calibration curve as obtained in a pure solvent. In order to study the influence of the injection solvent on the behaviour of macromolecules in SEC, the PE and iPP standards were individually analysed by SEC. The sample solvent for PE and iPP was either 1-decanol or TCB. SEC calibration curves constructed for both iPP and PE standards are shown in Fig. 3.42. There are variations in the calibration curves of iPP standards with different injection solvents, in contrast to PE standards that show no effect of the injection volume except for the low molar mass region. It is, therefore, important to

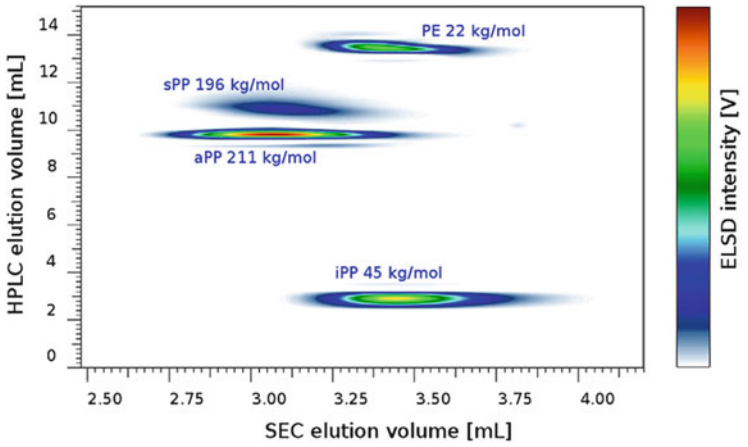

Fig. 3.41 2D-LC plot of a blend of iPP, sPP, aPP and PE with different molar masses; for experimental conditions see Fig. 3.40 (reprinted from [107] with permission of Elsevier)

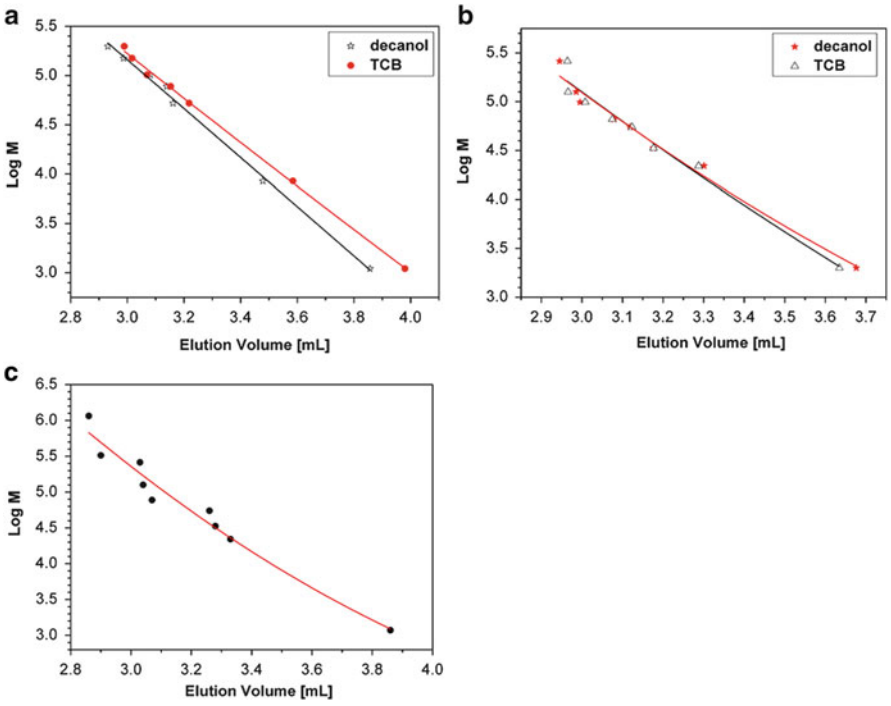

Fig. 3.42 2D-LC calibration curves for iPP (**a**) and PE (**b**) obtained by injection of the samples in the second dimension and for PE (**c**) obtained by injection in the 2D-LC (reprinted from [107] with permission of Elsevier)

investigate the calibration behaviour of different polyolefins in detail. An even more complex situation is encountered when the calibration standards are injected into the first dimension and undergo the entire 2D-LC separation. In this case, very scattered data have been obtained, as is seen in Fig. 3.42c, which cannot be explained at present.

3.4.2 Analysis of Ethylene-Vinyl Acetate Copolymers [106]

3.4.2.1 Aim

EVAs are copolymers of ethylene and vinyl acetate and are commercially important products. These products can be used for a variety of applications including the production of films, foams or hot melt adhesives, depending upon their comonomer content. As is true for all copolymers, these materials can exhibit distributions with respect to molar mass, chemical composition and branching. Therefore, it is essential to develop comprehensive characterization methods for these copolymers. The detailed characterization helps to optimize their synthesis and to develop structure–property correlations.

EVA with low vinyl acetate contents are semi-crystalline materials that can be separated according to composition by TREF. EVA copolymers containing 9–42 wt % VA were analysed. It was found that copolymers with VA contents higher than 20 wt% are fully amorphous and thus cannot be separated by TREF or CRYSTAF. It is, therefore, the aim of the present application to separate EVA copolymers over the entire comonomer concentration range by HT-HPLC. The molar mass information shall be obtained by online coupled SEC.

3.4.2.2 Materials

- *Calibration standards*. Linear PE standards (Polymer Standards Service, Mainz, Germany).
- *Polymers*. EVA copolymers were obtained from Exxon-Mobil Chemical (Meerhout, Belgium) and Bayer (Leverkusen, Germany). Their characteristics were as follows: M_w (kg/mol)/PDI/VA (mol%): Escorene 0019 (Exxon Mobil) 197.5/3.1/6.5; Levapren 450 (Bayer) 377.9/8.1/20; Levapren 800HV (Bayer) 224.6/4.1/57.

3.4.2.3 Equipment

- *Chromatographic system*. A prototype chromatographic system for HT-2D-LC (Polymer Char, Valencia, Spain) was used for all experiments. The system has an autosampler, two separate ovens, valves and two pumps equipped with vacuum degassers (Agilent, Waldbronn, Germany). The first oven is for thermostating the SEC column while the other one is used to thermostat the HPLC column. The injector and a switching valve are housed in the latter. An electronically controlled 8-port valve EC8W (VICI Valco instruments, Houston, Texas, USA) equipped with two 200 μL loops was employed for hyphenation of HT-HPLC and HT-SEC. The 8-port valve was switched every 2 min in order to

inject 200 µL of effluent from the HPLC into the SEC column from the moment of injection in the HPLC column (50 µL injection loop). The 2D-LC system was handled with software provided by Polymer Char (Valencia, Spain). The data acquisition and evaluation was performed by WinGPC-Software v. 7.0 (Polymer Standards Service, Mainz, Germany).

- *Columns*. Chromatograph 1: Perfectsil 300, 250 mm × 4.6 mm i.d., average particle size 5 µm (MZ Analysentechnik, Mainz, Germany). Chromatograph 2: PL Rapide H, 150 mm × 7.5 mm i.d. (Polymer Laboratories, Church Stretton, England).
- *Mobile phase*. Chromatograph 1: linear gradient TCB-cyclohexanone. The flow rate was 0.1 mL/min. Chromatograph 2: TCB with a flow rate of 2.5 mL/min.
- *Detectors*. ELSD PL-ELS 1000 (Polymer Laboratories, Church Stretton, England). The following parameters were set on the ELSD: air flow rate 1.5 L/min, nebulizer temperature 160 °C, evaporator temperature 260 °C.
- *Column temperature*. 150 °C.
- *Sample concentration*. 2 mg/mL. All samples were dissolved in TCB.
- *Injection volume*. 50 µL (first dimension).

3.4.2.4 Preparatory Investigations

The major prerequisite for the successful 2D-LC separation is a suitable chromatographic system. The successful separation of EVA copolymers with respect to the VA content has been shown on a bare silica column in a mobile phase composed of TCB and cyclohexanone [80]. EVA adsorbs on the stationary phase in the starting solvent (TCB) and is subsequently desorbed by a TCB-cyclohexanone solvent gradient.

3.4.2.5 Measurement and Evaluation

The contour plot in Fig. 3.43 shows the 2D-LC separation of a blend of the homopolymers PVAc and PE and three EVA copolymers. The y-axis represents the gradient HPLC separation and the x-axis represents the SEC separation. The samples are separated with respect to the polarity. PE is the least polar component and elutes first, while the last eluting component is PVAc, the most polar component. Between these two extremes, the three EVA copolymers elute with respect to their VA content. The separation of two of the EVA copolymers (6.5 mol% and 20 mol% VA) was not optimal; nonetheless, the presence of two components with different chemical compositions as well as with different molar masses can be concluded. The spot between 5.6 mL and 6.0 mL in the contour plot is an artifact produced by the WinGPC software.

In 2D-LC, typically only the second dimension providing the molar mass information is calibrated. In the present application, however, both dimensions shall be calibrated. The knowledge of the delay volume of the system, namely the time required by the gradient to reach the detector, is needed for calibration of the HPLC instrument.

The delay volume can be obtained by summing up the void volume and dwell volume of the corresponding system. The void volume corresponds to the volume

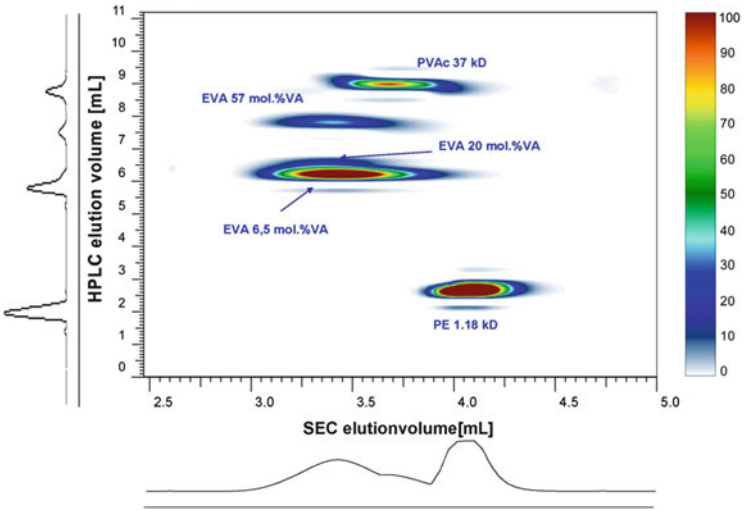

Fig. 3.43 2D-LC plot of a blend of PVAc, PE and three EVA copolymers. First dimension: Perfectsil, mobile phase: gradient TCB-cyclohexanone; second dimension: PL Rapide, TCB; detector: ELSD, column temperature 150 °C (reprinted from [106] with permission of Elsevier)

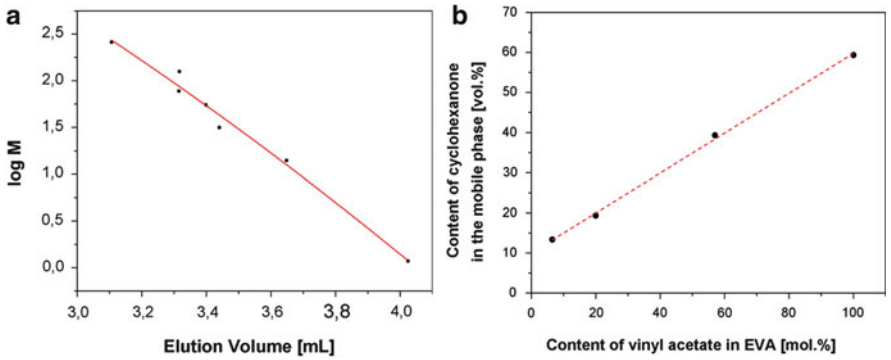

Fig. 3.44 Molar mass calibration curve for PE (**a**) and chemical composition calibration curve for VA content (**b**) obtained by injection in the 2D-LC (reprinted from [106] with permission of Elsevier)

of the mobile phase required to elute the unretained component. The dwell volume is the volume of the liquid between the injector and the point where the gradient is formed. The method proposed by Bashir et al. was modified to determine the void and dwell volume in HPLC [110]. According to the previous knowledge of the current system, there is a linear correlation between the elution volume and the average chemical composition of the EVA copolymers. The obtained relationship is depicted in Fig. 3.44 together with the SEC calibration curve. After the determination of the delay volume, the cyclohexanone content of the mobile phase at a

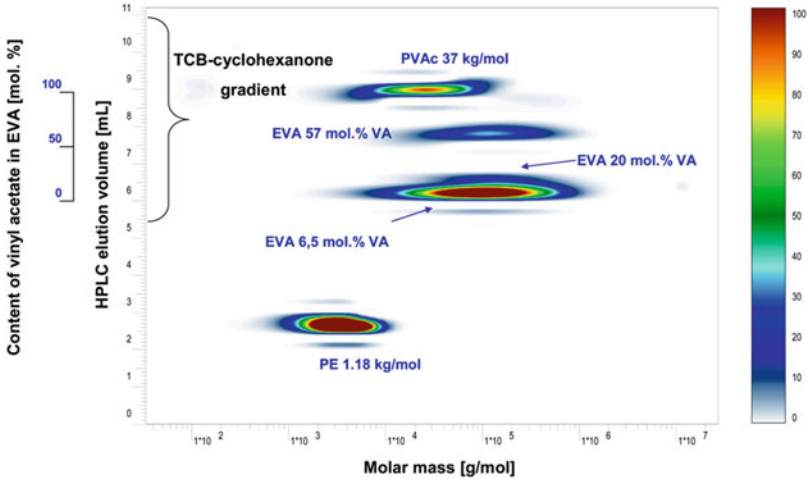

Fig. 3.45 2D-LC plot obtained from the original data in Fig. 3.43 after calibration of both dimensions (reprinted from [106] with permission of Elsevier)

particular elution volume can be found. The relation of the elution volume and the VA content of the copolymers was applied to the 2D contour plot. Consequently, the x- and y-axes of the contour plot were converted and thus a new (quantitative) contour plot was obtained; see Fig. 3.45.

3.4.3 Analysis Impact Polypropylene Copolymers [111]

The complexity of impact polypropylene copolymers (IPCs) is well documented. The major components of IPCs are iPP and ethylene-propylene (EP) copolymers of various compositions with small amounts of PE. The application range of iPP is significantly widened by introducing IPCs because these materials have improved low-temperature impact properties compared to pure iPP. The most widely used method for the preparation of IPCs is a two-step, two-reactor process. In the first reactor propylene is homopolymerized, followed by copolymerization of propylene and ethylene in the second reactor.

The meticulous characterization of these complex materials revealing MMD and CCD is very important for the understanding of the properties of materials during processing and in final applications. There is a direct correlation between MMD and physical properties such as toughness, melt viscosity and crystallinity. The tailoring and modifying of catalyst structures or polymerization conditions during synthesis in order to influence the final properties of the polymers also require accurate knowledge of the MMD. Although MMD is a very important factor, the final physical and mechanical properties of such complex copolymers are also greatly influenced by CCD [112].

A number of non-chromatographic separation techniques have been used to analyse the CCD of IPC, including TREF, CRYSTAF and CEF. Indeed, preparative

fractionation and subsequent analysis of the individual fractions by SEC-FTIR has been found to be an effective method for the determination of the chemical composition per molar mass slice [45]. This approach provides an average chemical composition per molar mass fraction; however, the CCD cannot be obtained since each molar mass fraction can be heterogeneous with respect to chemical composition.

The most recent development in the field of polyolefin analysis is the introduction of HT-HPLC that allows fractionation of polyolefins with respect to their chemical composition. Since final materials properties are dependent on MMD and CCD, fractionation with respect to both parameters is required. MMD and CCD overlap with each other; hence, a 2D mapping of this multivariate distribution (separation according to chemical composition and molar mass) is required. This mapping can be realized by HT-2D-LC. In a previous study, the individual components in selected TREF fractions of IPC were fractionated and analysed by the combination of P-TREF, HT-HPLC and HT-2D-LC [113, 114]. The analysis of the TREF fractions was accomplished by coupling HT-SEC to advanced thermal analysis. The analysis of TREF-SEC fractions by HyperDSC and Flash DSC 1 revealed that the fractions had complex molecular structures and exhibited complex thermal behaviours.

3.4.3.1 Aim

In this study, two complex IPC samples with different chemical compositions shall be analysed to evaluate the effectiveness of cross-fractionation techniques, obtained by a combination of various analytical separation methods as a tool for complex polyolefin characterization. The P-TREF fractionation will be the initial step that will provide different fractions, including EPR, EP-segmented copolymers and iPP. These fractions can still have distributions with respect to chemical composition and molar mass. Different coupled methods, namely SEC-FTIR, HT-HPLC-FTIR and HT-2D-LC, will be used for the analysis of the P-TREF fractions. In HT-2D-LC, the chemically homogeneous fractions obtained by HT-HPLC in the first dimension will be analysed for MMD by HT-SEC in the second dimension. For CCD analysis, HT-HPLC will be coupled to FTIR spectroscopy via the LC-Transform interface. The coupling to FTIR will reveal information on the ethylene and propylene contents of the samples, and also the ethylene and propylene crystallinities.

3.4.3.2 Materials

- *Polymers*. Two non-stabilized IPCs (designated 3V and 3VA) (SASOL Polymers, Secunda, South Africa). Molar mass dispersity and comonomer content of the samples are given as follows: 3V: 10.5 mol% ethylene, isotacticity 88.8 % (mmmm), M_w 228 kg/mol, M_w/M_n 3.5; 3VA: 11.8 mol% ethylene, isotacticity 87.5 % (mmmm), M_w 361 kg/mol, M_w/M_n 6.0.

3.4.3.3 Equipment

- *Chromatographic system for HPLC and 2D-LC*. A prototype chromatographic system for HT-2D-LC (Polymer Char, Valencia, Spain) was used for all experiments. The system has an autosampler, two separate ovens, valves and two pumps equipped with vacuum degassers (Agilent, Waldbronn, Germany). The first oven is for thermostating the SEC column while the other one is used to thermostat the HPLC column. The injector and a switching valve were housed in the latter. An electronically controlled 8-port valve EC8W (VICI Valco instruments, Houston, Texas, USA) equipped with two 100 μL loops was employed for hyphenation of HT-HPLC and HT-SEC.
- *HT-SEC*. PL GPC 220 high-temperature chromatograph (Polymer Laboratories, Church Stretton, UK) operating at 150 °C equipped with a differential RI detector, flow rate 1.0 mL/min, samples were dissolved at 160 °C at a concentration of 1 mg/mL for 1–2 h, injection volume 200 μL, calibration with narrowly distributed PS standards (Polymer Laboratories, Church Stretton, UK).
- *TREF*. Instrument developed and built in-house. For the fractionation, 3.0 g of polymer, ca. 2.0 wt% Irganox 1010 (Ciba® Speciality Chemicals, Switzerland) and 300 mL of xylene were placed in a glass reactor and dissolved at 130 ºC. The reactor was transferred to an oil bath maintained at 130 ºC. As a crystallization support, preheated sea sand (white quartz, Aldrich, South Africa) was added to the reactor. The reactor was cooled at the rate of 1 ºC/h to facilitate the controlled crystallization of the polymer. A stainless steel column was packed with the crystallized mixture and transferred to a modified GC oven for the elution step. The temperature of the oven was increased at a steady rate while preheated solvent (xylene) was pumped through the columns. Fractions were collected at predetermined intervals, isolated by precipitation in acetone followed by drying to a constant weight.
- *LC-transform interface*. LC-Transform series model 303 (Lab Connections, Carrboro, USA) coupled to the HT-HPLC system. Samples were dissolved at 160 °C in 1-decanol at a concentration of 1–1.2 mg/mL, with 110 μL of each sample being injected. The HPLC column outlet was connected to the LC-Transform interface through a heated transfer line set at 160 °C. The fractions were deposited by rotating a germanium disc (sample target in the LC-Transform) at a speed of 10° per minute. The disc stage and nozzle temperatures of the LC-Transform were set to 160 °C.
- *Columns*. **HT-2D-LC**: Chromatograph 1: Hypercarb column (Thermo Scientific, Dreieich, Germany) packed with porous graphite particles with the following parameters: column size 100 mm × 4.6 mm i.d., average particle size 5 μm, surface area 120 m^2/g, pore size 250 Å. Chromatograph 2: PL Rapide H, 100 mm × 10 mm i.d. (Polymer Laboratories, Church Stretton, England). **HT-SEC**: Column set of three 300 mm × 7.5 mm i.d. PLgel Olexis columns together with a 50 mm × 7.5 mm i.d. PLgel Olexis guard column (Polymer Laboratories, Church Stretton, UK).
- *Mobile phase*. **HT-2D-LC**: Chromatograph 1: linear gradient 1-decanol to TCB starting with 100 % of 1-decanol, flow rate 0.05 mL/min. Chromatograph 2:

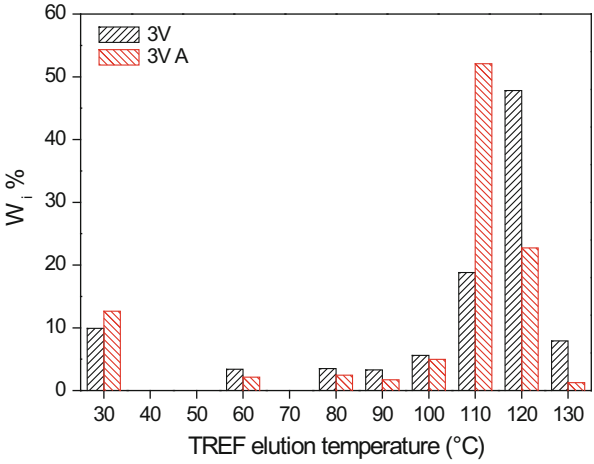

Fig. 3.46 P-TREF profile for samples 3V and 3VA, indicating the overall weight percentage of each fraction as a function of elution temperature (reprinted from [111] with permission of Elsevier)

TCB with a flow rate of 2.75 mL/min. **HT-SEC**: TCB with a flow rate of 1 mL/min.

- *Detectors*. ELSD PL-ELS 1000 (Polymer Laboratories, Church Stretton, England). The following parameters were set on the ELSD: air flow rate 1.5 L/min, nebulizer temperature 160 °C, evaporator temperature 270 °C.
- *Column temperature*. 160 °C.
- *Sample concentration*. 2.5 mg/mL. All samples were dissolved in 1-decanol.
- *Injection volume*. 50 µL (first dimension).

3.4.3.4 Preparatory Investigations

As the first part of the experiments, the IPC samples 3V and 3VA were fractionated into eight fractions by P-TREF. The TREF data in Fig. 3.46 show that the 30 °C fraction, together with those fractions eluting from 110 °C to 120 °C, constitute the largest weight percentages of both samples.

TREF is a crystallization-based technique and separates with regard to crystallizability; hence the low-temperature fraction (30 °C) should be amorphous. The fraction eluting at the highest temperature (around 120 °C) is expected to exhibit the highest crystallizability, while the fractions eluting between these two temperatures are expected to be semi-crystalline. The weight percentages of different fractions of both samples are quite different, as can be seen from the TREF profiles. Detailed analysis of the TREF fractions of sample 3V has been reported in previous work [45]. The fractions were analysed by HT-SEC, DSC and HT-^{13}C-NMR, and the most important fractions (60 °C, 80 °C, 90 °C and 100 °C) were analysed by SEC-FTIR. The HT-SEC and DSC curves for sample 3VA are presented in Figs. 3.47 and 3.48.

The shapes of the MMD curves obtained for the sample 3VA and its TREF fractions agree well with those observed for the sample 3V. Most of the fractions exhibit monomodal MMDs, but bimodal MMDs are obtained for fractions 3VA-60, -80 and -90. This bimodality indicates that the TREF fractions are not

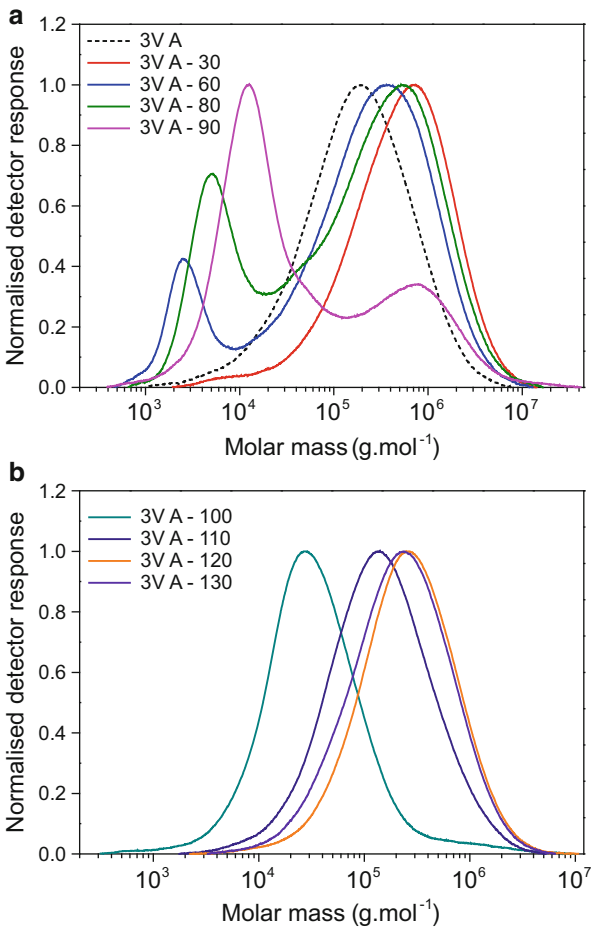

Fig. 3.47 HT-SEC results for the bulk sample 3VA and its TREF fractions (reprinted from [111] with permission of Elsevier)

homogeneous but contain different components. The chemical composition of these components will be elucidated later by HT-SEC-FTIR. The DSC analyses of the TREF fractions also indicate that the fractions contain different components, see Fig. 3.48. These are components that melt at different temperatures and, therefore, must have different copolymer compositions. As is the case with the SEC results, it can be assumed that the TREF fractions are still quite complex.

Obviously, the compositional heterogeneity of the TREF fractions could not be fully determined by only HT-SEC and DSC analyses. The combination of P-TREF with SEC-FTIR has been found to be a useful technique for the determination of the average chemical composition (identification of the constituents) per molar mass slice. However, it must be remembered that each fraction is not a single component, but consists of different chain structures having the same hydrodynamic volume, and thus only average values can be determined. Thus, it is challenging to

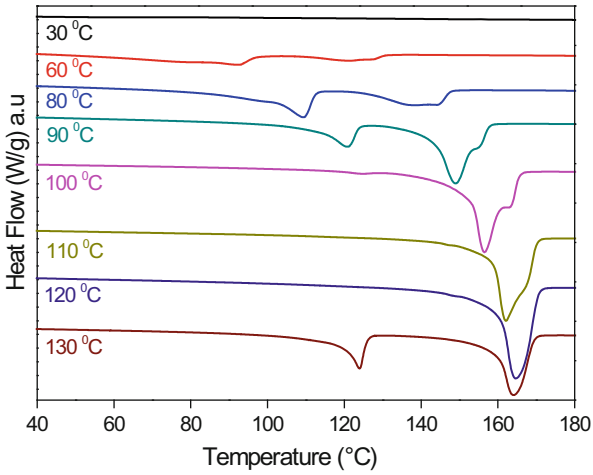

Fig. 3.48 DSC curves indicating the melt endotherms for the TREF fractions of 3VA and its TREF fractions (reprinted from [111] with permission of Elsevier)

differentiate between both samples according to the exact CCD, present in the various TREF fractions.

3.4.3.5 Measurement and Evaluation

To achieve the separation with regard to chemical composition of such complex polymeric materials in a fast and efficient manner, P-TREF must be combined with HT-HPLC, which reveals separation according to chemical composition and microstructure. The current study made use of the combination of P-TREF and HT-HPLC, with the additional use of FTIR as a composition detection method after HT-HPLC. The experimental set-up of the coupled HPLC-FTIR system is schematically presented in Fig. 3.49. All chromatographic separations are carried out on the SGIC system. From the column outlet, a heated transfer line is connected to the LC-Transform system. Fractions from chromatography are automatically sprayed on the germanium disc or a disc covered with aluminium foil.

The present system was used to separate the TREF fractions according to chemical composition by HT-HPLC. The corresponding chromatograms for samples 3V and 3VA are summarized in Fig. 3.50.

As reported by Pasch and Macko [85], linear ethylene sequences are strongly retained on the Hypercarb stationary phase and elute later than short ethylene sequences, while linear propylene sequences are not retained to the same extent. Although the chemical composition is the primary parameter and it governs the separation, the molar mass of the components also plays a role, especially for low molar masses. For all the TREF fractions, a fraction of iPP homopolymer having a low molar mass is not absorbed on the column, but elutes in 100 % 1-decanol before the start of the gradient. The concentration of this component increases as the TREF fractionation temperature increases.

The components of the 30 °C fraction are expected to be EP random copolymers, with some atactic PP or branched PE homopolymer being present. This can be seen

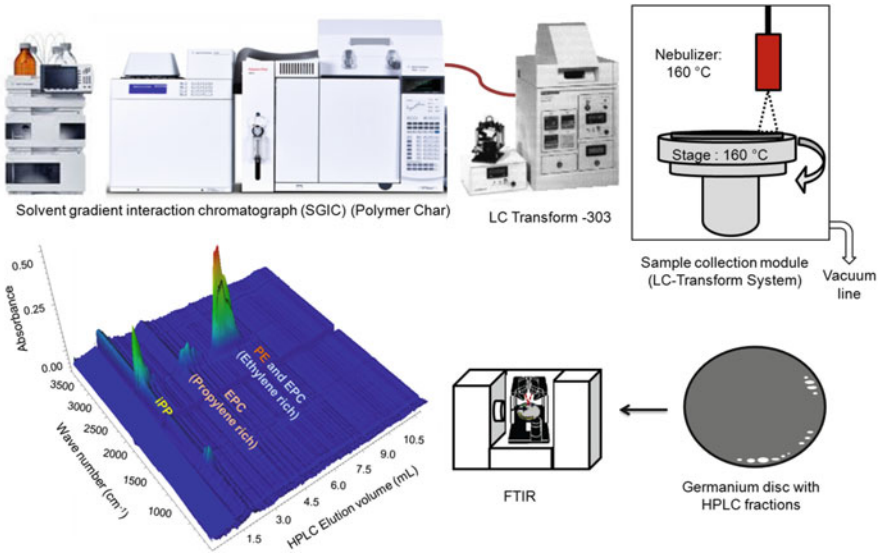

Fig. 3.49 Schematic representation of HT-HPLC-FTIR analysis (reprinted from [111] with permission of Elsevier)

in the chromatogram where the major component eluting at approximately 3.5–5.5 mL is mainly EP copolymer.

For the 60 °C fraction of 3V, two nearly baseline-separated peaks, in addition to some iPP, are observed (see Fig. 3.50c). The order of elution of the fractions is such that iPP with slightly higher molar mass elutes as the gradient starts (at approximately 3 mL). The fraction eluting between 3.25 mL and 4.8 mL is propylene-rich EP copolymer, followed by EP copolymer chains having longer ethylene sequences, and PE homopolymer (from 5 mL to 6.25 mL). The 60 °C fraction of sample 3VA contained three chemically different components in addition to low and high molar mass iPP components. The fractions eluting between 3 mL and 3.5 mL were high molar mass iPP and propylene-rich EP copolymers. The intense peak at 4.85 mL corresponds to the ethylene-rich EP copolymer while the peak at an elution volume of 5.5 mL belongs to PE (see Fig. 3.50d). The semi-crystalline TREF fractions that exhibit similar bimodal SEC profiles and two melt endotherms in DSC were efficiently and precisely separated into individual components by HT-HPLC. Sample 3VA contained a higher percentage of the late eluting fractions, clearly indicating the higher amounts of ethylene units in the fractions. The importance of the amounts and chemical compositions of the different components is clearly depicted by the results of the 60 °C fractions of the two IPC samples. The amount and chemical composition of this fraction plays an important role in connecting the dispersed EPR phase with the iPP matrix for enhancement of the interfacial interaction between the two phases, strongly influencing the total impact performance of IPC.

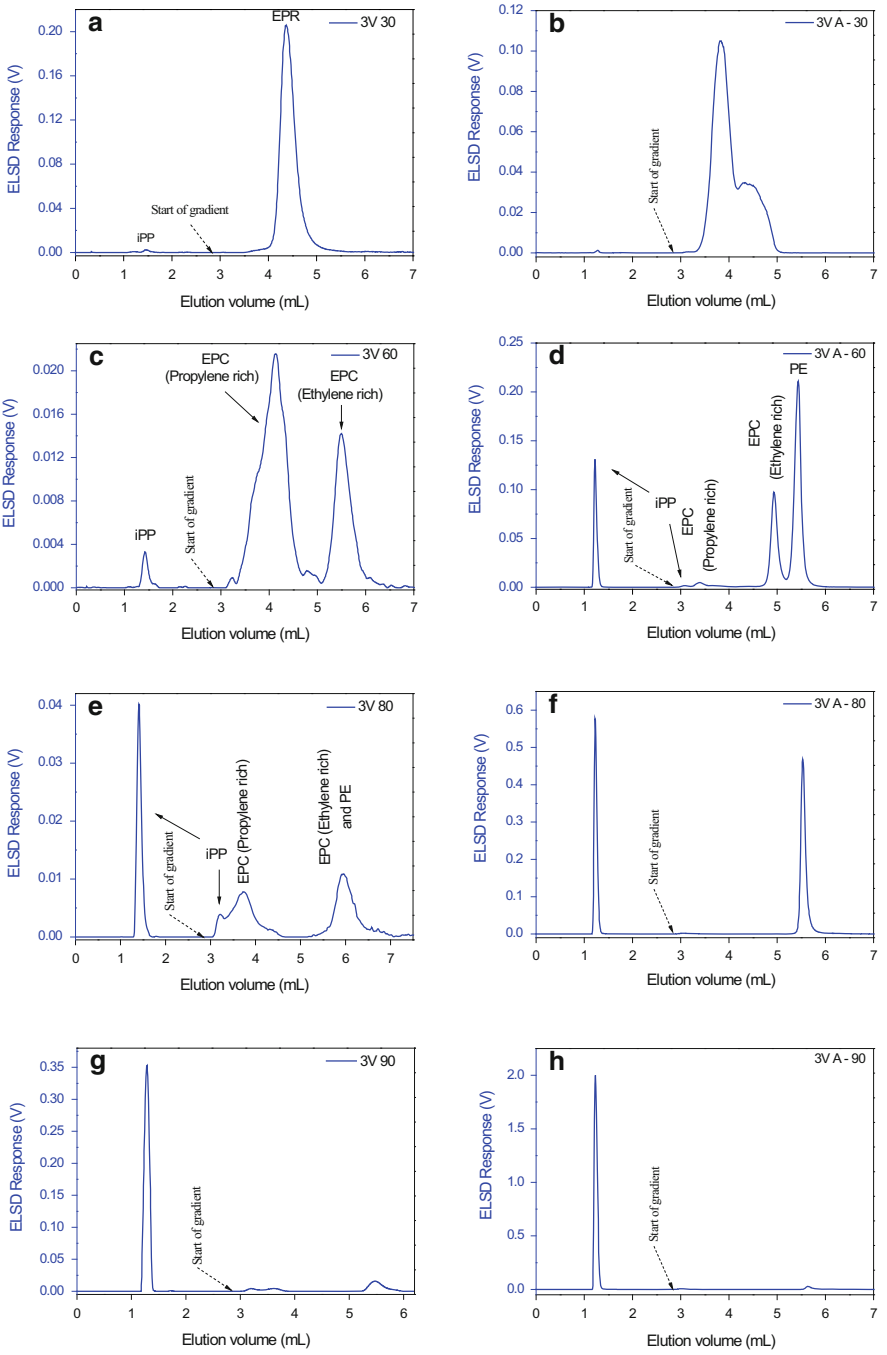

Fig. 3.50 HT-HPLC chromatograms of TREF fractions (30 °C, 60 °C, 80 °C and 90 °C) of samples 3V (**a**, **c**, **e**, **g**) and 3VA (**b**, **d**, **f**, **h**) (reprinted from [111] with permission of Elsevier)

Similar to the 60 °C fraction, the HPLC results for the 3V 80 °C fraction (Fig. 3.50e) show a complex distribution of different EP copolymers. In comparison, the chromatogram of the 80 °C fraction of 3VA (Fig. 3.50f) shows mainly iPP (that elutes before the start of the gradient) and a very late eluting component that may be assigned to PE. This comparison shows clearly that there are significant compositional differences between the two samples that are mainly due to the different ethylene contents. These results again confirm the capability of HT-HPLC as the only suitable method to distinguish the CCD present in such complex TREF fractions, which are indistinguishable by SEC (MMD) and DSC (melting behaviour). The chromatograms of the higher TREF fractions indicate mainly the presence of iPP eluting in two peaks, depending on molar mass and isotacticity.

More detailed information on the chemical composition of the fractions obtained by HT-HPLC is accessible by combining this fractionation with FTIR spectroscopy. The experimental background of such measurements has been outlined earlier and shall not be discussed again here. As an example, the analysis of the bulk sample 3VA is shown in Fig. 3.51. Hence, with the help of the corresponding FTIR spectra, it is proved that the early eluting fractions are PP while the late eluting fractions are EP copolymers and PE.

Figures 3.52 and 3.53 present the chemical composition (propylene and ethylene contents) and the crystallinity distributions of the TREF fractions as obtained by HT-HPLC-FTIR. The ratio of the peak areas CH_3/CH_2 decreased with increasing elution volume, indicating an increase in ethylene content. The results are in agreement with the separation mechanism, which assumes strong retention of ethylene sequences and no retention of linear propylene sequences. At an elution volume of approximately 6 mL, PE homopolymers with low branching elute (lower CH_3/CH_2 value for late eluting fractions). Propylene sequences with higher crystallinity were found in early eluting fractions where crystalline PE is not present. Crystalline PE is present only in the late eluting fractions. This again confirms the proposed adsorption-desorption mechanism on the Hypercarb stationary phase according to the E/P content and sequence lengths in the sample. According to the TREF separation mechanism, the higher temperature TREF fractions are mainly composed of highly crystalline iPP (not discussed here).

In order to further confirm these results, individual IR spectra at peak maximum for each component were analysed. These spectra proved that the component eluting at 2.0 mL is iPP homopolymer, and the component eluting at 4.2 mL is EP copolymer or a propylene-rich or branched copolymer. The individual spectrum for the component eluting at 5.5 mL was identical to that of PE homopolymer. In the HT-HPLC-FTIR results, it was observed that the elution volume of the first component in each fraction is nearly identical. The elution volume of the second component in the 80 °C and 90 °C fractions decreased compared to that of the similar component in the 30 °C and 60 °C fractions, and the elution volume of the late eluting fraction increased from the 30 °C to the 90 °C fraction. The first component of all the fractions is iPP homopolymer, which co-crystallized with other components during the TREF crystallization step, either due to differences in

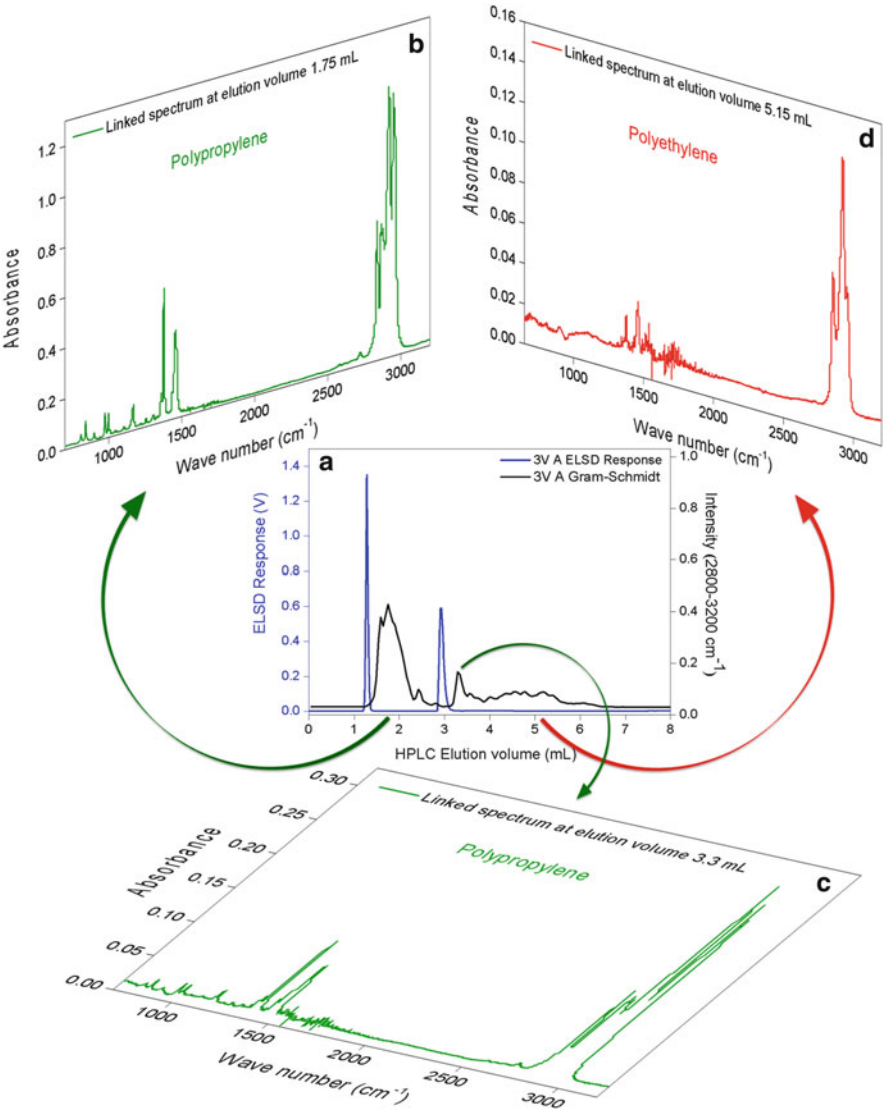

Fig. 3.51 HT-HPLC-FTIR analysis for the bulk sample 3VA. (**a**) Overlay of the ELSD response and Gram-Schmidt profile. (**b**), (**c**) and (**d**) show the individual linked spectra extracted from the Gram-Schmidt profile at elution volumes of 1.75 mL, 3.3 mL and 5.15 mL, respectively (reprinted from [111] with permission of Elsevier)

tacticity or MMD compared to other PP chains. The lower elution volume for the second component of the 80 °C and 90 °C fractions (3.7 mL) as compared to the same component for the 30 °C and 60 °C fractions (4.2 mL) indicates the longer ethylene sequences present in these fractions (30 °C and 60 °C). For the late eluting

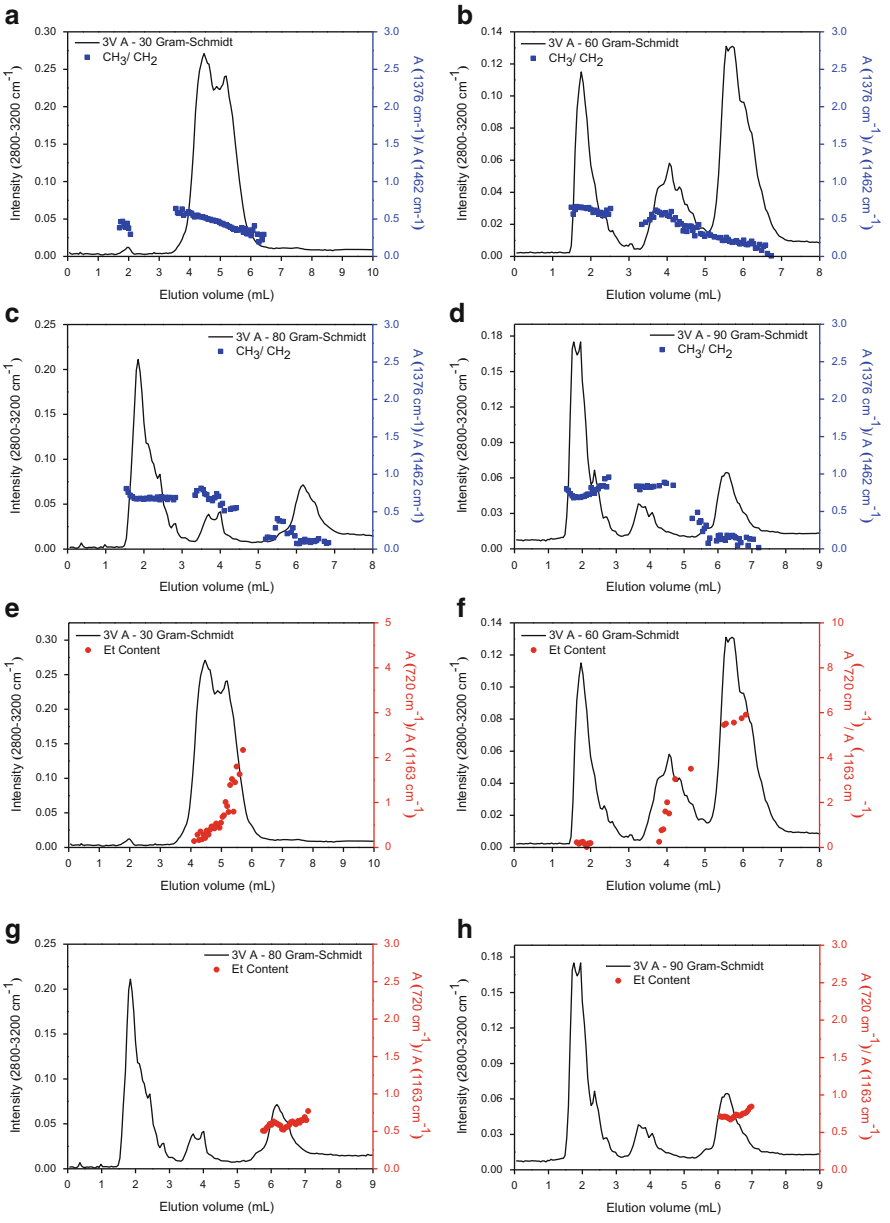

Fig. 3.52 HT-HPLC-FTIR analysis for the TREF fractions 30 °C, 60 °C, 80 °C and 90 °C of sample 3VA, illustrating propylene (CH_3/CH_2) (**a**–**d**) and ethylene (Et content) distributions (**e**–**h**) (reprinted from [111] with permission of Elsevier)

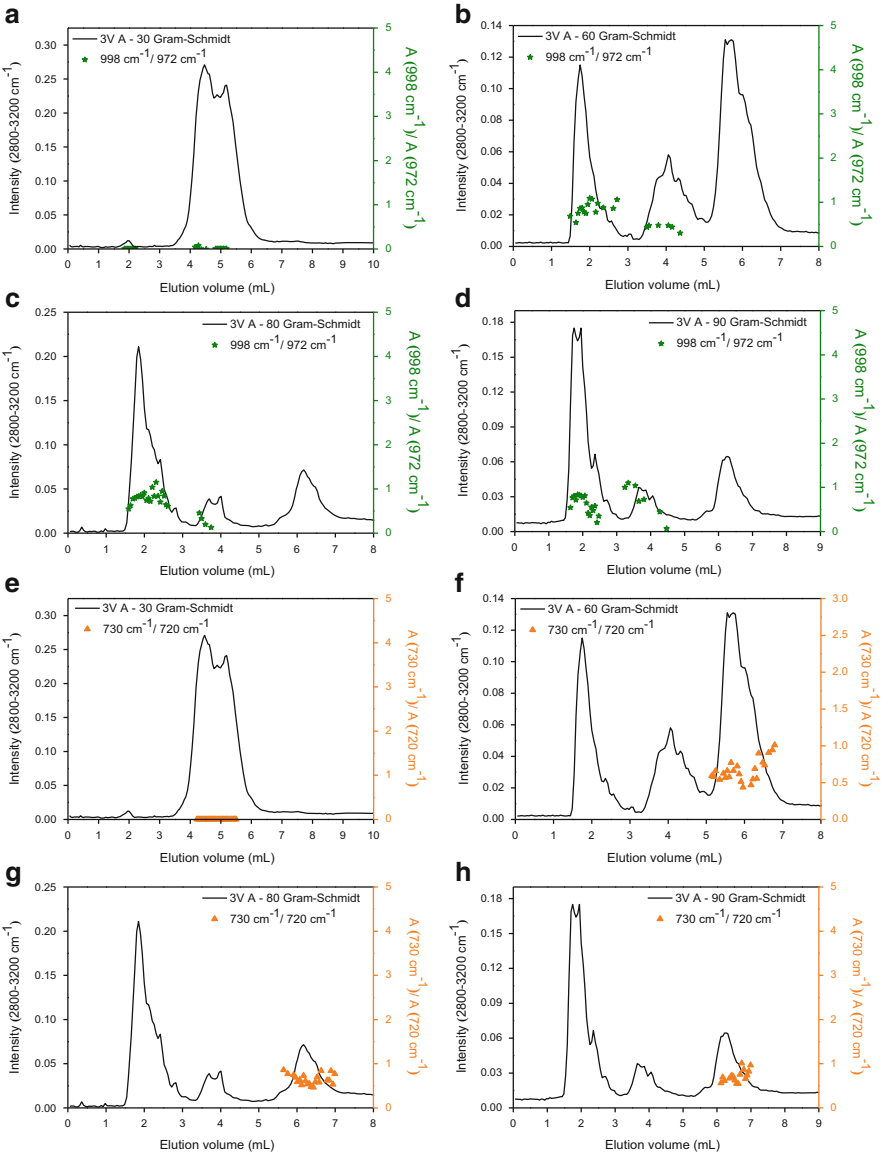

Fig. 3.53 HT-HPLC-FTIR analysis for the TREF fractions 30 °C, 60 °C, 80 °C and 90 °C of sample 3VA, illustrating propylene (**a–d**) and ethylene crystallinity distributions (**e–h**) (reprinted from [111] with permission of Elsevier)

component, the elution volume increases from 5.5 mL to 6.3 mL for all fractions (30–90 °C); accordingly, this indicates the difference in the chemical structure or distribution of the chemical composition in each component, which changes from

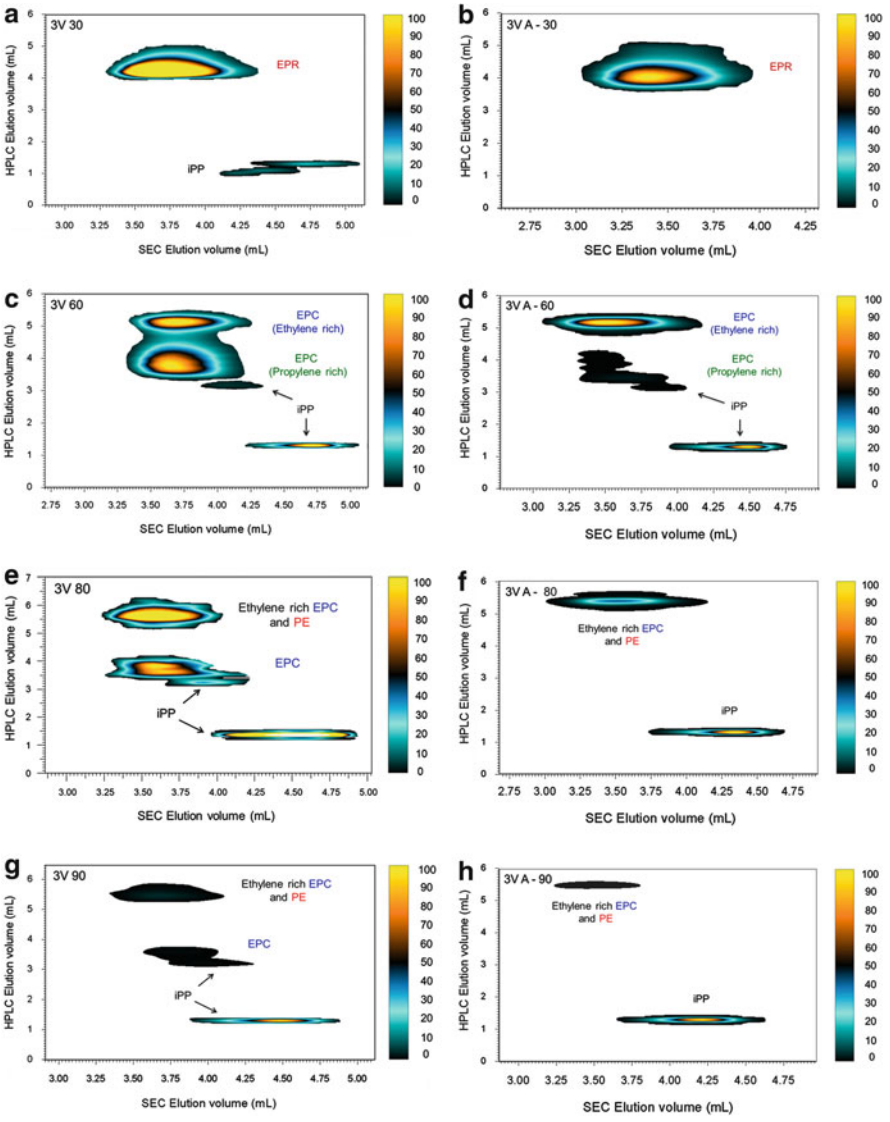

Fig. 3.54 HT 2D-LC contour plots for the fractions 30 °C, 60 °C, 80 °C and 90 °C of 3V (**a**, **c**, **e**, **g**) and 3VA (**b**, **d**, **f**, **h**) (reprinted from [111] with permission of Elsevier)

ethylene-rich EPCs to linear or slightly branched crystalline PE homopolymers as the TREF fractionation temperature increases.

Finally, a complete separation according to CCD and MMD for the TREF fractions was achieved by HT-2D-LC analysis, where the HT-HPLC separation is hyphenated to HT-SEC. The 2D contour plots for the 30 °C and all mid-elution-temperature TREF fractions of the two IPC samples are given in Fig. 3.54. Separation of low molar mass iPP and high molar mass EPR is seen for the 30 °C fraction

of 3V (Fig. 3.54a). For this fraction, there are two low molar mass components with a slight difference in their molar masses which elute in SEC mode. It is assumed that the first component (early eluting, approximately between 4.125 mL and 4.75 mL, SEC axis) comprises highly branched chains, which no longer show adsorption on the stationary phase due to the interruption of the long continuous methylene sequences by the branch points, or even random EP sequences in the backbone chain. EPR components of 3VA-30 show a higher molar mass compared to 3V-30, and no low molar mass iPP component is observed in this fraction (see Fig. 3.54b).

EPCs of similar molar masses but different ethylene and propylene sequence lengths as well as low and high molar mass iPP components were separated quite well for the 60 °C fraction of both samples (Fig. 3.54c, d). The 80 °C and 90 °C fractions of sample 3V (Fig. 3.54e, g) contain both lower and slightly higher molar mass iPP that eluted in pure 1-decanol and after the start of gradient, respectively. The ethylene content of the EP copolymers determines their elution behaviour in accordance with the elution behaviour of PE homopolymers on the Hypercarb column. The same fractions for 3VA show only low molar mass iPP and high molar mass EP copolymer (ethylene-rich). For 3VA-80, EP copolymer (ethylene-rich) eluted at approximately 5.5 mL together with PE homopolymers having similar molar masses.

To summarize, P-TREF fractionation and subsequent analysis of the individual fractions by high-temperature solvent gradient interaction chromatography and 2D-LC was found to be an effective method for the comprehensive characterization of complex polymeric materials such as IPCs. All components were identified by coupling of the chromatographic separation to FTIR spectroscopy. FTIR provides information not only on the ethylene and propylene contents but also on the ethylene and propylene crystallinities.

References

1. Francuskiewicz F (1994) Polymer fractionation. Springer, Berlin
2. Mori S, Barth HG (1999) Size exclusion chromatography. Springer, Berlin
3. Striegel AM, Yau WW, Kirkland JJ, Bly DD (2009) Modern size-exclusion liquid chromatography. John Wiley, Hoboken, NJ
4. Pasch H, Trathnigg B (1998) HPLC of polymers. Springer, Berlin
5. Pasch H, Trathnigg B (2013) Multidimensional HPLC of polymers. Springer, Berlin
6. Pasch H, Malik I, Macko T (2013) Adv Polym Sci 251:77
7. Housaki T, Satoh K, Nishikida K, Morimoto M (1988) Makromol Chem Rapid Commun 9:525
8. Nishikida K, Housaki T, Morimoto M, Kinoshita T (1990) J Chromatogr A 517:209
9. www.chem.agilent.com/en-US/. . ./lc/gpc. . ./pl-gpc220
10. www.malvern.com/ViscotekHT-GPC
11. http://www.polymerchar.com/gpc-ir
12. Markovich RP, Hazlitt LG, Smith-Courtney L (1993) In: Provder T (ed) Chromatography of polymers. Characterization by SEC and FFF, ACS symposium series 521. American Chemical Society, Washington, DC

13. DesLauriers PJ (2004) Measuring compositional heterogeneity in polyolefins using SEC/FTIR spectroscopy. In: Striegel A (ed) Multiple detection in size exclusion chromatography. ACS symposium series 893. American Chemical Society, Washington, DC
14. Pang S, Rudin A (1992) Polymer 33:1949
15. Wintermantel M, Antonietti M, Schmidt M (1993) J Appl Polym Sci Appl Polym Symp 52:91
16. Degoulet C, Nicolai T, Durand D, Busnel JP (1995) Macromolecules 28:6819–6824
17. Jackson C, Chen YJ, Mays JW (1996) J Appl Polym Sci 61:865
18. Yau WW, Arora KS (1994) Polym Mater Sci Eng 69:210
19. Jackson C, Barth HG (1994) Trends Polym Sci 2:203
20. Yau WW (1990) Chemtracts-Macromol Chem 1:1
21. Rao B, Balke ST, Mourey TH, Schunk TC (1996) J Chromatogr A 755:27
22. Ying Q, Xie P, Liu Y, Qian R (1986) J Liq Chromatogr 9:1233
23. Ibhadon AO (1991) J Appl Polym Sci 42:1887
24. Ying Q, Ye M (1985) Macromol Chem Rapid Commun 6:105
25. Pasti L, Melucci D, Contado C, Dondi F, Mingozzi I (2002) J Sep Sci 25:69
26. Sun T, Brant P, Chance RR, Graessley WW (2001) Macromolecules 34:6812
27. Parth M, Aust N, Lederer K (2003) Int J Polym Anal Charact 8:175
28. Mes EPC, De Jonge H, Klein T, Welz RR, Gillespie DT (2007) J Chromatogr A 1154:31
29. Barth HG, Carlin FJ Jr (1984) J Liq Chromatogr 7:1717
30. Pasch H (2012) Chromatography. In: Matyjaszewski K, Moeller M (eds) Polymer science: a comprehensive reference, vol 2. Elsevier, Amsterdam, pp 33–64
31. Provder T, Barth HG, Urban MW (eds) (1995) Chromatographic characterization of polymers. Adv Chem Ser 247. American Chemical Society, Washington, DC
32. Chu B (1995) Scattering methods in polymer science. Prentice Hall, London
33. Chu B (1997) Appl Optic 36:7645
34. Dhenin V, Rose LJ (2000) Polym Prepr 41:285
35. DesLauriers PJ, Battiste DR (1995) ANTEC-SPE 53:3639
36. DesLauriers PJ, Rohlfing DC, Hsieh ET (2002) Polymer 43:159
37. Piel C, Albrecht A, Neubauer C, Klampfl CW, Reussner J (2001) Anal Bioanal Chem 400:2607
38. Tackx P, Bremmers S (1997) Proceedings of the ISPAC-10, Toronto, p 42
39. Albrecht A, Brüll R, Macko T, Malz F, Pasch H (2009) Macromol Chem Phys 210:1319
40. Albrecht A, Brüll R, Macko T, Sinha P, Pasch H (2008) Macromol Chem Phys 209:1909
41. Heinz LC, Graef S, Macko T, Brüll R, Balk S, Keul H, Pasch H (2005) e-polymers no. 54
42. Macko T, Schulze U, Brüll R, Albrecht A, Pasch H, Fonagy T, Haeussler L, Ivan B (2008) Macromol Chem Phys 209:404
43. de Goede S, Brüll R, Pasch H, Marshall N (2003) Macromol Symp 193:35
44. de Goede S, Brüll R, Pasch H, Marshall N (2004) e-polymers no. 012
45. de Goede E, Mallon P, Pasch H (2010) Macromol Mater Eng 295:366
46. de Goede E, Mallon P, Pasch H (2012) Macromol Mater Eng 297:26
47. de Goede E, Mallon P, Pasch H (2011) Macromol Mater Eng 296:1018
48. Graef S, Brüll R, Pasch H, Wahner UM (2003) e-polymers no. 005
49. Luruli N, Pipers T, Brüll R, Grumel V, Pasch H, Mathot VBF (2007) J Polym Sci Polym Phys 45:2956
50. Kearney T, Dwyer JL (2008) Am Lab 40:8
51. Hiller W, Pasch H, Macko T, Hoffmann M, Ganz J, Spraul M, Braumann U, Streck R, Mason J, van Damme F (2006) J Magn Reson 183:290
52. Frauenrath H, Balk S, Keul H, Höcker H (2001) Macromol Rapid Commun 22:1147
53. Smallcombe SH, Patt SL, Keifer PA (1995) J Magn Reson A 117:295
54. Hiller W, Sinha P, Hehn M, Pasch H (2014) Prog Polym Sci 39:979
55. Zhou Z, Kuemmerle R, Stevens JC, Redwine D, He Y, Qiu X, Cong R, Klosin J, Montanez N, Roof G (2009) J Magn Reson 200:328

56. Zhou Z, Stevens JC, Klosin J, Kuemmerle R, Qiu X, Redwine D, Cong R, Taha A, Winniford B, Chauvel P, Montanez N (2009) Macromolecules 42:2291
57. Cong R, de Groot AW, Parrott A, Yau W, Hazlitt L, Brown R, Miller MD, Zhou Z (2011) Macromolecules 44:3062
58. Berek D (2000) Prog Polym Sci 25:873
59. Chang T (2003) Adv Polym Sci 163:1
60. Macko T, Pasch H, Kazakevich YV, Fadeev AY (2003) J Chromatogr A 988:69
61. Macko T, Pasch H, Denayer JF (2003) J Chromatogr A 1002:55
62. Macko T, Brüll R, Pasch H (2003) Chromatographia 57:S39
63. Macko T, Denayer JF, Pasch H, Baron GV (2003) J Sep Sci 26:1569
64. Macko T, Denayer JF, Pasch H, Pan L, Li J, Raphael A (2004) Chromatographia 59:461
65. Macko T, Pasch H, Denayer JF (2005) J Sep Sci 28:59
66. Wang X, Rusa CC, Hunt MA, Tonelli AE, Macko T, Pasch H (2005) Macromolecules 38:12040
67. Macko T, Brüll R, Brinkmann C, Pasch H (2009) J Autom Methods Manag Chem ID 357026 (electronic journal)
68. Macko T, Pasch H, Brüll R (2006) J Chromatogr A 1115:81
69. Macko T, Pasch H, Milonjic SK, Hiller W (2006) Chromatographia 64:183
70. Macko T, Brüll R, Zhu Y, Wang Y (2010) J Sep Sci 33:3446
71. Heinz LC, Macko T, Williams A, O'Donohue S, Pasch H (2006) The Column (electronic journal), February 13
72. http://www.polymerchar.com/SGIC_2D
73. Monrabal B (2013) Adv Polym Sci 257:203
74. Heinz LC, Macko T, Pasch H, Weiser MS, Mülhaupt R (2006) Int J Polym Anal Charact 11:47
75. Macko T, Hunkeler D (2003) Adv Polym Sci 163:61
76. Heinz LC, Pasch H (2005) Polymer 46:12040
77. Albrecht A, Heinz LC, Lilge D, Pasch H (2007) Macromol Symp 257:46
78. Weiser MS, Thomann Y, Heinz LC, Pasch H, Mülhaupt R (2006) Polymer 47:4505
79. Dolle V, Albrecht A, Brüll R, Macko T (2011) Macromol Chem Phys 212:959
80. Albrecht A, Brüll R, Macko T, Pasch H (2007) Macromolecules 40:5545
81. Pasch H, Albrecht A, Brüll R, Macko T, Hiller W (2009) Macromol Symp 282:71
82. http://www.interscience.be/promotiesites/hypersil/topics/promotiesites/hypersil/nieuws/hypercarb_technical.pdf
83. Gilbert MT, Knox JH, Kaur B (1982) Chromatographia 16:138
84. Macko T, Pasch H, Wang Y (2009) Macromol Symp 282:93
85. Macko T, Pasch H (2009) Macromolecules 42:6063
86. Macko T, Brüll R, Wang Y (2009) Polym Prepr 50:228
87. Macko T, Brüll R, Alamo RG, Thomann Y, Grumel V (2009) Polymer 50:5443
88. Macko T, Brüll R, Wang Y, Thomann Y (2009) The Column (electronic journal) 4:15
89. Macko T, Brüll R, Wang Y, Coto B, Suarez I (2011) J App Polym Sci 122:3211
90. Macko T, Cutillo F, Bussico V, Brüll R (2010) Macromol Symp 298:182
91. Chitta R, Macko T, Brüll R, van Doremaele G, Heinz LC (2011) J Polym Sci Polym Chem 49:1840
92. Macko T, Brüll R, Alamo RG, Stadler FJ, Losio S (2011) Anal Bioanal Chem 399:1547
93. Buback M, Wittkowski L, Lehmann SA, Mähling FO (1999) Macromol Chem Phys 200:1935
94. Kisparissidis C, Baltsas A, Papadopoulos S, Congalidis JP, Richards JR, Kelly MB, Ye Y (2005) Ind Eng Chem Res 44:2592
95. Kisparissidis C, Verros G, MacGregor JF (1993) J Macromol Sci Rev C33:437
96. Findenegg GH, Liphard M (1987) Carbon 25:119
97. Baukema PR, Hopfinger AJ (1982) J Polym Sci Polym Phys Ed 20:399
98. Lipatov YS, Sergeeva LM (1974) Adsorption of polymers. Wiley, New York, NY
99. Lochmüller CH, Moebus MA, Liu QC, Jung C, Elomaa M (1996) J Chromatogr Sci 34:69

100. Lee HC, Chang T (1996) Polymer 37:5747
101. Im K, Park S, Cho D, Chang T, Lee K, Choi N (2004) Anal Chem 76:2638
102. Monrabal B, Lopez E, Romero L (2013) Macromol Symp 330:9
103. Nakano S, Goto Y (1981) J Appl Polym Sci 26:4217
104. Ortin A, Monrabal B, Sancho-Tello J (2007) Macromol Symp 257:13
105. Monrabal B (2012) Advances in microstructure characterization of polyolefins. In: Proceedings of the Chemelot International Polyolefins Symposium (CIPS), Maastricht, 7–-10 October 2012
106. Ginzburg A, Macko T, Dolle V, Brüll R (2010) J Chromatogr A 1217:6867
107. Ginzburg A, Macko T, Dolle V, Brüll R (2011) Eur Polym J 47:319
108. Roy A, Miller MD, Meunier DM, de Groot AW, Winniford WL, van Damme FA, Pell RJ, Lyons JW (2010) Macromolecules 43:3710
109. Lee D, Miller MD, Meunier DM, Lyons JW, Bonner JM, Pell RJ, Li Pi Chan C, Huang T (2011) J Chromatogr A 1218:7173
110. Bashir MA, Brüll A, Radke W (2005) Polymer 46:3223
111. Cheruthazhekatt S, Harding GW, Pasch H (2013) J Chromatogr A 1286:69
112. Sperling LH (2006) Introduction to physical polymer science, 4th edn. John Wiley, Hoboken, NJ
113. Cheruthazhekatt S, Pijpers TFJ, Harding GW, Mathot VBF, Pasch H (2012) Macromolecules 45:2025
114. Cheruthazhekatt S, Pijpers TFJ, Harding GW, Mathot VBF, Pasch H (2012) Macromolecules 45:5866

Field-Flow Fractionation

4

4.1 Fundamentals

The molar mass distribution (MMD) of complex polymers is typically analysed by size exclusion chromatography (SEC). In the classical approach, the correlation between the experimentally determined elution volume and the molar mass is done using a set of well characterized calibration standards. For accurate results, the chemical compositions and molar masses of the calibration standards must be similar or close to the samples under investigation; see more details in Sect. 3.1. SEC separates according to hydrodynamic size in solution and it is assumed that one hydrodynamic size corresponds strictly to one molar mass. This, however, is not always the case as has been shown, e.g., for high molar mass branched polymers [1–7]. For such materials, co-elution of linear and branched molecules having different molar masses has been observed [8]. Accordingly, SEC is not the best tool for molar mass analysis in this case. Other problems associated with SEC relate to unwanted polar or ionic interactions with the stationary phase that disturb the SEC separation mechanism. Finally, samples with very high molar masses cause problems in SEC because the largest molecules are frequently shear degraded by the pores and frits of the columns, resulting in molar masses that are lower compared to those of the injected sample [7, 9–14]. All of the above-mentioned problems can lead to erroneous results and inaccurate interpretation of calculated results.

Field-flow fractionation (FFF) is a chromatography-like technique, discovered in the 1960s by J. Calvin Giddings, which has developed into a powerful alternative fractionation technique for complex polymers. Most of the problems associated with SEC can be overcome by FFF and additional information can be retrieved using the various sub-techniques of FFF. The most popular FFF techniques are asymmetric flow field-flow fractionation (AF4) and thermal field-flow fractionation (ThF3). Studies have been carried out on natural and synthetic polymers using organic and aqueous mobile phases, in various fields. Examples include the investigation of virus-like particles, starches and hyaluronic acid for aqueous

H. Pasch, M.I. Malik, *Advanced Separation Techniques for Polyolefins*, Springer Laboratory, DOI 10.1007/978-3-319-08632-3_4

applications [15–18]. Applications in organic mobile phases include branched polymers, high-temperature analysis of polyolefins, gel-containing polymers and rubber emulsions, to name a few [6, 7, 19–22]. The different FFF sub-techniques have their merits and limitations; nevertheless, for most of the analytical problems that complex polymers present, a suitable FFF method can be found.

A few advantages of FFF over SEC are summarized as follows:

1. Shear degradation of polymer is strongly minimized due to the absence of any stationary phase [15, 23].
2. Unwanted adsorption and secondary separation effects are avoided by the very low surface area of the accumulation wall in FFF [15, 24].
3. An open channel is used, therefore filtration is no longer necessary [6, 7].
4. Two orders higher exclusion limit is achieved compared to SEC [15].
5. Analysis of complex mixtures of suspended particles, gels and soluble polymers is possible in one measurement [15].
6. Working conditions in FFF are conducive for the analysis of sensitive molecules that degrade easily [23].

In FFF, a narrow ribbon-like channel is used to achieve the separation of the sample. This channel is composed of a thin piece of sheet material (usually 70–300 μm Mylar or polyimide film) known as the spacer, in which the channel is cut. Two walls of highly polished plane parallel surfaces are usually clamped by the spacer. The force can be applied through the two walls to achieve separation. The actual configuration of the spacer varies with the type of field being utilized. From the inlet, a carrier liquid is pumped through this channel to the outlet where detectors are connected, while the sample is injected at the inlet into the channel. A parabolic flow profile (laminar Newtonian flow) is established inside the channel, as in a capillary tube.

Interaction of the solute molecules with the field concentrates them at one of the channel walls, called the accumulation wall; see Fig. 4.1. The elution order of the analyte components is determined by the mode of operation being utilized.

In FFF, separation is achieved by applying a field force U on the molecules of interest. A counteracting motion of diffusion occurs in the opposite direction to U, resulting in a net flux J; see Fig. 4.2. D and U are both concentration dependent:

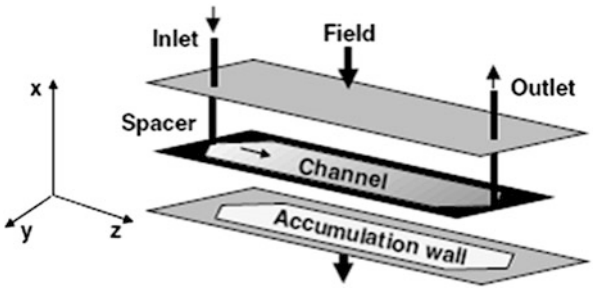

Fig. 4.1 Schematic representation of a FFF channel

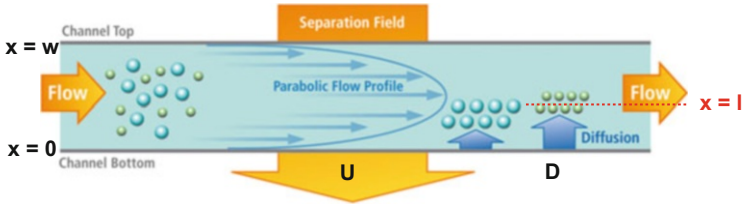

Fig. 4.2 Schematic presentation of the induced field U and counteracting diffusion D in FFF. $x = 0$ represents the accumulation wall while $x = w$ is the channel thickness and l the mean layer thickness (adapted from [25] with permission of Postnova)

$$J = Uc - D\frac{\mathrm{d}c}{\mathrm{d}x} \tag{4.1}$$

After reaching a steady-state condition where the two effects U and D cancel out each other, the net flux $J = 0$ and

$$Uc = D\frac{\mathrm{d}c}{\mathrm{d}x} \tag{4.2}$$

By means of integration and substituting the boundary values, a concentration profile is obtained with

$$c(x) = c_0\, \mathrm{e}^{\left(\frac{-|U|}{D}\right)x} \tag{4.3}$$

where c_0 is the solute concentration at the accumulation wall, U is the applied force velocity and D the diffusion coefficient of the solute. As a result of the concentration gradient, the concentration decreases exponentially as the solute molecules reside further away from the accumulation wall. The mean layer thickness of a zone of solute molecules is given by l

$$l = \frac{D}{U} \tag{4.4}$$

and the retention parameter, which is related to the interaction of the field with some physiochemical property of the solute, is given by

$$\lambda = \frac{l}{w} \tag{4.5}$$

where w is the thickness of the channel. λ is a representation of the zone density in relation to w as well as the zone fraction of the solute layer. Therefore, Eq. (4.3) can also be written as

$$c(x) = c_0 e^{\left(\frac{-x}{l}\right)} = c_0 e^{\left(\frac{-x}{\lambda w}\right)} \tag{4.6}$$

The diffusion coefficient D and the field induced by the force U can be related to the frictional drag f and is given by

$$D = \frac{kT}{f} \tag{4.7}$$

and

$$U = \frac{F}{f}, \tag{4.8}$$

respectively, where k, T and F are the Boltzmann constant, temperature and applied force, respectively. By substituting these two relationships in the λ term, the retention parameter can be expressed as

$$\lambda = \frac{l}{w} = \frac{kT}{Fw} \tag{4.9}$$

This is the basic equation for the retention parameter and the force F. The force will vary depending on the FFF technique used. Retention in FFF is based on the flow velocity $v(x)$, the concentration of solute molecules and the field induced force, and can be described solely based on the dimensionless retention parameter λ.

The retention parameter and the field force F differ for each sub-technique of FFF. They are tabulated in Table 4.1 for commercially available techniques [26].

Table 4.1 Commercial FFF techniques with corresponding external fields (reprinted from [26] with permission of the American Association for the Advancement of Science)

FFF technique	Force (F)	Variables
Normal mode AF4	$= f\|U\| = \frac{kT\|U\|}{D} = 3\pi\eta\|U\|\mathrm{d}$	η: viscosity of mobile phase d: diameter of molecule or particle D: diffusion coefficient U: field induced velocity
Thermal FFF (ThF3)	$= kT\frac{D_T}{D}\frac{\mathrm{d}T}{\mathrm{d}x}$	D_T: thermal diffusion coefficient dT/dx: temperature drop between hot and cold walls
Centrifugal FFF (CF3)	$= m'G = V_p\|\Delta p\|G = \frac{\pi}{6d^3}\|\Delta p\|\mathrm{G}$	m': effective mass V_p: particle volume Δp: difference in density between particle and mobile phase G: gravitational force

4.2 Application of Field-Flow Fractionation to Polyolefins

Similar to column-based chromatography, in FFF the sample under investigation must be dissolved in a suitable solvent and injected into the FFF system. Since most polyolefins are semi-crystalline materials, they dissolve only at high temperatures and, therefore, must be dissolved in high boiling point solvents. The rules that apply to HT-SEC regarding solvent preparation and the type of solvents also apply to HT-FFF; typical solvents are 1,2,4-trichlorobenzene (TCB), ortho-dichlorobenzene (ODCB), decaline, and similar. Working temperatures must be between 120 and 150 °C in order to ensure that the sample is completely dissolved.

The severe experimental conditions that must be used for HT-FFF limit the application of the various sub-techniques to AF4. ThFFF, which is based on a temperature gradient in the FFF channel, is not widely used for polyolefin analysis. One of the problems relates to the fact that typical temperature differences between the 'hot' and the 'cold' plate are around 50 °C. If the 'cold' plate must have a minimum temperature of 130–150 °C to keep the sample in solution, the hot plate should have a temperature of 180–200 °C. Considering the low thermo-oxidative stability of most polyolefins, these are not favourable experimental conditions.

AF4 for medium (MT) and high (HT) temperatures (MT-AF4 and HT-AF4) was developed and commercialized by Postnova Analytics (Landsberg, Germany) only a few years ago. HT-AF4 has been specifically developed for the separation and characterization of high molar mass complex polyolefins that are difficult to analyse by HT-SEC. Various detectors, such as infrared (IR), refractive index (RI), multi-angle light scattering (MALS) and dynamic light scattering (DLS), were applied in different experimental set-ups [27].

HT-AF4 is a specific variation of flow field-flow fractionation, in which separation is achieved by a cross-flow perpendicular to the solvent flow, as shown in Fig. 4.3. Through the empty channel, a constant solvent flow passes and forms a parabolic velocity profile. The macromolecules are held back by the cross-flow through a semipermeable membrane and, consequently, they are pushed against the membrane. From the accumulation membrane, the macromolecules move back into the channel by diffusion. The diffusion ability of the macromolecules is dependent upon their molecular size, i.e. small molecules diffuse faster than large molecules. This results in a distribution of the macromolecules with respect to their size in the channel. The macromolecules situated near the centre of the profile will be small in size. The maximum velocity of the flow profile will be in the centre and it decreases as it approaches the walls. Therefore, small molecules will elute earlier and larger molecules will elute later, opposite to the elution order in SEC.

A stainless steel channel and a flexible ceramic accumulation wall membrane are utilized in HT-AF4. Measurements with chlorinated organic solvents like TCB at temperatures up to 220 °C are possible because of the use of the above-mentioned materials. A Mylar spacer is cut to form the trapezoid channel with a thickness of 250–350 μm.

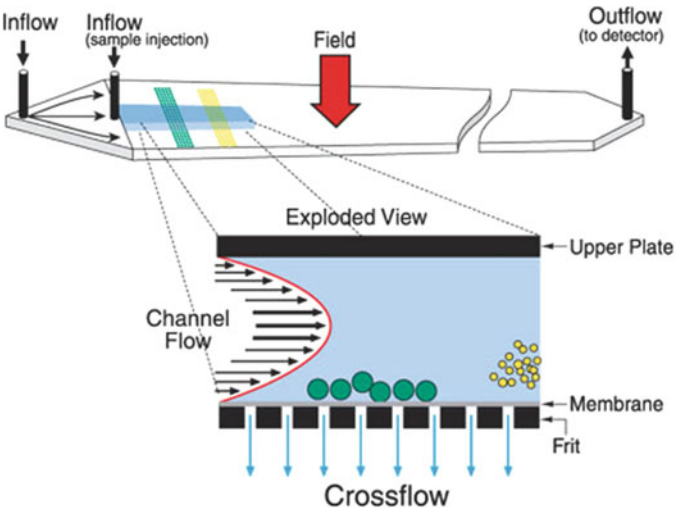

Fig. 4.3 Cross-section of the AF4 channel and scheme of size separation (reprinted from [28] with permission of Springer Science + Business Media)

A special focusing flow is implemented to enhance the performance of the polymer separation. The focusing flow enters the channel close to the center as a second input flow and divides itself into two sub-streams, as depicted in Fig. 4.4.

The injection flow meets the one part of the second input flow near the beginning of the channel. A sharp barrier is formed by the two flows. The sample transported by the injection flow is focused laterally in the region where both flows come into contact. The sample will rest at the same position until the focus flow stops. During the focusing step, a constant detector flow is provided by the second focus flow sub-stream. This focusing of the polymer molecules ensures the retention of the analytes at the beginning of the channel after the injection. The focusing step consequently provides separation of the polymer molecules with minimal longitudinal diffusion, which in turn results in less band broadening.

Giddings et al. [30] reported on the first AF4 separation at high temperature for polystyrene (PS). The possibility of separation of polyethylene (PE) by HT-AF4 was mentioned in the same article, but no results were included. Later, Mes et al. [6] reported on the successful separation of polyolefins with HT-AF4. Postnova Analytics (Landsberg, Germany) and Polymer Laboratories (Church Stretton, England) joined their efforts to develop the first commercial instrument for HT-AF4. Several different samples of high molar mass high density polyethylene (HDPE) and low density polyethylene (LDPE) were analysed by Mes et al. using a combination of HT-AF4 and IR, MALS and viscosity detectors. A comparison of the HT-AF4 results with the corresponding HT-SEC results has been presented [6]. A high molar mass shoulder was observed in the SEC chromatograms for the LDPE samples that was not noticed in the fractograms (Fig. 4.5) of the same samples. This shoulder was the consequence of lack of size separation at the exclusion limit of the SEC

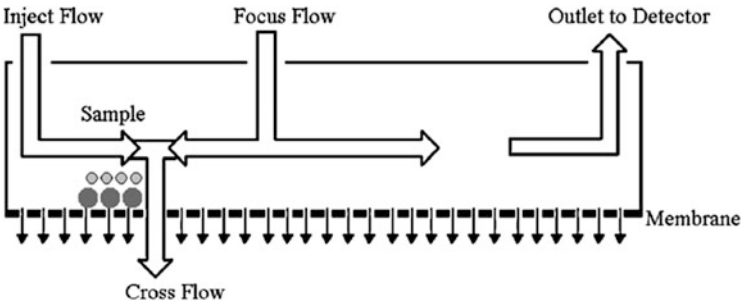

Fig. 4.4 Flow scheme of the AF4 focusing step (reprinted from [29] with permission of Elsevier Limited)

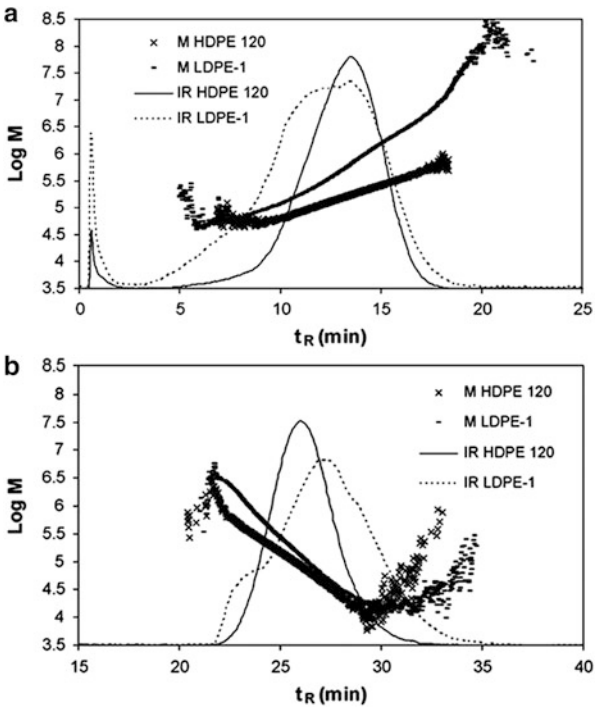

Fig. 4.5 Elution curves and molar mass plots of LDPE and HDPE samples; (**a**) separation by HT-AF4 and (**b**) separation by HT-SEC (reprinted from [6] with permission of Elsevier Limited)

column. This lack of separation at the higher molar mass end of the chromatogram results in incorrect molar mass average and long chain branching (LCB) calculations, as is depicted in the plot of the radius of gyration (R_g) or the intrinsic viscosity ($[\eta]$) versus molar mass (M) (Fig. 4.6). The separation and

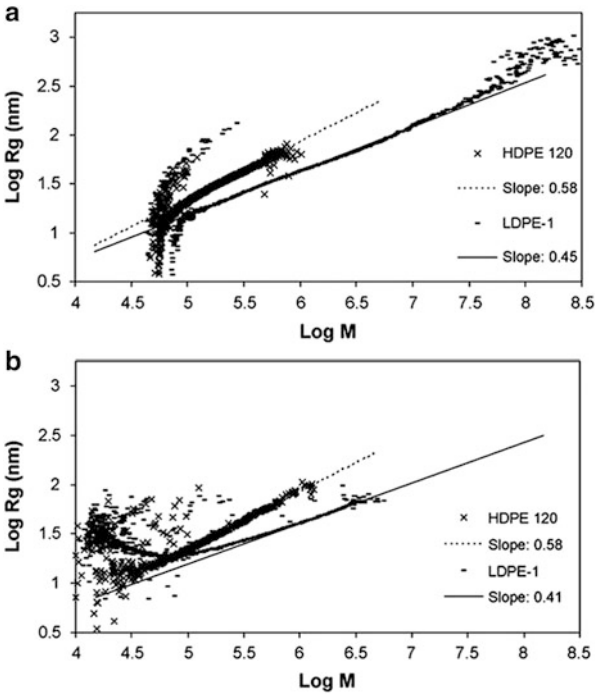

Fig. 4.6 Comparison of the conformation plots of HDPE and LDPE; (**a**) separation by HT-AF4 and (**b**) separation by HT-SEC (reprinted from [6] with permission of Elsevier Limited)

characterization of molar masses up to 10^8 g/mol are possible by using HT-AF4. On the other hand, SEC is not capable of discriminating such high molar mass samples with respect to molecular size due to shear degradation or the exclusion limit of the column. The shear degradation of high molar mass polymer samples during HT-SEC measurements was verified by the comparison with off-line low angle light scattering (LALS) measurements [29].

The abnormal late elution of a small amount of (probably branched) high molar mass material was also observed in HT-SEC of LDPE. A slight upward curvature in the R_g versus M plot of LDPE in HT-SEC (Fig. 4.6) was due to the co-elution of this fraction with the regularly eluting small molecules. The several advantages of HT-AF4 compared with HT-SEC are clearly illustrated in this application.

4.3 Analysis of Polyolefins by Asymmetric Flow FFF

In this section, a number of examples are discussed that show the potential of HT-AF4 as an alternative to high temperature liquid chromatography (HT-LC) for the analysis of complex polyolefins. It will be demonstrated that HT-AF4 is superior to column-based fractionations when ultrahigh molar mass (UHM) and branched samples must be analysed. Another important application is monitoring the thermo-oxidative degradation of polyolefins.

Otte et al. [7, 21, 22, 31] conducted several detailed studies on the analysis of UHM polyolefins following the work of Mes et al. [6]. The problems associated with SEC of UHM samples, namely the shear degradation of high molar mass structures and the anomalous late co-elution effects, can be successfully avoided in HT-AF4. This allows accurate molar mass analysis of samples up to $R_g > 1{,}000$ nm. The curvature that existed in the conformation plot based on SEC measurements is absent in similar AF4 plots. This curvature results in erroneous branching and molar mass calculations. Accordingly, molar mass averages calculated from HT-AF4 are significantly higher than those obtained from HT-SEC [7]. In addition, HT-AF4 allows the visualization of the thermo-oxidative degradation of polyolefins in solution [31]. Improper sample treatment, including sample preparation for HT-SEC, can be evaluated by this approach.

To summarize, the application of AF4 for the characterization of polyolefins enables wider insight into molecular properties, which are apparently more complex than has been found to date by traditional separation methods.

4.3.1 Characterization of Branched Ultrahigh Molar Mass Polyethylene by AF4 [7]

Polymers with weight average molar masses (M_w) > 500 kg/mol are typically considered as UHM polymers. The mechanical stability and specific weight of UHM PEs are superior compared to traditional materials. Therefore, UHM PE is used for special applications such as ultrastrong fibers, implants, or toothed wheels. Knowledge of the MMD and the chain structure of these materials is extremely important for the development of new products from UHMPE. The mechanical properties of the final products, the morphology and the rheological behaviour of the melt are influenced by these parameters [32].

SEC that is typically used for the molar mass analysis of polymers has its limitations regarding the measurements of UHM polymers. Such samples may undergo shear degradation during the chromatographic separation process. If the samples are not strictly linear, then co-elution of branched macromolecules with smaller linear macromolecules prevents an accurate analysis of the chain structure.

4.3.1.1 Aim

In the present study, UHM polyolefins shall be analysed regarding their molar masses. HT-SEC and HT-AF4 shall be used for fractionation; the detection shall be conducted by multiangle laser light scattering (MALLS). The molar mass and molecular size information obtained by both methods shall be compared and the effect of branching shall be discussed.

4.3.1.2 Materials

- *Polymers*. LDPE samples CSTR-LDPE 1 and 2 synthesized by free radical polymerization in a continuous stirred tank reactor (CSTR) using different amounts of chain transfer agent propionic aldehyde; technical PE samples PE

1 and PE 2 were broadly distributed HDPE and LDPE, respectively; technical PP samples PP 1 and 2 differed in molar mass and degree of branching. All polyolefins were produced by LyondellBasell (Frankfurt, Germany).

4.3.1.3 Equipment

- *AF4 instrument*. AF2000 (Postnova Analytics, Landsberg/Lech, Germany), specifically configured to be used at high temperature above 130 °C. For this aim, the AF4 pump system was connected to a PL GPC-220 chromatograph (Polymer Laboratories, Church Stretton, England). The HT-AF4 channel was placed inside the column oven. The AF4 channel was connected to three pumps from Postnova Analytics and to an additional pump management system which ensured a constant flow rate to the detectors during the entire separation. The HT channel had a spacer of 350 µm thickness; it was clamped between two plates made of stainless steel. For HT work, a ceramic membrane with a cut-off of approx. 50 kg/mol PE in TCB was used for separation. The flow rate at the detector was 0.5 mL/min. A schematic representation of the instrument is given in Fig. 4.7.
- *HT-SEC*. AF2000 (Postnova Analytics, Landsberg/Lech, Germany) was configured for HT-SEC work. The columns were installed inside the PL-220 chromatograph next to the AF4 channel. Three 6-port HT valves (Valco Instruments, Waterbury, USA) were used to control the injection and switching between the two separation systems. The detectors were connected to the outlet of the channel and the columns. A temperature of 145 °C and solvent TCB were used for all separations. Dissolution of the samples was accomplished at 160 °C under gentle rotation for 4 h. Butyl hydroxytoluene (1 mg/mL) was added to the solvent to minimize thermo-oxidative degradation of the polymers during the

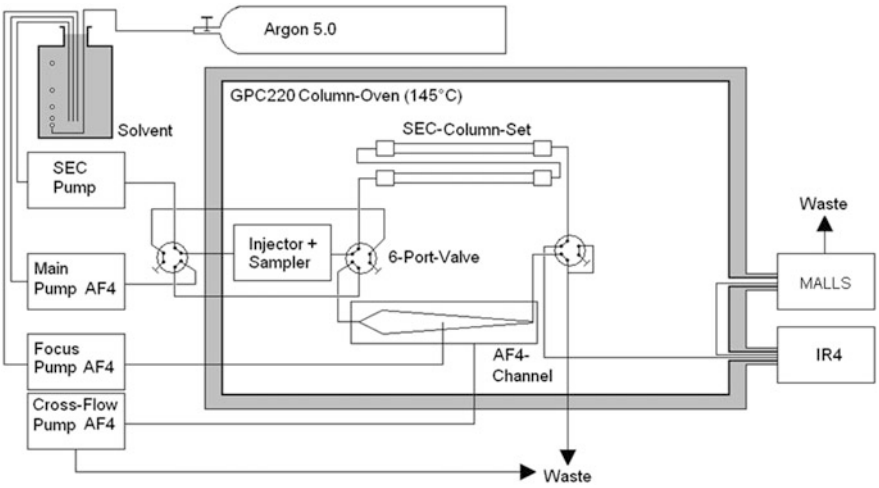

Fig. 4.7 Schematic representation of the HT-AF4-SEC-system (reprinted from [31] with permission of Wiley-VCH)

dissolution process. Argon was flushed through the solvent to remove any remaining oxygen. The flow rate was set at 0.5 mL/min.

- *Columns*. Two PLgel mixed B columns with particle sizes of 10 µm and column sizes of 300 × 8 mm i.d. (Polymer Laboratories, Church Stretton, England).
- *Mobile phase*. TCB for both AF4 and SEC, distilled prior to use.
- *Detectors*. IR detector (IR4, Polymer Char, Valencia, Spain) and a HT-MALLS detector (Heleos 2, Wyatt Technology, Santa Barbara, USA). The specific RI increments used in TCB at 145 °C were—0.091 for PE and 0.097 for PP.
- *Separation temperature*. 145 °C for both AF4 and SEC.
- *Sample concentration*. 2 mg/mL in TCB.
- *Injection volume*. 200 µL.

4.3.1.4 Preparatory Investigations

In the first part of the experiments, the correct operation of the HT-AF4-SEC system was investigated. In order to ensure that both AF4 and SEC yield the same results, an 'easy-to-analyse' sample of linear HDPE was selected and measured by both methods coupled to the MALLS detector. The sample was of rather low molar mass to minimize shear degradation in HT-SEC. The MALLS detector provided the weight-average molar mass (M_w) and the R_g values, which were then plotted as a conformation plot of log R_g vs. log M_w. Similar results were provided by both conformation plots; see Fig. 4.8.

The results of HT-SEC and HT-AF4 are fully congruent. The slope of the R_g–M relationship is 0.6, which is very close to the theoretical value (0.588) for a linear polymer in a good solvent. The correct adjustment of the system parameters is clearly indicated by the results. The separation as obtained by both methods was comparable.

As mentioned previously, the velocity of the cross flow is the major factor that determines the vertical position of the macromolecules in the channel. Therefore, good knowledge of the influence of cross-flow velocity is required for optimization

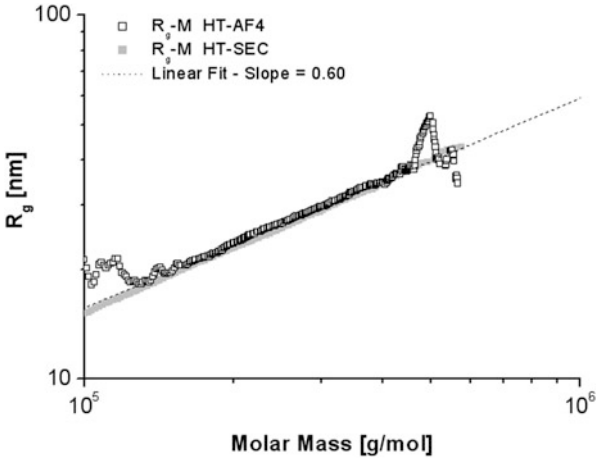

Fig. 4.8 Conformation plot from HT-SEC and HT-AF4 separation of linear HDPE, data obtained by IR-MALLS detection (reprinted from [7] with permission of Elsevier Limited)

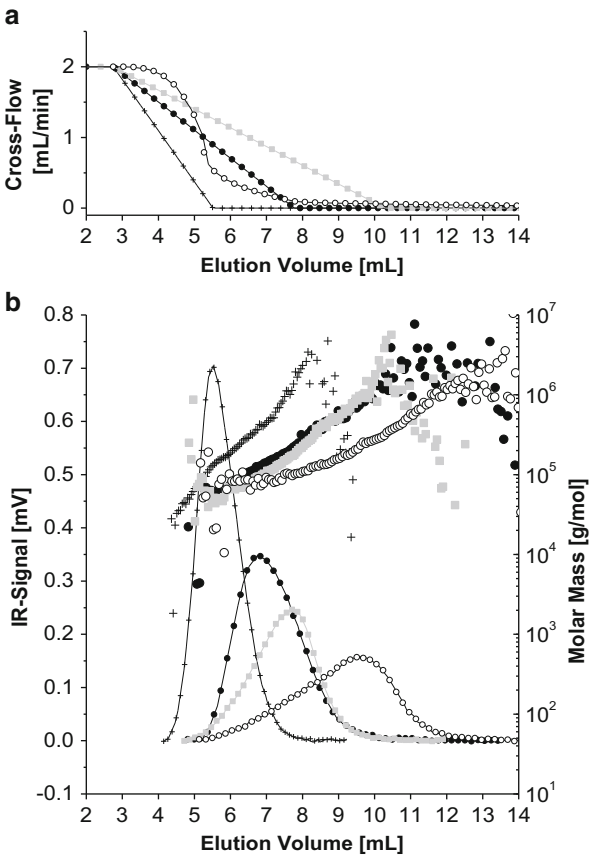

Fig. 4.9 Fractograms and molar mass calibration curves of PE 2 (**b**) separated with different cross-flow gradients (**a**) in HT-AF4-IR-MALLS (reprinted from [7] with permission of Elsevier Limited)

of separation. The analysis of sample PE 2 was conducted using different cross-flow gradients to study the influence of the cross-flow velocity on the separation. The obtained fractograms together with the molar mass calibration curves and the applied cross-flow gradients are shown in Fig. 4.9.

The quality of the separation is determined by both the steepness and the shape of the cross-flow gradient. An improved separation is obtained by a flat gradient, see Fig. **4.9**, as indicated by a decreased steepness of the molar mass vs. elution volume plot. One has to keep in mind, however, that the increase of the elution interval of the polymer for longer gradients is caused by peak broadening and improved separation. The separation of narrow PS standards at varying crossflows showed that increased separation strongly overcompensates for the band broadening [21].

In Fig. **4.9**, the advantage of a non-linear crossflow, represented by an exponential-like gradient, becomes obvious. A significantly better separation is obtained by this gradient in comparison to a linear gradient of the same duration. The selective retention of high molar mass molecules is promoted by the shape of the gradient, which leads to their better separation from the low molar mass

material. Furthermore, a decreased loss of small molecules through the pores of the membrane is observed due to the low average cross-flow value of the exponential gradient and, in turn, a large amount of solvent is saved.

The results demonstrate the enormous flexibility of AF4 as compared to SEC. The adjustment of the cross-flow function enables one to create tailor-made calibration curves. An expensive and time consuming change of the SEC columns is not necessary. Finally, an exponential-like gradient was chosen for further measurements because of the good separation and the lower material loss for low molar mass samples.

4.3.1.5 Measurement and Evaluation

The abnormal late elution of branched molecules that results in the co-elution of linear and branched molecules with different molar masses in HT-SEC causes severe problems in the accurate molar mass analysis of polyolefins with very high molar masses and significant branching (UHM HDPE or LDPE). This leads to errors in the calculated molar mass distributions. Macromolecules with molar masses above 1,000 kg/mol are known to be very sensitive to shear degradation in SEC. This is an additional source of error when molar masses are analysed by SEC.

The co-elution behaviour of two UHM LDPEs as investigated by HT-SEC and HT-AF4 is shown in Fig. **4.10**. An abnormal increase in the molar mass and R_g readings is observed at high elution volumes. The reason for this behaviour seems to be the late co-elution of high molar mass branched molecules together with low molar mass linear structures.

The R_g and the molar mass values as obtained by HT-SEC were clearly lower than the results obtained by HT-AF4, as illustrated in Fig. **4.10**. The enhanced shear degradation in either the packing or the frits of the SEC columns is apparent. The fractograms show that HT-AF4 enhanced the separation limit to radii up to 1,000 nm and molar mass values above 10^8 g/mol. A strong curvature of the radius and the molar mass readings at high elution volumes can be clearly seen for both

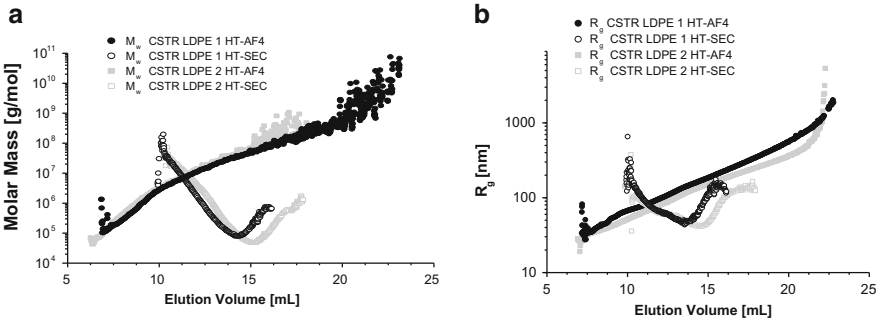

Fig. 4.10 Overlay of fractograms obtained by HT-AF4 and elugrams from HT-SEC, (**a**) CSTR-LDPE 1 and 2, molar masses obtained by light scattering detection, (**b**) CSTR-LDPE 1 and 2, R_g obtained by light scattering detection (adapted from [7] with permission of Elsevier Limited)

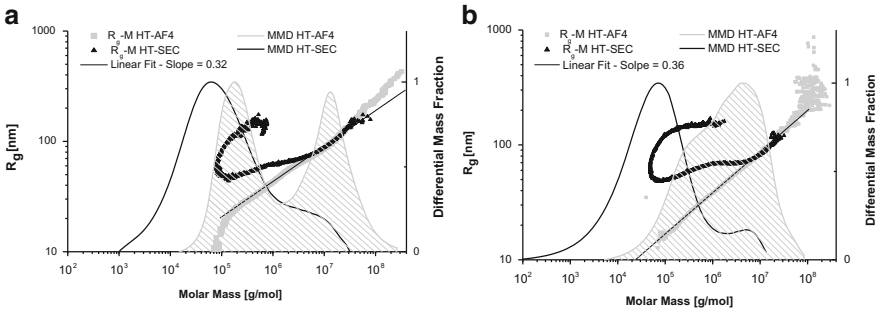

Fig. 4.11 MMD from HT-AF4 and HT-SEC overlaid with corresponding conformation plots obtained by IR-MALLS, (**a**) LDPE 1, (**b**) LDPE 2 (adapted from [7] with permission of Elsevier Limited)

samples in HT-SEC. The late co-elution of large branched macromolecules with small linear macromolecules affects the R_g values more pronouncedly than the molar mass values.

As no stationary phase is involved in HT-AF4, the co-elution effects are avoided. With increasing elution volume, the molar mass as well as R_g increase steadily. Consequently, HT-AF4 allows access to the lower R_g values that could not be obtained by HT-SEC. A linear dependence between R_g and the elution volume over the entire molar mass range is shown for HT-AF4 in contrary to HT-SEC, which is a clear indication for the separation of the macromolecules with respect to hydrodynamic size for the entire sample.

Figure **4.11** shows the differential MMDs and the conformation plots of both LDPE samples obtained by HT-SEC-IR-MALLS as well as HT-AF4-IR-MALLS. The negative effects in HT-SEC manifest themselves in a very pronounced way: the R_g curve in the conformation plot is strongly bent in the low molar mass range. The reason for this behaviour is the high sensitivity of the R_g value for high molar mass molecules in the case of co-elution. The curvature of the conformation plot from HT-SEC makes a correct determination of branching in the LDPE samples impossible. The lower hydrodynamic volume of branched molecules leads to a reduced slope of the R_g–M-relationship, which is significantly lower than the value of 0.588 for a linear polymer. As HT-AF4 shows no co-elution effects, the conformation plot provides correct information about the chain branching. The R_g–M_w dependence is linear and the reduced slopes of 0.32 and 0.36 for samples 1 and 2, respectively, indicate very compact macromolecules as a result of the very high degree of branching.

The late co-elution of large branched molecules in HT-SEC leads to incorrect information on the LDPE samples due to incorrect MMDs. There are various parameters that affect the extent of the shear force and late co-elution. Among them, the most important are the shape, size and type of the stationary phase particles, sample preparation methods as well as the flow rate of the mobile phase. The detrimental effects are reflected by the different molar mass averages

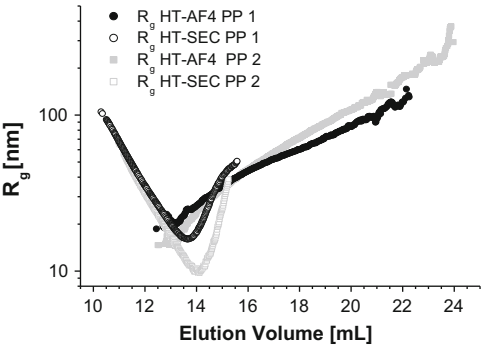

Fig. 4.12 Overlay of R_g vs. elution volume curves obtained with HT-AF4 and HT-SEC for branched PP 1 and PP 2, R_g obtained by IR-MALLS detection (adapted from [7] with permission of Elsevier Limited)

of LDPE samples as obtained by HT-SEC in different laboratories [14]. Therefore, there is a strong motivation to study the late elution phenomenon and the shear degradation dependence on different SEC parameters for different polyolefins.

In addition to branched LDPE, branched PP samples were analysed by HT-SEC and HT-AF4 to prove the universal applicability of HT-AF4. In Fig. **4.12** the R_g vs. elution volume curves from HT-SEC and HT-AF4 are displayed for the two branched PP samples. The PP samples show the same problems of late co-elution in SEC as the LDPE samples. For both PP samples, the radius re-increases at high elution volumes in HT-SEC; see Fig. **4.12**. HT-AF4 results do not show this behaviour. In addition, the radii from AF4 are significantly higher than those from SEC. These results show, impressively, that AF4 is not restricted to the analysis of PE but can be used for the analysis of all polyolefins.

4.3.2 Investigation of Thermo-oxidative Degradation of Polyolefins by AF4 [31]

Polyolefins are of enormous economic importance and the most important ones, polypropylene and polyethylene, represent the majority of the total polymer market. Polyolefins are, however, susceptible to degradation. Degradation of polyolefins takes place during processing, application and recycling. It influences the polymer properties, thereby limiting the lifetime of the materials and leading to economic loss. In particular, the increasing importance of polymer recycling is a strong motivation to search for new analytical methods to analyse the degradation of polyolefins.

One can distinguish photo-oxidative and thermo-oxidative degradation. The generally accepted free radical oxidation model consists of radical initiation, propagation and termination reactions. Following an initiation reaction, which usually results from the thermal or photo-initiated dissociation of chemical bonds, alkyl radicals react with molecular oxygen to form peroxy radicals. Propagation reactions result in the formation of oxygen-containing functionalities. Depending on the type of polyolefin, chain scission or cross-linking can occur.

Thermo-oxidative degradation is known to be a major problem in HT-SEC experiments of high molar mass polyolefins. Depending on the solvent used, the sample concentration, the dissolution temperature and time, chain scission can take place to a larger or lesser extent. Therefore, suitable protocols for SEC sample preparation are of utmost importance for the validity of the analytical results.

4.3.2.1 Aim

Thermo-oxidative degradation and shear stress in parts of the HT-SEC system are the main reasons for the decrease in PE molar masses [14, 33–36]. In the present application, the influence of the dissolution procedure on the molar mass of UHM PE shall be investigated. HT-SEC measurements shall be compared to results of HT-AF4 analyses, where shear stress or unwanted interaction of the macromolecules with the stationary phase (such as in SEC) are avoided. The absence of shear stress and co-elution in AF4 makes it possible to track the influence of the thermo-oxidative degradation process on the molar mass distribution without disturbing secondary effects that often significantly influence the SEC results.

4.3.2.2 Materials

- *Polymers*. HDPE, LDPE, linear and branched PP. HDPE and PP were technical products (Basell, Frankfurt, Germany). The UHM PE AK1 was obtained from the University of Freiburg, Germany. The LDPE samples were synthesized by a free radical polymerization process.

4.3.2.3 Equipment

- *AF4 instrument*. AF2000 (Postnova Analytics, Landsberg/Lech, Germany) which was specifically configured to be used at high temperature above 130 °C. For this aim the AF4 pump system was connected to a PL GPC-220 chromatograph (Polymer Laboratories, Church Stretton, England). The HT-AF4 channel was placed inside the column oven. The AF4 channel was connected to three pumps from Postnova Analytics and to an additional pump management system which ensured a constant flow rate to the detectors during the entire separation. The HT channel had a spacer of 350 μm thickness; it was clamped between two plates made of stainless steel. For HT work, a ceramic membrane with a cut-off of approx. 50 kg/mol PE in TCB was used for separation. The flow rate at the detector was 0.5 mL/min.
- *HT-SEC*. AF2000 (Postnova Analytics, Landsberg/Lech, Germany) was configured for HT-SEC work. The columns were installed inside the PL-220 chromatograph next to the AF4 channel. Three 6-port HT valves (Valco Instruments, Waterbury, USA) were used to control the injection and switching between two separation systems. The detectors were connected to the outlet of the channel and the columns. A temperature of 145 °C in TCB was used for all separations. Argon was flushed through the solvent to remove any remaining oxygen. The flow rate was set at 0.5 mL/min.

- *Columns*. Two SDV (styrene–divinylbenzene copolymer) Olexis columns with particle diameters of 13 µm and column sizes of 300 × 8 mm i.d. (Polymer Laboratories, Church Stretton, England).
- *Mobile phase*. TCB for both AF4 and SEC, distilled prior to use.
- *Detectors*. IR detector (IR4, Polymer Char, Valencia, Spain) and a HT-MALLS detector (Heleos 2, Wyatt Technology, Santa Barbara, USA). The specific RI increments used in TCB at 145 °C were—0.091 for PE and 0.097 for PP.
- *Separation temperature*. 145 °C for both AF4 and SEC.
- *Sample preparation*. Stirring and shaking of polymers during sample preparation was avoided to reduce shear degradation. Samples were prepared by dissolving the polymers in distilled TCB (2 mg/mL). Various parameters of sample preparation, namely the amount of stabilizer, the dissolution temperature and time were varied. The absence of oxygen in the vials was ensured by the addition of argon for some samples before dissolution. The remaining oxygen from the solvent for all the measurements was removed with a degasser. For the samples to which argon was added, the sample solvent was also flushed before passing the degasser. Butylated hydroxytoluene (1 mg/mL) was added to the sample solvent and the mobile phase for stabilization. An aluminium block was used to heat the sample solutions in the vials. The temperature control during the sample dissolution was ensured by a sensor inside the aluminium block. PTFE-silicone septa work well at high temperature and were used to close the vials.
- *Injection volume*. 200 µL.

4.3.2.4 Measurement and Evaluation

A high dissolution temperature of 160 °C had to be used for the samples to ensure complete dissolution of samples containing significant amounts of UHM material (consideration of the latter being the focus of this study). As a result, an initial thermal degradation has to be accepted, especially for the PP samples. A sample of UHM PE was dissolved under various conditions (see Table 4.2) and separated with HT-AF4 and HT-SEC, resulting in MMDs as shown in Fig. 4.13.

Comparison of the MMDs and the average molar masses shows that the absence of both antioxidant BHT and argon in the sample solution leads to a very pronounced decrease in molar masses. A few hours difference in the dissolving time of the samples without BHT or argon leads to a very strong shift of the MMDs towards lower values. The addition of argon alone or argon and BHT stabilizer slows down the degradation process, but does not stop it completely.

There are large differences in the molar mass averages obtained from HT-SEC and HT-AF4. In general, molar masses obtained from HT-AF4 are much higher than the molar masses obtained from HT-SEC. The low and incorrect MMDs obtained by SEC are attributed to shear degradation of the polymer samples during SEC separation in the column packing and the inlet frits [9–11, 33, 34, 37–39]. Furthermore, the thermo-oxidative degradation of the macromolecules during the dissolution step superimposes the intensive shear degradation in SEC. In comparison to SEC, polymer molecules are less exposed to shear degradation in AF4 due to the absence of a stationary phase and, therefore, higher MMDs are

Table 4.2 Average molecular parameters of linear PE and PP separated by HT-AF4 and HT-SEC, calculation performed with data from IR-MALLS (reprinted from [31] with permission of Wiley-VCH)

Sample	Separation method	Stabilization	Dissolving time (h)	$\overline{M}_w$ (kg/mol)	Degradation (%)	$\langle R_g^2 \rangle_z^{0.5}$ (nm)	PDI
PE AK01 linear (slope $R_g/M = 0.58$)[a]	HT-AF4	BHT + Ar	2	3,570	100	176	1.15
			4	2,423	68	149	1.11
			6	2,232	63	112	1.11
			8	2,054	58	107	1.09
			12	761	21	68	1.28
			14	552	15	66	1.24
	HT-AF4	Ar	2	2,890	80	163	1.09
			4	1,230	34	98	1.11
			6	956	27	84	1.10
	HT-AF4		2	1,310	37	103	1.10
			4	749	21	72	1.08
			6	571	16	64	1.10
	HT-SEC	BHT + Ar	2	1,656	46	133	1.35
			4	1,297	36	87	1.45
			6	1,162	33	77	1.49
	HT-SEC		2	918	26	66	1.42
			4	516	14	62	1.43
			6	382	11	49	1.38
			8	339	9	46	1.49

PP LIN 1 linear (slope $R_g/M = 0.58$)[a]	HT-AF4	BHT + Ar	2	1,656	100	133	1.35
			4	1,297	78	87	1.45
			6	1,162	70	77	1.49
	HT-AF4		2	786	47	65	1.42
			4	719	43	59	1.33
			6	650	39	53	1.24
	HT-SEC	BHT + Ar	2	539	33	35	1.55
			4	454	27	33	1.83
			6	357	22	29	2.46
	HT-SEC		2	427	26	31	1.90
			4	380	26	31	2.62
			6	349	21	29	2.81

[a] R_g/M relationship obtained from HT-AF4-IR-MALS, linear polymer dissolved in a good solvent: slope $R_g/M = 0.588$

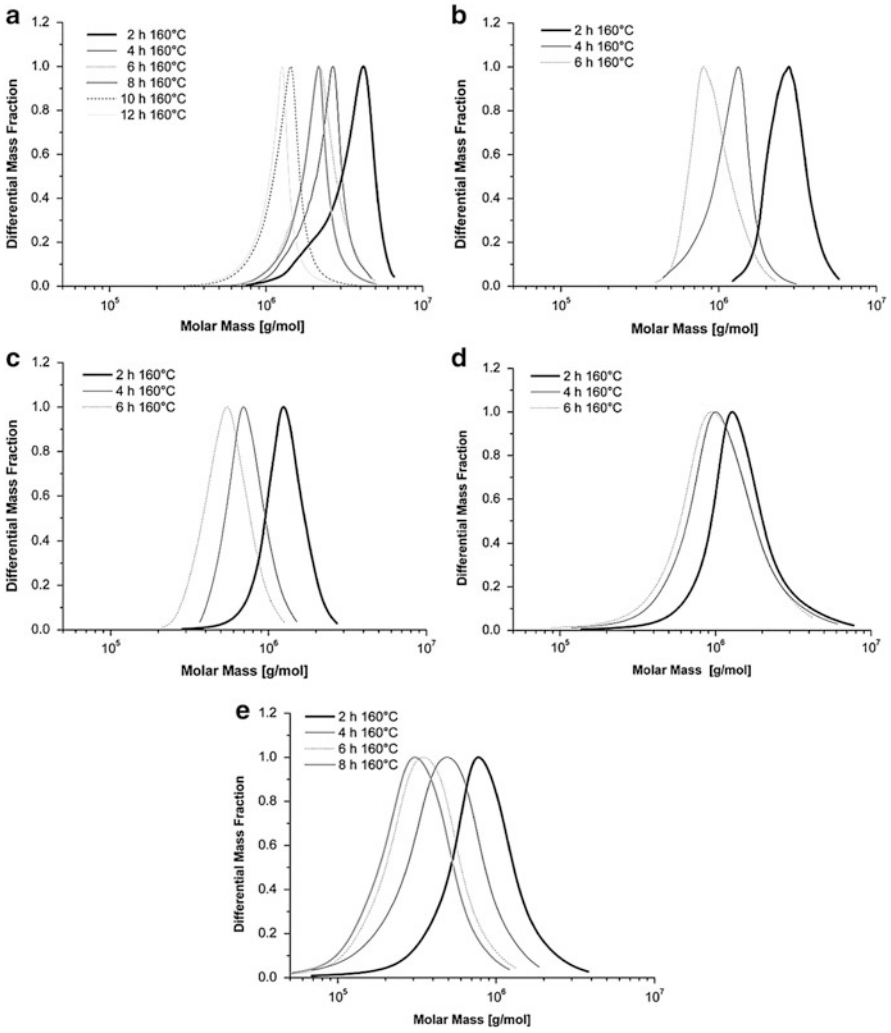

Fig. 4.13 MMDs of linear UHM PE sample AK01 from HT-SEC and HT-AF4, dissolution time and stabilization were varied, (**a**) HT-AF4, BHT and argon added; (**b**) HT-AF4, only argon added; (**c**) HT-AF4, not stabilized; (**d**) HT-SEC, BHT and argon added; (**e**) HT-SEC, not stabilized (reprinted from [31] with permission of Wiley-VCH)

obtained. For linear polyolefin samples, the extent of molar mass degradation as a function of dissolution time is given in Fig. 4.14 for different methods and different conditions. In the present case, 100 % stands for the initial molar mass before degradation.

The molar masses obtained from HT-AF4 are significantly higher than the molar masses obtained from HT-SEC at similar dissolution times, indicating significantly higher degradation for the separations by HT-SEC. Quantification by HT-SEC only

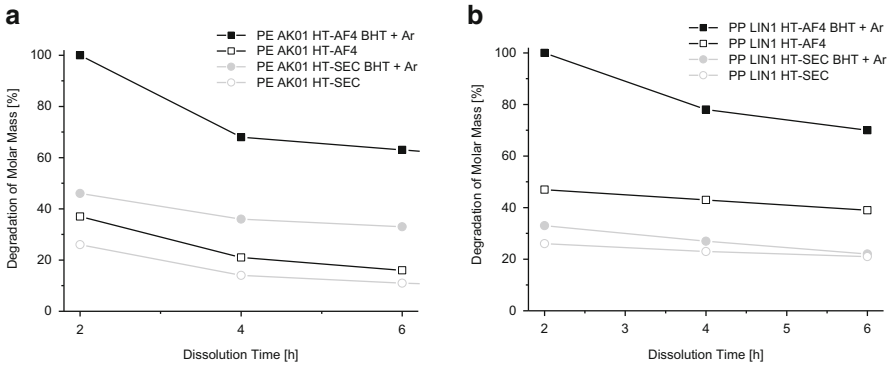

Fig. 4.14 Comparison of the percentage of molar mass degradation obtained with different separation methods, after different dissolution times and with different stabilization, (**a**) linear sample PE AK01, (**b**) linear sample PP LIN1 (reprinted from [31] with permission of Wiley-VCH)

is very difficult, or impossible, because shear-offset overlays the thermo-oxidative degradation. For non-stabilized samples, differences between the molar masses from SEC and AF4 are lower due to prior reduction of the molar mass by the thermo-oxidative degradation. Shear degradation of the polymer sample is molar mass dependent. Hence, samples already degraded by high temperatures during the dissolution process will undergo considerably less shear degradation and the resulting differences between the molar mass values from SEC and AF4 will not be as great as would otherwise be obtained. The molar mass of the PP sample is much lower than that of the UHM PE. It nonetheless sheared to a comparable or even higher extent, which is an indication of the higher shear sensitivity of PP compared to PE.

PP, like PE, tends to degrade thermally during the dissolution process. A significant decrease in molar mass of non-stabilized linear PE or PP is observed after 2 h of dissolution time. Further thermal degradation of the polymer samples is rather small when dissolution times are increased from 2 to 4 and 6 h. The molar mass degradation induced by thermal oxidation seems to decrease for lower initial average molar masses. The absolute degree of degradation for the stabilized samples is significantly lower than the non-stabilized material. For the non-stabilized samples, more pronounced differences in molar masses between 2 and 4 h of heat treatment are obtained. The assumption that the rate of molar mass degradation depends on the initial molar mass is also supported by these results. The thermo-oxidative degradation process is decelerated for the stabilized polymer. Therefore, sufficiently high average molar masses still exist after 2 h dissolution time and further degradation occurs. Similar thermal degradation behaviour is obtained for PE and PP, despite the fact that PP has a significantly lower molar mass than the PE sample. The results show that PP is more sensitive towards degradation, which supports the trend of the shear degradation process.

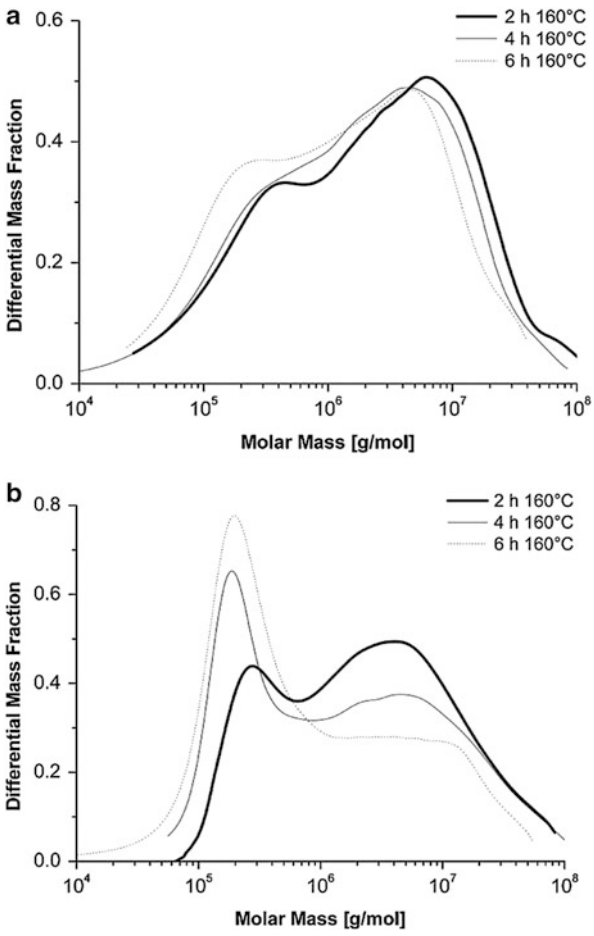

Fig. 4.15 Differential molar mass distributions of CSTR LDPE 2 obtained with HT-AF4-IR-MALLS, the dissolving times and stabilization were varied, (**a**) HT-AF4, BHT and argon added; (**b**) HT-AF4, not stabilized (reprinted from [31] with permission of Wiley-VCH)

Degradation can be decelerated and minimized by stabilization, but it cannot be fully stopped, as can be seen from the data shown in Figs. 4.13 and 4.14.

In a next step, HT-AF4-MALLS analyses of PE and PP samples with different degrees of branching were conducted to investigate the relationship between thermal degradation and the architecture of the polymer chain. The most important outcome of this study was the abnormal late elution of highly branched polymers with high molar mass molecules in SEC. Accordingly, it is not possible to determine the degree of branching by SEC-MALLS. As discussed previously, the late elution and co-elution effects are not shown by HT-AF4. Therefore, the branched samples were characterized by HT-AF4. The analyses of UHM linear PE and highly branched LDPE were conducted under similar conditions. Figure 4.15 depicts the differential MMDs of the bimodal LDPE sample. A summary of the corresponding molar masses and radii of gyration for the LDPE as well as for other branched PEs and PPs is given in Table 4.3. The low degradation of the high molar mass fraction

Table 4.3 Average molecular parameters of branched PE and PP separated by HT-AF4, calculation performed with data from IR-MALLS (reprinted from [31] with permission of Wiley-VCH)

Sample	Separation method	Stabilization	Dissolving time (h)	$\overline{M}_w$ (kg/mol)	Degradation (%)	$\langle R_g^2 \rangle_z^{0.5}$ (nm)	PDI
CSTR LDPE 2 branched (slope $R_g/M = 0.36$)[a]	HT-AF4 branched	BHT + Ar	2	7,726	100	116	17.40
			4	6,246	81	117	12.78
			6	5,110	66	102	14.28
	HT-AF4 branched		2	6,605	85	113	9.63
			4	6,006	78	109	15.67
			6	4,423	57	99	11.36
PE B branched (slope $R_g/M = 0.47$)[a]	HT-AF4	BHT + Ar	2	937	100	70	1.13
			4	583	62	59	1.12
			6	447	48	49	1.08
	HT-AF4		2	784	84	64	1.13
			4	543	58	53	1.16
			6	450	48	45	1.09
PP 180 long-chain branching (slope $R_g/M = 0.50$)[a]	HT-AF4	BHT + Ar	2	1,275	100	80	1.62
			4	976	77	69	1.67
			6	723	57	42	1.31
	HT-AF4		2	600	47	58	1.40
			4	575	45	52	1.44
			6	437	34	49	1.45
PP LCB 1 long-chain branching (slope $R_g/M = 0.42$)[a]	HT-AF4	BHT + Ar	2	2,759	100	74	1.82
			4	1,267	46	50	1.51

(continued)

Table 4.3 (continued)

Sample	Separation method	Stabilization	Dissolving time (h)	$\overline{M}_w$ (kg/mol)	Degradation (%)	$\langle R_g^2 \rangle_z^{0.5}$ (nm)	PDI
			6	939	34	48	1.43
	HT-AF4		2	1,995	72	65	1.66
			4	857	31	52	1.44
			6	485	18	35	1.13

[a] R_g/M relationship obtained from HT-AF4-IR-MALS, linear polymer dissolved in a good solvent: slope $R_g/M = 0.588$

due to the intensive stabilization is indicated by Fig. 4.15a. A slight shift of the entire distribution curve in the direction of low molar masses manifests degradation. The strong degradation of the same sample without BHT and argon is shown in Fig. 4.15b as indicated by the decrease of the high molar mass region in favour of a shoulder which is formed in the low molar mass region. In addition the whole molar mass distribution is shifted towards lower molar masses.

The average molar masses of branched polymers as given in Table 4.3 stay high in comparison to the linear materials (see Table 4.2) despite the changes in the molar mass distribution curves even for long dissolving times and without stabilization. The tertiary C-H bonds, that have low dissociation energy and result in more stable radicals, are the preferred sites for the start of the thermo-oxidative degradation. More tertiary C-H bonds are present in LDPE than in linear materials because free radical polymerization induces the formation of long- and short-chain branches at the main chain and at the side chains [40, 41]. Accordingly, the probability of chain scission or radical formation during thermal treatment at the various side chains that contain additional branching points is rather high. The lower molar mass degradation for the branched samples seems to contradict, therefore, the degradation mechanism. However, one has to keep in mind that side chains in branched samples are significantly shorter than the main backbone of a linear or slightly branched polymer. Even a significant number of chain scissions resulting in the abstraction of a number of side chains will not lead to a significant decrease in average molar mass. The amount of low molar mass material will increase at the expense of the highest molar mass fractions as depicted in Fig. 4.15. It can, therefore, be assumed that the impact of degradation on the entire molar mass distribution of LDPE will not be as pronounced as for a comparable linear or slightly branched PE.

In conclusion, the effects of the dissolution process, as well as the separation conditions and methods on the obtained molar masses are, impressively demonstrated. All samples undergo shear degradation in SEC, but this has been successfully eliminated in HT-AF4. The molar mass dependence of shear degradation is also shown, which prevents the possible use of correction factors for the molar mass analysis by SEC.

Most problems in SEC are caused by the stationary phase, which is not used in HT-AF4. Without the effects of the stationary phase, HT-AF4 gives a clear picture on the thermo-oxidative degradation of polyolefins that is a result of sample preparation and treatment. The results have shown that the thermal degradation is equally molar mass dependent. Degradation can be significantly reduced by stabilization using BHT and/or argon gas. However, even stabilized samples show a decrease in molar mass when long dissolution times are used.

References

1. Johann C, Kilz P (1991) J Appl Polym Sci Appl Polym Symp 48:111
2. Wintermantel M, Antonietti M, Schmidt M (1993) J Appl Polym Sci Appl Polym Symp 5:91
3. Podzimek S (1994) J Appl Polym Sci 54:91
4. Percec V, Ahn CH, Cho WD, Jamieson AM, Kim J, Leman T, Schmidt M, Gerle M, Möller M, Prokhorova SA, Sheiko SS, Cheng SD, Zhang A, Ungar G, Yeardley DJ (1998) J Am Chem Soc 120:8619
5. Gerle M, Fischer K, Roos S, Muller AHE, Schmidt M (1999) Macromolecules 32:2629
6. Mes EPC, de Jonge H, Klein T, Welz RR, Gillespie DT (2007) J Chromatogr A 1154:319
7. Otte T, Pasch H, Macko T, Brüll R, Stadler FJ, Kaschta J, Becker F, Buback MJ (2011) Chromatogr A 1218:4257
8. Makan AC, Otte T, Pasch H (2012) Macromolecules 45:5247
9. Slagowski EL, Fetters LJ, McIntyre D (1974) Macromolecules 7:394
10. Zammit MD, Davis TP, Suddaby KG (1998) Polymer 39:5789
11. Aust N (2003) J Biochem Biophys Methods 56:323
12. Cave RA, Seabrook SA, Gidley MJ, Gilbert RG (2009) Biomacromolecules 10:2245
13. Messaud FA, Sanderson RD, Runyon JR, Otte T, Pasch H, Williams SKR (2009) Prog Polym Sci 34:351
14. Stadler FJ, Kaschta J, Münstedt H, Becker F, Buback M (2009) Rheol Acta 48:479
15. Schimpf ME, Caldwell K, Giddings JC (2000) Field flow fractionation handbook. John Wiley, Hoboken, NJ
16. van Bruijnsvoort M, Wahlund KG, Nilsson G, Kok WTJ (2001) Chromatogr A 925:171
17. Rojas CC, Wahlund KG, Bergenstahl B, Nilsson L (2008) Biomacromolecules 9:1684
18. Rolland-Sabaté A, Guilois S, Jaillais B, Colonna P (2011) Anal Bioanal Chem 399:1493
19. Podzimek S (2011) Light scattering, size exclusion chromatography and asymmetric flow field flow fractionation: powerful tools for the characterization of polymers, proteins and nanoparticles. John Wiley, Hoboken, NJ
20. Bang DY, Shin DY, Lee S, Moon MH (2007) J Chromatogr A 1147:200
21. Otte T, Brüll R, Macko T, Pasch H, Klein T (2010) J Chromatogr A 1217:722
22. Otte T, Klein T, Brüll R, Macko T, Pasch H (2011) J Chromatogr A 1218:4240
23. White RJ (1997) Polym Int 43:373
24. Liu Y, Radke W, Pasch H (2006) Macromolecules 39:2004
25. http://www.postnova.com/general-theory.html
26. Giddings JC (1993) Science 260:1456
27. http://www.postnova.com/fff-systems.html
28. Pasch H, Malik MI, Macko T (2013) Adv Polym Sci 251:77
29. Gao S, Caldwell D, Myers N, Giddings JC (1985) Macromolecules 18:1272
30. Miller ME, Giddings JC (1998) J Micro Sep 10:75
31. Otte T, Pasch H, Brüll R, Macko T (2011) Macromol Chem Phys 212:401
32. Trinkle S, Friedrich C (2001) Rheol Acta 40:322
33. Aust N, Parth M, Lederer K (2001) Int J Polym Anal Charact 6:245
34. Parth M, Aust N, Lederer K (2003) Int J Polym Anal Charact 8:175
35. Grinshpun V, Rudin A (1985) J Appl Polym Sci 30:2413
36. Pasti L, Melucci D, Contado C, Dondi F, Mingozzi I (2002) J Sep Sci 25:691
37. de Groot AW, Hamre WJ (1993) J Chromatogr A 648:33
38. Barth HG, Carlin FJ Jr (1984) J Liq Chromatogr 7:1717
39. Zigon M, The NK, Shuyao C, Grubisic-Gallot Z (1997) J Liq Chromatogr 20:2155
40. Schnabel M (1981) Polymer degradation: principles and practical applications. Hanser International, Munich
41. Constantin D, Hert M, Machon JP (1981) Eur Polym J 17:115

Conclusions and Future Trends

5

Polyolefins are one of the most important synthetic polymeric materials in all spheres of human activities ranging from packaging and construction to computer science and medicine. Of all synthetic polymers produced today, they account for more than 50 %. Similar to other polymeric materials, polyolefins are distributed in their molecular properties and in-depth analysis of these properties is required using the most sophisticated analytical methods. This helps to establish structure–property relationships and broadens the application of polyolefins in science and technology.

The classical techniques for chemical composition analysis of polyolefins are based on crystallization behaviour of different components of these materials. These techniques are only applicable for the crystalline part of the sample and the amorphous part is obtained as a bulk fraction. Although the methods themselves are very reliable and robust, they require long analysis times and significant amounts of solvents. Nevertheless, these techniques are still the analytical workhorse in most polyolefin research laboratories. The reason behind this is that most of the commercially important polyolefin materials are semi-crystalline.

There are a number of recent advancements in these techniques that allow to decrease analysis times significantly, to obtain better resolution and more detailed understanding of the underlying physical processes through mathematical modelling. The most fascinating innovation in this regard is development of crystallization elution fractionation (CEF). CEF combines the separation power of both temperature rising elution fractionation and crystallization analysis fractionation resulting in better separation of fractions along with considerable reduction in analysis time. CEF has the promise and potential to be the major technique in crystallization analysis in future.

High-temperature (HT) size exclusion chromatography (SEC) is the premier technique for information with regard to molar masses. A number of different concentration detectors as well as molar mass sensitive detectors can be used. The coupling of HT-SEC with spectroscopic techniques like FTIR and ^{1}H-NMR reveals the chemical composition across the MMD of the sample. Other important

H. Pasch, M.I. Malik, *Advanced Separation Techniques for Polyolefins*, Springer Laboratory, DOI 10.1007/978-3-319-08632-3_5

structural features like long chain branching and stereoregularity can also be obtained by these method combinations.

A fascinating new development in column-based chromatographic techniques for polyolefin analysis is high-temperature interaction chromatography. In contrast to crystallization-based techniques, interaction chromatography can address the complete sample irrespective of whether it is crystalline or amorphous. The use of gradient HT high performance liquid chromatography (HPLC), liquid chromatography at critical conditions at high temperatures above 120 °C, HT-HPLC based on precipitation–redissolution or adsorption–desorption for chemical composition analysis of polyolefins have been reported in recent years. These methods are a major breakthrough in the field of chemical composition analysis of polyolefins. They overcome the drawbacks of other techniques used previously for chemical composition analysis as they address both the amorphous and the crystalline part of the sample. The ultimate recent development in polyolefin analysis is coupling of HT-HPLC with online size exclusion chromatography. This fascinating development leads to the molar mass distribution of the sample as a function of its chemical composition. Two-dimensional (2D) HT-HPLC is a major advancement in polyolefin analysis and promises to be the future for research-oriented polyolefin laboratories. The most recent step regarding hyphenation of 2D-HT-HPLC is the coupling with infrared and light scattering detectors.

High-temperature field-flow fractionation (HT-AF4) overcomes the column-related problems of previous separation techniques like sample degradation or sample loss due to interactions with the stationary phase or the column frits. HT-AF4 is particularly useful for ultrahigh molar mass samples and can emerge as the first choice for very high molar mass polyolefins in future. It remains to be seen if HT-AF4 (similar to column-based fractionation methods) will be hyphenated with spectroscopic detectors or will be used as one dimension in two-dimensional experimental set-ups in the future.

To summarize, all techniques used for polyolefin characterization have advantages and disadvantages. Some information can be obtained more reliably from one technique and some other from other techniques. One has to decide on the problems to be addressed using a given technique. Nevertheless, 2D-HT-HPLC seems to be one major technique to be used for polyolefin analysis in the future due to its ability to provide molar mass distribution as a function of chemical composition distribution of the sample which is not possible by other approaches.

The fact that there is constant progress in developing new separation methods for polyolefins has been demonstrated very recently by introducing high-temperature thermal gradient interaction chromatography. In addition to using an interacting stationary phase, temperature gradients are used to enhance separation of complex olefin copolymers.

Index

H. Pasch, M.I. Malik, *Advanced Separation Techniques for Polyolefins*, Springer Laboratory, DOI 10.1007/978-3-319-08632-3